Generating useful tools for future studies in the center of the circadian clock – defined knockout mutants for PERIOD and TIMELESS

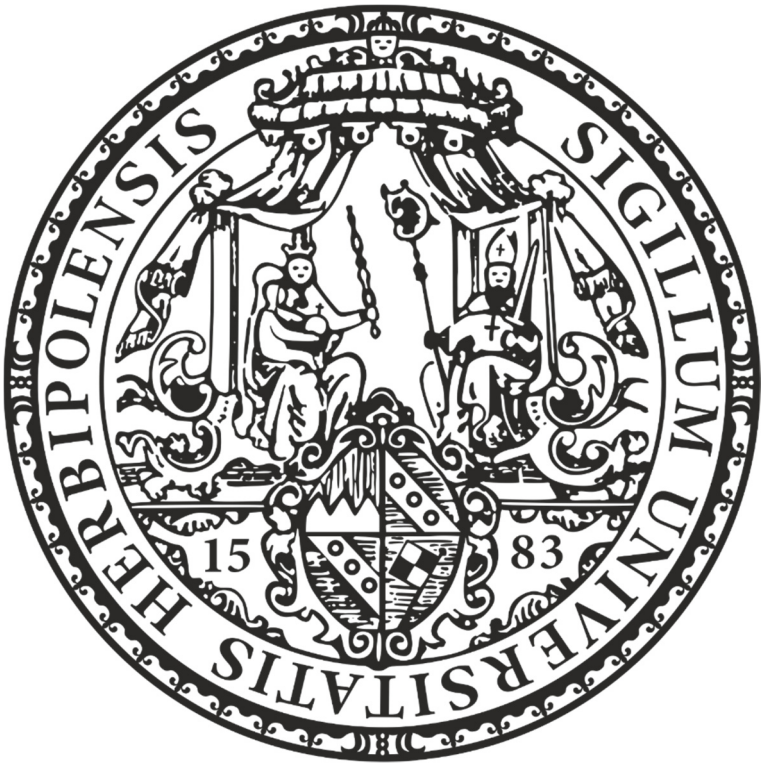

Dissertation for a doctoral degree

at the

Julius-Maximilians-Universität Würzburg

Chair for Neurobiology and Genetics

Submitted by

Robin Fischer

Würzburg, 2015

Submitted on: _____

Members of the thesis committee (Promotionskomitee):

Chairperson:

First Supervisor: Dr. Nicolai Peschel

Second Supervisor: Dr. Tobias Langenhan

Date of public defense: _____

Date of Receipt of Certificates: _____

Table of contents

1 Abstract

To unravel the role of single genes underlying certain biological processes, scientists often use amorphic or hypomorphic alleles. In the past, such mutants were often created by chance. Enormous approaches with many animals and massive screening effort for striking phenotypes were necessary to find a needle in the haystack. Therefore at the beginning chemical mutagens or radiation were used to induce mutations in the genome. Later P-element insertions and inaccurate jump-outs enabled the advantage of potential larger deletions or inversions. The mutations were characterized and subsequently kept in smaller populations in the laboratories. Thus additional mutations with unknown background effects could accumulate.

The precision of the knockout through homologous recombination and the additional advantage of being able to generate many useful rescue constructs that can be easily reintegrated into the target locus made us trying an ends-out targeting procedure of the two core clock genes *period* and *timeless* in *Drosophila melanogaster*. Instead of the endogenous region, a small fragment of approximately 100 base pairs remains including an *attP*-site that can be used as integration site for *in vitro* created rescue constructs. After a successful ends-out targeting procedure, the locus will be restored with e.g. flies expressing the endogenous gene under the native promoter at the original locus coupled to a fluorescence tag or expressing luciferase.

We also linked this project to other research interests of our work group, like the epigenetic related ADAR-editing project of the Timeless protein, a promising newly discovered feature of time point specific *timeless* mRNA modification after transcription with yet unexplored consequences. The editing position within the Timeless protein is likewise interesting and not only noticed for the first time. This will render new insights into the otherwise not-satisfying investigation and quest for functional important sequences of the Timeless protein, which anyway shows less homology to other yet characterized proteins.

Last but not least, we bothered with the question of the role of Shaggy on the circadian clock. The impact of an overexpression or downregulation of Shaggy on the pace of the clock is obvious and often described. The influence of Shaggy on Period and Timeless was also shown, but for the latter it is still controversially discussed. Some are talking of a Cryptochrome stabilization effect and rhythmic animals in constant light due to Shaggy overexpression, others show a decrease of Cryptochrome levels under these conditions. Also the constant light rhythmicity of the flies, as it was published, could not be repeated so far. We were able to expose the conditions behind the Cryptochrome stabilization and

discuss possibilities for the phenomenon of rhythmicity under constant light due to Shaggy overexpression.

Zusammenfassung

Um die Rolle einzelner Gene hinter biologischen Prozessen zu entschlüsseln, bedienen sich Wissenschaftler häufig amorpher oder hypomorpher Allele. Diese wurden in der Vergangenheit oft auf Zufall basierend generiert. Gewaltige Ansätze mit zahllosen Tieren unter enormem Selektionsaufwand bei der Suche nach markanten Phänotypen waren notwendig um sprichwörtlich die Nadel im Heuhaufen zu finden. Zunächst wurden chemische Mutagene oder Strahlung verwendet um Mutationen im Genom zu induzieren. Später kamen P-element Insertionen und induziertes unpräzises Herausspringen der Transposons dazu. Das hatte den Vorteil, dass so unter Umstände größere Deletionen oder Inversionen entstanden. Die Mutationen wurden charakterisiert und die Tiere anschließend in kleinen Populationen gehalten. Dadurch konnten sich zusätzliche Mutationen mit möglichen Hintergrundeffekten unbemerkt ansammeln. Ebenso blieben weitere durchaus mögliche Mutationen aufgrund der Mutagene und dem deutlicheren Phänotyp der primären Mutation oftmals unbemerkt.

Die Präzision eines Knockouts durch homologe Rekombination und der Vorteil, zusätzlich im Stande zu sein, jedes entworfene Rettungskonstrukt auf einfache Weise wieder einsetzen zu können, überzeugte uns, eine Ends-out Targeting Prozedur mit den zwei Uhr Basisgenen *period* und *timeless* in *Drosophila melanogaster* durchzuführen. Dabei soll ein geplanter Knockout zu einer kompletten Deletion des gesamten Bereichs durch homologe Rekombination führen. Anstelle der endogenen Region verbleibt lediglich ein kleines Fragment von ungefähr 100 Basenpaaren inklusive einer *attP*-Stelle, die als Insertionsstelle für *in vitro* hergestellte Konstrukte genutzt werden kann. Angestrebte Ziele sind beispielsweise Fliegen, die das endogene Gen unter der Kontrolle des ursprünglichen Promoters am originalen Lokus gebunden an einen Fluoreszenzmarker oder aber gekoppelt an Luziferase exprimieren.

Wir koppelten dieses Projekt zusätzlich mit anderen Forschungsinteressen unserer Arbeitsgruppe, wie zum Beispiel dem epigenetischen ADAR-Editierungsprojekt des Timeless Proteins, einer vielversprechenden Neuentdeckung zeitpunktspezifischer und posttranskriptionaler Modifizierung der *timeless* mRNA, mit bisher noch unbekannten Folgen. Die Position der Editierung innerhalb des Timeless Proteins ist ebenfalls sehr interessant und nicht zum ersten Mal im Fokus von Wissenschaftlern. Dies wird neue Einblicke in die sonst bislang nicht zufriedenstellende Suche nach

funktionell wichtigen Strukturen von Timeless bringen, welche aufgrund der geringen Homologie zu anderen bisher charakterisierten Proteinen bislang nur unzureichend bestimmt werden konnten.

Zuletzt beschäftigten wir uns mit der Frage nach der Rolle von Shaggy bezüglich der inneren Uhr. Der Einfluss einer Überexpression oder Herabregulierung von Shaggy auf die Taktung der Uhr ist eindeutig und wurde schon oft beschrieben. Der Einfluss von Shaggy auf Period und Timeless wurde ebenfalls bereits gezeigt, wird jedoch im Falle des letzteren Proteins noch sehr kontrovers diskutiert. Während einige von einem Cryptochrom stabilisierenden Effekt und rhythmischen Tieren in konstanter Beleuchtung aufgrund von Shaggy Überexpression sprechen, zeigen andere einen Abfall des Cryptochromlevels unter eben genau diesen Umständen. Es war uns möglich die Umstände hinter der Cryptochromstabilisierung aufzudecken. Darüber hinaus zeigen wir mögliche Gründe für das Phänomen des Rhythmus im Dauerlicht von Shaggy Überexpressionstieren auf.

2 Introduction

2.1 The clock – function and basics

'And God said, Let there be light: and there was light. And God saw the light, that it was good: and God divided the light from the darkness. And God called the light Day, and the darkness he called Night. And the evening and the morning were the first day.' *1. Mose 1: 3-5*

Some conditions can be assumed as standards for all living beings on this planet. Like for the law of gravity or thermodynamics, every living being on earth is exposed to the daily change of night and day[a] established by the rotation of the earth around its own axis in a 24 h cycle. Adaptation to this condition can be quite useful for all creatures, especially for the occupation of an individual ecological niche (Peschel and Helfrich-Förster 2011). Thus, also temporal activity differences emerged like nocturnal (night active), diurnal (day active) or crepuscular (active at twilight) ways of life. Since the endogenous pacemaker[b] does not exactly fit to the daily 24 h rhythm, an ongoing adaptation (re-entrainment) is unavoidable to generate a proper behavioral output. But nevertheless, it is quite astonishing that a series of molecular processes, that establish the core clock pacemaker, can generate a rhythm so close to natural conditions. The endogenous rhythm can be aligned and adapted to environmental time cues (called Zeitgeber) like light, temperature, food availability or social interactions (Dubruille and Emery 2008). If a creature gets deprived from all these Zeitgeber, it would yet show an activity rhythm of approximately 24 h (Helfrich-Förster 2002, 2004), a condition called free-run. One famous example for such an experiment was done by J. Aschoff in the 1960s in a bunker in Andechs, where he observed human volunteers under simulated free-run conditions. The circadian clock is a meanwhile well studied mechanism of animals to create an endogenous rhythm of around 24 h in the absence of any external time cues (Schibler 2006, Helfrich-Förster 2004, 2002) , but still plastic and able to be adjusted to erratic seasonal changes in photoperiod or temperature (Dubruille and Emery 2008).

From this point onwards, the focus of this work will be on the fruit fly *Drosophila melanogaster*. Since this small insect is the cuddly toy of geneticists, its genome is already sequenced, a bulk of genes are described and meanwhile there is a great variety of genetic 'gadgetry' established for this model organism. Especially for researchers of biological rhythms *Drosophila* is an excellent model, because the fly shows many different large scale measurable patterns of behavior like locomotion, eclosion or

[a] Except e. g. of deepsea fishes and cave living animals

[b] Another word for the endogenous rhythm. Also used by *Drosophila* scientists to describe a set of neurons rhythmically expressing a small group of clock genes that set the pace of this functional unit.

egg laying. Another advantage is the simplicity of its neuronal network. A manageable number of only 150 clock neurons forming the core oscillator (Peschel and Helfrich-Förster 2011) (see part 2.2). On the molecular level the clock is made up of two interlocked negative feedback loops consisting of two main proteins, respectively: Period (PER)/Timeless (TIM) (Figure 1) on the one hand and Clock (CLK)/Cycle (CYC) (Figure 2) on the other side. These loops are controlled and adjusted by a set of major kinases like double-time (DBT, more precise at 2.3), casein kinase 2 (CK2) or Shaggy (SGG, see 2.4). They enable a precise timing of *per* and *tim* transcription – the constant restart of a new cycle (Dubruille and Emery 2008).

2.1.1 The PER/TIM feedback loop and the connection to light

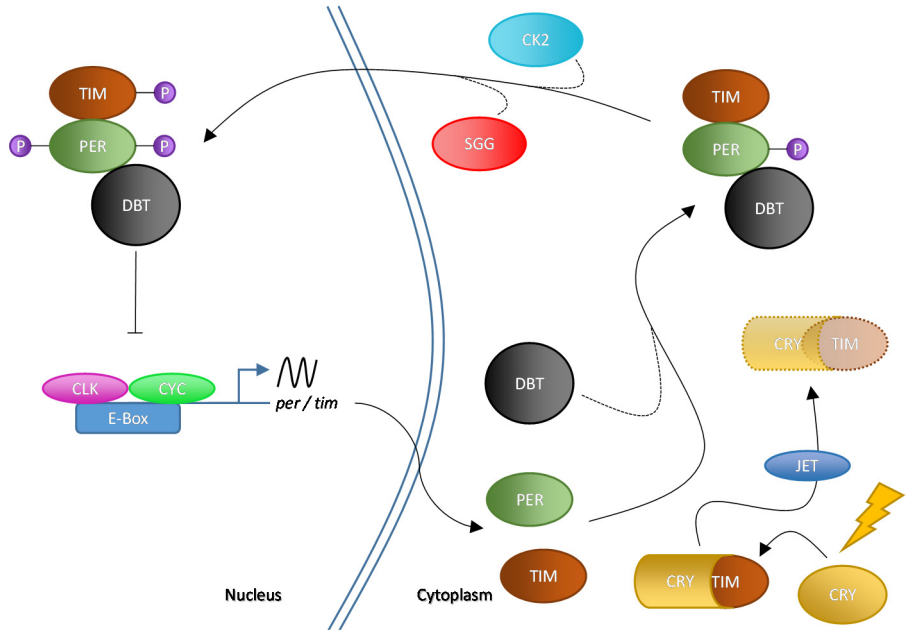

Figure 1: The PER/TIM feedback loop.

Simplified figure of the core feedback loop of the circadian clock. Due to binding of the activation factors CLK and CYC on E-Box regulatory elements, *per* and *tim* get transcribed and subsequently translated in the cytoplasm. Certain kinases regulate degradation, accumulation, dimerization and localization of PER and TIM (details in the main text). Finally they are transported back to the nucleus, where they inhibit their own expression and with that restart the cycle. CRY is necessary for the adaptation of the loop towards light. It gets activated through light, binds to TIM whereupon both proteins are degraded via JET-mediated ubiquitination. Figure adapted from Hardin et al., 2011 (Hardin 2011).

The initiation of the loop is done by the binding of CLK-CYC heterodimers to the E-Box regulatory elements, thereby activating the transcription of *period (per)* and *timeless (tim)* genes (Dubruille and Emery 2008). But due to phosphorylation dependent destabilization of PER by e.g. DBT, PER and TIM levels peak later than their own RNA levels do. The enrichment is only possible by PER stabilization via PER-TIM heterodimerization and thus the resulting reciprocal dependency of both proteins (Hardin 2005). In this way, the PER-DBT complex gets stabilized, too, and the three proteins accumulate together (Hardin 2011). The formation of this complex is not only thought to be important for protein

accumulation, but also for nuclear entry, enabled through phosphorylation by certain kinases (Shafer, Rosbash, and Truman 2002) like SGG (see 2.4.1) or CK2. Once located in the nucleus, PER binds CLK, thereby reducing the binding capacity of CLK-CYC heterodimers, which ends in the reduction of *per* and *tim* transcription (Hardin 2005). Light, the most important Zeitgeber, acts on the feedback loop via the blue light sensor Cryptochrome (CRY, more detailed in 2.5), which in turn regulates the function of TIM (Stanewsky 2002) through degradation mediated by the F-box protein Jetlag (JET) (Koh, Zheng, and Sehgal 2006, Hardin 2011).

2.1.2 The *Clk* loop

The second (*Clk*) loop regulates the transcription of CLK and is hence interconnected with the PER-TIM loop (Figure 2). Here, CLK-CYC dimers activate the transcription of Vrille (VRI) and PDP1ε (PAR-domain protein 1), which in turn bind to V/P boxes (VRI/PDP1) in the promoter region of *Clk* (Peschel and Helfrich-Förster 2011). Thereby VRI, in contrast to PDP1, is attributed to repress *Clk* transcription. The peak levels of both proteins are postponed, whereas VRI peaks around Zeitgeber time (ZT)14, PDP1 reaches its highest level at ZT18 (Hardin 2011, Blau and Young 1999).

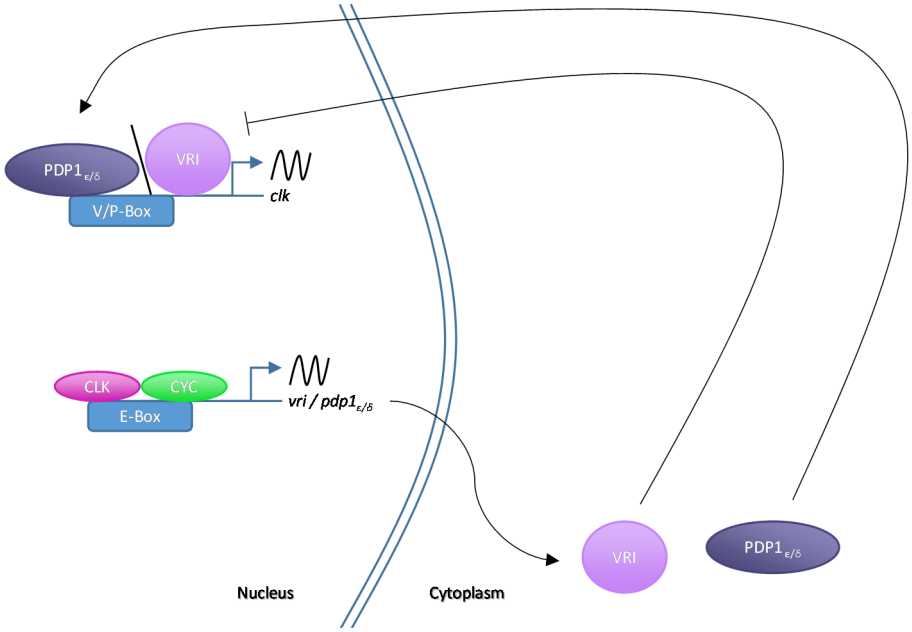

Figure 2: The *Clk* feedback loop.

CLK and CYC bind to E-Box regulatory sequences of *vri* and *pdp1*$_{\varepsilon/\delta}$. The figure is a broad simplification, but shows the key features. As in case of *per* and *tim*, the *vri* and *pdp1*$_{\varepsilon/\delta}$ mRNA gets translated in the cytoplasm, where the proteins accumulate, reenter the nucleus and inhibit (VRI) or activate (PDP1) *Clk* expression. Thereby both loops are interconnected. Figure adapted from Hardin et al., 2011 (Hardin 2011).

That shows us, both loops control mRNA cycling in opposite phases and are not equally important for the core oscillator. The PER loop is inevitable for the *Clk* loop, since CLK-CYC regulates *vri* transcription.

On the other hand the *Clk* mRNA level does not influence its own protein level and has little effect on molecular and behavioral rhythms (Kim et al. 2002). However, it is thought that the *Clk* loop is important for the regulation of rhythmic transcription of output genes, especially those that peak at dawn (Hardin 2011).

2.2 Clock networks and anatomy

Drosophila melanogaster is a crepuscular animal that displays two activity peaks, one at dawn (morning) and one at dusk (evening), separated by a midday siesta. These anticipatory responses are thought to derive from two separate functional units of neurons, also called oscillators (Vanin et al. 2012, Grima et al. 2004, Stoleru et al. 2004, Yoshii, Rieger, and Helfrich-Förster 2012). The previously mentioned 150 clock neurons in the brain of *Drosophila melanogaster* are divided in seven major groups based on their anatomical position (Figure 3). There are three cell clusters located more dorsally and are thus referred to as dorsal neurons (DNs). They are further subdivided into about 16 DN_1, 2 DN_2 and 40 DN_3 neurons according to their position, protein content, size and/or function. The residual four groups are located more laterally and are therefore called lateral neurons (LNs). Here a distinction is made between 4 l-LN_vs, 4 s-LN_vs, a 5th s-LN_v, the LN_ds and the LPNs based on the same criteria used for the DNs' subdivision. An important neuropeptide used for the classification is the pigment dispersing factor (PDF) (Peschel and Helfrich-Förster 2011), which is derived from the closely related crustacean pigment-dispersing hormones (PDH). Its receptor belongs to the class II GPCRs (G-protein coupled receptors). PDF is interesting, because it is the major output factor[c] of s-LN_vs and l-LN_vs. The theory is, that PDF is used from these cells to communicate with other brain centers controlling the behavior of the animal and also for signaling within the clock network (Shafer and Yao 2014). The s-LN_vs - amongst others - are thought to regulate the morning activity in the fly. That is the reason, why null mutations in the *pdf* gene result in animals with defect rhythms during prolonged constant darkness (DD = 'DarkDark'), especially concerning the morning peak (Stoleru et al. 2004, Grima et al. 2004). In total they are much less rhythmic than wild types, most often they lose their rhythm after 2-3 days in DD. In light-dark conditions (LD) they show an advanced evening activity peak and a lack of lights-on anticipation (Renn et al. 1999). This term describes an expectation of the light change, the fact that the animals start getting active not exactly with lights-on or -off, instead they increase their activity level a certain time before.

[c] Output factor means a kind of signal or substance the neuron sequesters upon stimulation or excitation to communicate with its environment.

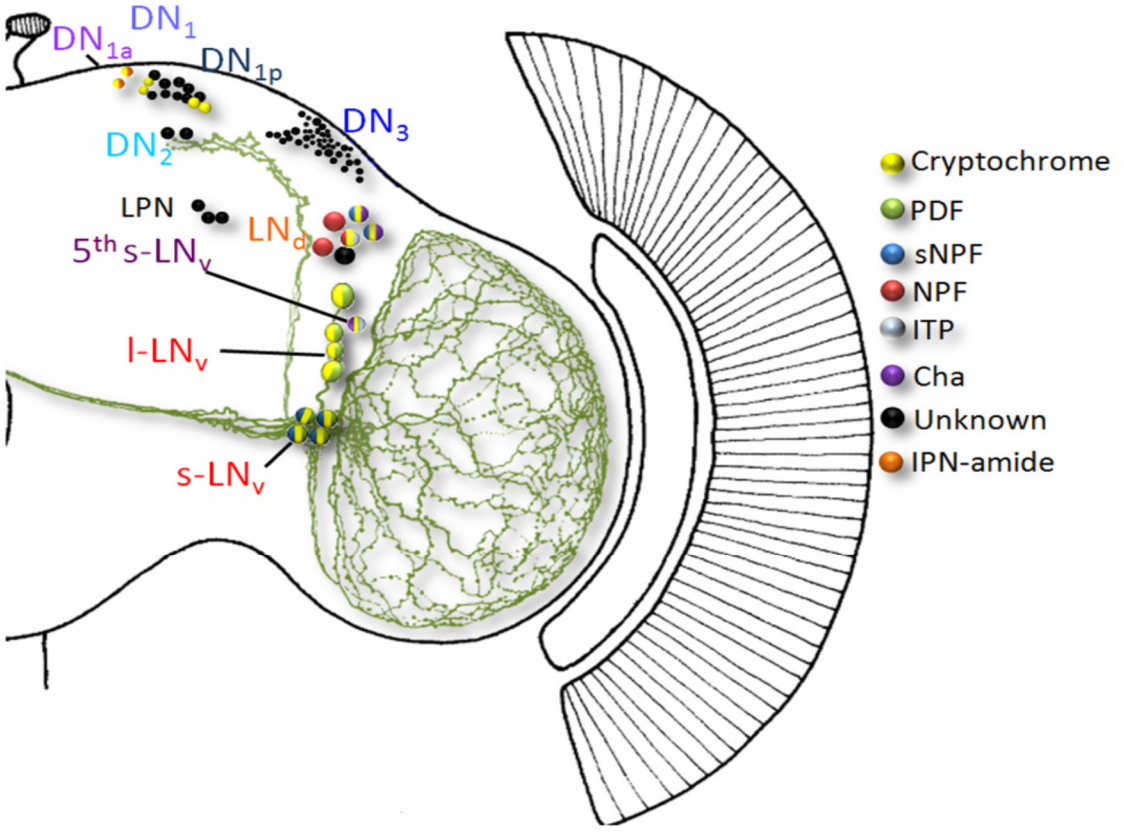

Figure 3: Clock network in *Drosophila*.

The clock neurons are divided in seven major groups and named after their anatomical position. Three clusters are located more dorsally and are thus called dorsal neurons (DNs_{1-3}). The other 4 groups (LN_d, l-LN_v, LPN, and s-LN_v) can be found more laterally. They are named lateral neurons (LNs). Colors indicate neurochemical contents, listed on the right side. To enable an easier overview, not all peptides are explained in detail in the main text. NPF (Neuropeptide F), sNPF (short Neuropeptide F), ITP (ion transport peptide), Cha (choline acetyltransferase). Taken from N. Peschel and C. Helfrich-Förster, 2011 (Peschel and Helfrich-Förster 2011).

Since *Drosophila melanogaster* shows two distinct peak levels of activity over the day - one in the morning, the other in the evening – one speaks of a bimodal activity pattern. The existence of two circadian oscillators was already proposed in the 70s (Daan and Pittendrigh 1976). The morning oscillator (M) regulates the activity in the morning and is accelerated by light. Thus, in a changing environment involving a light increase, like the prolonged photoperiod in long summer days, it usually answers with an advanced morning activity peak. It is mainly located in the s-LN_vs (except of the 5th s-LN_v), which are also described to be the main circadian pacemaker cells, because they are inevitable for maintaining a rhythmic behavior under

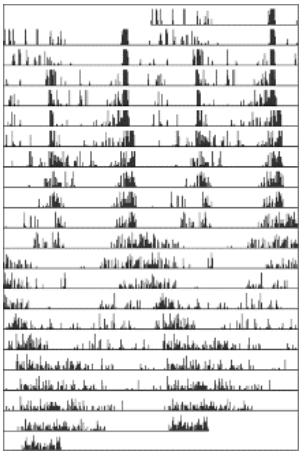

Figure 4: Split activity rhythm.

An actogram shows the periods of activity and rest of an organism over a 24 hour cycle, so that trends in activity can be identified. Depicted is a double plotted actogram of a single fly. The X-axis shows two consecutive days next to each other - for a better overview. Every line on the Y-axis corresponds to one day. After 10 days of LD cycles of 12 h light and 12 h darkness, the system is changed to LL. The example is taken from an experiment with *cry*^{01} flies.

DD. The evening oscillator (E) induces activity in the evening and is slowed down by light, thus delaying the onset of evening activity in long summer days. The LN_ds, part of the DNs and the 5^{th} s-LN_v make up this functional unit (Grima et al. 2004, Peschel and Helfrich-Förster 2011, Rieger et al. 2006). One verification of this theory can be seen in the rhythmicity of cry^b flies (2.5) in constant light conditions (LL). Here the animals display a split activity rhythm, observable as an 'X' in the actogram (Figure 4) made up of two activity components running with a faster (~22 h) and a slower (~25 h) period (Peschel and Helfrich-Förster 2011, Rieger et al. 2006, Yoshii et al. 2004).

2.3 The gene *per* – started it all.

2.3.1 *per* alleles

In the early 70s R.J. Konopka and S. Benzer discovered new mutations in flies treated with chemical agents. Thereby they screened for flies showing abnormal circadian behavior and found three lines with conspicuous phenotypes. Observed in free-run conditions in DD one would normally expect a rhythmic change of activity and rest in a roughly 24 h pattern. Three rhythmically abnormal phenotypes could be found. The first mutant was totally arrhythmic (later denoted as per^{01}), whereas the other two displayed periods of 19 h and 28 h (per^S/per^L), respectively. Surprisingly all three phenotypes could be assigned to one genetic locus on the X-chromosome. The responsible gene was identified and named *period* (*per*). Unraveling the details about how the *per* gene exactly contributes to the circadian timekeeping lasted until 1984, when it was isolated (Hardin 2011). It turned out, that its protein is one core protein establishing the cycling that triggers and drives the circadian time machine (Konopka and Benzer 1971). The reason for the arrhythmicity produced by the per^{01} allele can be found in a nonsense point mutation (TAG → Stop instead of CAG → glutamine) in one of the coding exons at amino acid (AA) position 464 leading to a truncated polypeptide with 463 AA instead of possible 1218 (Yu et al. 1987). The result is a loss of function allele (Stanewsky, Frisch, et al. 1997). It is used since its characterization, assuming that these flies contain no functional PER at all, although a shortened per^{01} nonsense fragment - that is thought to retain some aberrant biological activity - is still observable (Yu et al. 1987). per^S as well as per^L can be ascribed to point mutations or more precisely single AA changes (per^S: S589N and per^L: V243D)[d]. The short mutation (per^S) is located in a part of PER coding for a region called 'short-domain' because other AA exchanges in this region also lead to individuals with shorter circadian periods (Baylies et al. 1992, Garbe et al. 2013). The PER^S protein shows fastened hyperphosphorylation and with that disappearance from the nucleus. per^L falls into a binding domain

[d] An overview of all amino acids and used abbreviations in the text is shown in the appendix in Figure 58.

of PER called PAS (PER-ARNT-SIM) and is thought to alter interactions between PER and TIM (Gekakis et al. 1995) (Figure 5). Here, the timing of nuclear entry is retarded (Ko et al. 2007), because interaction of both proteins is required for the entry into the nucleus and protection of PER phosphorylation by DBT (Rothenfluh, Young, and Saez 2000). Recent publications postulate a catalytic function for TIM towards PER instead of a direct heterodimerization as necessity for entrance into the nucleus (Shafer, Rosbash, and Truman 2002).

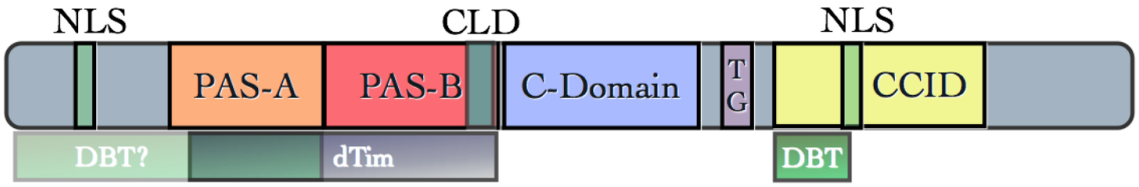

Figure 5: Functional domains and grouped phosphorylation sites of PER (schematic).

NLS: nuclear localization signal. PAS: PER-ARNT-SIM. CLD: cellular localization domain. TG: threonine-glycine rich region. CCID: dCLK:CYC inhibition domain. Shaded boxes beneath the protein depict protein-protein interaction domains. The per^{L} mutation falls into the PAS-A region, per^{S} into the C-Domain. per^{01} lies somewhere in between. Taken from Garbe et al., 2013 (Garbe et al. 2013).

per (*CG2647*) is located on the X-chromosome (3B1-3B2). Two transcripts are known, but they result in only one polypeptide. The PER protein belongs to the category of transcriptional repressors and functions and cycles together with another core clock protein (TIM) as heterodimer to inhibit the function of CLK-CYC and VRI (Hardin 2005). The *per* expression level, however, peaks at the mid- to late-night and it gets repressed by accumulation of its own protein (Hardin 2011). Daybreak and with that light-dependent degradation of TIM is followed by a slightly delayed decrease in PER level, which was stabilized in the TIM-PER complex before. The expression begins to increase anew at middle-late day.

2.3.2 DBT – PER phosphorylation pattern

One major kinase of PER is DBT– the *Drosophila* orthologue of the mammalian casein kinase Iε. It has a primary role in the regulation of PER as it post-translationally influences PERs phosphorylation status at several time points throughout the day and thus controls a variety of aspects like protein stability, subcellular localization, protein-protein interactions and transcriptional repression. But, although DBT is expressed constitutively, its subcellular localization varies (Stanewsky 2002) due to its direct physical interaction with PER. Thus it is dependent on PERs' localization and in complex with TIM and PER, DBT is also able to enter the nucleus of the cell (Kloss et al. 1998). Interestingly, phosphorylation by the DBT kinase on the one hand inhibits the accumulation of PER in the cytoplasm – thereby prolonging the period. On the other hand it sets the endpoint of the cycle by first converting PER into a potent repressor before degradation in the nucleus (Stanewsky 2002). This is done by SLIMB, a protein from

the ubiquitin-proteasome system that preferentially interacts with phosphorylated PER, thus stimulating its degradation (Ko, Jiang, and Edery 2002). Further important examples for PER acting enzymes are CK2 (Lin et al. 2002, Akten et al. 2003) or protein phosphatase 2A (PP2A) (Dubruille and Emery 2008, Ko, Jiang, and Edery 2002). The latter, like DBT, also regulates CLK phosphorylation levels (Kim and Edery 2006). D.S. Garbe (Garbe et al. 2013) gives a good overview of all yet identified phosphorylation sites of PER. Summed up, the phosphorylation of PER increases with its accumulation and peaks, when PER is degraded - due to progressive phosphorylation and final ubiquitination - in the proteasome shortly after dawn (Hardin 2011).

2.4 TIM – the light switch

The discovery of *tim* took until the 90s of the last century, when Sehgal et al. described a new mutation leading to arrhythmia in circadian behaviors (Sehgal et al. 1994). It is located on the left arm of the second chromosome (23F6) and encodes for eight reported transcripts of different size (Figure 6).

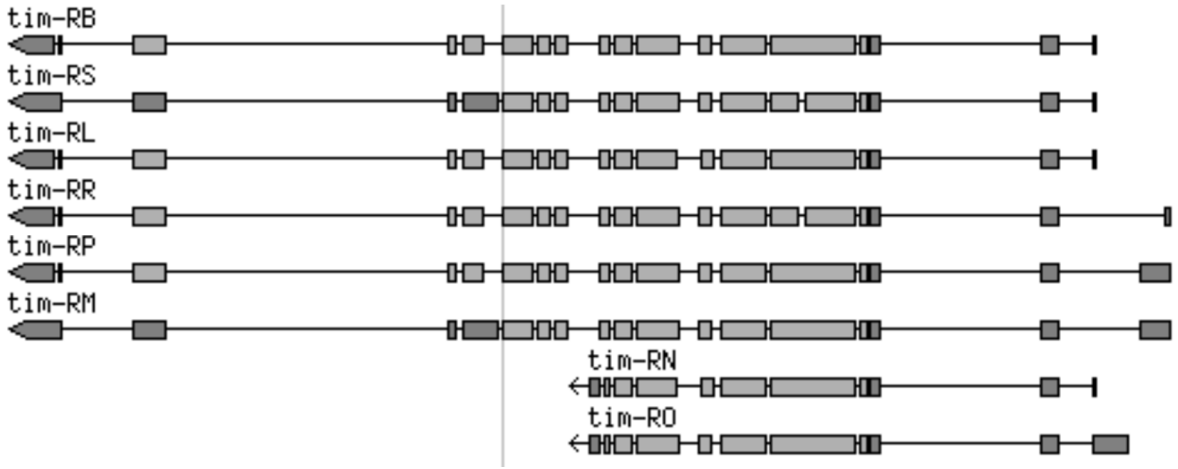

Figure 6: The *tim* (*CG3234*) transcripts as reported on flybase.org.

Eight transcripts are noted (890-1398 bp long). Translation start is depicted concerning the *s-tim* polymorphism. They are coding for seven different polypeptides with the size ranging from 100 to 156 kDa (reported as ~180 kDa). Translated exons leading to the polypeptides are depicted in light grey. Untranslated regions (UTRs) occurring in the RNA are shown in dark grey. Introns are drawn as thin lines in between. The single transcripts are labeled with different letters. The gene is orientated with the future N-terminal site facing to the right (Source: http://flybase.org).

TIM is inevitable for establishing the molecular core of the clock as it allows accumulation and nuclear entry of PER or adapts the circadian clock to different light circumstances (Sehgal et al. 1995). Nuclear entry is promoted by the dimerization of PER and TIM through the PAS-domain of PER (Gekakis et al. 1995). TIM itself does not have a typical protein-protein interaction domain that can be found with protein modeling algorithms, but three ARMADILLO-like dimerization domains, two of which overlap with the PER binding region (Stanewsky 2002, Kyriacou and Hastings 2001, Saez and Young 1996). Another example is the cytoplasmic localization domain (CLD), that restrains TIM in the cytoplasm until

PER is bound (Rothenfluh et al. 2000). In general TIM lacks sequence similarities to any other described protein (Kyriacou and Hastings 2001).

Important TIM-influencing proteins are SGG (2.4.1), CRY (2.5) and JET. The last one is applicably named after the phenomenon of dysrhythmia resulting from alterations in the light-dark system existing in the environment around the body. Appropriate because JET plays a key role in mediating light-dependent degradation of TIM through signaling of the light-receptor CRY (Koh, Zheng, and Sehgal 2006). But not only TIM, also CRY gets ubiquitinated in a light-dependent fashion by JET, which is thought to be a putative component of an E3 ubiquitin ligase complex (Peschel et al. 2009). The antagonist responsible for dephosphorylation of TIM is the protein phosphatase 1 (PP1). Reduced levels of this phosphatase lead to lengthened circadian periods and an altered response towards light through stabilization of TIM, but not by affecting the nuclear entry of TIM (Fang, Sathyanarayanan, and Sehgal 2007). Putatively separate phosphorylation sites are addressed by the kinase SGG and the phosphatase PP1 (Peschel and Helfrich-Förster 2011, Fang, Sathyanarayanan, and Sehgal 2007).

2.4.1 SGG – regulation of TIM

A multifunctional key player, regulator and pivot also known from many other research areas, but still remaining a myth for many scientists is SGG, the *Drosophila* orthologue of the mammalian Glycogen synthase kinase 3 beta (GSK3-β). SGG is a very versatile kinase, involved in many different events like protein synthesis, cell proliferation and differentiation or contributions in important signaling pathways like the Wnt signaling pathway (Frame and Cohen 2001). Described as a serine/threonine and tyrosine kinase, it usually needs priming phosphates at position P_{+4} from other kinases at its target sites (= P). The first phosphate thereupon tends to be the next priming phosphate for subsequent phosphorylations executed by SSG (Harwood 2001). Besides publications showing a coherence between SGG and PER phosphorylation (Ko et al. 2010), it is now generally acknowledged that TIM phosphorylation levels are in part controlled by SGG (Martinek et al. 2001). A change in SGG levels leads to distinct effects on the rhythm of the animals in DD and LD conditions. A commonly accepted fact is, that an overexpression shortens and a reduction lengthens the period (Figure 7). Both is also observable by a prominent shift in the morning and evening peak of activity in LD (Stoleru et al. 2007, Martinek et al. 2001).

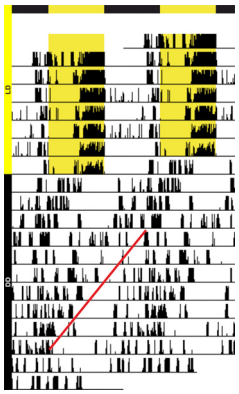

UAS-SGG^{11008} x tim-GAL4

Figure 7: The influence of SGG on the circadian clock.

If SGG is overexpressed (*SGG^{11008}*) by the GAL4-UAS system or down regulated (*SGG^{35364}*) via RNAi in clock neurons (*tim-GAL4*), it has severe impact on the behavior of the flies regarding their rhythm. Thereby, overexpression leads to shorter rhythms. Prolonged periods can also be observed caused by hypomorphic *sgg* alleles.

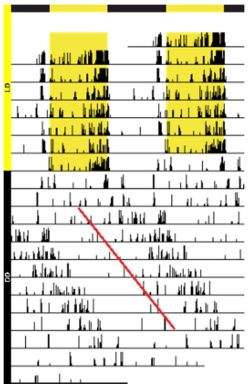

UAS-SGG-RNAi^{35364} x tim-GAL4

Connections between the Wnt signaling and the circadian clock are discussed, mainly for SGG but also for DBT, whose vertebrate orthologue – casein kinase 1ε – is thought to participate in the developmental pathway (Martinek et al. 2001).

The effect under LL and with that the influence on CRY is still controversially discussed. Whereas some scientists are convinced that SGG stabilizes CRY, proven by LL-rhythmicity due to SGG overexpression (Stoleru et al. 2007), these results could not be reproduced so far and were shown to be just contradictory to past publications (Martinek et al. 2001). The idea behind is a binding of SGG to CRY leading to its stabilization, but somehow reducing the degrading effect of CRY on TIM (Peschel and Helfrich-Förster 2011, Stoleru et al. 2007). However, the effect in DD cannot be denied, is quite prominent and is therefore a topic in our study (see appendix 6.1).

2.4.2 The *tim* alleles

Because of a natural polymorphism there are two forms of *tim*, a 'long' and a 'short' form, referred to as *ls-tim* or *s-tim*, respectively. Considered in detail, there is a single nucleotide insertion that produces an alternative start codon for the long form, which contains 23 additional AA at its N-terminus. The expression '*Ls-tim'* refers to the ability of the longer form to express both alleles, because both start codons exist. In contrast, the *s-tim* form just encodes for the short form of TIM (Peschel, Veleri, and Stanewsky 2006)[e]. Withal, the long form has a much weaker binding affinity to CRY and thus a consequence of this polymorphism is that both TIM isoforms show different sensitivities towards light (Peschel, Veleri, and Stanewsky 2006, Tauber et al. 2007, Sandrelli et al. 2007).

[e] 'A single nucleotide insertion' is a simplified description. Detail are explained in the original publication from Peschel et al. Figure 4A.

To date, many different *tim* alleles are described. The most common null allele for *tim* is tim^{01}. It was first described in 1994 by Sehgal et al. as a result from a genetic screen for new mutations affecting circadian rhythms in *Drosophila*. For mutagenesis they remobilized single P-elements inserted by L. Cooley (Cooley, Kelley, and Spradling 1988) via a transposase-encoding Δ2-3 P-element and screened for abnormalities in the hatching behavior of the flies. Thereby they found one strain behaving similar to per^{01} – it neither showed a discernible rhythm in eclosion, nor did it maintain any rhythm in adulthood, when LD cycles were removed and DD was applied. The mutation was mapped to the outer part of the left arm of the second chromosome and referred to as *timeless*. Furthermore they observed no *per* mRNA oscillation in these mutants. From this they concluded a direct interaction of both loci (Sehgal et al. 1994). One year later the changes on nucleotide level leading to tim^{01} were revealed by Myers et al. (Myers et al. 1995). It is a 64-base pair deletion, resulting in a frameshift and with that in a premature breakup of transcription. The consequent polypeptide is therefore truncated to 749 AA and described as a loss of function allele (Yoshii et al. 2008).

Another mutation leading to a striking phenotype is the $tim^{UltraLong}$ (tim^{UL}) allele. Flies homozygous for tim^{UL} show free-running periods of 33 h and 26 h in heterozygous constellation, caused by an increased stability of the TIM^{UL}-PER complex in the nucleus. The result is a prolonged accumulation duration of nuclear PER and with that also a delayed degradation. On DNA level, the reason of the mutation can be found in a missense mutation leading to an AA change from glutamic acid to lysine at positon 260. There are no protein fragments described for this region that bind independently to PER, but it might contribute to the full length association of PER and TIM *in vivo* (Rothenfluh, Young, and Saez 2000). The glutamic acid (K^{260}) is a key acidic residue close to a potential phosphorylation site of CK2 at S^{256}. Thus, a decreased influence of CK2 on the molecular oscillator can be suggested (Akten et al. 2003, Meissner et al. 2008).

2.5 CRY – the light sensor

Cryptochromes are blue light photoreceptors also known from plants and related to photolyases - proteins that use the light energy to repair UV-damaged DNA - but with distinctive C-terminal domains. The photolyase-like part is highly conserved whereas the C-terminus is mostly diverged (Dissel et al. 2004). In animals and plants, CRY also functions as photoreceptor in circadian systems (Cashmore 2003). But in contrast to *Drosophila*, the mammalian system contains two *cry* genes (*cry1* and *cry2*). Here *cry2* is mainly expressed in retinal ganglion cells that detect light and project to the

suprachiasmatic nucleus (SCN)[f] and thus are known to be the photosensitive cells important for entrainment of the circadian clock in mammals. *Cry1* instead is active in the SCN and thought to be required for the functioning of the master clock. This also reflects a major difference of the circadian photoperception between flies and mammals, where it is solely dependent on the eye (Cashmore 2003). In *Drosophila*, CRY acts as a photoreceptor in brain and peripheral tissues (Krishnan et al. 2001). To complete the story, it has to be mentioned that there are also additional photoreceptors including the compound eyes and the Hofbauer-Buchner eyelets contributing to the light synchronization (Rieger, Stanewsky, and Helfrich-Förster 2003, Helfrich-Förster et al. 2001, Veleri et al. 2007). In the brain, CRY is expressed in most clock cells, in particular in all LN_vs, in three LN_ds and in 8 DN1s (Emery, Stanewsky, Helfrich-Förster, et al. 2000, Yoshii et al. 2008). One example for a non-photoreceptive role of CRY is a peripheral oscillator that drives circadian olfactory responses in the antennae also in cry^b animals (explained further down in the text). Krishnan et al. propose that the role of CRY is reversed in *Drosophila* compared to mice, meaning a core clock function in the periphery and a more photoreceptive role in the brain (Krishnan, Dryer, and Hardin 1999). Upon light absorption CRY undergoes conformational changes (Ceriani et al. 1999). This opens a binding site for TIM, which is subsequently bound and marked for degradation (Peschel, Veleri, and Stanewsky 2006) by a yet unidentified tyrosine kinase (Naidoo et al. 1999) - a crucial step for resetting the clock in a light-dependent manner. 30 minutes of light leads to a drastic reduction of TIM levels (Hardin 2011). Constant illumination therefore leads to an arrhythmic behavior of wild type flies, but not in CRY mutants (Emery et al. 2000). However, not only TIM, also CRY gets degraded by the proteasome after illumination (Busza et al. 2004, Lin et al. 2001) and interaction with JET or Ramshackle (BRWD3) (Ozturk et al. 2013) in a light-dependent manner. The affinity of TIM for CRY and JET determines the order of degradation for TIM and CRY, since CRY association to TIM is different in *s*- and *ls-tim* flies. The result is a faster degeneration of s-TIM followed by CRY, compared to l-TIM. The lower affinity of l-TIM for CRY yields in ubiquitination of CRY, because the binding probability of JET to CRY hence gets increased (Peschel et al. 2009). More recent studies thereby postulate a linked control of the degradation of CRY and TIM (Peschel et al. 2009), which was claimed to be independent before (Busza et al. 2004, Sathyanarayanan et al. 2008).

In 1998 R. Stanewsky et al. chemically mutagenized transgenic flies carrying a PER-LUC fusion protein and screened the offspring for abnormalities in bioluminescence rhythms. They found a recessive mutation on the third chromosome resulting in abnormal rhythms. The reason was a missense mutation in the C-terminal part within the CRY polypeptide – hence called cry^{baby} (cry^b). The affected

[f] Central brain nucleus in mammals, homing the main oscillator of the circadian system.

AA is highly conserved and is involved in the flavin binding, which is thought to participate in the capacity of blue light absorption. Since western blot analyzes show that *cry*^{b} is a null mutant, the reason is assumed in the altered flavin-binding capacity that influences the integrity of the protein and causes its degradation (Stanewsky et al. 1998). It turned out that this mutant is not completely circadianly blind. Instead, the perception of light is just strongly impaired. Dolezelova et al. designed a new *cry*^{0} mutant by ends-out homologous recombination targeting strategy, exchanging the whole coding area of *cry* (Dolezelova, Dolezel, and Hall 2007). These flies showed more severely abnormal light-response phenotypes, meaning the majority of *cry*^{0} flies displayed two free-running periodic components in LL (Figure 4), a condition that normally results in total arrhythmicity for wild type flies.

2.6 RNA editing by ADAR

RNA editing is a process that enables cells to make discrete changes to specific nucleotide sequences and thus allows an organism to generate diversity on its RNA (and thereby also on protein) level, which is not encoded in its genome (Zinshteyn and Nishikura 2009). The modification of the nucleotides takes place after the transcription of the RNA by the RNA polymerase. Consequences can occur for the protein product or the RNA molecule itself, which in turn can influence coding capacity, si-/miRNA target effects, nuclear sequestration or alter splicing processes for instance. Next to insertions or deletions, which are also reported, there are two enzymatically catalyzed forms of editing by deamination named after the exchanged bases, C-U editing and A-I editing, respectively. The deamination of adenosine is the most common form and carried out by the ADAR protein family. The reaction is catalyzed in dsRNAs and yields inosine (Figure 8), which pairs with cytidine instead of uridine (Jepson and Reenan 2010).

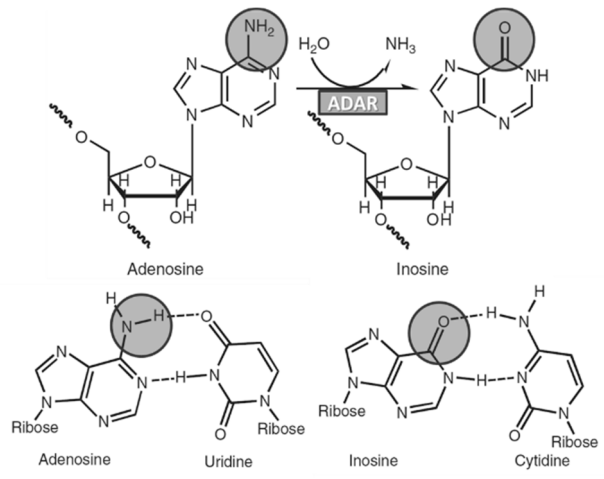

Figure 8: Impact of the deamination by ADAR.

The ADAR enzyme is exchanging adenosine (A) for inosine (I). An amino group is exchanged to a single oxygen molecule. Inosine is recognized as G, binding to C instead of U.

The edited portion of a single site can range from 0-100% in an RNA population, but is at 50% on average. Thereby it is highly unlikely that the ADAR proteins bind specifically to their own target sites.

Instead, the editing activity seems to be determined by the stability of the substrate dsRNA. The RNA double strand itself tends to be destabilized by the editing effect and stops the process through its own degradation, because it is no longer recognized by the enzyme. More specifically, editing gets possible through certain secondary structures within the dsRNA molecule, reducing the threshold of stability and allowing only few deaminations before decay (Zinshteyn and Nishikura 2009).

The genome of *Drosophila melanogaster* contains one X-linked *adar* gene locus, but mRNA modification sites for ADAR in the three-digit range, primarily coding for voltage- and ligand-gated ion channels, as well as presynaptic proteins. That makes *Drosophila* a good model system for studying the correlation between deamination and its output (Jepson et al. 2011). Deletion of the single *adar* locus ($dADAR^{5g1}$) resulted in a complete loss of courtship in males and other extreme behavioral abnormalities like loss of coordination. Therefor $dADAR^{5g1}$ animals are not cultivable in a homozygous genotype (Jepson et al. 2011). Another *adar* mutant strain carrying a $white^{+}$ mini-gene insertion in a C-terminal intron was generated through homologous recombination, similar to the technique that was used in this study (Maggert, Gong, and Golic 2008). The insertion created a hypomorphic allele ($adar^{hypomorph}$) that showed a >80% reduced protein level on western blots. But notably the editing efficiency concerning different adenosines in an arbitrary nucleotide sequence is very diverse and only conditionally dependent on the ADAR level. The spectrum is quite broad, ranging from 70-100% reduction to nearly wild type modification levels (Jepson et al. 2011) (here the authors already talk of 'high and low efficiency' groups of ADAR-substrates). Because of that, these flies do not show such severe behavioral abnormalities and can be sustained as a homozygous strain.

2.7 Genetic engineering – or how to build my own fly as desired

The first development and identification of mutations in the genome of *Drosophila* were mainly done via mutagens. These are physical or chemical agents that change the genetic material of an organism and thus increase the frequency of mutations. Examples often used as mutagens for the genome of *Drosophila* are ethyl methanesulfonate as a chemical or x-rays. By this very time consuming method, the genome of the fly is suspended to these agents and the following progeny is screened for new undescribed phenotypes. This approach is untargeted, random and beyond control.

Figure 9: Health hazard.

Pictogram for chemicals that are sensitizing, mutagenic, carcinogenic or toxic to reproduction.

Later, after P-elements became useful tools of *Drosophila* genetics, a more purposeful and targeted method of generating mutations was developed. By using a transposase[g], previously incorporated P-elements were mobilized anew. This often leads to errors or failures through an additional jump out of adjacent regions. Not rarely, this results in deletions of different sizes. The difficulties thereby are in defining the deletion, particular determining which parts of the locus are deleted, concluding if there is a remaining region leading to a still functional polypeptide or observing if neighboring gene regions are likewise affected. A rescue experiment is only possible with duplications of the deleted locus located elsewhere in the genome and often fails on already available fly strains. However, it is an important verification of the reliability of the collected deletion-data and not being an artefact due to destruction of other important genetic structures.

A clear and well defined knockout of a complete gene region can be managed through a double homologous recombination occurring up- and downstream of the target locus and thereby replacing the endogenous part with a designed construct. The process of homologous recombination is not an artificial but natural process for generation of genetic diversity, maintenance of genomic integrity and segregation of chromosomes[h]. The advantages of an induced knockout through homologous regions are obvious: first, the deletion is precise and previously well-conceived. No residual pieces of the gene locus remain, if correctly arranged in the preparatory work and if there is a sufficient amount of Fortuna's good-will. Also 3' and 5' regulatory regions can be deleted, too, without disturbing adjacent genes. Second, by generating a founder line by exchanging the locus with a site-specific recombination site, every desired rescue construct can be reintegrated easily. That gives a high amount of opportunities for the researcher: integration of a fluorescence tag, N- or C-terminally coupled to the polypeptide, inserting specific mutations at important sites of the protein or the regulatory sequences or setting the gene under control of an extrinsic controllable promoter, just to mention a few examples. But the event of a double homologous recombination is a very rare process. A lot of research spirit was necessary to increase the probability of this event and to minimize the work load to be done by the scientists.

Specifically and directly modifying the genome of mouse and yeast with artificial DNA via homologous recombination is nothing new *per se* and possible for a longer time. But by the turn of the millennium, only one form of gene targeting was possible for *Drosophila* – the ends-in targeting. A reason was that for a long time it had not been possible to create linearized transgenic constructs containing double

[g] Enzyme that binds to the end of a transposon and catalyzes its movement through cut-and-paste mechanism or replicative transposition.

[h] For those who are interested in the details of the mechanism I suggest the work from Kowalczykowski et al., 1994 (Kowalczykowski et al. 1994).

strand breaks *in vivo* in *Drosophila*, a given condition necessary for a successful ends-out targeting. The two forms of targeting are explained in Figure 10.

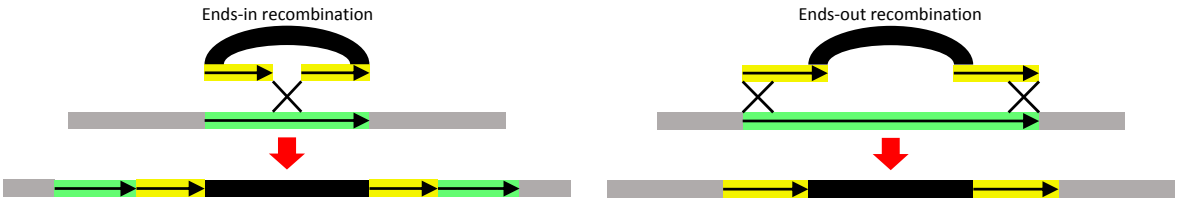

Figure 10: The two forms of gene targeting.

The target gene is depicted in light green, the donor gene in dark green and the marker gene in black. Donor constructs are located above the target region. The event and result of both targeting procedures are shown. The graph was modified from W.J. Gong and K.G. Golic (Gong and Golic 2003).

The technique for genetic manipulation and locus exchange in *Drosophila melanogaster* we used in this study is mainly based on the former research and review of Y.S. Rong and K.G. Golic (Rong and Golic 2000, Gong and Golic 2003) and the work of J. Huang and Y. Hong (Huang et al. 2008, Huang, Zhou, Dong, Watson, et al. 2009), that was based on these studies. An original working plan was established by K. A. Maggert (Maggert, Gong, and Golic 2008), refined by T. Langenhan (Scholz et al. 2015) and most widely borrowed by us. Smaller deviations are always mentioned in the methods paragraph.

Genetic engineering by homologous recombination uses endogenously existing mechanisms for DNA repair and recombination. The aim is to substitute a certain genetic cassette with a native target locus and with that integrate the construct site-directed by sequence homology. Three conditions are mandatory to generate the requirements for the recombination of construct and target gene: transgenes that express a site-specific recombinase (first condition) and a site-specific endonuclease (second condition). Of course this requires a donor construct that carries recognition sites for both enzymes and DNA from the locus to be targeted – as third condition. The current method makes use of an Flp site-specific recombinase and the I-SceI site-specific endonuclease. Thereby the recombinase catalyzes recombination between copies of the *Flp recombination target* (*FRT*) inserted into the genome. The intervening DNA gets excised in form of a circular molecule, if the FRTs are located in the same relative orientation as the chromosome. A close proximity of the *FRT* sites thereby enables a nearly 100% efficiency (Golic and Lindquist 1989). Because DNA molecules with double-strand broken ends have proven to be more recombinogenic than circular DNA (Rong and Golic 2000), Rong and Golic introduced the I-SceI intron-homing endonuclease from *yeast* into *Drosophila*. This endonuclease belongs to a group of enzymes that cleave the phosphodiester bond within a polynucleotide chain. A specific sequence of 18 bp is enough to be recognized and cut by I-SceI. Both enzymes got incorporated

into transgenic flies via P-element-mediated germline transformation and coupled to the control of a heat shock promoter to be available through simple crosses and heat activation. Further simplifications, especially concerning the work load of crossings and fly pushing, were achieved by inserting distinct lethal genes (Huang et al. 2008). Activatable through heat shock (in the genome of the transgenic flies) or the GAL4-UAS system (on the designed construct), these genes help the scientists to kill most, if not all, unwanted offspring carrying the wrong genotypes. Details are explained in the methods paragraph.

So far only the question of generating a suitable environment for a homologous recombination was discussed, but another important factor is a certain sequence homology between the target locus and the construct that is supposed to be exchanged. For that, adjacent parts of the target gene region have to be amplified. Regarding the size, J. Huang (Huang, Zhou, Dong, Watson, et al. 2009) for example used homology regions ranging from 2.8 – 5.3 kb[i].

Another key modification and upgrade by Huang et al. of the original method was to couple the ends-out (replacement) gene targeting with a phage integrase ϕC31-mediated DNA integration. That means first creating a founder knockout line by deleting the target gene and replacing it with an integration site of ϕC31, referred to as *attP-site*. Thereby the integration is irreversible and proceeds between a bacterial (*attB*) and a phage attachment site (*attP*). This leads to stable transformants containing the gene of interest between *attL* and *attR* sites. An integration efficiency of around 1.4% for different loci is described by Huang et al. (Huang, Zhou, Dong, Watson, et al. 2009), but is nowadays part of an affordable offering of *Drosophila* genetic engineering companies like BestGene Inc.

2.8 Aims and outlook

Because of the advantage of easily gaining nearly every desired rescue in the endogenous genomic locus we came up with the idea of generating fly lines carrying an exact defined deletion of the total *per* and *tim* loci by help of an earlier developed and from the Huang lab improved method, the ends-out targeting procedure (Gong and Golic 2003, Huang et al. 2008, Huang, Zhou, Dong, Watson, et al. 2009). We designed the knockout area including also the genetic regions next to the target genes to encompass predicted promoter sites. At the end we succeeded and received new tools not only for more precise projects referred to *per*/*tim* null studies, but also with the possibility to have a closer look on PER/TIM itself, its single structural domains and its expression.

[i] We tried to make a compromise between our knockout locus size that demands a longer homology region and the complications we predicted for working with large sized constructs for PCR and cloning.

A first goal for *per* knockout (*per*^{Out}) is to investigate *per*^{01} and *per*^{Out} to see if the residual piece of PER in *per*^{01} still shows influences on the clock mechanism. We could not manage to do all this work in time, so it is still in progress and we do not show preliminary results in this thesis. This encompasses protein investigations through immunohistochemistry and western blot analyzes and in additional behavioral tests. Additionally, we want to observe TIM levels in *per*^{Out} individuals to unravel remaining influences of the truncated PER^{01} on TIM. Our first preliminary comparisons showed that there are indeed differences between the amorphic allele and the complete knockout fly, which also includes the already observed residual endogenous rhythm of the *per*^{01} flies, as well as the level of the partner protein TIM. Since genome sequencing of the *per*^{Out} flies revealed a small deviation in the knockout flies compared to wild type, we first cloned a rescue construct identical to the original locus, to restore initial circumstances. A next project is to generate a fusion construct of PER and the green fluorescence protein (GFP) to localize PER in living animals.

For TIM the initial plan also comprises a rescue coupled to a fluorescence tag, which is in best case distinguishable from that fused to PER, so that both proteins can be investigated in one experiment. But we first focused our attention on a special site inside TIM close to the *tim*^{UL} mutation site and created GAL4-constructs that should be integrated into the genome through P-element insertion. These constructs then will be activated through the UAS/GAL4 system, with help of a *tim*-GAL4 driver integrated through recombination crosses on the second chromosome.

In a first attempt (temporally viewed) our aim was to repeat the results from Stoleru et al. concerning SGG and its stabilizing effect on CRY under LL conditions (Stoleru et al. 2007). Instead, we revealed a small negligence in their work and propose how the acquisition of their results might have unfortunately been achieved. Although contradicting Stoleru et al. and therefore appearing to be negative, our results are nevertheless interesting and contribute to our understanding of the role of SGG. We therefore provide this information in form of a publication to the community of our field of study (Fischer et al., 2015, submitted).

3 Materials and Methods

3.1 Materials

3.1.1 Fly strains

Flies were raised on a standard cornmeal/agar medium containing 0.8% agar, 2.2% sugar beet molasses, 8.0% malt extract, 1.8% yeast, 1.0% soy flour, 8.0% corn flour and 0.3% hydroxybenzoic acid, at 25°C (constant usage)/18°C (long-term keeping), respectively, in LD 12:12. Humidity was kept between 60 and 65%.

Table 1: Fly lines used in this study.

Fly strain name	Genotype	Description	Donor
PerStart (1-4M-C2)	*w^{1118};P{per}$^{Rpr+}$;+*	Flies containing P-element for homologous recombination	Designed in this study
Bl#25679	*y^1 w*/Dp (2;Y)G, P{hs-hid}Y; P{70FLP}23 P{70I-SceI}4A/TM3, P{hs-hid}14, Sb1*	Flippase under heat shock promoter	Yang Hong (Huang et al. 2008)
Bl#26258	*w*; P{?GawB}477w-; TM2/TM6B, Tb1*	Drives GAL4 expression in a subset of dendritic arborization neurons	Yang Hong (Huang et al. 2008)
Bl#1092	*y^1 w^{67c23}; snaSco/CyO, P{Crew}DH1*	Cre recombinase on second chromosome	Dan Hartl (Siegal and Hartl 2000)
Per^{01}	*per^{01}*	Point mutation – loss of function allele	Konopka, Benzer (Konopka and Benzer 1971)
Per^{Out} w^-	*per^{Out}, w^-*	Deletion of the *per* locus, floxed-out *mini-white* gene.	Designed in this study
Per^{Out} (w^+)	*per^{Out}, w^+*	Deletion of the *per* locus	Designed in this study
Per^{Out} red	*per^{Out}, w^+*	Deletion of the *per* locus. Exclusively males out of a heterozygous strain.	Designed in this study

Fly strain name	Genotype	Description	Donor
Per^{Out} white	*w^{1118}*	Genetically wild type. Exclusively males out of a heterozygous knockout strain.	Designed in this study
w^{1118}	*w^{1118}*	Partial deletion of *white*	BDSC
TimStart (2-3M-C3)	*w^{1118};+; P{tim}$^{Rpr+}$*	Flies containing P-element for homologous recombination	Designed in this study
Tim^{Out}	*w*; tim^{Out}; +*	Deletion of *tim* locus	Designed in this study
Sco/Cyo	*yw; Sco/Cyo*	Balanced on C2. Used for *tim* targeting.	BDSC
$ADAR^{Hypomorph}$	*$adar^{hyp}$*	Bearing a *mini-white* inside the coding regions of *adar*.	Jepson (Jepson et al. 2011)
SGG^{11008}	*P{w[+mC]=EP}sgg[EP1576] w^{1118}*	SGG overexpression	Martinek (Martinek et al. 2001)
SGG^{35364}	*y^1 sc* v^1; P{TRiP.GL00277}attP2*	SGG RNAi	Ni (Ni et al. 2009)
TimGAL4	*w; tim (UAS)-GAL4; +*	GAL4 expression line	Young (Blau and Young 1999)

3.1.2 Primer

All primers were ordered from Sigma-Aldrich® in deprotected and desalinated condition. Oligomers of 20 to 25 nucleotides were used and if necessary restriction sites were directly attached with a four nucleotides overhang at the 3' site.

Table 2: All primers used in this study.

Purposely integrated restriction sites are cited on the right side. Rv = reverse primer, orientated 3' → 5' regarding the sense strand of the DNA, Fw = forward, orientated 5' → 3'.

Primer name	Sequence 5' → 3'	Orientation	Restriction site
PerL antisense	GCGGAAGGGTTCGTAGCT	Rv	
PerL sense	GTTCGACAAGACCTGGGAGG	Fw	
11	AATTGGTACCCAAGCAAACAAGTTAAAGTTG	Rv	*Kpn*I
12	ATAGCGGCCGCATCATTAAAATTTGCGAAAAA	Fw	*Not*I
13	AATTCTCGAGATCGTACACCTGTTTGGGTTT	Rv	*Xho*I
14	GCCGACTAGTAAAGCGATTATGTCTAGAAGC	Fw	*Spe*I
15	ACGTACTAGTAACTGTGCAGGATATACGAATC	Fw	*Spe*I

Primer name	Sequence 5' → 3'	Orientation	Restriction site
16	ATCGCTCGAGGGTCAAGATCTATTGGGAGTT	Rv	*Xho*I
17	CGATGGTACCATACCCTAATCGAAGTTGGTT	Rv	*Kpn*I
31	ATAGCGGCCGCGAAGATTGTATACTCTAGAAG	Fw	*Not*I
80	AACTGAGAGAACTCAAAGGTT	Rv	
81	ACACATATCTTGTGGGGAAAT	Fw	
82	ATGTATGCTATACGAAGTTAT	Fw	
83	AAATATGACTTACCAGGGAT	Rv	
84	CAACCTTGTGCTTGGTCAGA	Fw	
85	TCGGGTATGTAGAATGCCAC	Rv	
109	CATAATCAGTAGAAGGTGTCAA	Fw	
111	TTGACTGGCGGTGACTGGACATT	Rv	
113	CAAGGACGAAGACAAGGAGGAA	Fw	
117	TAGAGTGCCGTTTACTGTGCG	Rv	
120	TCCTGCTCTTTGGCGGCTTCTTCTTGA	Fw	
121	TTGGGTTCGCTTTTGCCACACTTCTGG	Rv	
138	TTCTGATACTCCTGACCCTTGCGGCT	Fw	
151	ATTACTCGAGGTGTGATGCTTTTTCAAATCGAGAG	Fw	*Xho*I
153	ATGGGTAGTAGCCACACCTGCAGGTGCTGC	Fw	*Sbf*I
154	GCAGCACCTGCAGGTGTGGCTACTACCCAT	Rv	*Sbf*I
155	AAGCTGGAGAACCTAGGCACCATGGAGGGC	Fw	*Avr*II
156	GCCCTCCATGGTGCCTAGGTTCTCCAGCTT	Rv	*Avr*II
158	TAACGGTACCACGTGCTTCTAGACATAATCGCTTT	Rv	*Kpn*I
163	TGTCCGTGTATTTCTTGTTGTTGGCG	Rv	
164	ATTCCACTCGGTCACCACTCCT	Fw	

3.1.3 Cloning vectors

3.1.3.1 pGX-attP

This vector (Figure 11) was designed for the ends-out targeting procedure by the Huang lab (Huang et al. 2008). We got it as a kind gift from T. Langenhan (Institute of Physiology – Department of Neurophysiology, University of Würzburg). It contains two multiple cloning sites (MCS) flanking a short (CDS only) form of a *Drosophila* marker gene called *mini-white.* The *mini-white* is under control of a strong hsp70 promoter. Integrated into flies with a white eyed genetic background, the observer is able to verify the existence of the construct by the presence of red eyes. Two *loxP* sites surrounding

the *mini-white* allow an easy way to get rid of the marker gene by a Cre recombinase mediated excision, if necessary.

The 3’ and 5’ P-element insertion sites facilitate the random incorporation of the construct into the genome of a fly. A new jump out can then be done with help of a Flp recombinase, recognizing the *FRT* sites. A special feature of the plasmid is the *reaper* gene that can be used for negative selection of false positive integrations during the ends-out targeting crosses. Section 3.2.12 gives a more precise explanation. During cloning procedures positive clones can be selected by beta-lactamase mediated resistance to ampicillin.

Figure 11: Ends-out targeting vector pGX-*attP*.

This vector contains two multiple cloning sites for the 5’ and 3’ homologous arm, respectively. With help of 5’ and 3’ P-element insertion sites, the construct can be randomly inserted into the genome of the fly. *FRT* and *I-SceI* recombination sites enable a new jump out from the genome to start the homologous recombination between the homologous arms and the right targeting site to exchange the genomic locus with the cloning cassette. The *mini-white* allows screening for recombinants by eye color. *LoxP* sites can be used to flox-out the marker gene in the end of a successful experiment.

3.1.3.2 pGE-attB GMR

This vector (Figure 12) is used to reintegrate any desired rescue construct at the place, where once the target locus was located. We got it as a kind gift from T. Langenhan (Institute of Physiology – Department of Neurophysiology, University of Würzburg). It was also introduced by the Huang lab

(Huang et al. 2008). After the ends-out targeting process and the cut-out of the marker gene, only one *loxP* site and an *attB-site* are left. The remaining *loxP* site in the genome can be used together with the single *loxP* site of the pGE-vector to cut out the marker gene in the end. The *attP-site* in the genome and the *attB-site* in the vector allow the integration of a rescue construct by the phiC31 recombination system. This is a sequence-specific recombinase within the genome of the bacteriophage phiC31. Thereby the phiC31 integrase mediates recombination between two 34 bp sequences termed *att sites*. An *attB* containing donor plasmid can be integrated into the target genome through recombination at an *attP-site*.

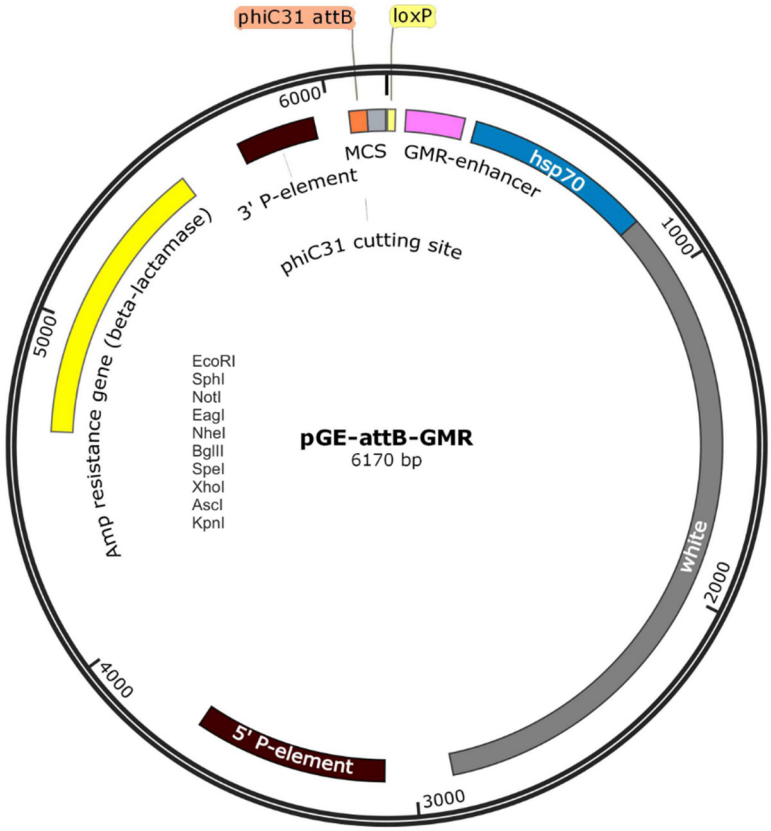

Figure 12: pGE-*attB*-GMR vector for site specific recombination.

The pGE vector can be used to reintegrate any desired construct at the location, where the *attP-site* was integrated into the genome via ends-out targeting. The system is based on the site-specific recombinase technology with the phiC31 integrase.

3.1.3.3 pJet1.2

The pJet1.2 (Figure 13) cloning system from Thermo Scientific (3.1.5) just served as transitory vector for easy storing and amplification of bigger constructs. The advantage of this vector is the blunt end cloning site that can be used to directly integrate the PCR products into the vector without the additional step of a restriction digest.

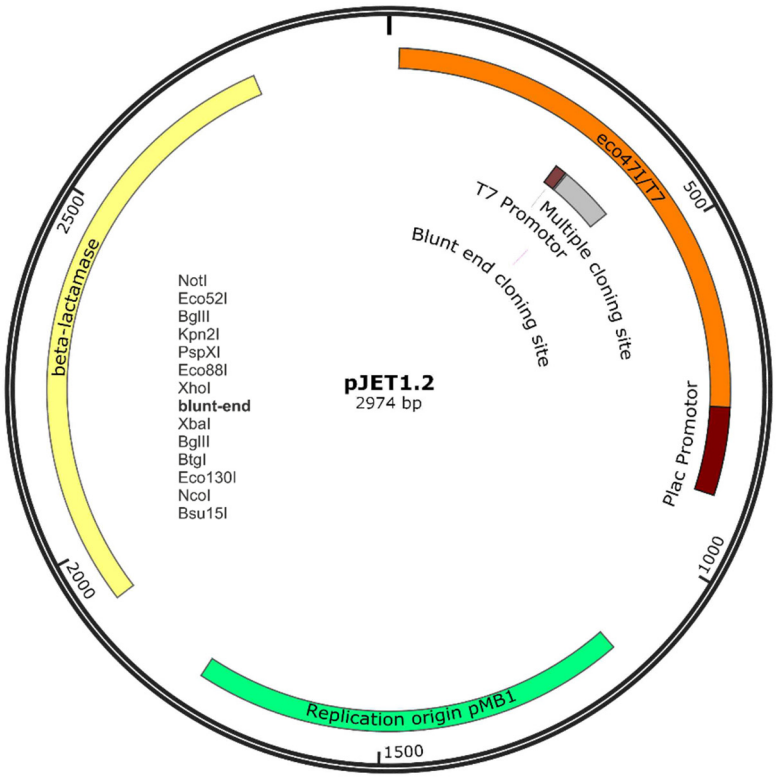

Figure 13: pJet1.2 cloning vector.

The pJet vector is a small assistance vector and was primarily used to amplify and safely store certain PCR products. It was taken from the CloneJet PCR cloning kit (Thermo Scientific), due to the advantage of an integration possibility via blunt end cloning. Restriction sites of the *MCS* are indicated inside the vector.

3.1.3.4 pUAST

The pUAST vector (Figure 14) was introduced by Brand and Perrimon in 1993 (Brand and Perrimon 1993). It contains five tandemly arranged optimized GAL4 binding sites followed by the hsp70 TATA box and transcriptional start. A target open reading frame (ORF) cloned downstream of these sites can be controlled by a special GAL4 driver. The whole construct can be incorporated into the genome by P-element insertion.

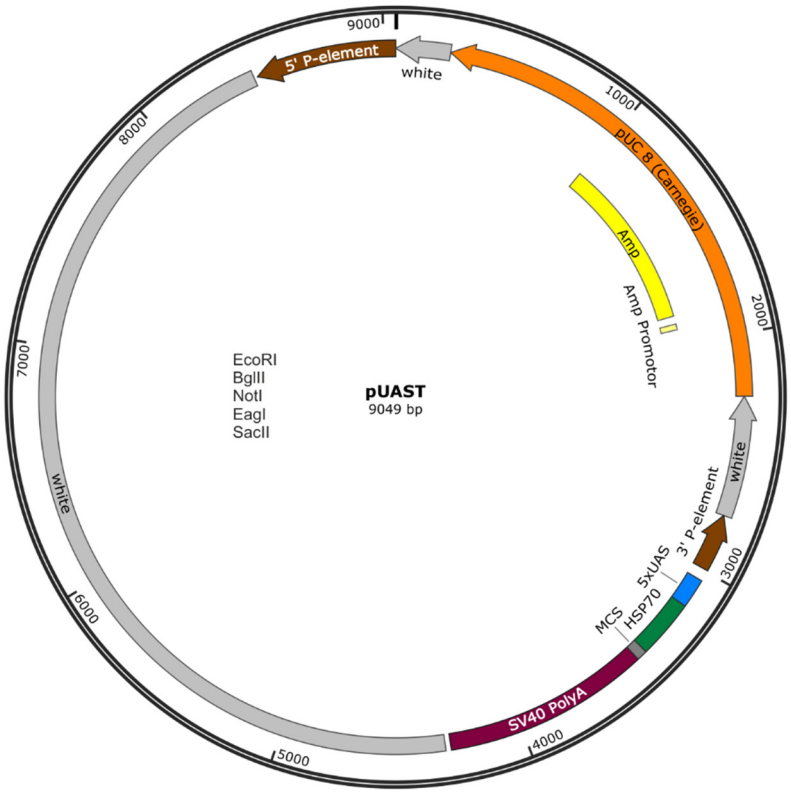

Figure 14: pUAST vector for random integration into the fly genome.

Along with the P-element insertion sites for integration, this vector also contains a strong UAS-promoter. Downstream of the promoter the *MCS* can be used to clone the desired ORF into the vector. Afterwards it is integrated into the fly and can be activated using the GAL4-UAS system.

3.1.3.5 pAc5.1/V5-His A

For cell culture expression experiments we used the pAc5.1/V5-His A vector (Figure 15), purchased from Life Technologies GmbH. This is a high copy plasmid that can be used for transfection and constitutive expression of recombinant proteins. Its promoter originates from the *Drosophila* actin 5C gene and allows a strong expression rate. It contains a C-terminal V5 and a 6xHis tag for simple purification and protein staining.

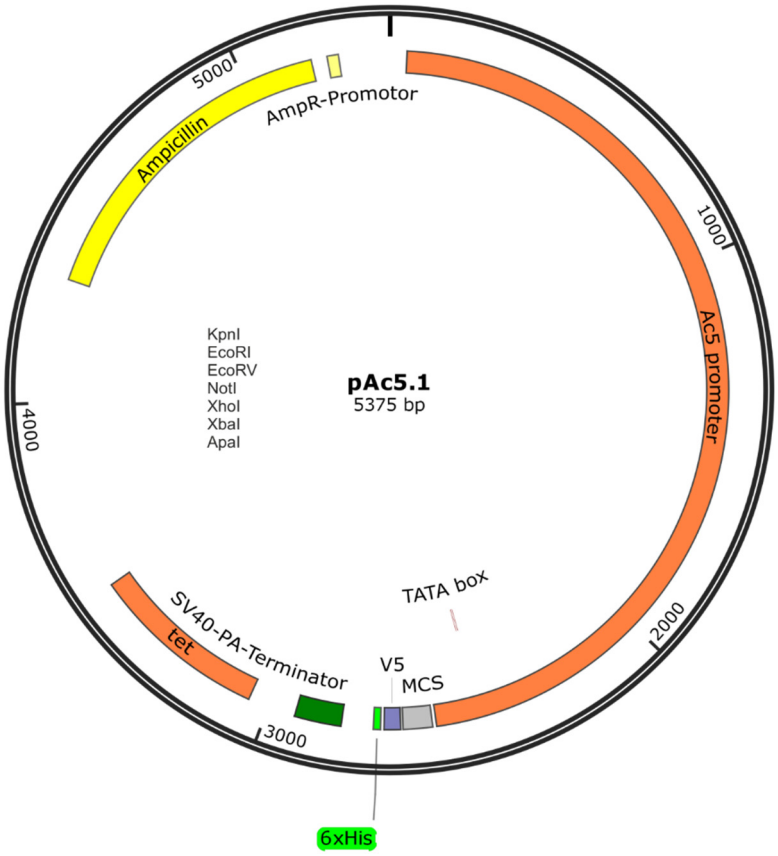

Figure 15: pAc5.1/V5-His A vector.

This vector was used for transfection and expression in *S2* cell culture. Two different types of tags can be added to the protein by deleting the stop-codon.

3.1.4 Antibodies

3.1.4.1 Primary antibodies

Working solutions of primary antibodies for western blotting were diluted in 1x TBST, 5% milk powder, 0.02% NaN_3 and stored at +4°C. Antibody stocks were kept 1:1 in glycerol or in the manufacturer's solution at -20°C.

Table 3: List of all primary antibodies.

Antibody	Immunogen	Donor animal	Dilution	Reference
Anti-PER IgG (d-300)	epitope corresponding to AA 925-1224 mapping at the C-terminus of PER of *Drosophila melanogaster* origin	Rabbit, poly	1:100	Sc-33742, Santa Cruz, USA
Anti-PER	Baculovirus expressed full length Drosophila PER protein	Rabbit, poly	1:1000	Stanewsky (Stanewsky, Frisch, et al. 1997)
Anti-TIM	Polyhistidine fused TIM fragment expressed in *E. coli* (AA 222–577)	Rat, poly	1:1000	Edery (Sidote et al. 1998)

3.1.4.2 Secondary antibodies

Working solutions of secondary antibodies for western blotting were diluted in 1x TBST, 5% milk powder, 0.02% NaN_3 and stored at +4°C. Antibody stocks were kept in the manufacturer's solution at -20°C.

Table 4: List of all secondary antibodies.

Antibody	Immunogen	Donor animal	Dilution	Manufacturer
Goat anti-Rabbit IgG	Rabbit	Goat, poly	1:7500	Alexa Fluor® 680, Life Technologies
Goat anti-Rat IgG	Rat	Goat, poly	1:7500	Alexa Fluor® 680, Life Technologies

3.1.5 Kits

Table 5: All kits from external manufacturers regularly used in this study.

Concern	Name	Manufacturer
Cloning Vector	CloneJET PCR Cloning Kit (K1231)	Thermo Scientific
DNA Ladder	GeneRuler 1kb DNA Ladder (SM0311)	Thermo Scientific
dNTP	dNTP Set, 100mM Solutions (R0181)	Thermo Scientific
Electrocompetent cells	One Shot® TOP10 Electrocomp™ *E. coli*, (C4040-50)	Invitrogen
gDNA cleanup	NucleoSpin® gDNA Clean-up (740230.50)	Macherey-Nagel
Gel purification	GenElute™ Gel Extraction Kit (NA1111)	Sigma-Aldrich
Midi prep	GenElute™ HP Plasmid Midiprep Kit (NA0200)	Sigma-Aldrich
PCR purification	GeneJet PCR Purification Kit (K0701)	Thermo Scientific
Protein Ladder	PageRuler Prestained Protein Ladder (26616)	Thermo Scientific
qPCR	SensiFAST™ SYBR® No-ROX Kit (BIO-98002)	Bioline
RNA prep	Quick-RNA™ MicroPrep (R1050)	Zymo Research
RT PCR	QuantiTect Reverse Transcription Kit (205310)	Qiagen

3.1.6 Buffers, solutions and media

3.1.6.1 Tris-acetate (TAE, 50x, 1 l)

Tris	242 g
Na_2EDTA (pH 8.0)	100 ml
Glacial acid	57.1 ml
H_2O	Adjust to 1 l

3.1.6.2 Protein extraction buffer (PEP)

HEPES 1 M pH 7.5	5 µl
KCl 3 M	8.3 ml
Glycerol 50%	25 ml
EDTA 0.5 M	5 ml
Triton X-100 10%	2.5 ml
β-Glycerophosphate 1 M	5 ml
Na_3VO_4 10 mM pH 10-12	2.5 ml
H_2O	Adjust to 250 ml

3.1.6.3 DGLP (5x, 10 ml)

Tris	0.375 g
SDS	1 g
Glycerol	5 ml
β-Mercaptoethanol	2.5 ml
Bromophenol blue	0.01 g
H_2O	Adjust to 10 ml

3.1.6.4 Semi-dry blotting buffer (SDBB, 1x, 1 l)

Tris	5.82 g
Glycine	2.93 g
Methanol	200 ml
SDS 10%	3.75 ml
H_2O	Adjust to 1 l

3.1.6.5 Transfer buffer (1 l)

Tris	3 g
Glycin	15 g
SDS 20%	10 ml
Methanol	200 ml
H_2O	Adjust to 1 l

3.1.6.6 TBS(T) (1x, 1 l)

Tris 50 mM	6.05 g
NaCl 150 mM	8.76 g
H_2O	Adjust to 1 l

Adjust pH to 7.5 with HCl.

(0.5 ml Tween-20 in 1 l 1x TBS)

3.1.6.7 Elpho buffer (5x, 2 l)

Tris	30 g
Glycine	144 g
SDS 10%	100 ml
H_2O	Adjust to 2 l

3.1.6.8 Buffer A

Tris HCl 1 M pH 7.5	40 µl
EDTA 500 mM pH 8.0	80 µl
NaCl 4 M	10 µl
SDS 10%	20 µl
H_2O	250 µl

3.1.6.9 Squishing Buffer

Tris HCl 1 M pH 8.0	100 µl
EDTA 0.5 M pH 8.0	20 µl
NaCl 4 M	62.5 µl
H_2O	Adjust to 10 ml

3.1.6.10 LB-Medium/-plates

Bacto-Tryptone	10 g
Bacto-Yeast	5 g
NaCl	10 g
H_2O	Adjust to 1 l

Adjust pH to 7.0 with 10 M NaOH, sterilize by autoclaving and store at room temperature.

For LB_{Amp} add appropriate amount of the ampicillin stock solution (100 mg/ml) to a final working concentration of 80 µg/ml and store at 4°C.

For Agar plates prepare liquid LB-media and add 15 g Bacto-Agar to 1 l of medium and sterilize by autoclaving. Allow cooling down to 50°C and add appropriate amount of antibiotic and immediately pour into sterile plates. Allow to solidify and store at 4°C in inverted position.

3.1.6.11 STET buffer (250 ml)

Na_2EDTA, pH 8.0	0.093 g
NaCl	1.46 g
Tris	0.3 g
Triton X-100	12.5 ml
H_2O	Adjust to 250 ml

3.1.6.12 Ammonium acetate (500 ml)

$NH_4C_2H_3O_2$	385.4 g
H_2O	Adjust to 500 ml

3.1.7 Enzymes

Table 6: All kinds of enzymes used in this study.

Type	**Enzyme**	**Manufacturer**
DNA Ligase	T4 DNA Ligase 1000 units (EL0011)	Thermo Scientific
DNA Ligase	T4 DNA Ligase, 20.000 units (M0202 S)	New England Biolabs
DNA Polymerase	Phusion High-Fidelity DNA Polymerase (F-530L)	Thermo Scientific
DNA Polymerase	JumpStart™ REDTaq® ReadyMix™ Reaction Mix (P0982)	Sigma-Aldrich
Lysozyme	Lysozyme Biochemica (A3711)	Applichem
Phosphatase	FastAP Thermosensitive Alkaline Phosphatase (EF0654)	Thermo Scientific
Restriction Enzyme	FastDigest *Avr*II (*Xma*JI) (FD1564)	Thermo Scientific
Restriction Enzyme	FastDigest *Xho*I (FD0694)	Thermo Scientific
Restriction Enzyme	FastDigest *Not*I (FD0593)	Thermo Scientific
Restriction Enzyme	FastDigest *Kpn*I (FD0524)	Thermo Scientific
Restriction Enzyme	FastDigest *Spe*I (*Bcu*I) (FD1253)	Thermo Scientific
Restriction Enzyme	FastDigest *Sbf*I (*Sda*I) (FD1194)	Thermo Scientific
Restriction Enzyme	FastDigest *Xba*I (FD0684)	Thermo Scientific
Restriction Enzyme	*Hind*III (R0104S)	New England BioLabs

3.1.8 Chemicals and materials

Table 7: Important chemicals used in this study.

Chemical	Manufacturer
2-Propanol	Sigma-Aldrich (59300)
Agarose	peqGOLD Universal-Agarose, Peqlab (35-1020)
Ammonium persulfate (APS, 10%)	Applichem (A2941)
Ampicillin	Ampicillin sodium salt, Roth (K029), 100 mg/ml in H_20
Blocking buffer (western blot)	Odyssey® Blocking Buffer (TBS), Li-cor (927-50000)
Blotting membrane, 0,45 µm, 85 µg/cm²	Nitrocellulose membrane, Whatman (Protran BA85)
DNA dye	Midori Green Advance, Nippon Genetics (MG04)
Electroporation cuvettes	2 mm gap size, 40-400 µl volume, VWR (732-1136)
Ethanol	Absolut, Sigma-Aldrich (24102)
Filter paper	Blotting paper 3 mm, Whatman (GB3M)
H_2O	Water Molecular Biology Reagent, Sigma (W4502)
Methanol	Applichem (A0688)
Milk powder	Roth (T145)
dNTP	dNTP Mix, 10mM each, Thermo Scientific (R0192)
Polyacrylamide gels	Rotiphorese® Gel 30 (37,5:1), Roth (3029)
Protease inhibitor cocktail	c0mplete, Mini, EDTA free, Roche (11697498001)
Sodium azide (NaN_3)	0.02% in 1x PBS from 2% stock, Sigma-Aldrich
Sodium dodecyl sulfate (SDS 10%)	Applichem (A0676)
Tetramethylethylenediamine (TEMED)	Roth (2367)
Tween-20	Applichem, Biochemica (A1389)

3.1.9 Software and data

3.1.9.1 Programs

Nucleotide sequence specific planning of cloning experiments, digestions and PCR reactions were done with ApE – A plasmid editor v2.0.47.

Figures of vectors and gene regions were designed using SnapGene viewer 2.6.2.

Pictures of agarose gels were obtained with an E-Box version 15.05 (Vilber Lourmat) and processed and evaluated with E-Capt version 15.06 for windows.

For depiction of certain images and evaluation of behavioral data, ImageJ 1.48v with the plugin ActogramJ was used.

For primer design we used Oligo Analyze 1.0.2 and ApE (described above), as well as online tools (3.1.9.2).

Western blot images were obtained and adjusted with Image Studio Lite software version 4.3 (Li-cor).

Quantitative PCRs were done with a Rotor Gene-Q cycler (5-Plex, Qiagen) and evaluated with the Rotor Gene-Q series software version 2.1.0.

3.1.9.2 Online sources

Sequence files from genes and vectors were based on http://flybase.org or http://www.ncbi.nlm.nih.gov. Also blasts were done with these online tools.

For determining primer annealing temperatures specific for PCR reactions in buffers from Thermo Scientific, we used the online tool from the manufacturer: http://www.thermoscientificbio.com/webtools/tmc/

Prediction for putative phosphorylation sites, an online tool named NetPhosK 1.0 server was used: http://www.cbsdtu.dk/services/NetPhosK/

3.2 Methods

3.2.1 GAL4-UAS System

One of the most common methods used in genetic studies on *Drosophila melanogaster*, is the GAL4-UAS system, first described by Brand and Perrimon in 1993 (Brand and Perrimon 1993). This system allows the expression of a certain genetic construct under spatial and temporal control and regulation *in vivo*. The basic principle thereby consists of two distinct transgenic fly lines, the GAL4 (driver) line and the UAS (responder) line. In the driver line, a yeast transcriptional activator sequence called GAL4 is cloned downstream of a particular promoter region of interest. This can be an endogenous promoter for spatial and temporal restricted expression or a very strong transgenic ubiquitous promoter e.g. originally from the gene *actin*. The responder line then contains the upstream-activating-sequence (UAS), which is the target sequence of the transcriptional activator. Inserted upstream of a requested ORF, this can be overexpressed or subjected to the regulation of the promoter region controlling the GAL4. Crossing both fly lines in the right way results in an offspring containing both genetic constructs and with that the defined expression of the ORF.

3.2.2 Fly entrainment

Entrainment of the flies means equalizing the circadian clocks of the animals by synchronizing them with an external time cue cycle and harvest at a definite time point within this regime. Thereby the external time cue, that is used by the animals to orientate in the given time cycle, is called Zeitgeber. For example, this can be light or temperature as the most common Zeitgeber. A new cycle starts at ZT0 and is normally set to 24 h, the naturally given duration of a day-night cycle on earth. Thus, for a LD cycle ZT0 means lights-on. If there is no external Zeitgeber, the activity of the animals is only defined through their internal clock. Scientists now talk of circadian time (CT) 0 as the time point of the restart of the subjective, individual cycle.

We entrained the flies by putting about forty males into a new glass vial with standard food and subsequently placed it into light tight boxes equipped with white light LEDs (Lumitronix, LED-Technik, Hechingen, Germany), which were set to an intensity of 100 lux. The LEDs thereby simulated a LD regime of 12 h light and 12 h darkness. To ensure that there was no light perceptible also during harvesting of the flies by putting them into liquid nitrogen, these boxes were placed in a special temperature-controlled red light chamber. Entrainment was done for at least 3 days.

3.2.3 Behavioral analyzes

Locomotor activity of individual flies was recorded using the Drosophila Activity Monitoring (DAM) System (Trikinetics, Waltham MA, USA) as previously described (Hermann et al. 2012). CO_2-anaesthetized male flies were isolated in small glass tubes, filled to one third with food (2% agar, 4% sucrose) and closed on the other end with an air permeable plug. Filled tubes were then placed in an activity monitor with an infrared light beam crossing the tube at its approximate middle. The number of light beam disruptions by an active fly was then registered by the DAMSystem Collection Software in 1-minute bins for each fly and the raw data were read out as text files. Seven Days in LD 12:12 were followed by ten days in constant darkness. Light was supplied by an LED-lamp at an intensity < 1000 lux. Recordings were done at 25°C in controlled climate chambers (Sanyo, Japan). Text files with raw data were displayed as double-plotted actograms using ActogramJ, a Java plugin of the program ImageJ (Schmid, Helfrich-Förster, and Yoshii 2011) (3.1.9.1). Data of the first day was always discarded to exclude untypical adaptive behavior of the animals to the new environment. Average activity rhythms for each genotype were calculated by taking the activity bins of each minute of every single fly and averaging them over the last seven days of the LD-condition. Data of all single flies were again averaged and finally the curves of the activity profile and the standard error of the mean (SEM) were smoothed by a moving average of eleven values. For determining the individual free-running period (τ) of

rhythmic flies, DD data from day 2–12 were analyzed using χ2-periodogram analysis and average period length of each genotype was calculated. Finally, data were averaged across the genotype. For defining the free-running period and rhythmicity, we analyzed LL data from day 2-12 in the same way.

3.2.4 Genomic DNA (gDNA) prep

Approximately ten male flies were collected and anaesthetized in a small 1.5 ml tube on ice. Afterwards they were grinded with a disposable tissue grinder in 200 µl of Buffer A. Another 200 µl Buffer A were added and grinding was continued until only cuticle parts remained. In the next step the solution was incubated at 65°C for 30 min on a heating block. Afterwards 230 µl 5 M potassium acetate and 570 µl 6 M lithium chloride solution were added, the mixture inverted and incubated on ice for at least 10 min. Subsequently the tubes were centrifuged at room temperature with 12,000 rpm. 1 ml of the supernatant was transferred into a new tube, avoiding floating crud. If this didn't succeed successfully, the step was repeated. To precipitate the DNA, 600 µl of isopropanol were added and the solution was spun for 20 min at room temperature with 12,000 rpm. The supernatant was removed; the remaining pellet washed with 1 ml of 70% ethanol, further centrifuged for 5 min with 12,000 rpm and dried on air. Finally, the pellet was resuspended in 50 µl H_2O and incubated over night at room temperature to dissolve the pellet. DNA content was measured with a NanoDrop 2000/2000c Spectrophotometer. Short-term storage was done at 4°C. For longer time we stored nucleic acids at -20°C.

In certain cases, e.g. for difficult PCR reactions, the gDNA solution was additionally purified using a gDNA preparation kit (3.1.5). Thereby we followed the manufacturers' instructions.

3.2.4.1 Single fly gDNA prep

Flies were ground in 50 µl SB-Buffer mixed with 0.4% Proteinase K. Afterwards the solution was incubated at 37°C for 30 minutes and furthermore 3 minutes at 95°C to inactivate Proteinase K. The mash was spun down at top speed for 10 minutes and the supernatant was transferred into a new tube. DNA was stored at -20°C.

3.2.5 cDNA synthesis

After entrainment we took 5 flies for RNA extraction and followed the manufacturer instructions (RNA prep, 3.1.5). The isolated RNA was then translated to cDNA using a reverse transcriptase from Qiagen (RT PCR, 3.1.5, see manufacturer instructions).

3.2.6 PCR

3.2.6.1 PCR recipe for high accuracy

For PCR amplification with a preferably high accuracy, the Phusion high fidelity DNA polymerase from Thermo Scientic with proofreading function was used. Normally reactions were done in a PCR mastercycler gradient (Eppendorf). We adapted the recipe under submission of the manufacturer's manual for difficult genomic templates as followed:

Table 8: Recipe for Phusion polymerase PCRs

Ingredient	**Amount**
5x Phusion HF Buffer	10 µl
dNTP	1 µl
Primer forward	1.25 µl
Primer backward	1.25 µl
DMSO	1.5 µl
$MgCl_2$	0.5 µl
DNA template	2 µl (~100 ng/µl)
H_2O	32 µl
Phusion Polymerase	0.5 µl
Total	50 µl

Table 9: Program for Phusion polymerase PCRs

Temperature [°C]	**Time [s]**	**Cycles**
98	30	1
98	15	35
~ lower melting temperature of both primers minus 5°C	30	
72	30/kb	
72	300	1
4	∞	1

3.2.6.2 PCR recipe for standard PCR

Simple proof PCRs were done with Taq DNA polymerase without proofreading from Sigma-Aldrich (RedTaq, 3.1.7). We followed the proposed recipe from the manufacturer:

Table 10: Recipe for Tag polymerase PCRs

Ingredient	Amount
JumpStart REDTaq ReadyMix	12.5 µl
Primer forward	1 µl
Primer reverse	1 µl
DNA template[j]	1 µl
H_2O	9.5 µl
Total	25 µl

Table 11: Program for Tag polymerase PCRs

Temperature [°C]	Time [s]	Cycles
94	120	1
94	30	35
~ lower melting temperature of both primers minus 5°C	30	
72	60/kb	
72	300	1
4	∞	1

We also followed the instructions for the setup of the program. For simple PCRs we normally used a PCR-cycler from Peqlab.

3.2.7 Gel electrophoresis

As a standard procedure, we worked with 1% agarose gels in 1xTAE buffer, added a DNA dye (5 µl/100 ml, Table 7) directly into the gels before polymerization and used a commercial DNA loading dye and ladder for fractionation and sizing. The electrophoresis was performed at 140 V for 45 min in an appropriate chamber from Peqlab and 1xTAE buffer (3.1.6.1).

3.2.8 Sequencing

Sequencing was done by the company LGC as Ready2/Flexi Run (Berlin, Germany) or Macrogen (Amsterdam, Netherlands) and subsequently analyzed using ApE software (3.1.9.1).

3.2.9 Cloning

Standardized cloning procedures just for amplifying a certain nucleotide sequence for restriction digest, cloning or sequencing was done with help of the pJet1.2 cloning kit (3.1.5, 0). We followed the instructions of the manufacturer, whereby we normally stick to an insert to vector ratio of 3: 1. Because the pJet1.2 cloning procedure is based on blunt end cloning, we did the previous PCRs with the Phusion polymerase (3.2.6.1).

Cloning was done using electro- or chemo-competent *E.coli* stored at -80°C from unknown origin and followed either the protocol for electroporation or transformation by heat shock. For more difficult

[j] Concentration was not determined for Taq polymerase amplification, but should also be around 100 ng/µl.

transformations (vectors from 12-20 kb) commercial One Shot® TOP10 Electrocomp™ *E. coli* (Invitrogen) were used.

Successfully transformed clones were selected using LB-agar plates containing ampicillin (3.1.6.10).

3.2.9.1 Restriction digest

Restriction digests were performed with fast digest enzymes and buffers from Thermo Scientific (3.1.7). Reaction mixtures were set up following the instructions of the producer. We digested 1 µg of DNA in a 20 µl reaction volume with 1 unit of enzyme and incubated the digestion mixture at 37°C for one hour/µg DNA on a heating block. For bigger amounts of DNA we scaled up the whole reaction mixture.

In case of a direct further processing with the digested DNA without any case of purification by gel or kit, we did an appropriate inactivation of the enzyme.

3.2.9.2 Ligation

We used insert to vector ratios ranging from 3:1 – 7:1. Ligation was done with a T4 DNA Ligase (3.1.7) at room temperature for one hour if not differently described by the manufacturer. Some cloning procedures linking large constructs were ligated at 16°C overnight in a PCR cycler.

3.2.9.3 Transformation via heat shock

Cells were thawed on ice for 10 min, mixed with 10 µl of DNA solution and incubated for 20 min again on ice. Afterwards, the transformation was done by putting the cells to 42°C for 1 min on a heating block or water bath. Immediately after heat shock, the cells get covered with 500 µl LB_0 (3.1.6.10) medium and incubated for 90 min at 37°C under constant shaking.

3.2.9.4 Transformation via electroporation

Previous to the electroporation, the samples were purified either by gel electrophoresis and gel purification or PCR purification (3.1.5). Then 5 µl template were mixed with 25 µl cell suspension (3.1.5), or 50 µl for self-made competent cells), incubated for one minute and transferred into a new precooled electroporation cuvette (3.1.8). The electroshock was applied with an Electroporator 2510 (Eppendorf), with voltage set to 2500 V and the time constant to 5 ms. Immediately after the shock, the cells were covered with 500 µl SOC (3.1.5) medium and transferred into a new tube. Incubation at 37°C for 90 min under constant shacking followed.

3.2.10 Plasmid preparation

Cultures for plasmid preparations were placed in an incubator at 37°C under constant shaking for 16 h. Cloning success was checked by an appropriate restriction digest or colony PCR and gel electrophoresis.

3.2.10.1 Mini preparation

Small bacterial cultures (2 ml) were placed in glass test tubes. After incubation the culture was transferred into a 1.5 ml plastic reaction vessel and pelletized in a centrifuge with 4500 rpm for 5 min. The supernatant was discarded and the pellet was again dissolved under rough vortexing in 250 µl STET buffer (3.1.6.11) and 20 µl lysozyme (3.1.7, 20 mg/ml). Afterwards the solution was boiled for 2 min on 95°C and subsequently cooled down on ice. Another centrifugation step for 10 min at full speed collected all cell crud at the bottom of the reaction vessel. Leaving the crud in the vessel, the supernatant got transferred into a new tube that was previously filled with 250 µl of a mixture between 2-propanol and 10 M ammonium acetate in the ratio 2:1. The solution was again spun at full speed for 10 min, the supernatant discarded, the pellet washed with 500 µl 70% ethanol and again centrifuged at top speed for 5 min. After removing the ethanol with a pipet the pellet was air dried and resuspended in 20 µl H_2O.

3.2.10.2 Midi preparation

For a bigger amount of plasmid DNA, highly purified for following experiments we made cell cultures of 50 ml. For purification we used a kit from Sigma-Aldrich (3.1.5) and stuck to the instructions of the manufacturer.

3.2.11 Western blot

Flies were harvested by freezing in liquid nitrogen. In case of temporally entrained flies, this was done under red light. The heads were separated from the bodies by rough vortexing for a few seconds. On a metal plate placed on dry ice, 20 heads were collected and subsequently doused with 60 µl protein extraction buffer (PEP, 3.1.6.2) and 10 µl 7 x Protease inhibitor cocktail (3.1.8). The tissue was ground with a suitable tissue grinder and spun down at 4°C and 14,000 rpm for 10 min. The supernatant was transferred into a new tube without including any floating crud. 15 µl of 5 x DGLP (3.1.6.3) were added and the total mixture was incubated at 95°C for 5 min before loading onto the gel.

For electrophoresis we used 6-15% polyacrylamide stacking gels depending on protein size and 5% loading gels following the recipe from the manufacturer of the ready to use solution Gel 30 (3.1.8).

Devices for polymerization and running of the gel were from Peqlab (PerfectBlue™ Dual Gel System Twin). We applied 160 V and started separation for around 3 h.

For proteins < 100 kDa, we usually performed semi-dry blotting in an adequate setup (PerfectBlue™ 'Semi-Dry'-Elektroblotter, Peqlab). Concerning larger proteins, we also worked with the wet-blot procedure (TE62 Standard Transfer Tank with Cooling Chamber, Hoefer), but always used the same nitrocellulose blotting membrane (3.1.8), which was embedded between two layers of 3 filter paper (3.1.8), adjacent to the polyacrylamide gel on the side facing the negative pole. For semi-dry blotting, we used SDBB (3.1.6.4), for wet-blot we used transfer buffer (3.1.6.5), respectively. A current of 400 mA (2.67 mA/cm²) was applied for 1 h (1 A and 2 h for wet-blot). We normally used gels sized 10 to 15 cm (150 cm²).

Blocking was done for 2 h at room temperature under constant shaking in blocking buffer (3.1.8) 1:1 diluted in TBST (3.1.6.6).

Primary antibody binding was allowed over night at 4°C under constant shaking.

Secondary antibodies were incubated for 2 h at room temperature. Washing steps between and after the antibody staining were performed with 1x TBST. One short rinse was thereby followed by three washing steps for 5 min each under constant shaking.

Membrane scans and analyzes were done with an Odyssey® Classic infrared imaging system (Li-cor biosystems, Bad Homburg, Germany).

3.2.12 Ends-out targeting procedure

For the ends-out targeting of the genomic locus of *per* and *tim* including predicted up- and downstream regulatory sites, two homologous arms (3-5 kb in size) complementary to the genomic sequence were created by amplification from gDNA (3.2.4) via PCR (3.2.6.1). For gDNA extraction we used flies from strain w^{1118} (3.1.1). These homologous arms were subsequently cloned into the multiple cloning sites of the targeting vector pGX-*attP* (Figure 11, 3.1.3.1). Thereby we used adequate restriction sites directly coupled to the primers with an overhang of four nucleotides. The purpose of these homologous regions is to allow a double homologous recombination between the genomic site next to the target gene and the amplified parts flanking the marker gene on the designed construct (Figure 16).

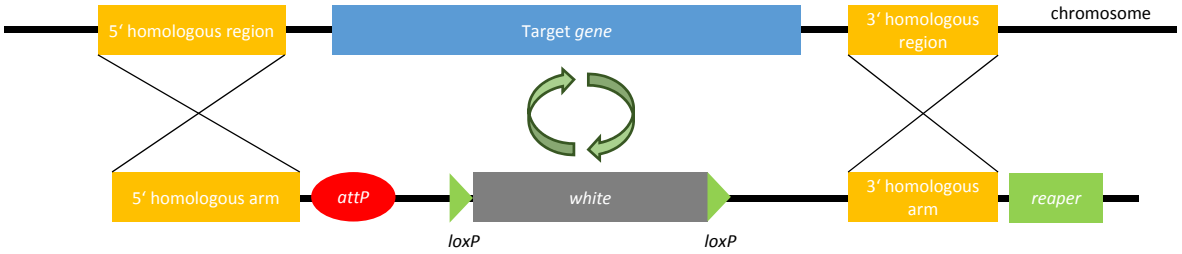

Figure 16: Simplified schematic depiction of the recombination process.

With the recombination, mediated by the homologous regions up- and downstream of the target gene, the genomic area in between should be exchanged with the vector cassette.

This construct was then injected into fly embryos of w1118 flies (3.1.1) by BestGene Inc. (CA, USA [Service type: Plan C; Qty: 1]) and mapped to the chromosome through balancer crossings. Flies carrying insertions on different chromosomes were sent back from BestGene Inc. and screened for homozygous genotypes. Afterwards they were tested by crossings to the later used driver strains. Subsequently, the F1 generation was counted, the values evaluated and a starting strain for the targeting procedure determined. All in all, the ends-out procedure consists of a series of three major crosses. In the first cross, called targeting cross, a high number of virgin flies from the starting strain (carrying the integrated construct) were crossed (proportion of 1:1) to a strain (BL#25679, Table 1) containing a gene for a flippase (Flp-/FRT-system) under a heat shock promoter to start the targeting process (Huang et al. 2008, Huang, Zhou, Dong, Watson, et al. 2009) (for a more detailed overview of all numbers of the single ends-out targeting processes see Table 27/Table 29). The Flp recombinase thereby recognizes and binds to the *FRT* sequences surrounding the construct (3.1.3.1) and catalyzes the recombination between them. In consequence the construct gets freed from the chromosome and is able to get in spatial proximity to the targeting locus, an inevitable requirement for the double homologous recombination.

On day three and four after the first contact of both genders and subsequent to flipping the parent flies to new vials (also on day three), the larvae were suspended to a one hour heat shock at 37°C in a water bath. We pressed down the plugs close to the level of food to prevent larvae from crawling up the glass walls and thus to ensure a maximum exposure of the animals to the warmed-up temperature. Due to *hid* (head involution defective (Grether et al. 1995)) genes on the Y- and third chromosome, which are also controlled by a heat shock promoter, the whole offspring has the same genotype and is exclusively of female gender with a red-white patchy eye color (Figure 17).

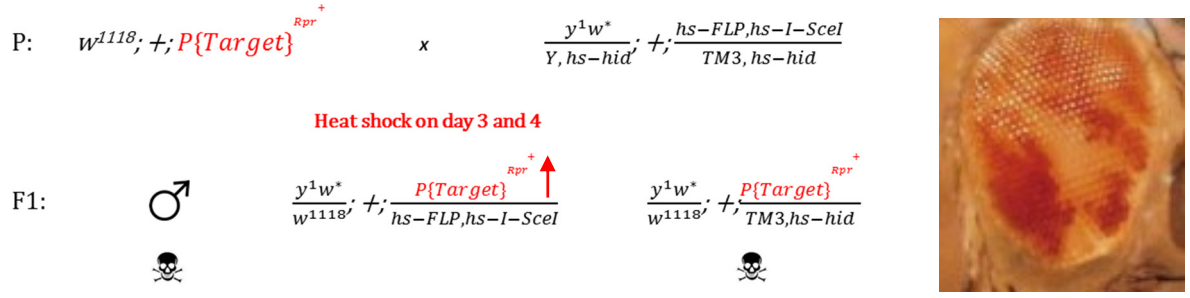

Figure 17: Genetic background of the targeting cross.

Left: Virgin flies of the starting strain *(P{Target}$^{Rpr+}$* = targeting construct including the *reaper* gene) are crossed with males bearing several *hid-* and the *Flp recombinase* genes under control of heat shock promoters. By activation of this promoter, only one genotype reaches adulthood. Additionally, the target construct gets excised from the genome allowing the homologous recombination on the desired locus (indicated as a red upwards directed arrow). Starting on chromosome 3, as it is shown here, serves as an overview and is not true for the single targeting procedures. Red letters indicate that this construct also leads to a red eye color. Right: red-white patched eye color, as it can be seen in the offspring of the targeting cross.

All vials were checked for males one or two times a day. If no male offspring was observable, all female flies were used for the next step, the screening cross. Occasionally (also depending on the age of the vials and with that the crosses), some unhealthy, small looking male flies hatched, too. Thus, it was necessary to check the offspring as often as possible to be able to use a high amount of female flies from this cross. Otherwise we just used the virgin females. In the ratio of 2:1, these females were crossed with males bearing an ubiquitous GAL4 driver (BL#26258, 3.1.1) to negatively screen for false positive integrations (Figure 18).

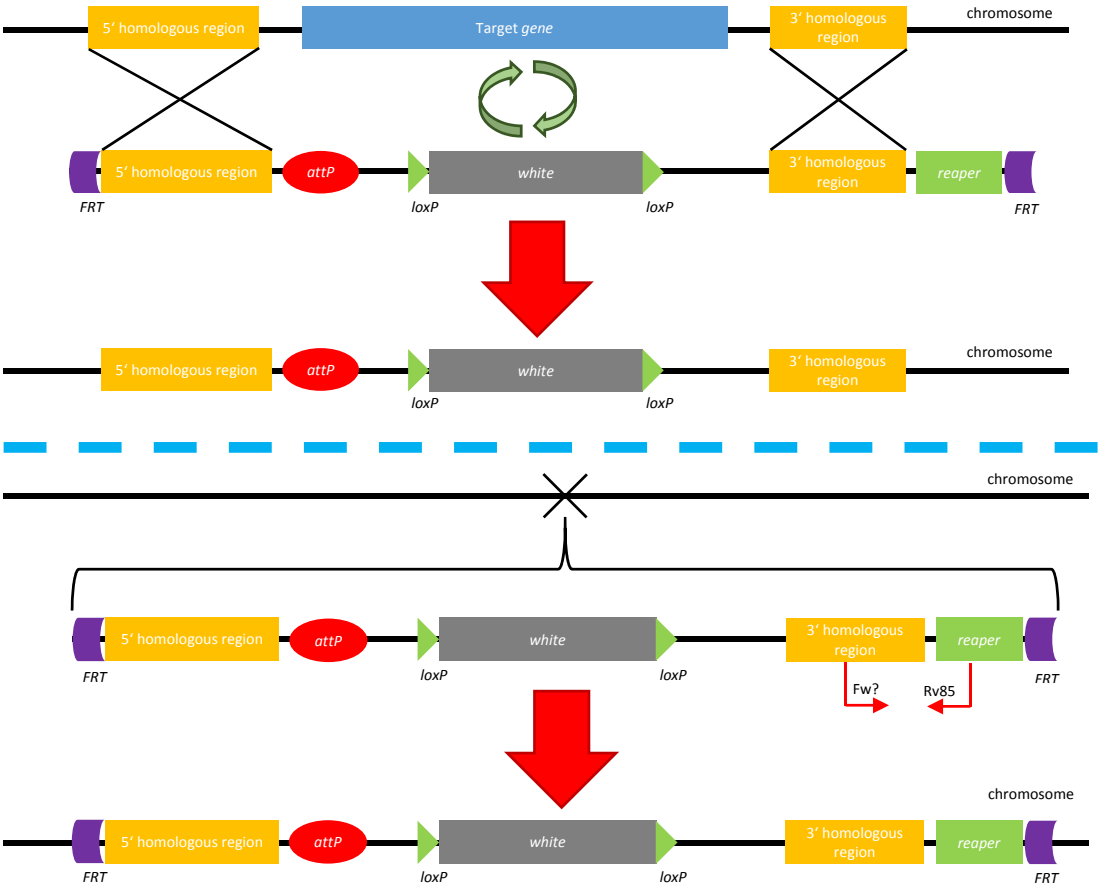

Figure 18: Integration possibilities of the linearized construct.

On top: In case of a double homologous recombination at the right locus, only the part between the homologous arms of the construct exchanges with the target region (in graphs indicated as *P{Target}*$^{rpr-}$). Below: If the integration occurs somewhere else, the whole constructs gets integrated into the genome also including the *reaper* gene (*P{Target}*$^{rpr+}$). The primer binding sites for the first verification through PCR are schematically depicted with red arrows. 'Fw?' = The forward primer was dependent on the 3' homologous region and with that on the target gene.

The construct is designed with a lethal gene next to the 3' homologous arm, but still inside the *FRT* sites to be cut out for catalyzing the homologous recombination. In case of a false integration somewhere in the genome, the gene – called *reaper* (White, Tahaoglu, and Steller 1996) - will also be integrated into the genome of the fly, as it is shown in Figure 18. Since this gene is under control of an UAS promoter it can be activated by expression of GAL4. This is fulfilled by including an ubiquitous GAL4 driver by crossing with an appropriate fly line (BL#26258, Table 1). This step minimizes the work amount by approximately 90% for screening and crossing false positive flies afterwards. The screening crosses were also flipped for three times, adults discarded and the newly hatched flies screened for red eyes within 20 days, before they were discarded.

In the last cross - mapping cross - all red eyed progeny (red eyed males 1:3 balancer females, red eyed females 1:2 balancer males) was crossed to appropriate balancer flies to map the insertion onto the chromosome number (at least for *per*).

Male progeny with red eyes were used for gDNA prep for verification on the genome level (3.2.4.1, 3.2.6.2). As a first filter, the attendance of the *reaper* gene was used, because the main proportion of the red eyed progeny pointed out to be false positive. For that, we designed primers located in the *reaper* gene and in the 3' homologous arm, respectively (Rv85/Fw? (locus specific), indicated in Figure 18, sequences shown in Table 2). In case there was no product observable after PCR and gel electrophoresis, we tried to gain homologous offspring and screened gDNA via PCR for the genetic locus that should be deleted. Additionally, we checked the location and size of the homologous arms with a primer pair binding first inside the gene cassette of the construct and second up- or downstream of the homologous arms inside the genomic area surrounding the gene locus. For closer description and smaller deviations, see the according paragraphs for the ends-out targeting process for the individual genes.

We also performed verification experiments on RNA, protein and behavioral level. These are explained in the following chapters.

After confirming that the knockout was complete, the marker gene had to be deleted. This was done by a cross with a fly line carrying a *Cre recombinase* gene, which recognizes the *loxP* sites surrounding the *mini-white* (The Cre-/*loxP*-system is functionally similar to the Flp-/*FRT*-system). So only the *attP-site* and one *loxP* site is left, where once the target locus was located (Figure 19). The remaining area corresponds to around 100 bp and future new integrations can also be done by using a *mini-white* marker gene.

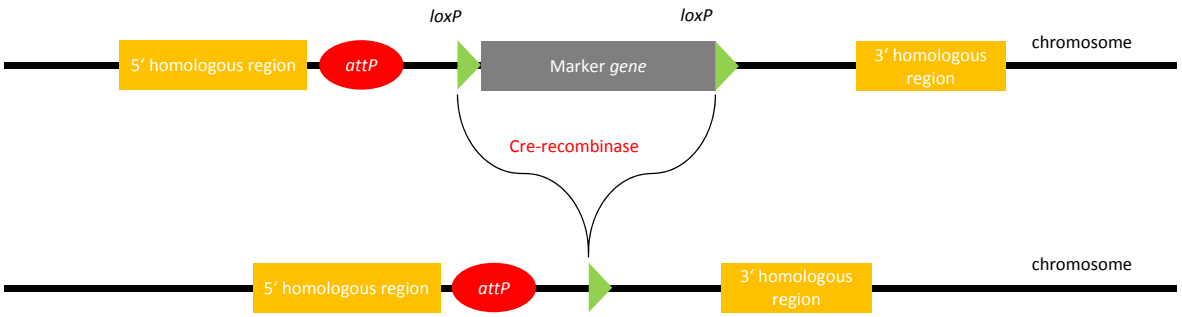

Figure 19: The flox-out process.

The Cre recombinase recognizes the 34 nucleotides of the *loxP* sites surrounding the marker gene and catalyzes the recombination between them. If both *loxP* sites are orientated in the same direction the part in between them is cut out and the halves of both *loxP* sites are getting ligated.

3.2.13 Ends-out gene targeting for the *per* locus

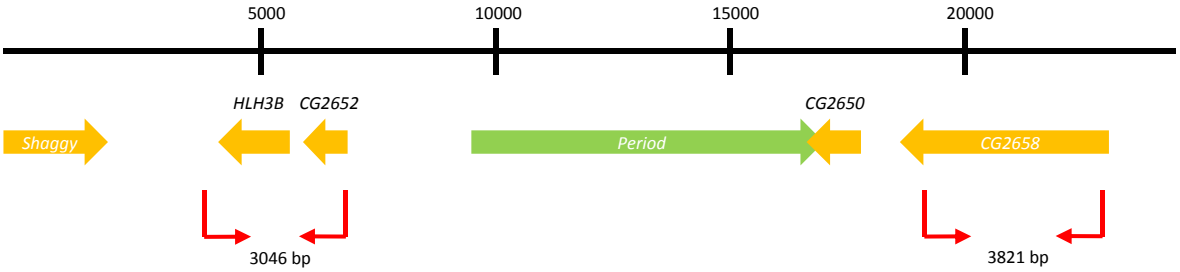

Figure 20: Overview of *per* genomic locus.

The graphic depicts *per* genomic locus with adjacent gene regions. Red arrows imply the binding sites of the primers used for the amplification of the homologous regions. These were cloned into the ends-out targeting vector pGX-*attP* (Figure 11). Numbers on top are a hint for the size of the depicted genetic region and are not shown for orientation on the chromosome. The exact coordinates for the *per* gene are X:2,685,580..2,692,780 [+] or 3B1-3B2 on X.

For creating the 5' homologous arm primer Fw12 and Rv11 were used. Fw14 and Rv13 for the 3' homologous arm (Table 2). The following program was designed for the PCR reaction (3.2.6.1):

Table 12: Program for the 3' homologous arm (3841 bp).

Temperature [°C]	Time [s]	Cycles
98	30	1
98	15	45
57	40	
72	120	
72	600	1
4	∞	1

Table 13: Program for the 5' homologous arm (3067 bp).

Temperature [°C]	Time [s]	Cycles
98	30	1
98	15	40
60	40	
72	90	
72	600	1
4	∞	1

The subsequently performed restriction digest was done successively first with *Spe*I/*Xho*I for the 3' or second with *Kpn*I/*Not*I for the 5' homologous arm and the pGX-*attP* vector, respectively. After ligation, the constructs were sent to BestGene Inc. and 6 strains with integrations of the construct on different chromosomes were generated:

Table 14: Putative *per* ends-out starting strains.

The construct is integrated on different genomic positions.
The successful experiment was done with strain 1-4M-C2.

Strain	Hit chromosome
1-1M-C3	3
1-2M-C3	3
1-3M-C2	2
1-4M-C2 (*perStart*)	2
1-5M-C2	2
1-6F-X	X

For targeting the *per* locus, we started with around 1,080 virgin females of a fly line containing the recombination construct on chromosome pair two (*perStart*, Table 1). The vials were further handled as described in 3.2.12. One difference to the *tim* targeting was that we did not remove the flies from the water bath between the heat shocks on day three and four, so the flies were also suspended to the warm up and cool down phase of the water. An overview about all numbers and stats of the targeting can be found in the results paragraph (Table 27).

For the mapping crosses we used w^{1118} flies to map the integration to the X-chromosome, before starting the verification on the molecular level by PCR. For that, we just checked the distribution of the red eye color in the progeny, when we mated red eyed males with w^{1118} females. In case all sons showed white eyes, whereas all daughters were red-eyed, the integration took place on the first chromosome pair (Figure 21 and Figure 22).

All female offspring was first crossed to w^{1118} flies to gain males showing red eyes and with that bearing the *mini-white* marker putatively on the X-chromosome. In this case one can propose: these males are hemizygous for the marker gene. We proceeded with these male animals in the same way, as we did in the beginning with male red-eyed candidates. That means we crossed them with virgin w^{1118} flies. If the insert had struck the X-chromosome, all females and 50% of the male progeny should express the red eye color (the *mini-white* appears dominant). If white eyed females were found, the strain was discarded. Strains that correspond to these notions were further tested by PCR.

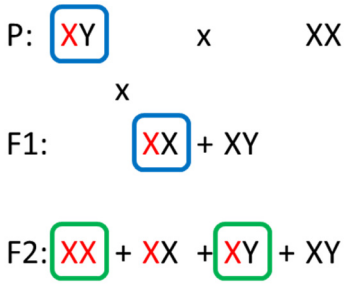

Figure 21: Mapping schedule for male progeny.

P: Male red eyed offspring (*XY*) was crossed 1:3 to w^{1118} virgins (*XX*). The insertion is mapped to the X-chromosome, if all daughters show red eyes (*XX*), whereas all male progeny is white eyed (*XY*). F1: Virgins with red eyes were than backcrossed with the red eyed father (blue edging) to gain homozygous female flies for the insertion. F2: Afterwards they were randomly single crossed to their red eyed brothers (green), leading to a homozygous strain, which was obvious by the eye color of the progeny (all red).

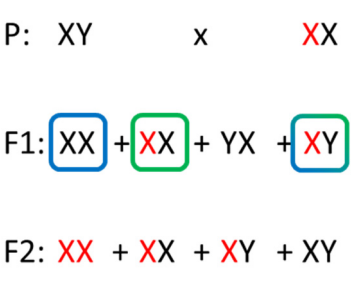

Figure 22: Mapping schedule for female progeny.

P: Red eyed females (*XX*) were crossed to w^{1118} males (*XY*). F1: Red eyed male offspring (blue-green edging, *XY*) was further crossed as red eyed males from the screening cross to map the insertion to the X-chromosome (blue, see Figure 21, *XX*) or crossed with their red eyed sisters (*XX*) to gain homozygous daughters (green, F2). With the following offspring we continued as with the F2-generation in Figure 21.

For the first genetic test for attendance of the *reaper* gene, we used the standard backward primer (Rv85, Table 2) binding inside the *reaper* gene locus and a forward primer located in the 3' homolgous arm (Fw113, Table 2). We predicted a product with the size of 691 bp. Since *per* is located on the X-chromosome, it was possible to test hemizygous male candidates, that were negative in the *reaper* PCR (no signal), for attendance of the *per* gene. This was done with primer PerL-sense and PerL-antisense (Table 2), both located in exon regions of the *per* gene, leading to a product with 409 bp in size. Both first PCRs were prepared after 3.2.4.1 and 3.2.6.2.

We went on amplifying both homologous arms (5' arm: Fw109/Rv117, 3' arm: Fw120/Rv111, Table 2) with primer pairs resulting in a product corresponding to the genetic region next to the ends-out area until the *mini-white* gene on the construct. For this we switched to 3.2.4 and 3.2.6.1. The PCR reaction was done with the setup shown in Table 15 and Table 16. The products were gel-purified (3.1.5), cloned into an assistance vector (3.2.9) and sent in for sequencing (3.2.8).

Table 15: PCR program for the verification of the 3' homologous arm of *per*^{Out} (4444 bp).

Temperature [°C]	Time [s]	Cycles
98	30	1
98	5	35
68	30	
72	150	
72	300	1
4	∞	1

Table 16: PCR program for the verification of the 5' homologous arm of *per*^{Out} (3629 bp).

Temperature [°C]	Time [s]	Cycles
98	30	1
98	5	35
55	30	
72	150	
72	300	1
4	∞	1

After the verification on DNA level, we went on with checking the RNA from *per*^{Out} flies. For that, we took complete flies, that were entrained and further harvested at ZT 15, when we expected the highest level of *per* mRNA throughout the day under normal circumstances (Hardin, Hall, and Rosbash 1992). We extracted the RNA (3.1.5) and designed primers (Rv163/Fw164) over exon-exon boundaries to exclude residual gDNA. A 212 bp sized product was expected. We adapted the standard recipe and program for simple PCRs for cDNA:

Table 17: PCR recipe for reactions with cDNA templates.

Ingredient	Amount
JumpStart REDTaq ReadyMix	12.5 µl
Primer forward	1 µl
Primer reverse	1 µl
cDNA template	2.5 µl
H_2O	8.5 µl
Total	25 µl

Table 18: PCR program for PCRs with cDNA template.

Temperature [°C]	Time [s]	Cycles
94	120	1
94	30	35
69	30	
72	30	
72	300	1
4	∞	1

The next logical step was to have a look on the protein level. So we extracted the proteome out of the lysate from flies' heads at ZT 23, the peak level of the PER protein expression. To examine the amount of protein we performed a standard western blot (3.2.11).

In the end we additionally investigated the animals' behavior. The setup and procedure is explained in 3.2.3.

After the knockout of the *per* locus was confirmed on the level of nucleic acids, proteome and behavior, the marker gene in the central part of the construct was floxed-out with help of the two *loxP* sites surrounding the *mini-white* (details to the procedure in Figure 23 and paragraph 3.2.12).

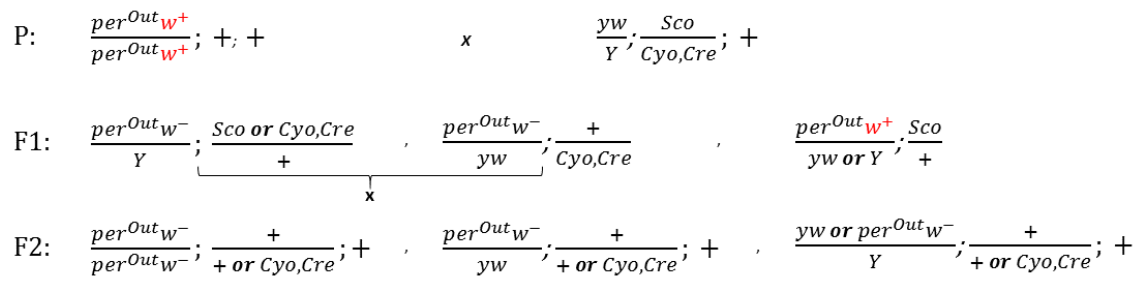

Figure 23: Flox-out crossing for removal of the *mini-white*.

Homozygous per^{Out} flies were crossed with male flies containing a *Cre recombinase* gene. In the F1 generation, male and female flies with a white eye color were allowed to mate, red eyed offspring was removed. Because the *mini-white* is dominant, a white eye color is only possible, if a jump out of the marker gene occurred. All female flies in the F2 generation were checked for their rhythmicity in behavior experiments. Arrhythmic flies should contain no *per* gene and were again crossed with white eyed males from the F1 generation to establish a homozygous flox-out strain. w^-: white eye color based on the cut out of the *mini-white*; w^+: *mini-white* is present leading to a red eye color.

3.2.14 Design for the rescue construct of *per*

For two major reasons we divided the locus, that should be rescued, into three parts (Figure 24). First, we expected that the size of more than 12 kb would make PCR reactions - necessary for introducing putative mutations - extremely difficult. Second, our aim was to create a tool that could be simply adapted with new mutations and to diminish the work amount to be done for later cloning steps. Hence, new mutations are integrated easily into the smaller subparts and can be exchanged in the vector. Thereby we considered it to be useful to divide the rescue locus into functional parts of the genomic region and checked the entire sequence for single restriction enzyme cutting sites. We were able to find two sites close to the start and the end of the *per* CDS, where we could insert two distinct restriction sites by just mutating one or two base pairs, respectively.

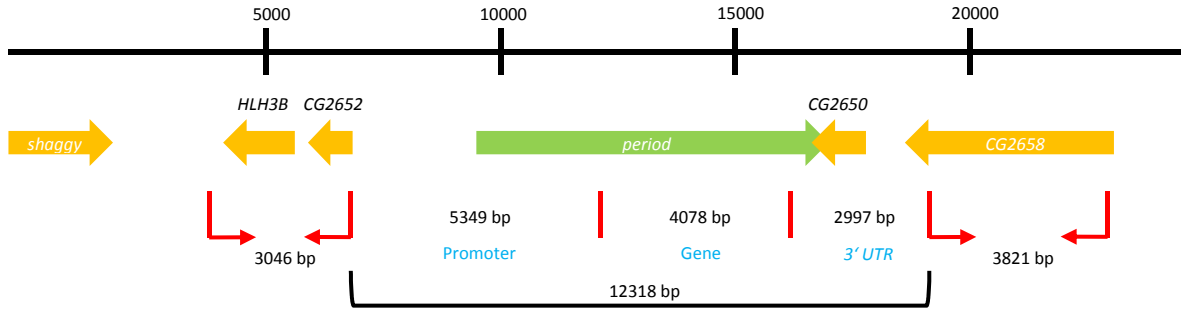

Figure 24: The *per* genomic locus with the rescue part divided into 3 pieces.

The whole area that was deleted by the recombination spans around 12 kb. This region was divided into three parts. First, the promoter region including the part until the next gene plus *5' UTR* sequences from *per*. Second, the CDS from *per*, spanning all described transcripts and third, the *3' UTR* and the adjacent gene *CG2650*. The sizes of the parts are indicated in the graph including the regions of the homologous arms (red arrows) we used to induce the recombination. Numbers on top are a hint for the size of the depicted genetic region and are not shown for orientation on the chromosome. The exact coordinates for the *per* gene are X:2,685,580..2,692,780 [+] or 3B1-3B2 on X.

This leads to three parts of rescue constructs. For future promoter studies the first sequence spans the whole area between gene *CG2652* and *per* also including its *5' UTR* region. Starting with the AA methionine, the second part involves all exons and introns of the ORF from *per*. By mutating the stop codon, one can e.g. insert a fluorescent tag here. The last piece covers the *3' UTR* of *per* plus the neighboring gene *CG2650*. This could not be prevented, because the ends of both genes are overlapping. We ensured that the mutations, that had to be included for inserting the restriction sites, were not located inside the CDS of *per* or affected any exon structure. They were inserted by changing the bases in the primers used for PCR. Table 19 and Table 20 show the sequences, in which the mutations were made.

Table 19: Sequence of the first cutting region (translation start).

The border between the *5' UTR* and the translated region of *per* is depicted. The primers used for mutation span the bases that are drawn in red letters. The beginning of *per* CDS is marked with a purple 'ATG'. The cutting site is shaded in green with a blue underlined letter that shows the mutated base to insert the *Avr*II restriction site. This restriction site is unique for the whole *per* locus.

5'…AACCAACTGGGCAAGCTGGAGAACCTAAGCACCATGGAGGGCGGCGAGTC…3'	*Avr*II: 5'...C↓C T A G G...3'
5'…AACCAACTGGGCAAGCTGGAGAACCTAGGCACCATGGAGGGCGGCGAGTC…3'	

Table 20: Sequence of the second cutting region (translation stop).

The region of and around the primer used for inserting the necessary mutations is shown. Red letters depict the primer region. The purple 'TAG' marks the end of *per* CDS. The restriction site for *Sbf*I is shaded in green and enabled by mutating the two underlined bases in blue. This restriction site is unique for the whole *per* locus.

5'…CACAGCACGGGGATGGGTAGTAGCCACACCCGCAGTTGCTGCTGACCGAC…3'	*Sbf*I: 5'...C C T G C A↓G G...3'
5'…CACAGCACGGGGATGGGTAGTAGCCACACCTGCAGGTGCTGCTGACCGAC…3'	

For the promoter region the primers Fw151/Rv154 were used. Fw153/Rv156 were designed for the gene region and Fw155/Rv152 for the *3' UTR*. As template for PCR (3.2.6.1), we used gDNA (3.2.4) from w^{1118} flies. All reactions were done with one program:

Table 21: PCR reaction profile for amplifying the three parts of the *per* locus.

Temperature [°C]	Time [s]	Cycles
98	30	1
98	15	35
65	30	
72	350	
72	600	1
4	∞	1

The products were separated by gel electrophoresis (3.2.7), cut out and purified using a standard gel purification kit (3.1.5). We first cloned the DNA strands into an assistance vector called pJet1.2 (0, 3.1.5) to gain a high amount of product (3.2.10.2). Furthermore, this was recloned into the pGE-*attB* vector (3.1.3.2), designed for inserting the rescue constructs. To simplify the cloning procedure, we successively inserted the three pieces starting with the *3' UTR*. The procedure is described in Figure 25.

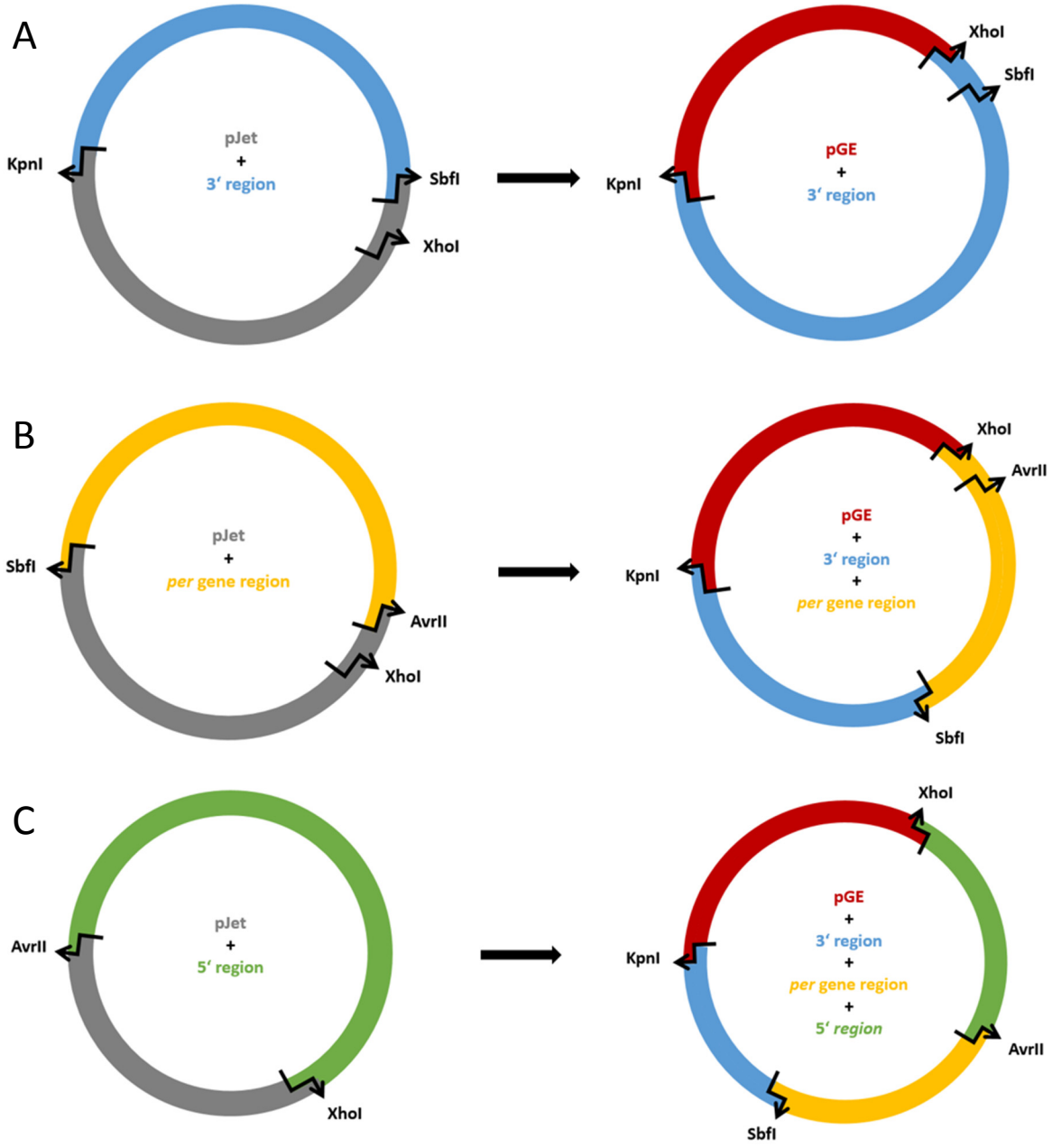

Figure 25: The *per* rescue cloning procedure in three steps.

The pJet1.2 vector *MCS* includes a *Xho*I restriction site upstream of the blunt end cloning site (3.1.3.3). This restriction site plus the restriction site integrated in the primer on the 3’ site of the constructs, was used to successively insert all constructs into the pGE-*attB* vector. A: In a first step, digestion with *Xho*I and *Kpn*I including a following ligation led to the integration of the *3’ UTR* construct. B: The gene construct was integrated with *Sbf*I and *Xho*I. C: The promoter region completed the whole rescue and was integrated with *Xho*I and *Avr*II. The figure was taken from the bachelor thesis of S. Lichtblau.

Every step includes the whole cloning procedure – digestion, ligation, transfection, selection and plasmid preparation (3.2.9).

Finally we sequenced (3.2.8) and checked the breaking points between the single pieces and between the pieces and the vector to ensure a right integration.

The pGE-*attB* vector containing all constructs was sent to BestGene Inc. (CA, USA [Service type: Plan H; Qty: 1]) to get integrated into per^{Out} w^{-} flies by PhiC31 integrase-mediated transgenesis systems.

3.2.15 Ends-out targeting for the *tim* locus

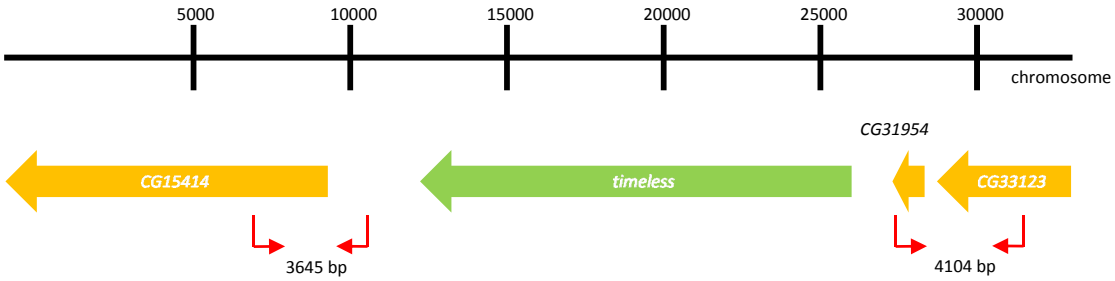

Figure 26: Genomic locus of *tim*.

The gene *tim* and the genomic region next to it are depicted. Also the primers with binding sites that were used to amplify the homologous arms. The chromosome is orientated that the 5' site is on the left side, whereas the gene lies opposed. So the *3' UTR* of *tim* is located upstream referred to the chromosome. Numbers on top indicate the size of the area and not the position on the second chromosome. This is: 2L: 3,493,986. 3,508,119 [-] or 23F6-23F6.

For the *tim* ends-out targeting, we used primer Fw31/Rv17 for the 5' and Fw15/Rv16 for the 3' homologous arm, respectively. PCRs were performed with the same gDNA (3.2.4) and the same recipe (3.2.6.1) as for the construction of the *per*-pGX-*attP* ends-out vector.

The attentive reader may ask, why we did not expand the knockout region for the total 3' region of *tim* until the beginning of *CG15414*. Mainly, this was because the whole locus already spans around 17 kb and we tried to keep the deletion preferably small. So we decided to search for a not conserved region to reduce the probability of destroying a putatively important sequence with the breaking point between knockout region and 3' homologous arm. This is where Rv16 is located.

Table 22: PCR program for both homology arms of *tim* ends-out targeting vector.

(3' homologous arm: 4124 bp/5' homologous arm: 3666 bp).

Temperature [°C]	Time [s]	Cycles
98	30	1
98	15	45
45	30	
72	150	
72	600	1
4	∞	1

We digested the 5' homologous arm with *Not*I/*Kpn*I, the 3' homologous arm with *Spe*I/*Xho*I and opened the pGX-*attP* vector with the same enzymes. After sending the constructs to BestGene Inc., we received 7 strains containing the integration of the construct on different chromosomes (Table 23):

Table 23: Putative *tim* ends-out starting strains.

The construct is integrated on different genomic positions. The successful experiment was started with strain 2-3M-C3.

Strain	Hit chromosome
2-1M-C2	2
2-2M-C2	2
2-3M-C3 (*timStart*)	3
2-4M-C2	2
2-5M-C2	2
2-6M-C2	2
2-7M-C2	2

We started the *tim* ends-out targeting with approximately 1090 virgin female flies from the strain *timStart* (Table 1) carrying the integrated construct on the third chromosome. Fly pushing was done similarly as for *per* ends-out targeting process explained in 3.2.12.

One crucial difference we made in this round of targeting was setting and removing the flies out of the water bath at 37°C for the heat shock just in time. That means exactly one hour on day three and four at 37°C, resulting in a significantly higher amount of offspring from the targeting cross. All states and numbers of the targeting procedure for *tim* are shown in Table 29.

For balancing the insertion, we had to use another balancer fly line, containing markers on the second chromosome pair (Table 1). Here we crossed red eyed males 1:3 with virgin females and red eyed females 1: 2 with males of the balancer fly strain. We did not invest the time for screening by eye, what

would have been possible through the balancer phenotypes. Instead we isolated gDNA from all putative candidates.

Because *tim* is located on the second chromosome and thereby there are no hemizygous male flies bearing only one copy of the *tim* allele, it was not possible to check the flies for the presence of *tim* gene locus, before passing a high number of single crosses and tests to gain homozygous flies. So we skipped this in the beginning and went on with the screening for *reaper* instead. For that, we used the primers Rv85/Fw84, isolated the gDNA in standard manner (3.2.4) and established an easy PCR program (3.2.6.2). Fw84 (Table 2) thereby binds to the 3' homologous arm of *tim* (see also Figure 18).

All flies showing negative results for *reaper* were than further tested for the 5' and 3' homologous arm. For the *tim* homologous arms, we used Rv80/Fw81 for the 5' and Fw82/Rv83 for the 3' homologous arm, respectively. The PCR reaction was performed in an Eppendorf gradient mastercycler with the standard recipe for more complicated PCR reactions (3.2.6.2) and following programs:

Table 24: Program for the 3' homologous region of the tim^{Out} flies (4197 bp).

Temperature [°C]	Time [s]	Cycles
98	30	1
98	5	35
49	30	
72	140	
72	600	1
4	∞	1

Table 25: Program for the 5' homologous region of the tim^{Out} flies (3861 bp).

Temperature [°C]	Time [s]	Cycles
98	30	1
98	5	35
50	30	
72	120	
72	600	1
4	∞	1

Again, the DNA was extracted from the gel (3.1.5), cloned into the assistance vector pJet1.2 (3.1.3.3) and sent for sequencing (3.2.8).

For *tim* we did not do any confirmation of the knockout on RNA level.

For western blots (3.2.11) we entrained the flies and extracted the proteome from flies' heads at Zeitgeber time 23, the time point with the highest presence of TIM.

The behavior experiments were done in the same way as described in 3.2.3.

Also the flox-out procedure in the end was the same as for *per* knockout. Figure 27 shows an overview of the participating genotypes

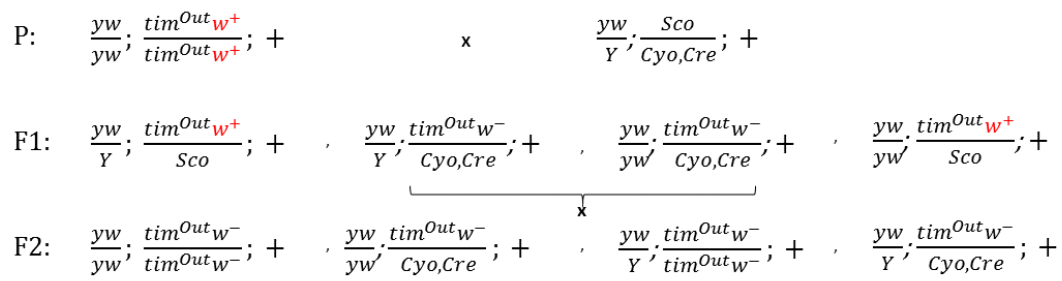

Figure 27: Flox-out crossings to remove the marker gene for the *tim* targeting.

We used the same strain carrying the *Cre recombinase* as for *per* ends-out targeting. But here we were able to easily select for heterozygous flox-out animals in the F1 generation, first, because of the eye color and, second, because of the Cyo phenotype. In the F2 generation, we mated individuals showing white eyes and no balancer phenotype to gain a homozygous strain. To be really sure, we yet tested these strains in behavior experiments. w^-: white eye color based on the cut out of the *mini-white*; w^+: *mini-white* is present leading to a red eye color.

3.2.16 Rescue of *tim^{Out}*

Due to time constraints and practical reasons we decided not to start with the rescue of the complete *tim* locus. Instead, we designed a rescue based on the GAL4-UAS system. We used already available *tim-PD* CDS constructs cloned into the pAC5.1 vector, generated by F. Cao and N. Peschel for *S2* cell culture experiments (unpublished results). In previous studies these scientists created four different constructs, containing either no mutation or nucleotide substitutions on one or both editing sites, respectively (see Table 26, from the top to the bottom: *timCDS* without mutation, *timCDS* with mutation 1, *timCDS* with mutation 2 and *timCDS* with mutation 1+2). They exchanged the nucleotides in a way that it simulates an ongoing, permanent editing (A→G).

Table 26: *tim^{Out}* GAL4-UAS rescue constructs.

The four different constructs are depicted. One with both sites as they are encoded in the genome (adenosine), one with both sites mutated (A→G), mimicking the deamination by ADAR. The two constructs in the middle are designed with only one of both mutations. The depicted sequence shows the important part of the whole construct, exclusively.

.....	AGC	CTC	TGG	TTC	GAA	GCC	TCT	CTG	TCG	GAG	AGC	TCT	GAG	GAT	AAT	GAG	AGT	AAT	ACC	TCG	.....
.....	AGC	CTC	TGG	TTC	GAG	GCC	TCT	CTG	TCG	GAG	AGC	TCT	GAG	GAT	AAT	GAG	AGT	AAT	ACC	TCG	.....
.....	AGC	CTC	TGG	TTC	GAA	GCC	TCT	CTG	TCG	GGG	AGC	TCT	GAG	GAT	AAT	GAG	AGT	AAT	ACC	TCG	.....
.....	AGC	CTC	TGG	TTC	GAG	GCC	TCT	CTG	TCG	GGG	AGC	TCT	GAG	GAT	AAT	GAG	AGT	AAT	ACC	TCG	.....

With a simple cloning procedure including *Xho*I and *Xba*I, the inserts in the pAC5.1 vector were subcloned into the pUAST vector – containing the important sites for fly integration and the GAL4-UAS system (3.2.1).

Finally, after checking the pUAST-*tim* constructs with a control digest, we sequenced the mutation sites and the breaking point between vector and insert to ensure a proper assembly (results are not shown in this thesis).

4 Results

4.1 Ends-out targeting *per*

4.1.1 The crosses

For all scientists, who think about designing a knockout fly, we collected all data from the ends-out targeting procedure to give an overview about the work amount that has to be expected. Table 27 summarizes all data.

Table 27: Statistics for the ends-out targeting process of the *per* locus.

We only PCR-verified those flies, in which we were able to map the integration on the X-chromosome. The ratio and size of the crosses are indicated in brackets.

Gene	*period*
Target chromosome	X
3' + 5' arm (kb)	3.821 bp + 3.046 bp
Target gDNA deletion (kb)	12.381 bp
Attempts	3
Targeting crosses (30♀ x 30♂)	~ 36 (~1080 x 1080)
Screening crosses (20♀ x 10♂)	205 (4.100 x 2.050)
Mapping crosses (3♀ x 1♂/1♀ x 1♂)	123 (84♀, 36♂, 3?[k])
PCR tested/Integration mapped on X	10 (8♀, 2♂)
PCR verified	1♂

In the end we noted a clear decrease in offspring compared to the *tim* procedure. Therefore, we recommend to precisely stick to the heat shock times. We can clearly say that the reason for the low amount of offspring here is not due to the different genotypes. Instead, it must be the consequence of the longer exposure to the warmed environment. In total, we started three attempts to end up successful. At this point, it might be helpful for other scientists to mention, to what extend we changed or adjusted some settings compared to former authors that turned out to be important for the reduction of work amount and also for its success. First, we minimized the workload of the fly pushing

[k] The '?' stands for flies that died in the food before we noticed their gender.

by increasing the amount of animals per cross in each vial and prolonging the time from 3-4 to 4-5 days between the transfers. Second, we strictly discarded all vials 20 days after the first contact with the flies, to exclude animals from the F2 generation. Third, we started screening for progeny 10 days after mating and used male and female flies for the mapping cross independent of virginity. The last, but most effective difference was to change the GAL4-driver line in the screening cross from BL#26259 to BL#26258. It turned out, that this minimizes the outcome of false positive flies tremendously. Although, both strains seemed to be almost identical, strain BL#26258 is much more effective. With that, we minimized red eyed progeny hatching from the screening cross from 1.140 to 123 individuals to be further processed in the mapping cross. 68% of the 123 red eyed candidate flies we found in the offspring of the screening cross were of female gender. Ten carried the *mini-white* on the X-chromosome and were further tested via PCR.

As the result of crossing around 1080 virgin flies at the beginning, we got one single male fly, in which the *per* locus was completely exchanged with the targeting construct.

4.1.2 Genomic verification

As described in the methods paragraph, we started the genomic verification by PCRs proofing the existence of the *reaper* (Figure 28) and *per* (Figure 29) gene. Both genes should not be detectable in male flies bearing the correct knockout of *per*.

The numbers labeling the flies in the gel pictures refer to the succession of individuals with red eyes that were selected from the offspring of the screening cross[l]. *#911* dates back to a former attempt, in which we found much more candidates. It just served as a positive control in this experiment. However, there is a weak signal in all lanes, also in the negative control. Since this is just very faint, compared to *#991*, it is most probably because of contamination.

[l] All candidate flies showing a red eye color were selected and just counted.

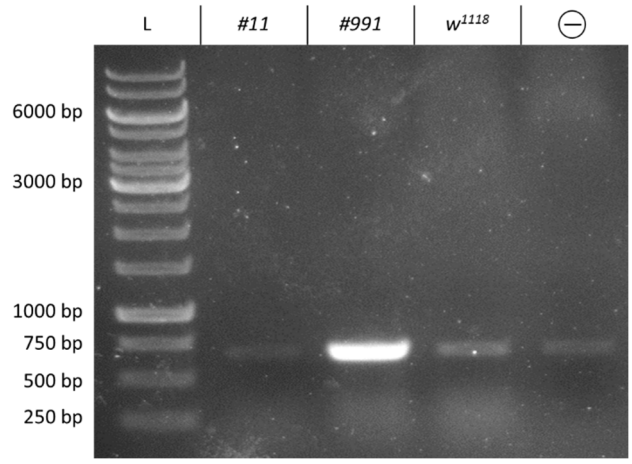

Figure 28: PCR verification of an integration without *reaper*.

As shown in 3.2.12 the *reaper* gene should not be integrated into the genome of the fly in case of a right exchange. We used the 'not existence' for a first PCR test. #*11*: verified as knockout. #*911*: randomly chosen control fly that survived the *reaper*-based negative selection. Θ: negative control without DNA. w^{1118}: wild type control. L: DNA ladder.

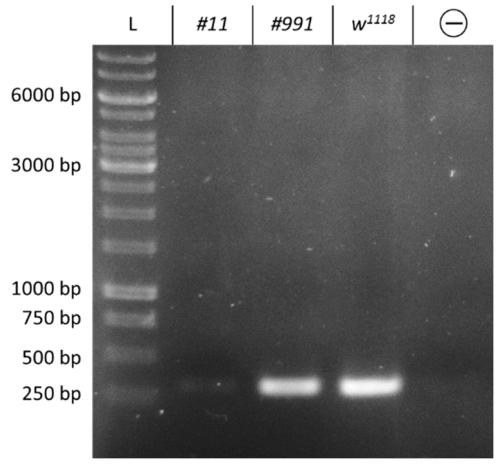

Figure 29: PCR verification of the deletion of *per*.

With a primer pair located inside the genomic region of *per*, we ensured the deficit of the targeting region. #*11*: verified as knockout. #*911*: randomly chosen control fly that survived the *reaper*-based negative selection. Θ: negative control without DNA. w^{1118}: wild type control. L: DNA ladder.

The PCR validation clearly ensured the loss of at least a part of the *per* locus, without integrating the lethal gene *reaper* in the genome. To see, if the construct with the *mini-white* exchanged correctly with the whole genomic locus, we performed another PCR proofing the size and location of the homologous arms (Figure 30).

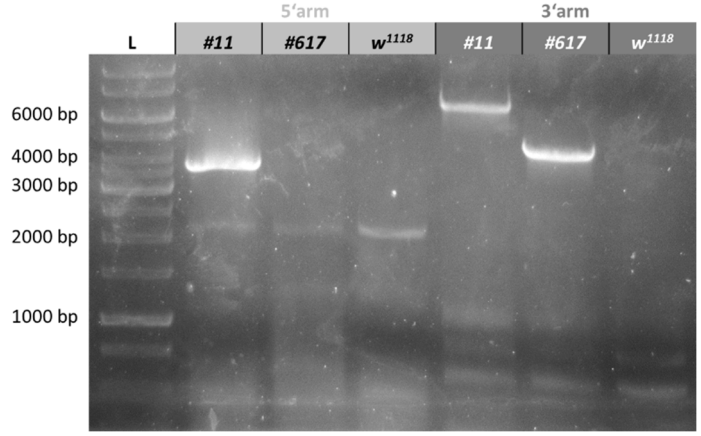

Figure 30: PCR verification of the homologous arms.

The *per* knockout positive fly was also tested for the location and size of the homologous recombination arms. It is obvious that the 3' homologous arm, that should measure around 3.8 kb in size, is bigger. Although the PCR yielded a clear signal. *#617*: A fly that showed positive results for the 3' homologous arm, but failed in deficit tests for the *per* gene locus. Results like this show, why it is inevitable to perform more than one PCR test. w^{1118}: wild type control. L: DNA ladder.

Besides the correct knockout fly, we also found a few flies, in which we mapped the integration to the X-chromosome (Table 27) and that were positive for one of both homology arm PCR tests. The majority of these flies, positive in the PCR of the 5' homologous arm, also showed a signal in *reaper* PCRs, whereas the 3' homologous arm positive individuals did not show any positive result in *reaper* PCRs. But in all of them the existence of the *per* gene was proven. We often used these flies as positive controls for further PCR reactions, so done in Figure 30. We only found one fly that was negative for

both gene proving PCRs, *per* and *reaper*, and showed a clear signal for both homologous arms. In most figures, this individual is denoted as *per#11* (candidate number) or per^{Out} (final name). 99 (of 123) individuals were preserved as a strain, the rest died before mating or seemed to be unfertile.

Because the signal for the 3' homologous arm was on a higher level than it was predicted, we went on with sequencing. For that, the bands were cut out, purified, cloned into the assistance vector pJet1.2 and sent for sequencing. We started with primers located inside the vector, but facing towards the MCS. The rest was done successively, generating the next sequencing primer on the results of the former sequencing reaction. The results verified the assumption of a longer 3' homologous region than it had been initially. An overview of the sequencing results depicted as a genomic map is shown in Figure 31.

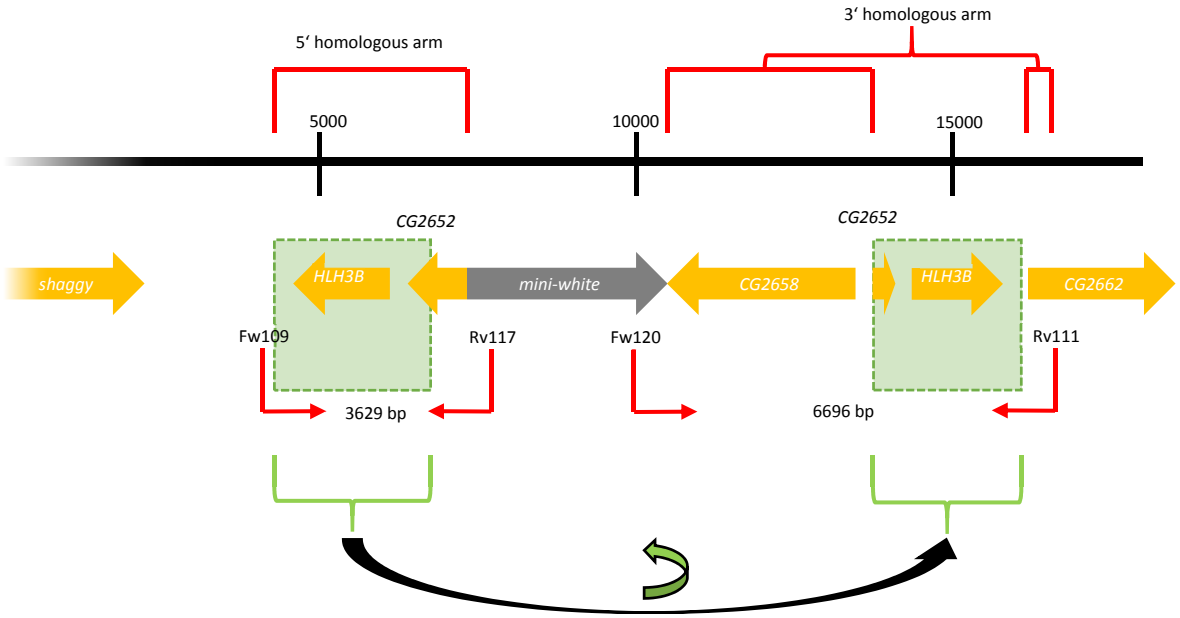

Figure 31: The *per* locus after recombination.

The complete *per* locus (as planned) was exchanged with the designed construct cassette (grey). It is depicted in a simplified scheme and comprises not only the *mini-white*, but all elements between the *MCS'* of the pGX-*attP* vector (3.1.3.1). The real breaking points between endogenous region and construct cassette are located somewhere inside the homologous arms. On the 5' site, the homologous recombination occurred without complications, whereas on the 3' site, somehow a part from the 5' homologous arm was duplicated and reintegrated into the 3' homologous arm in reverse direction (green brackets). Thereby luckily no gene of the 3' homologous arm was interrupted or destroyed. The integration took place exactly between the gene region of *CG2658* and *CG2662*. The duplicated part includes a piece of gene *CG2652* and the whole gene region of *HLH3B*. Numbers on top indicate the size of the area and are no position information concerning the second chromosome. The binding sites for the primers used for the proof of the homologous arms are indicated with red arrows. The location, where the homologous arms actually would be expected are represented with red arrows from above.

By chance, a part of the 5' homologous arm was duplicated and reintegrated in reverse orientation into the 3' homologous arm. The original genomic map can be found in Figure 20. However, the exact process of the duplication remains pure speculation. But it makes it inevitable to generate a rescue for the knockout locus, to see if the duplication somehow shows consequences on the phenotype. It is obvious that the insertion of the duplication did not disrupt the ORF of gene *CG2658* or *CG2662*, which are located up- and downstream. Instead, it occurred between both genes. The duplicated region contains a part of *CG2652* and the total area of *HLH3B* (*helix loop helix protein 3B*), but in reverse orientation. It is hard to make any proposition about consequences, which later experiments will show.

4.1.3 Evidence of *per* mRNA

In a next step the verification on RNA level, as described in 3.2.13, was done. During the further procedure, other positive/negative controls with more closely related genotypes to the knockout animals were available and used for the experiments. per^{Out} (w^{+}) is a strain carrying the knockout of *per* and still including the *mini-white* in a homozygous constellation. per^{Out} *red* and per^{Out} *white* are male siblings from a heterozygous strain. Since *per* is located on the X-chromosome, males are hemizygous (meaning they have the X-chromosome and all its alleles in a single version) and hence, one can select *per* knockout and wild type individuals easily by eye color out of the same vial.

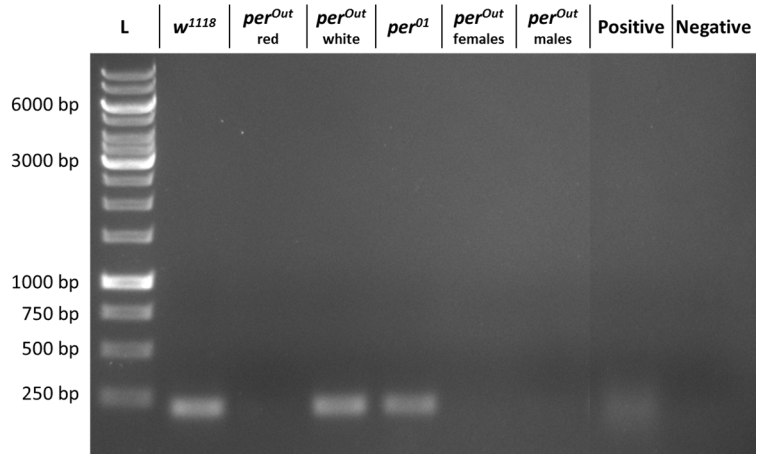

Figure 32: cDNA PCR of per^{Out} animals.

per mRNA amplified with primer pair Rv163/Fw164 yields a signal of 212 bp in size. *per* mRNA could be detected in w^{1118}, per^{Out} *white* and per^{01}. Per^{Out} *red*: males with red eyes taken out from a heterozygous stock. Per^{Out} *white*: males with white eyes taken out from the same heterozygous stock as the red eyed males. Per^{Out} males/females: Flies from a homozygous *per* knockout strain. Positive: Normal gDNA from w^{1118} flies. A faint band is obvious because of a weak primer binding despite a design over exon-exon borders. Negative: Reaction mix without any nucleic acid.

The result of the PCR (Figure 32) shows clearly, that there is no *per* mRNA detectable using cDNA templates from per^{Out} flies. We tested both genders from a homozygous stock, as well as red eyed

males from a heterozygous strain (*per*^{Out} *red*). The white eyed brothers (*per*^{Out} *white*) of the latter flies were used as a positive control. Also *per*^{01} showed a distinct signal, because the knockout phenotype of *per*^{01} is based on a point mutation within the *per* gene, that leads to a nonsense mutation and with that to a shortened, not functional peptide (Hardin, Hall, and Rosbash 1990). For this reason, the phenotype is only obvious on protein level. As positive control, we used gDNA from *w*^{1118} flies. Primer Rv163 (Table 2) is designed to bind over exon-exon borders, preventing from detecting the genomic locus. However, there is a faint signal that can be ascribed to a residual primer binding on the gDNA.

4.1.4 Protein – search for PER

Following natural conditions, after the RNA validation PER protein level were checked. Initially, we spared a time point specific study of PER. Instead, we just observed ZT 19, the time point described for the highest PER level (Stanewsky, Frisch, et al. 1997). We did not detect any PER signal in *per* mutant strains, neither in *per*^{Out} nor in *per*^{01}. Also *tim*^{Out} did not display PER at ZT 19, but at other time points PER was detectable in this strain (data not shown). The only signal was observed in the *w*^{1118} wild type control (Figure 33).

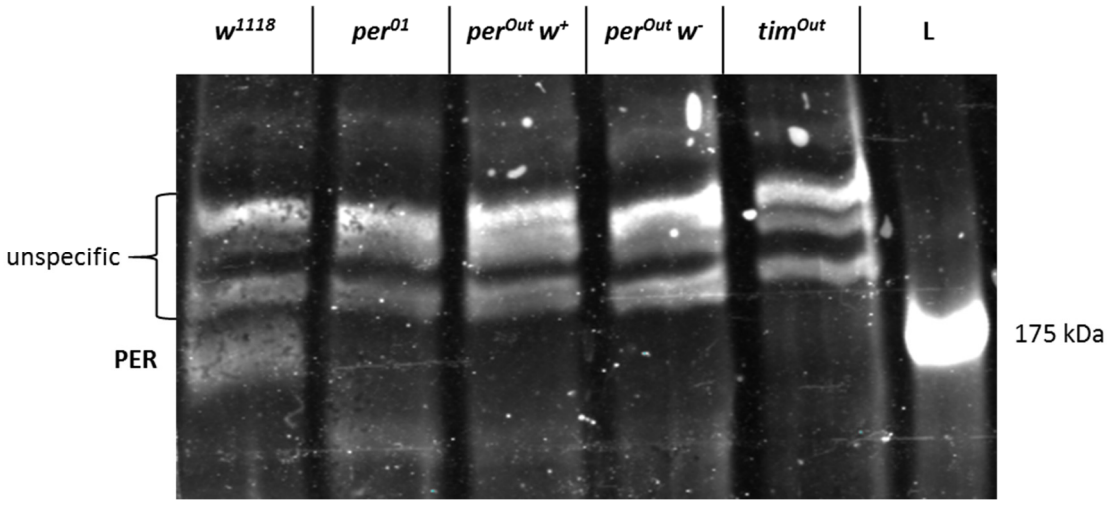

Figure 33: Western blot of *per*^{Out}.

Flies were harvested at ZT 19, heads were cut off and used for western blot. Staining was done with a commercial antibody against PER from Santa Cruz. The only genotype showing a signal for PER is *w*^{1118}. Also *tim*^{Out} did not display any PER.

Because PER is cycling throughout the day we decided to check different time points, too. Another antibody from R. Stanewsky (Stanewsky, Frisch, et al. 1997) was tested in this experiment. As expected, different protein amounts and also variations in the phosphorylation can be seen for PER in the wild type flies (Figure 34). *Per*^{Out} shows a blot without any specific mark.

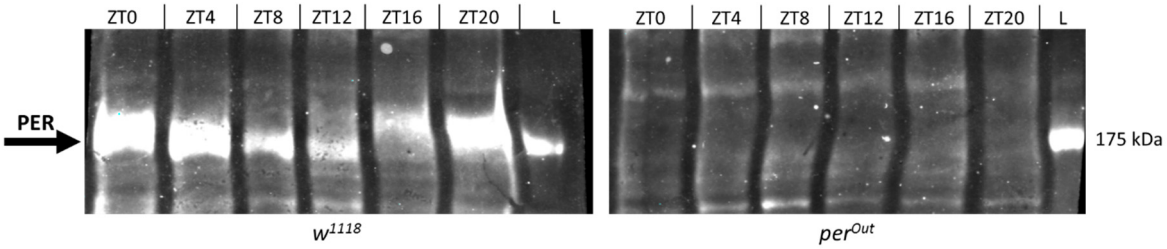

Figure 34: Anti-PER western blot of different time points of wild type and *per*^{Out} flies.

The flies were entrained in a 12/12 LD cycle and harvested at different time points. For the wild type flies (*w*^{1118}), the typical cycling of PER is observable. High amount of protein late in the dark phase and different phosphorylation levels indicated through varying heights of the bands. *Per*^{Out} does not show any kind of PER signal. For this experiment, we changed the primary antibody to one from Stanewsky et al. (Stanewsky, Frisch, et al. 1997).

4.1.5 Behavior

per^{Out} animals were also checked in behavior experiments. Table 28 summarizes the results under constant darkness.

Table 28: Periodogram analyzes from *per*^{Out} flies with controls.

The periods of the rhythmic flies, detected by the computer program, were averaged. The power value gives a hint for the reliability of the evaluated period. For *per*^{Out} *red* it is quite low, but most of these flies were arrhythmic anyway. Judged by eye, we could not find any rhythmic fly (see Figure 54). Genotypes are explained in detail in the main text.

Genotype	Quantity (n)	Period (SEM)	Power (SEM)	Arrhythmicity
perStart	16	23.93 (0.103)	29.96 (2.27)	0%
per^{01}	15	-	-	100%
per^{Out} *white*	14	23.58 (0.092)	26 (2.89)	0%
per^{Out} *red*	30	27.28 (3.3)	15.29 (1.43)	86.67%

Albeit there are a few *per*^{Out} flies with red eyes (4/30) that show a weak rhythm, they just display low power values. For more transparency see discussion chapter.

The activity of the flies in the average actogram of all participating flies is equally distributed in both *per*^{01} and *per*^{Out} during DD (Figure 35). Two single artefacts (marked with red background) on day 2 and 7 in DD are discernible in both genotypes and can be ascribed to artefacts due to disturbances of the experimental conditions from outside. They can be found in *per*^{Out} *white* and *perStart* as well, although they are not as prominent there.

The average day graphs show (Figure 35), that there is no morning and evening anticipation in *per*^{Out} and *per*^{01}, but obviously in the flies expressing PER. One can recognize a slight rise in activity throughout the dark phase, but this increase proceeds evenly without a distinct slope increase in the graph immediately before lights-on. Whereas in the *per*^{Out} flies the activity seems to be nearly equally distributed throughout the day – times of switching the light status excluded and with a little less

activity in the dark – the *per*^{01} animals show clearly more activity in the night. There is also no midday siesta and also not such strong reactions to lights-on.

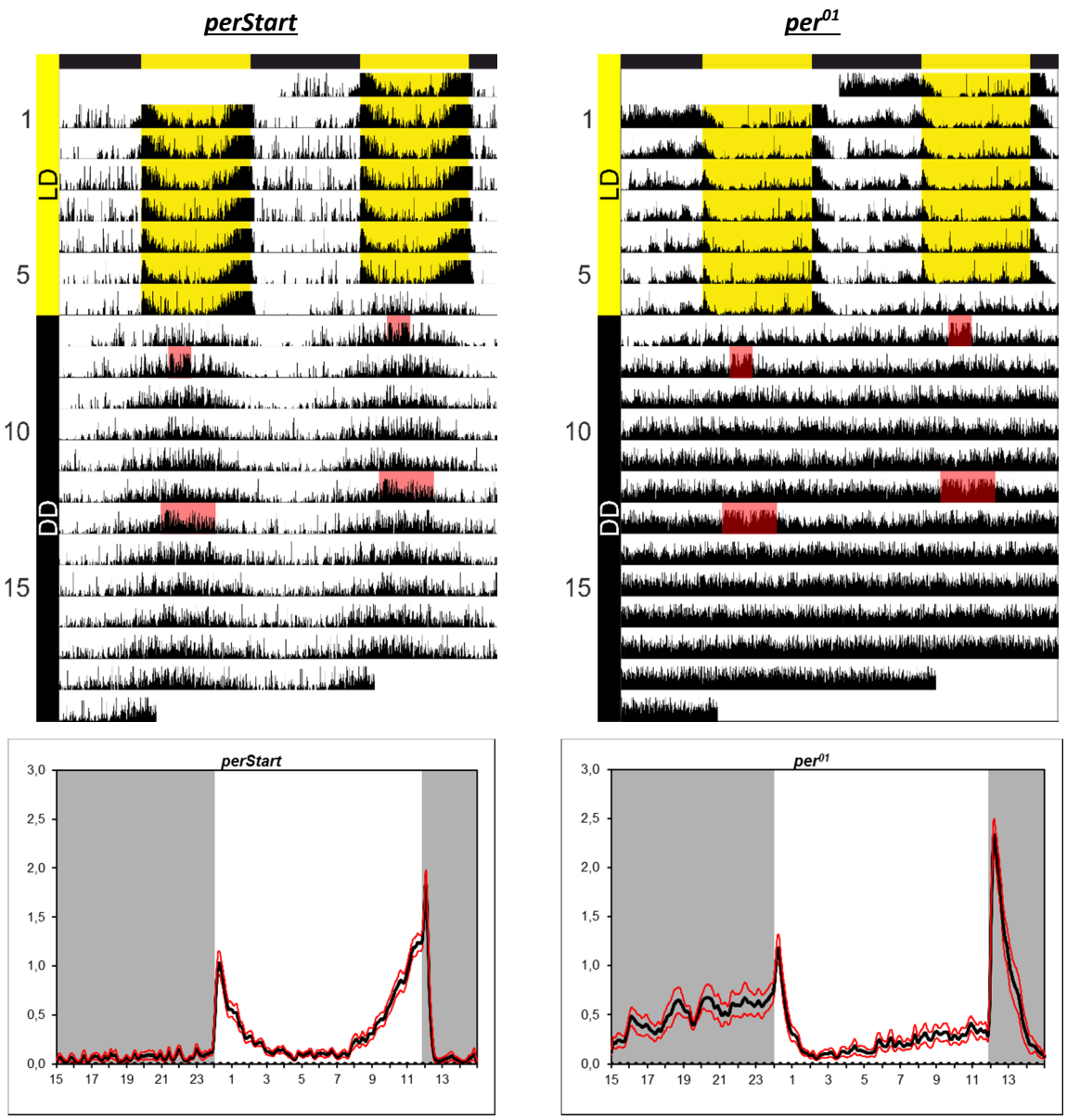

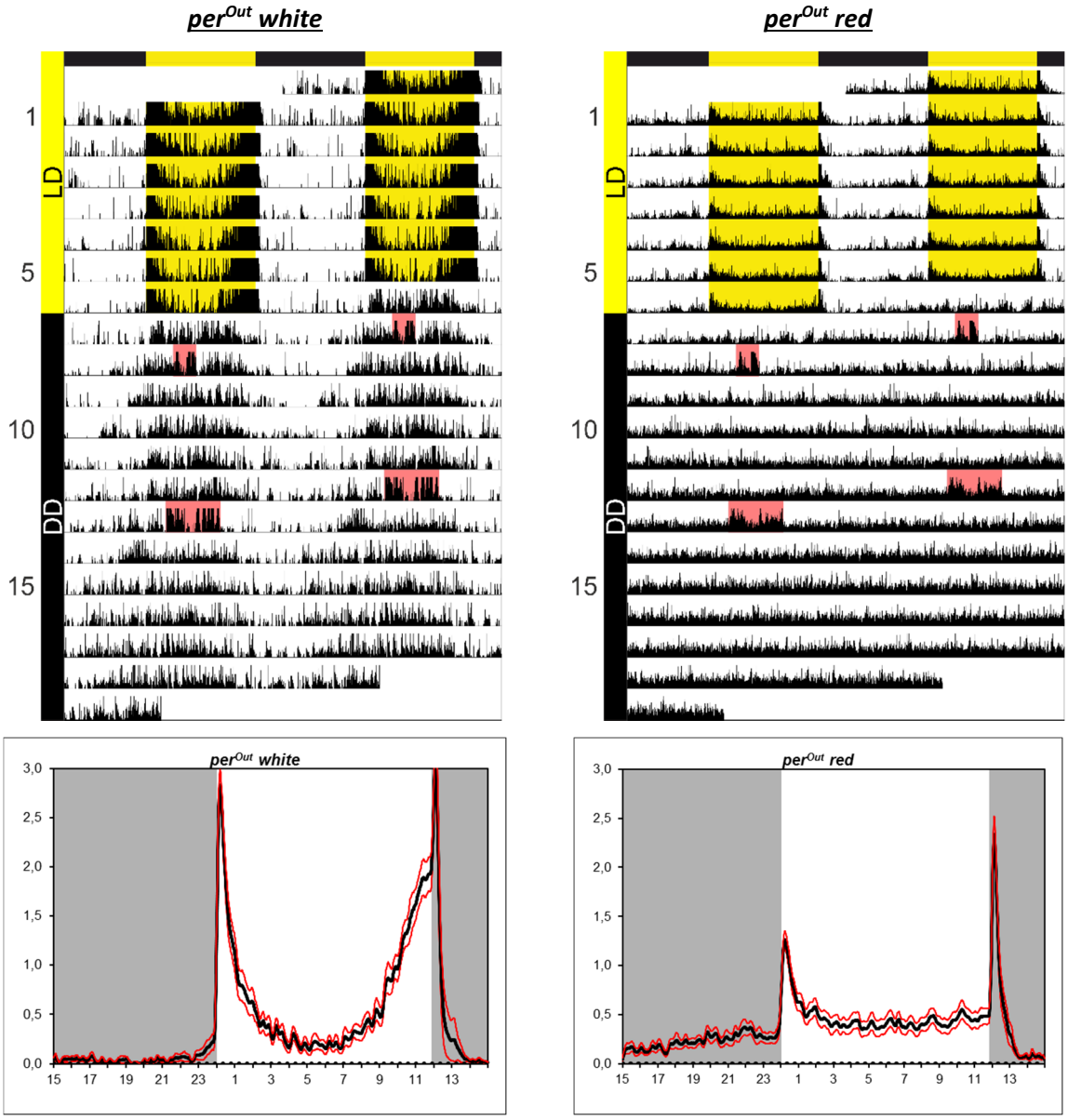

Figure 35: Average actograms and average day graphs from behavior experiments of *per*^{Out}.

For each genotype the actogram for the whole timespan of the experiment (upper figure) and an average day graph for the LD part of the experiment (lower graph) is shown. Black bars show crosses of the light beam inside the monitor by the fly. Numbers on the left side count the days of the experiment. The yellow/black bars on top show the existing light regime of the first 6 days. For a better view yellow background also shows timespans with lights-on. All actograms from flies participating in the test were averaged. In the average day graphs, the dark phase is deposited with gray background. ZT values are plotted on the X-axis, whereby ZT0 means lights-on. *PerStart*: Flies with the construct integrated on the second chromosome. These flies were used as starter line in the ends-out targeting procedure. *per*^{01} served as a control for not functional PER protein. N values were: *perStart* = 16, *per*^{01} = 15, *per*^{Out} *white* = 14, *per*^{Out} *red* = 32.

The *per*^{01} flies tend to shift their activity into the night. This is obvious after lights-off where activity in the other genotypes decreases faster, whereas in *per*^{01} a shift of the evening peak towards the night is clear, but the total activity stays quite high throughout the night (compared to the day). It is also worth to keep in mind, that we did not perform these experiments under high light intensity, instead we used an intensity of around 300 lux.

4.1.6 Construct for the *per* rescue

The *per* rescue was designed as close as possible to the native locus. We cloned the rescue in a stepwise manner as described in 3.2.14. Here, just the final result before shipping the vector for injection is shown (Figure 36).

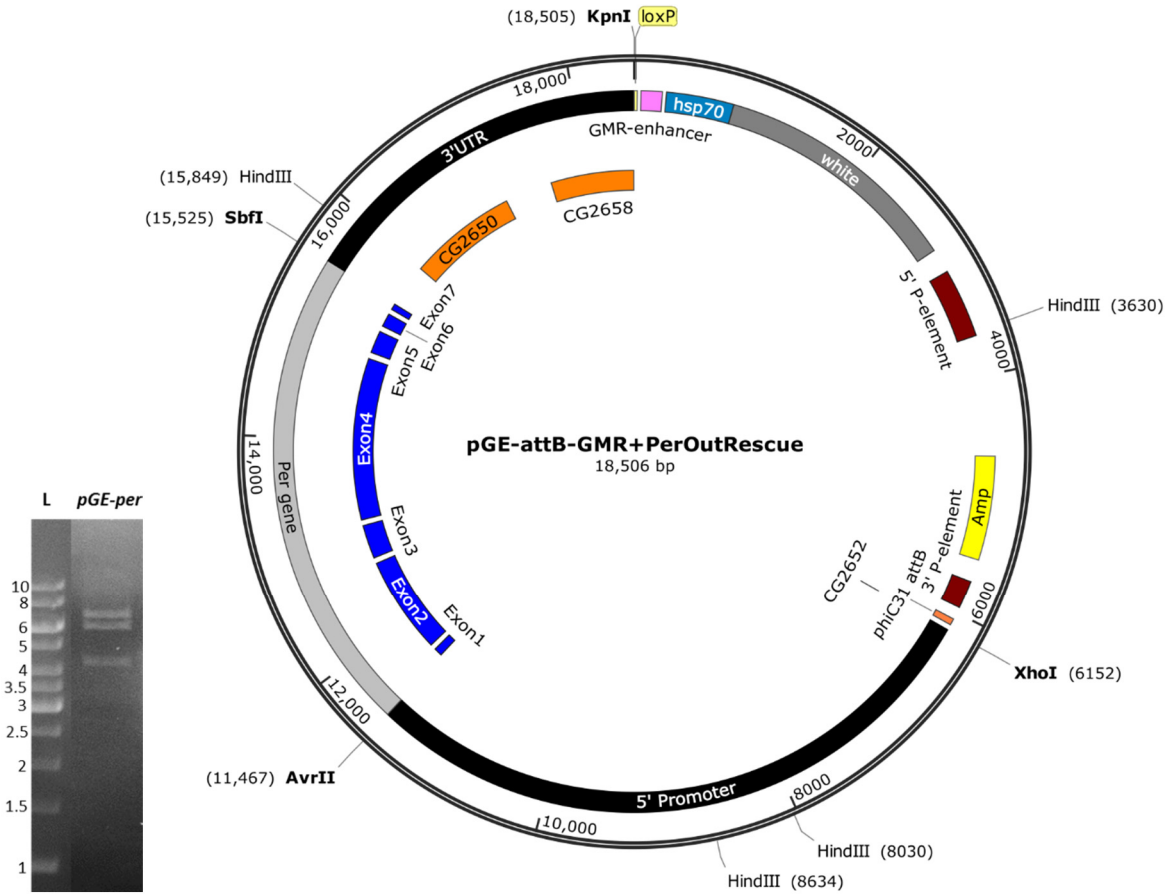

Figure 36: Rescue construct of *per*.

The vector map of the pGE-*attB*-GMR vector plus the complete rescue locus for the knockout of *per* is displayed. The area was subdivided into three units (*3' UTR*, *per* gene, 5' Promoter). The restriction sites between the single units and the vector are depicted in bold type. A test digest was done with *Hind*III, the inherent cutting sites are also listed. The result of the test digest is shown on the left side next to a gene ladder (numbers indicate the size of the rungs x1000 bp).

4.2 Ends-out targeting *tim*

4.2.1 The crosses

All numbers concerning the ends-out targeting crosses for *tim* are collected in Table 29.

Table 29: Statistics of *tim* ends-out targeting.

We started 3 attempts with slightly different settings to be successful with the deletion of the *tim* locus.

Gene	*timeless*
Target chromosome	2
3' + 5' arm (kb)	3.666 bp + 4.124 bp
Target gDNA deletion (kb)	16.828 bp
Attempts	3
Targeting crosses (30♀ x 30♂)	~ 36 (~1090 x 1090)
Screening crosses (20♀ x 10♂)	1037 (20.740 x 10.370)
Mapping crosses (3♀ x 1♂/1♀ x 1♂)	73 (44♀, 28♂, 1?[m])
PCR verified	1♀

Three attempts were necessary to end up successful. The amount of starting crosses was nearly the same compared to *per*. We also adapted the setting for the *tim* targeting in the same way. The only difference was in giving the heat shocks, explained in 3.2.15. That might be one reason for the high amount of screening crosses we obtained out of the targeting cross. Another reason should be the different genetic locus and size we targeted here. The latter should also be responsible for the small number of positive flies out of the screening cross, although the number of screening crosses was that high.

Again, the number of female positive candidates was higher compared to males. We handled them similarly to virgins or male flies, meaning we crossed them to balancer flies. For further work, we selected the red-eyed progeny.

4.2.2 Genomic verification

The gene *tim* is located on the left arm of the second chromosome. Because of that, we could not simply take male flies to screen for the loss of *tim* via PCR. But we started again with the attendance of *reaper* (Figure 37).

[m] The '?' stands for a fly that died in the food before we could notice its gender.

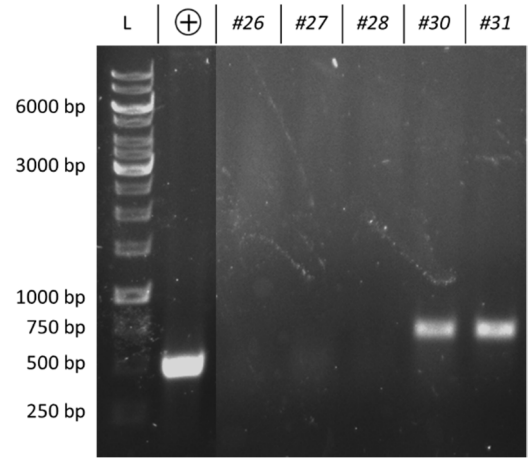

Figure 37: *Reaper* presence PCR in tim^{Out}.

As positive control, we used the pGX-*attP* vector (Figure 11) with the integrated homologous arms. The numbers on top depict the counted number of candidate flies out of the screening cross. *#26* turned out to be the right fly in the end. An additional positive control for the gDNA of *#26* was not done here. Its functionality is indirectly proven through the PCR reactions from Figure 38. Obvious size shifts between the positive control and *#30/#31* are discussed later.

All *reaper* negative flies were further tested for the location and size of the 3' and 5' homologous arm, respectively (Figure 38).

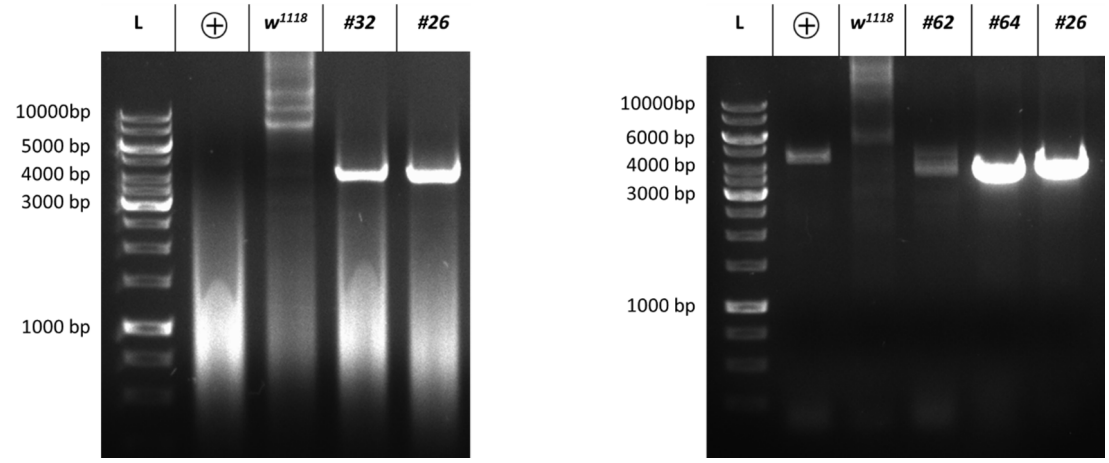

Figure 38: Proof of integration on the right spot via 3' and 5' homologeous arm PCR.

As pseudo-positive but only similar control we used the pGX-*attP* vector with the integrated homologous arms (Figure 11) we had designed at the beginning. Only *#26* showed positive results for both homology arms. For the PCR of the 3' arm we used heterozygous flies, whereas for the 5' arm we already got homologous individuals.

We found more than one individual positive for the 3' or 5' homologous arm, but only one fly that showed distinct signals for both (fly *#26*). Ongoing work was equal to *per* targeting. The DNA bands were purified, cloned into the assistance vector pJet1.2 and sent for sequencing. Thereby no greater difference to the predicted sequence was detected. The exchange of the *tim* locus with the construct cassette via double homologous recombination proceeded flawless.

After homozygous flies for tim^{Out} (from the homozygous status on we switched the name from *tim#26* to tim^{Out}) were available, we started the tests for the deletion of the *tim* locus by PCR, which confirmed the results of the former PCRs (Figure 39).

Here we used homo- and heterozygous individuals for the knockout and w^{1118} as standard positive control. Additionally, we also checked the flies for *per* to ensure, that the DNA template was properly working. The signals for *per* are not as obvious as they are for *tim*, but still they are present for all genotypes.

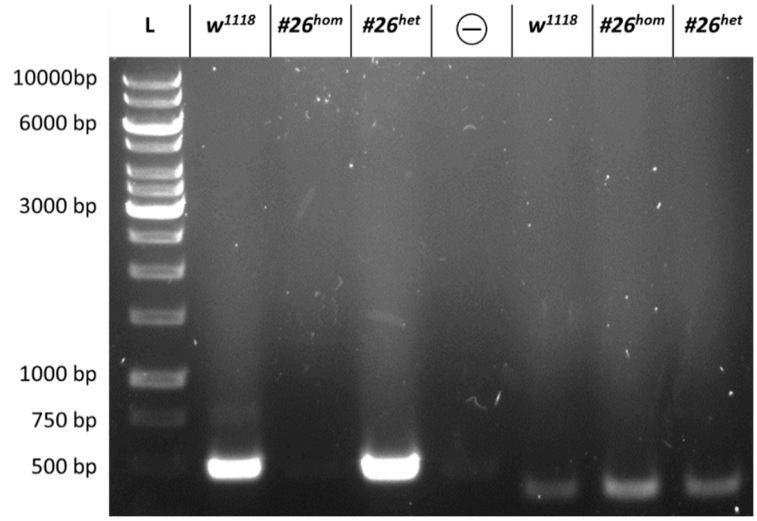

Figure 39: *tim* presence PCR.

Homozygous knockout flies were tested for the presence of the *tim* locus in this experiment. To ensure that the DNA sample is working properly, we used the same DNA for a PCR, proofing the existence of the *per* gene locus (three samples on the right side). In the homozygous *tim* knockout flies there is no signal detectable.

4.2.3 Proteome

Following cellular processes from gene to phenotype, but skipping the RNA stage, the protein level was observed (Figure 40). Additionally, we examined control flies from the tim^{Out} strain, which means, we preserved a heterozygous, *mini-white* containing line and selected the white eyed flies as homologous controls for *tim*.

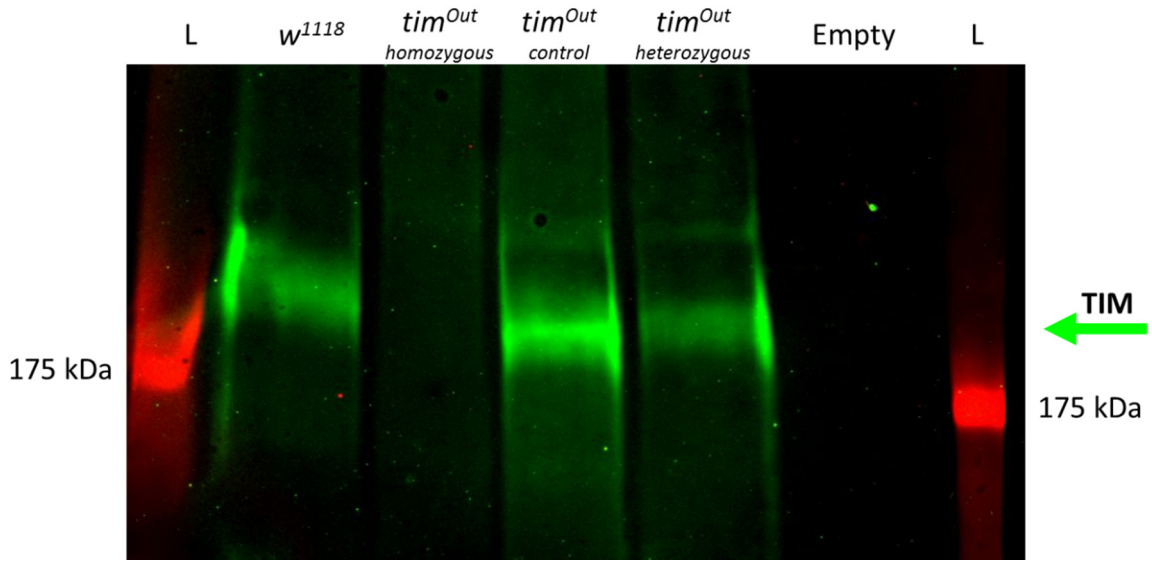

Figure 40: Western blot of *tim*^{Out} flies.

There is no TIM-specific signal obvious in homozygous *tim*^{Out} flies with the anti-TIM antibody we got from I. Edery (Sidote et al. 1998). *tim*^{Out} controls are white-eyed and thus homozygous *tim* positive. They were selected from a heterozygous *tim*^{Out} strain. Compared to their siblings, the heterozygous individuals, it is clearly visible that the protein signal in the *tim*^{Out} heterozygous flies is decreased.

The result was as clear as for *tim* presence PCR: no signal for homologous *tim*^{Out} flies. The controls showed an adequate strength in signal and the heterozygous control flies depicted a decreased level of TIM compared to their homozygous siblings.

4.2.4 Behavior

The same genotypes were also checked in behavior experiments. Free-run behavior results are summarized in Table 30.

Table 30: Periodogram analyzes from *tim*^{Out} flies.

The periods of the rhythmic flies, detected by the computer program, were averaged. The power value gives a hint for the reliability of the evaluated period. For *tim*^{Out} it is quite low and most of these flies were arrhythmic anyway. Genotypes are explained in detail in the main text.

Genotype	Quantity (n)	Period (SEM)	Power (SEM)	Arrhythmicity
w^{1118}	12	23.58 (0.069)	20.64 (1.59)	0%
tim^{01}	15	26.26 (1.622)	14.91 (1.16)	46.67%
tim^{Out} *white*	15	23.89 (0.622)	19.99 (2.51)	13.33%
tim^{Out}	29	32.19 (0.893)	15.03 (0.55)	75.86%

It is obvious, that despite the fact that *tim*^{Out} are not totally arrhythmic, they are still less rhythmic than *tim*^{01} flies (Figure 41) and also show a low power value. In addition, the few rhythmic flies display an extremely long free-running period, which is longer than in *tim*^{01} flies.

A look on the actograms, which are an average of all flies of the experiment, shows no discernible rhythm in the *tim*^{Out} flies. Even under LD conditions there is no morning or evening anticipation. Only the lights-on/-off peaks represent a disruption of the otherwise more or less flat activity curve throughout the day. The evening peak of the *tim*^{01} flies is shifted towards the night. They also show an evening anticipation.

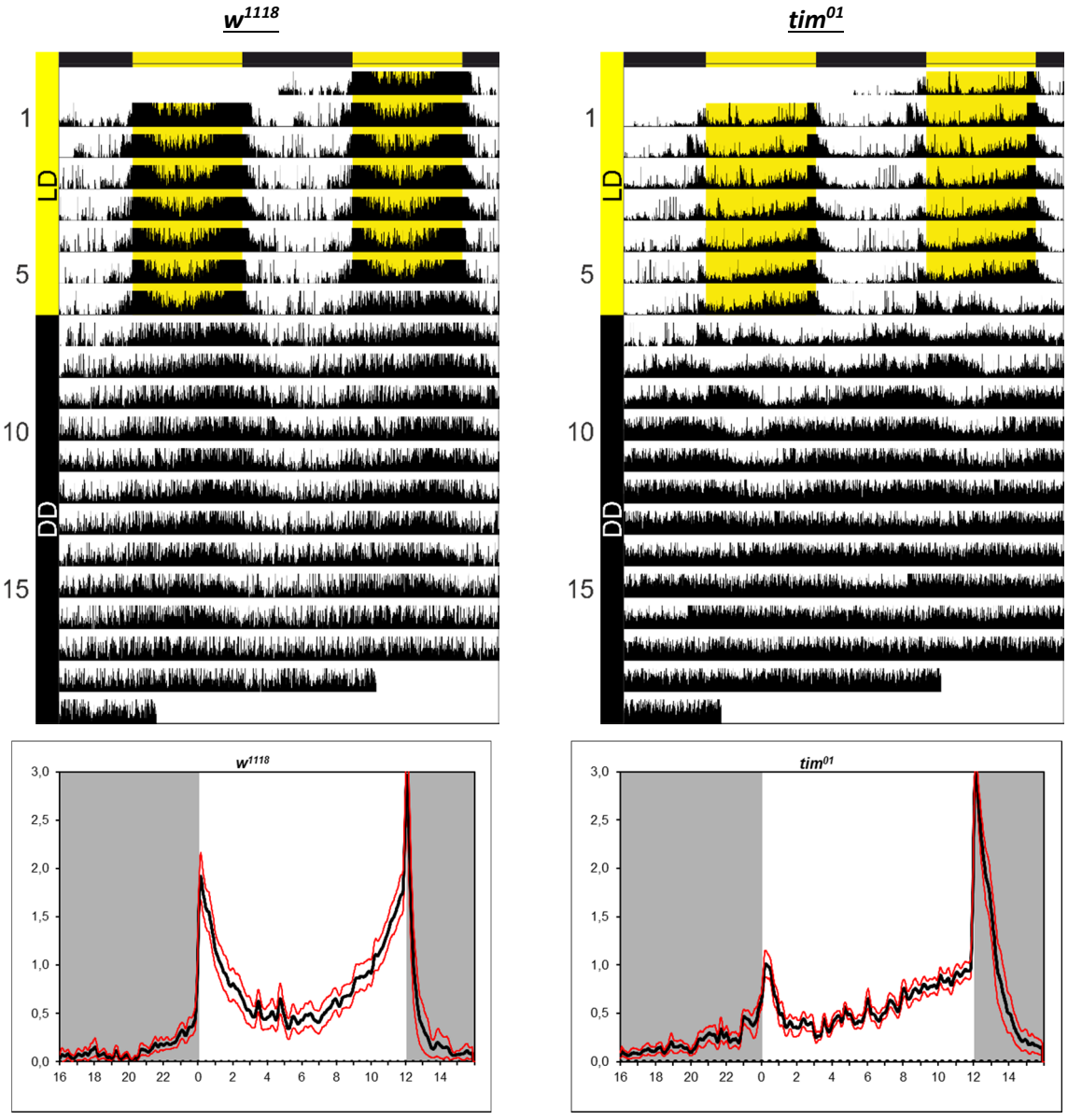

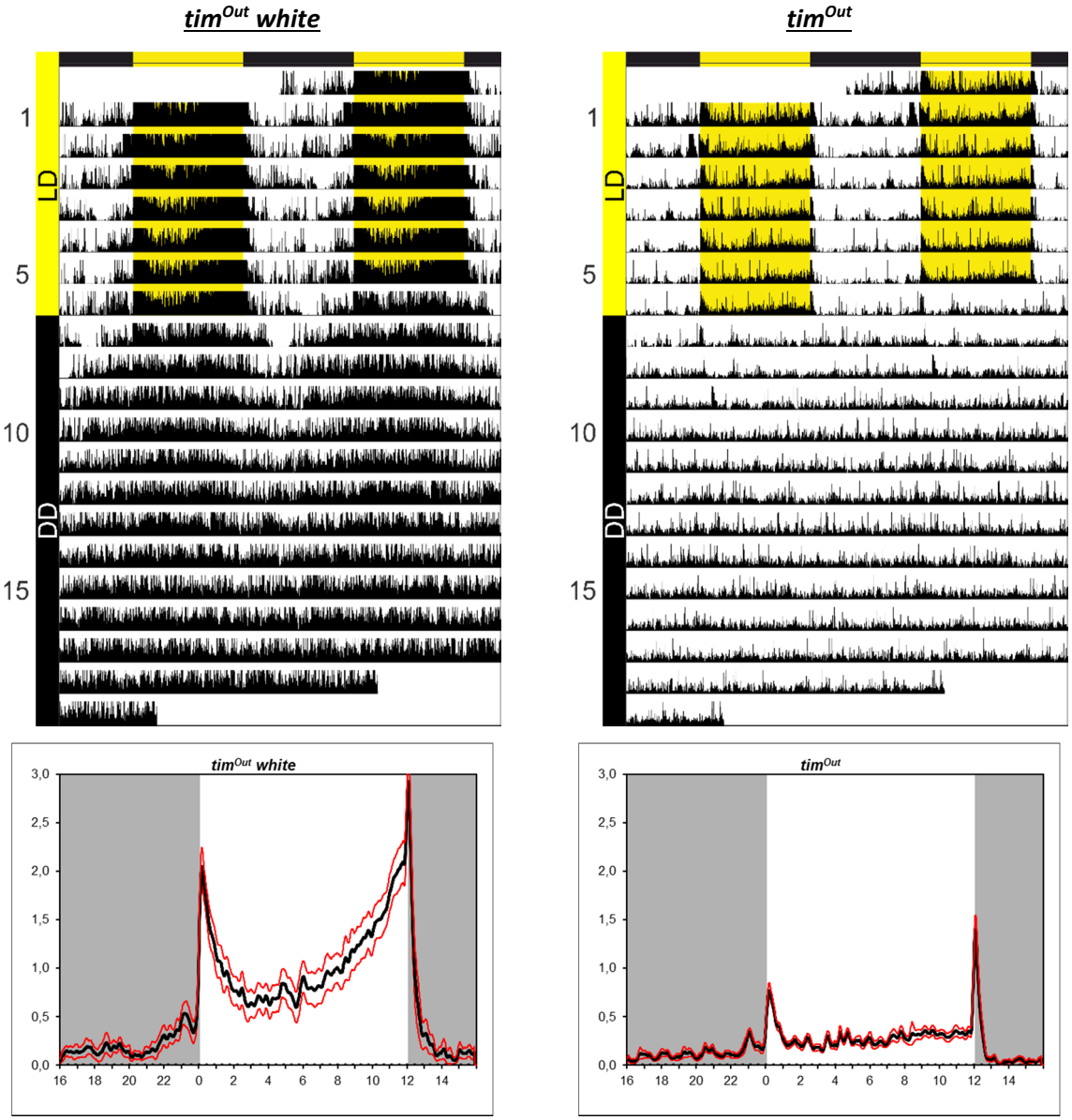

Figure 41: Average actograms and average day graphs from behavior experiments of *tim*^{Out}.

For each genotype the actogram for the whole timespan of the experiment (upper figure) and an average day graph for the LD part of the experiment (lower graph) is shown. Black bars show crosses of the light beam inside the monitor by the fly. Numbers on the left side count the days of the experiment. The yellow/black bars on top show the existing light regime of the first 6 days. For a better view yellow background also shows timespans with lights-on. All flies of the behavior experiment were averaged. In the average day graphs, the dark phase is deposited with grey background. ZT values are plotted on the X-axis, whereby ZT0 means lights-on. N values are: *w*^{1118} = 14, *tim*^{01} = 15, *tim*^{Out} *white* = 15, *tim*^{Out} = 30.

4.3 Construct for the *tim* rescue

4.3.1 Prologue - *tim* editing

Our focus of attention was drawn close to the *tim*^{UL} mutation site. The trigger therefore came from former, yet unpublished studies of F. Cao and N. Peschel back in 2012. The scientists sequenced *tim* cDNA of different time points from *Drosophila melanogaster* and observed nucleotide and time point

specific differences in the sequence of the transcripts among themselves and compared to the gDNA. Because the changes were restricted to a certain time window and always encompassed only changes from adenine to guanine, they postulated that modification by RNA editing could be the reason. RNA editing is a process, through which some single cells are able to apply discrete changes to the sequence of their RNA molecules, after they are transcribed by the RNA polymerase. For an overview of the described part concerning the *tim* genetic region, Figure 42 is recommended.

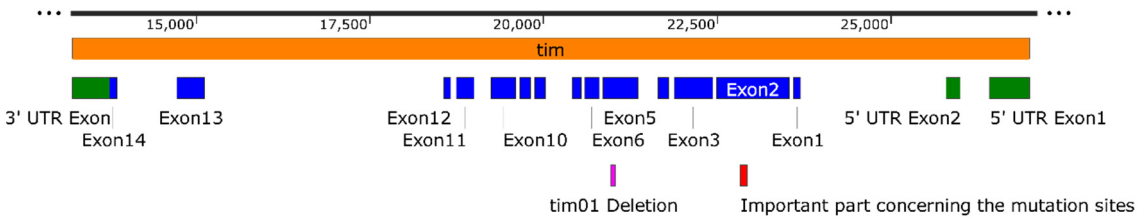

Figure 42: Gene region of *(s-) tim*.

Translated exons of the PD-transcript of *tim* are depicted in blue. Green exons do not exist in the protein, but belong to the *tim* transcript. A purple bar marks the area that is deleted in the tim^{01} mutation, which leads to a frameshift in the reading frame and with that to a truncated, not functional protein in the end. Upstream of this site, another part is shown in red. This region is determined as an intron in some transcript isoforms and contains the mutation site for the tim^{UL} mutation and the two editing sites.

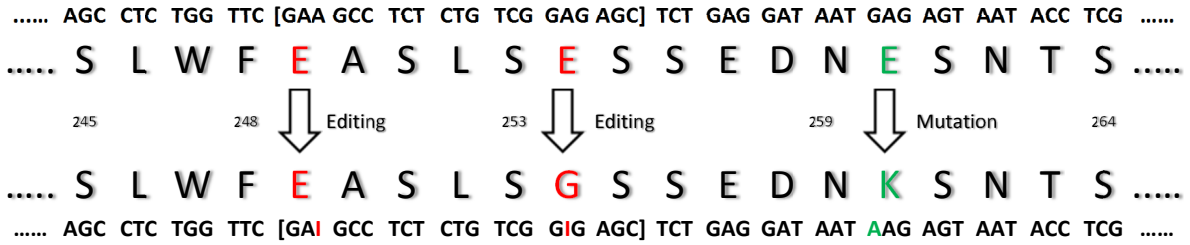

Figure 43: *tim* region affected by editing on the level of nucleotides and AA.

Single letters stand for the AA sequence of TIM starting at number 245 and ending with AA 264. The upper row is without editing and mutation. Red letters show the sites affected by the editing process. Only the second site leads to an AA exchange from glutamic acid to glycine. The tim^{UL} mutation is shown in green (E260K). Corresponding nucleotide codons are depicted above and below. 'I' stands for inosine and is the result of the deamination by the ADAR (adenosine deaminases acting on RNA) enzyme. Please note, that the sequence here is depicted in reverse complementary orientation referred to the chromosome, but N- to C-terminal related to the protein. The part in between the square brackets is sequenced in Figure 44. The small numbers between the AA strands indicate the numbers of the residues inside the TIM polypeptide. The AA numbers are concerning the *s-tim* isoform that is depicted on http://flybase.org.

The area depicted as a red beam in Figure 42 is 96 bp long and in most, but not all of the known *tim* transcripts read as a part of exon 2, but sometimes also spliced out as an intron. Both detected editing sites and the tim^{UL} mutation lie inside this region. A section of it is shown in Figure 43. The AA sequence is written in standard abbreviation letters. Corresponding codons are depicted above and below, respectively. Only the second editing leads to an AA exchange.

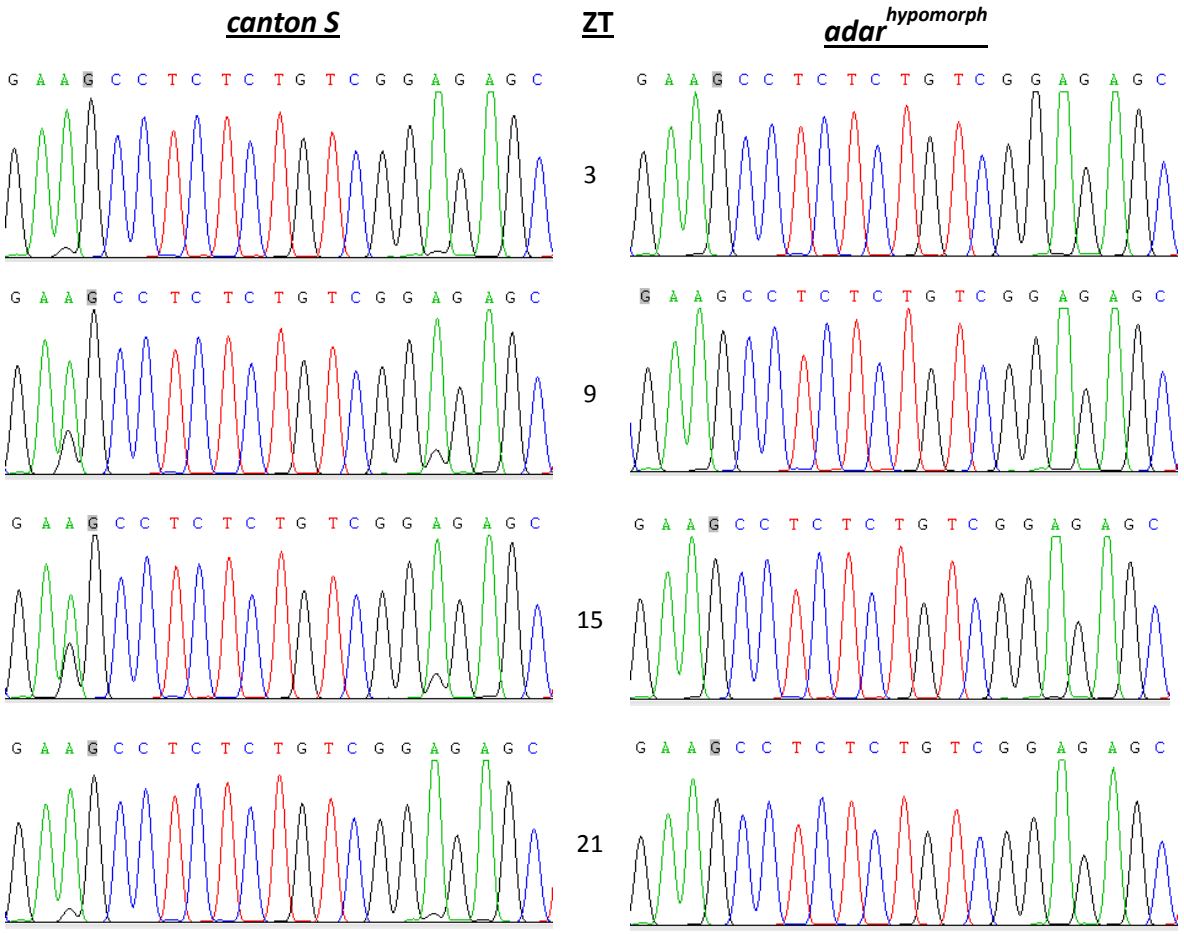

Figure 44: Sequencing results of different time points in *adar*^{hypomorph} and wild type (*canton S*) flies.

The locus inside *tim* containing the editing sites was sequenced and is compared in this figure. It is obvious, that at the third nucleotide from the left (adenine) and the fifth nucleotide from the right (adenine) a second smaller peak appears next to the main adenine signal. This peak increases until ZT 15 and exhibits a polymorphism of adenine for guanine. In *adar*^{hypomorph} (*adar*^{hyp}) flies, this phenomenon is not detectable (graphs taken and modified from N. Peschel).

Possible consequences for the AA exchange, the proximity of the editing sites to the *tim*^{UL} mutation, altering possibilities for phosphorylation sites and the location inside this putative intron renders a great variety of ideas for discussing the question, why.

First, there was the idea of a variety in RNA folding. When making RNA folding predictions for both sequences with or without editing, the differences are not serious, but still obvious. There are a lot of online tools for calculating RNA secondary structures and all show deviations, but small ones compared to the whole RNA molecule, impairing only a single loop structure (Figure 45). Since these results were not that striking, we primarily skipped further research in this field.

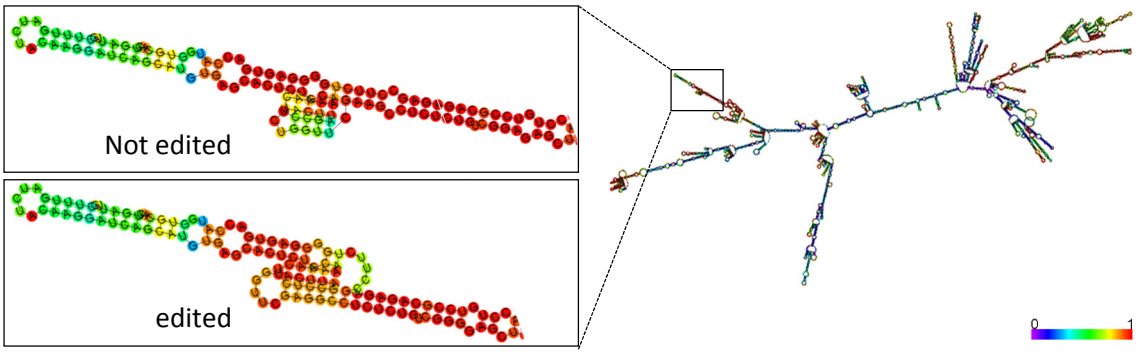

Figure 45: Secondary structure prediction for the *tim* mRNA-molecule with and without editing.

The RNA of the *tim-TD* transcript in total without editing is shown on the right side. The sequence inside the small rectangle confers to exon 2 of this transcript, especially on the part, where the editing sites are located. A magnification is depicted with and without editing on the left side. This is only one example for a prediction, which was made with the RNAfold WebServer from Vienna University (http://rna.tbi.univie.ac.at/cgi-bin/RNAfold.cgi). It should only serve as an example. The colors in the secondary structure plot give reliability annotation from positional entropy and base-pairing probabilities.

Furthermore, we had a look on the RNA expression levels of *adar* compared to *tim*, to see whether ADAR levels are expressed rhythmically or if the editing process is somehow regulated in a time dependent manner. It is clearly observable, that *adar* mRNA expression levels are not changing, so the theory of regulatory variances should be taken into count in more detail (Figure 46).

Interestingly, the comparison within the *Drosophila* genus shows that a few species already established the first adenine to guanine editing base-exchange in their genome. However, that does not apply for the second exchange. The juxtaposition shows, that the rest of the sequence seems to be highly conserved over the whole genus. Often, this is an indication for a functional unit or other important structures (Figure 47).

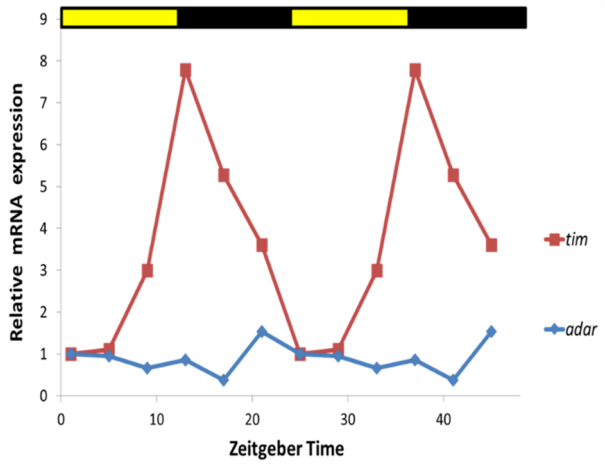

Figure 46: RNA expression levels of *adar* and *tim*.

Whereas *tim* mRNA expression cycles throughout the day, adar mRNA levels stay unaltered. LD cycles are indicated on top.

Drosophila species	Sequence
Melanogaster	TGGTTCGAAGCCTCTCTGTCGGAGAGCTCTGAGGA
Simulans	TGGTTCGAAGCCTCTCTGTCGGAGAGCTCTGAGGA
Erecta	TGGTTCGAAGCCTCTCTGTCGGAGAGCTCTGAGGA
Sechellia	TGGTTCGAAGCCTCTCTGTCGGAGAGCTCTGAGGA
Yakuba	TGGTTCGAAGCCTCTCTGTCGGAGAGCTCTGAGGA
Eugracilis	TGGTTCGAAGCCTCTCTGTCGGAGAGTTCTGAGGA
Biarmipes	TGGTTCGAAGCCTCTCTGTCGGAGAGTTCTGAGGA
Takahashii	TGGTTCGAAGCCTCTCTGTCGGAGAGTTCTGAGGA
Elegans	TGGTTCGAAGCCTCGCTGTCGGAGAGTTCTGAGGA
Miranda	TGGTTCGAGGCATCGCTTTCGGAGAGCTCCGAGGA
Persimilis	TGGTTCGAGGCATCGCTTTCGGAGAGCTCCGAGGA
Pseudoobscura	TGGTTCGAGGCATCGCTTTCGGAGAGCTCCGAGGA
Kikkawai	TGGTTCGAGGCCTCGCTCTCGGAGAGCTCCGAAGA
Mojavenisis	TGGTTCGAGGCATCGCTGTCGGAGAGCTCCGAGGA
Bipectina	TGGTTCGAGGCTTCGCTCTCCGAGAGCTCGGAGGA
Ananassae	TGGTTCGAGGCTTCGCTCTCCGAGAGCTCGGAGGA
Ficusphila	TGGTTCGAGGCCTCCCTCTCCGAGAGCTCCGAGGA

Figure 47: Comparison of the editing locus.

Some Drosophila species already exchanged the adenine to guanine in their genome making an editing event obsolete.

Next, we had a look at the behavior of flies with a reduced ADAR level. Because *adar* null mutations are lethal, $adar^{hyp}$ animals were investigated. These animals, generated by Jepson et al. (Jepson et al. 2011) (more details in 2.5), are not very healthy and display no strong rhythmic behavior under constant darkness (DD) conditions. Under LD $adar^{hyp}$ animals show a strongly diminished evening activity peak.

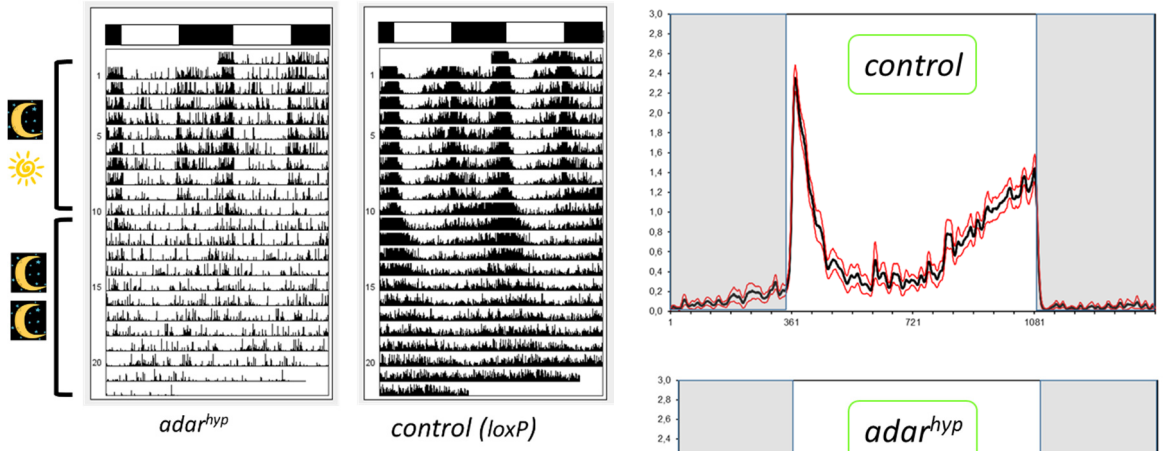

Figure 48: Behavior under LD12/12 and free-run.

To generate appropriate control animals the *mini-white* inside the *adar* locus of *adar*^{hyp} was deleted through a flox-out. Example actograms of single flies with the LD cycle indicated on top are shown above. Average activities during the LD cycle are plotted on the right side.

Another astonishing observation on the behavioral level was that the induced weak rhythmicity and the absent evening peak for *adar*^{hyp} flies can be rescued by the *tim*^{UL} mutation (Figure 49). The reason might be the antagonistic effect of the *tim*^{UL} mutation and the *adar*^{hyp} animals with regard to their CK2 phosphorylation (2.4.2).

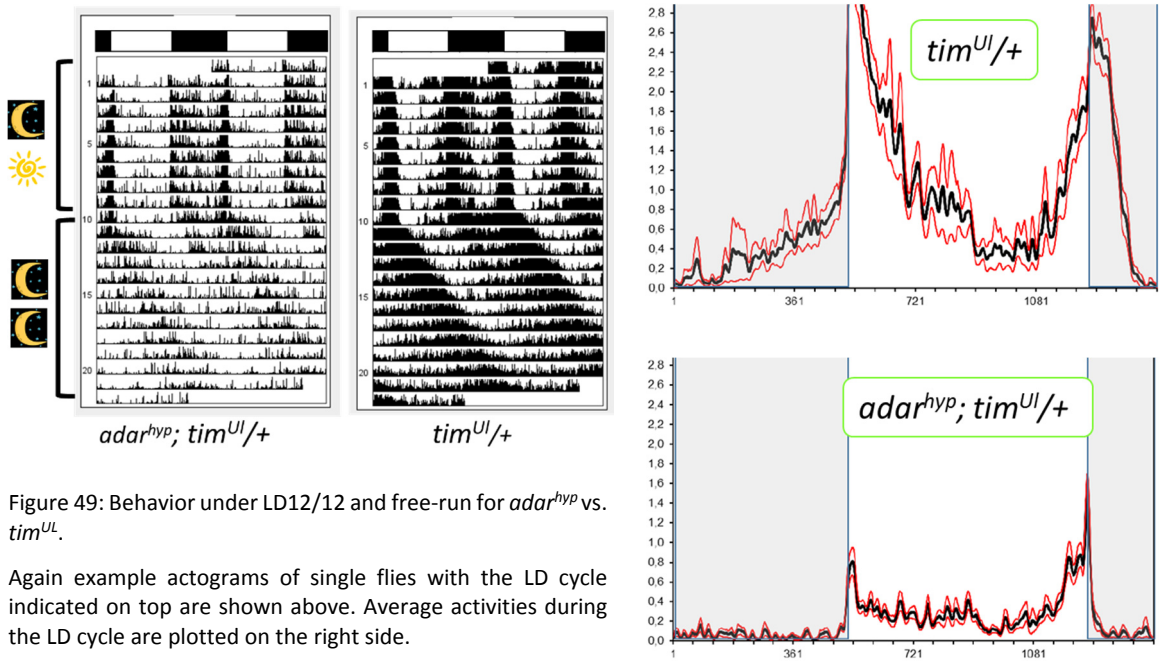

Figure 49: Behavior under LD12/12 and free-run for *adar*^{hyp} vs. *tim*^{UL}.

Again example actograms of single flies with the LD cycle indicated on top are shown above. Average activities during the LD cycle are plotted on the right side.

Table 31: Rhythmicity in free-run conditions, numbers and statistics.

The period and appertaining power values are shown with standard deviation. 16 male flies were tested in each experiment. The percentage of rhythmic individuals is indicated, too.

Genotype	n	% Rhythmic	Period ± SEM	Power ± SEM
adar^{hYP}	16	18,75	26,60 ± 1,49	1,6 ±0,24
control (loxP)	16	93,75	24,40 ± 0,11	11,47 ± 2,04
control tim^{UL}/+	16	75	26,04 ± 0,23	2,6± 0,41
adar^{hyp}; tim^{UL}/+	16	100	26,06 ±0,08	18,09± 1,76

In a work from Meissner et al., 2008 (Meissner et al. 2008), the authors showed that the expression of a dominant negative form of CK2α (called *Tik*) leads to a couple of interesting phenotypes. First, a long behavioral rhythm[n] of ~30 (Meissner et al. 2008)/~33 h (Smith et al. 2008) and just a weak oscillation of TIM and *tim* mRNA levels, when *Tik* is expressed homozygously in all circadian cells. Additionally, TIM remains mostly cytoplasmic in the LN_vs of these animals, too, but exposure to a LD cycle can restore a robust cycling of both, TIM and *tim* mRNA (Meissner et al. 2008). They also already linked *tim^{UL}* and the CK2 phosphorylation activity by postulating that *Tik* and *tim^{UL}* might affect the same molecular pathway due to phenotypic similarities. That was, why N. Peschel and F. Cao also made predictions for possible phosphorylation sites of certain kinases on serine residues located close to the editing sites. For the calculations, they used an online tool named NetPhosK 1.0, published by N. Blom et al. (Blom et al. 2004). They observed that editing changes the probability of a phosphorylation event on two putative phosphorylation sites next to the second edited adenine. Additionally, we did the same for the *tim^{UL}* mutation. Interestingly the prediction revealed a changed kinase score for CK2, also true for the *tim^{UL}* mutation. The results of the predictions are shown in Figure 50. Figure 51 shows the result of a western blot from head extracts of *adar^{hyp}* and wild type flies, stained with an anti-TIM antibody (3.1.4.1). It is recognizable that the signal for TIM always tends to run slightly higher than in the wild type flies – an indication for an increased protein size. This is also another hint for an additional phosphor residue due to CK2 activity that is not observable, if there is no ADAR specific editing, because of the reduced ADAR levels in *adar^{hyp}* flies.

[n] Different provided statements. Both paper used the same *tim-GAL4–62* driver line.

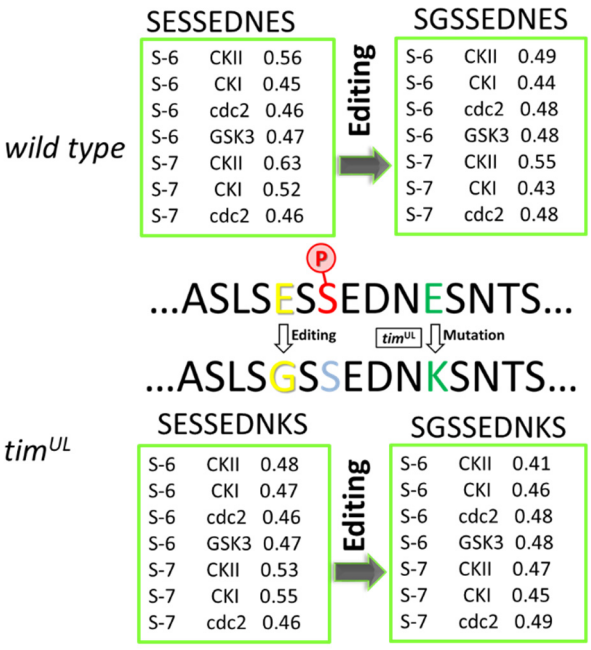

Figure 50: NetPhosK prediction of phosphorylation events by certain kinases.

Casein kinase 1 and 2 (CK1 and 2), the cyclin dependent kinase 2 (CDC2) and GSK3 were tested. For wild type and *tim*^{UL} specific AA sequence, with and without editing, respectively. The score for CK2 was the highest and therefore the most probable one. In both cases – editing and/or *tim*^{UL} mutation - the probability of a phosphorylation event is decreased. The value for CK1 is also quite high, but CK2 was suggested as a *tim* modifying kinase before (Meissner et al. 2008). For a better overview, the AA sequence with editing, mutation and phosphorylation site is depicted in between.

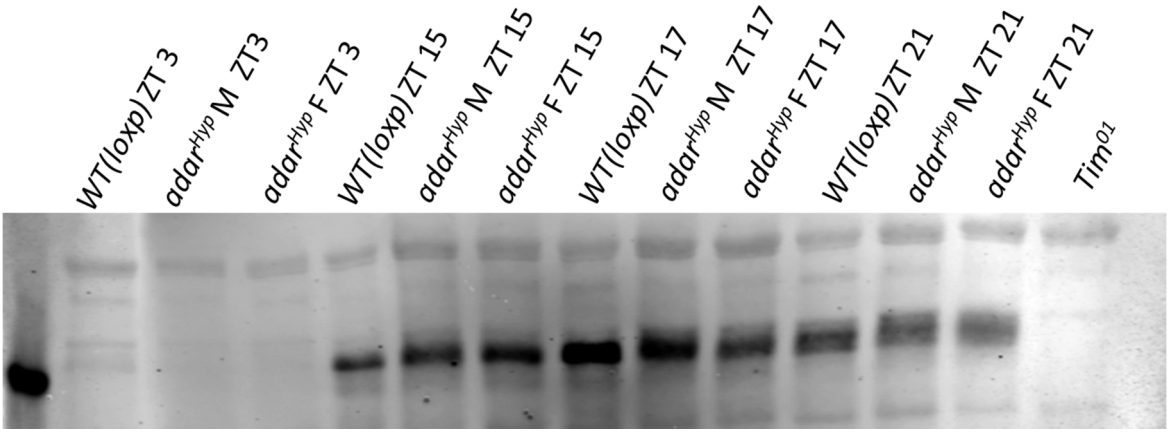

Figure 51: anti-TIM western blot of *adar*^{hyp} and wild type flies.

Whole head protein extracts of *adar*^{hyp} male (M) or female (F) animals have the tendency to hyperphosphorylated TIM protein, compared to the wild type (*loxP*) control. This is confirming the suspicion, that unedited TIM protein is phosphorylated by CK2. *tim*^{01} serves as negative control to confirm the antibodies' binding affinity. Four different time points, taken out of a 12/12 LD cycle are shown. Blot made by F. Cao.

A possible next step for us was to observe if the expression of only one type of editing would somehow interfere with the phenotype of the flies. Four different possibilities are conceivable: editing on only one or both sites, or no editing at all. To simulate a permanent editing event, we exchanged the adenosines with guanosines at these sites. Because this was much easier to be achieved with the CDS of *tim* only, we decided to couple these questions to the *tim* knockout project and designed a rescue through the GAL4-UAS system with different constructs containing the exchanges to mimic a permanent editing at the mentioned locus in the above discussed possibilities. The integration then was done via P-element insertion followed by selection of a hit on the second chromosome. The

expression of only one form of rescue construct in the *tim* knockout background should possibly show differences in the phenotype of the flies.

4.3.2 Design of the *tim* rescue constructs

For verification of a successful recloning experiment, we just sequenced the important sites inside the vectors. These are shown in Figure 52.

……	CGA	GGT	ATT	ACT	CTC	ATT	ATC	CTC	AGA	GCT	CTC	CGA	CAG	AGA	GGC	TTC	GAA	CCA	GAG	GCT	……
……	CGA	GGT	ATT	ACT	CTC	ATT	ATC	CTC	AGA	GCT	CTC	CGA	CAG	AGA	GGC	CTC	GAA	CCA	GAG	GCT	……
……	CGA	GGT	ATT	ACT	CTC	ATT	ATC	CTC	AGA	GCT	CCC	CGA	CAG	AGA	GGC	TTC	GAA	CCA	GAG	GCT	……
……	CGA	GGT	ATT	ACT	CTC	ATT	ATC	CTC	AGA	GCT	CCC	CGA	CAG	AGA	GGC	CTC	GAA	CCA	GAG	GCT	……

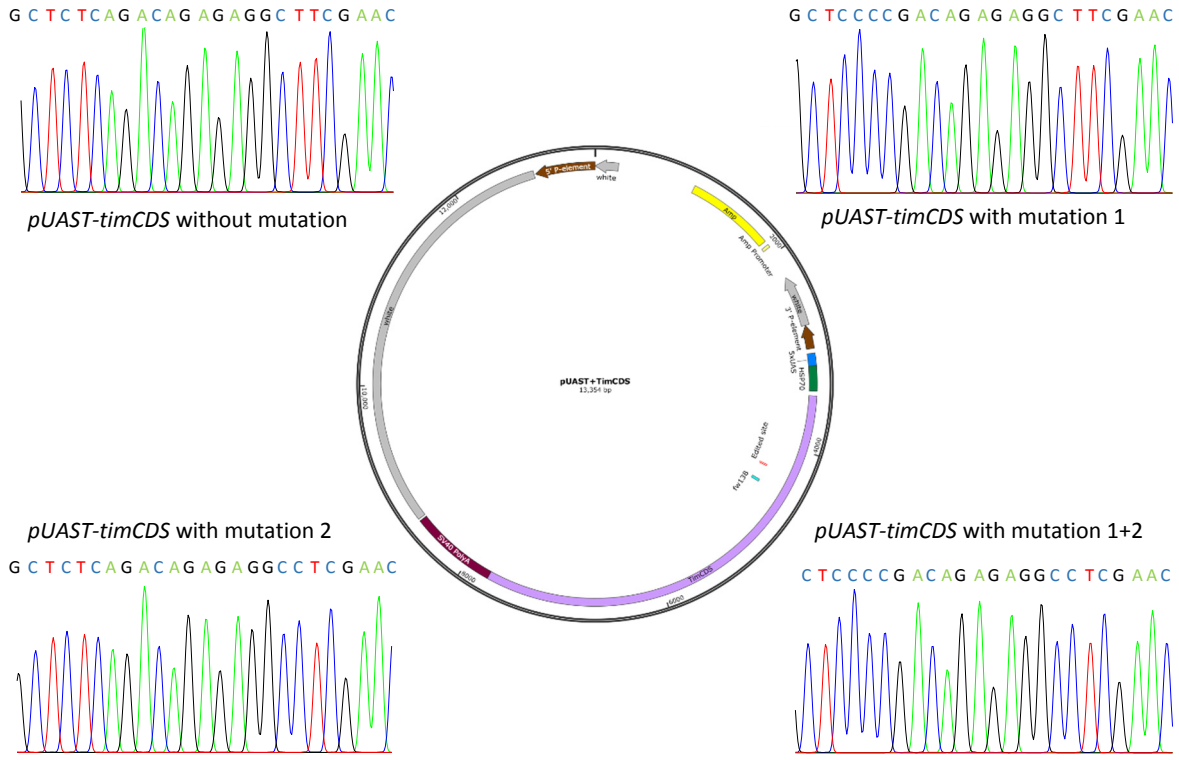

Figure 52: Result of the cloning process of the pUAST-*timCDS* constructs.

The sequence on top is the same as in 4.3, but in reverse complement orientation for a better comparison with the sequencing results shown below. The part, that was sequenced, is shaded in yellow. The bases, that should be mutated, are indicated in red. There are two more mutations in two constructs, but these do not lead to any changes in the AA sequence. The vector map in the center shows the pUAST-vector with an integrated *tim* CDS. Primer Fw138 was used for sequencing.

5 Discussion

5.1 The ends-out targeting technique

We made some small adaptions in the ends-out targeting procedure as they are described in paragraph 4.1.1., concerning mainly the fly handling. Particularly for labs with limited manpower - like ours - it is important to reduce the workload that is mainly due to the high amount of flies that have to be kept and screened. Although we used the same procedure - and wherever possible - also the same driver and balancer strains, we observed genome locus specific differences in both targeting experiments. This became apparent mainly in the number of red-eyed positive flies that we found in the offspring of the screening crosses – an indication for the accessibility of the target locus, for the size of the generated deletion and the design of the homology arms.

5.2 Generating the knockout strain for *per*

5.2.1 Why ends-out targeting of *per*

Often, the question arose why we did not use the CRISPR/Cas9 system for the project? Simply, the boom of this new genetic tool came up in 2013 (Bassett and Liu 2014), but we started in 2011 with the planning procedure. Additionally, a knockout of such a big locus was not often done, at least not with the CRISPR/Cas9 system.

One motivation for our work was the missing, clear defined knockout mutant for *per*. So far, most work with *per* null mutants was done using the per^{01} allele, which is going back to the 70s of the last century (Konopka and Benzer 1971). But there is a residual *per* mRNA (Hardin, Hall, and Rosbash 1990) and also a residual rhythmicity described for per^{01} animals by a handful of authors (Helfrich and Engelmann 1987, Dowse, Hall, and Ringo 1987, Helfrich-Förster 2001, Menegazzi, Yoshii, and Helfrich-Förster 2012, Bywalez et al. 2012). In detail, they claimed that a fly with dysfunctional circadian system should on the one hand show an unlimited range of entrainment[o] under LD cycles and on the other hand display a simple lights-on/-off reaction. But in per^{01}, the entrainment range was limited and the mutant flies started their activity before lights-on (Helfrich and Engelmann 1987). Residual PER could not be proven until today, but is a component of hypothesis and explanations (Collins et al. 2005, Kempinger

[o] Meaning, the flies should be able to adapt and react directly to lights-on/-off independent of the applied LD regime. Instead, the animals prolonged their activity into the dark phase in short cycles and started prematurely in long LD periods.

et al. 2009). One future task thus will be to perform comparable studies with per^{Out} and per^{01}, to see if and what differences occur on all levels from RNA to behavior.

The initial idea behind the project actually was not the knockout of *per*, but to create a fusion protein consisting of PER and a fluorescence tag like GFP or a luminescence protein like luciferase, since those tools are not existing to date. This was supposed to be done for PER and TIM with different labels, emitting significantly distinct wavelengths, thus being able to be activated and detected next to each other in the same sample. One big advantage of the ends-out targeting method is the generated founder line carrying the *attP* site in the genome at the place of the native gene locus. This site can be used for site specific recombination to insert any rescue construct with a reasonable work load.

5.2.2 Genetic design of *per* knockout and rescue

All *in silico* preplanning and BLAST analyzes were based on actual sequence data reported in FastA format on http://flybase.org (June 2011 – March 2015) for *Drosophila melanogaster*. We did not use gateway cloning, especially for rescue cloning, because for the integration into the genome of the flies either through P-element insertion or phage induced site specific recombinase, we had to stick to certain vectors (Figure 11, Figure 12) containing essential elements for these procedures. These vectors were generated earlier and were repeatedly modified or improved (Gong and Golic 2003, Huang et al. 2008, Huang, Zhou, Dong, Watson, et al. 2009, Huang, Zhou, Dong, and Hong 2009, Maggert, Gong, and Golic 2008). They are not available for gateway cloning.

5.2.2.1 The knockout

Actually, we had three options how to design the knockout. The first option with the smallest construct: deletion of the CDS region of *per* only, beginning with the start codon (*ATG*) of translation until the stop (*TAG*). The second possibility was to additionally include the 3' and 5' *UTR*s in the recombination-based exchange. The advantage would be that also putative regulatory sequences concerning the transcript would be deleted. Finally, we decided upon a third option (largest construct), a knockout of the whole genomic region including putative 3' and 5' regulatory regions, but without disturbing neighboring genes. For *per*, that was unconvertible, because *CG2650*, the next gene in downstream direction, shares overlapping *UTR* sequences with *per*. So we included the - as noncoding described - regions next to *per* and *CG2650* and placed the homologous arms over the genes *HLH3B* and *CG2652* upstream and *CG2658* downstream of the knockout locus. In future, a partial rescue including gene *CG2650* should determine its possible influence on the clock or other phenotypes (see also 5.1.3.1). Due to the cloning procedure, a small piece (the part between the *attR*/*L* and restriction site) is left between the homology arm and the knockout region in the end. We ensured, that the

border lies over an unimportant region (if known so far and defined as not conserved regions by BLAST analyzes).

5.2.2.2 The rescue

A first rescue construct should include all genomic parts, which were deleted with the exchange of locus and construct, to restore the native phenotype. Hence, the natural phenotype should be recovered, unless we had accidentally disturbed other important genomic structures. The reason, why we divided the rescue in three parts and therefore even substituted a few bases, was on the one hand to avoid cloning the rescue construct with a size of over 18 kb in one step and on the other hand because of further planed rescue constructs. The advantage of this procedure is the generation of a plasmid, in which certain functional parts can be exchanged or additional tags getting inserted at different positions.

5.2.3 The result – *per^{Out}* and the duplicated region

Genomic verification for *per* knockout was achieved more easily than for the *tim* locus, since *per* is located on the X-chromosome and male individuals carry only one allele. A quick observation of the eye color distribution of the male offspring was enough to map the insertion of the construct to the X-chromosome (detailed explanation see Figure 21 and Figure 22). All X-selected males were then checked for attendance of the *per* locus by a simple PCR. In Figure 29 (and also Figure 28) faint bands can be seen in fly *#11* (the later proven *per^{Out}* individual) and the negative control. The reason for this should be contamination. First, because all following tests verified the knockout, and second, due to our used gDNA extraction process. Since we had to make the compromise between being fast and productive besides being exact and we extracted gDNA from many strains in parallel, it is well conceivable, that contaminations could have happened. To ensure this, we additionally performed a second test and screened for the absence of the *reaper* locus, that should not be observable in case of a positive integration event.

We often found integration events on the X-chromosome due to single homologous recombination. These flies showed positive signals for one of both homologous arms and in most cases also for *reaper*. Therefore we always checked both sides of the knockout locus and verified them again by sequencing.

The same result, a complete knockout, was obtained by screening the RNA of *per^{Out}* flies for *per* mRNA existence. Because *per^{01}* is a loss of function allele due to a single point mutation (Yu et al. 1987) and the cDNA primers used in this experiment bound to the still expressed part of *per*, these flies showed a mRNA signal (Figure 32). Also the positive control – gDNA from *w^{1118}* flies – showed a faint band. This

was a first unexpected result, because the primers were designed over exon-exon borders to exclude gDNA from being template for the polymerase. It is most likely, that a small portion of primers nevertheless bound to the genomic DNA, leading to a faint signal. An improved annealing temperature or adjusted primer design should help in this case.

Proteome investigations via western blot strengthened the result of a clear knockout of *per* (Figure 33 and Figure 34). Neither the commercial anti-PER antibody from Santa Cruz Biotechnology Inc. directed against an epitope corresponding to AA at the C-terminus (AS925-1224) of PER, nor an antibody raised against full length PER, expressed in a baculovirus expression system (Stanewsky, Frisch, et al. 1997) (a kind gift from R. Stanewsky), did detect PER protein at the presumed highest level around ZT20 or at any time point during the light phase. The commercial anti-PER antibody is not able to detect PER^{01} residual protein, which is a truncated form of PER ending at AS464 (Yu et al. 1987) (see also Figure 34 and paragraph 2.3.1). The anti-PER antibody from Liu et al. could theoretically prove the truncated PER^{01}, but we were not able to detect any specific signal. This coincides with the common literature, according to which no PER^{01} detection was described so far.

Unfortunately not everything worked out as imagined. The knockout of *per* succeeded, but with small blemishes. Obviously, the homologous recombination was incorrect at least on the 3' site. An area of ~2.5 kb was inserted in the 3' homologous arm compared to the original genome (see Figure 31). This encompasses mainly sequences from the 5' homologous arm inserted in reverse direction. Fortunately, the incorporation took place exactly in between gene *CG2658* and *CG2662* and did not disturb any open reading frames. Putative effects should therefore rather be due to the duplicated region of the 5' homologous region (comprising a part of *CG2652* and total *HLH3B*) than emerging from the disruption of the 3' homologous arm, although the non-coding part between *CG2658* and *CG2662* is not really large. But these putative consequences first have to be measured. Hints are maybe given from knowledge about these genes that was acquired so far. For that reason, we first designed a rescue that should exactly encompass the original sequences. Comparable studies with w^{1118} flies (the wild type that was used for the insertion of the recombination constructs at the beginning) are thus intended and are getting injected with the rescue plasmid at the moment.

To date we can say, that the knockout - despite of the duplication - yielded in viable, fertile and externally healthy flies with no observable striking extrinsic phenotypes. This is true for hemizygous males as well as for homozygous females.

Under LD conditions, the per^{Out} flies show a similar behavior like tim^{Out}: neither morning nor evening anticipation or midday trough in activity was observable. The activity curve increases slowly throughout the day, starting after lights-off at its minimum and ending before lights-off at its

maximum. The only distinct disruptions are the lights-on/-off reaction peaks in activity. *per*^{01} looks similar, but here the start/end of the slope is after/before lights-on shifting the major proportion of activity into the dark phase (Figure 53).

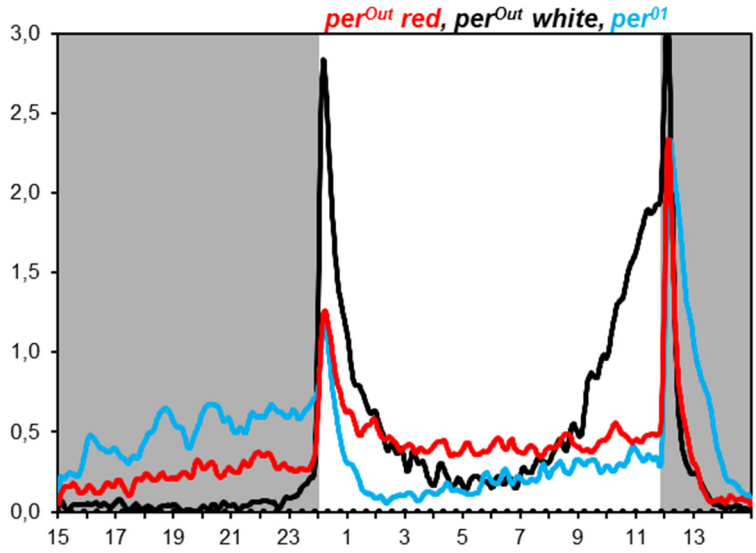

Figure 53: Direct comparison of *per*^{Out}, *per*^{01} and control.

Only male flies were used for behavioral experiments. Red and white is concerning the eye color of flies out of a heterozygous strain. Red eyes showing a knockout because *per* is exchanged with the *mini-white*. The x-axis shows the ZT values, starting with ZT0 = lights-on. On the y-axis the activity is plotted in light beam disruptions per minute.

In DD, *per*^{01} is totally arrhythmic (Konopka and Benzer 1971), a fact that was verified by our results (Table 28). But our data was not achieved under such severe[p] evaluation like it was done by C. Helfrich in 1987, who found residual activity rhythms in *per*^{01} flies (Helfrich and Engelmann 1987). Indeed, we calculated (3.2.3) an arrhythmicity rate of 87% for *per*^{Out}, a value that cannot be verified by judgment with naked eyes. That is the compromise between the objective, but sometimes vulnerable result of a computer calculation on the one hand and artifact insensitive, but often more subjective decisions by human eye on the other side. For a better illustration, Figure 54 shows examples for a rhythmic *per*^{Out} fly with the highest power value we found, an arrhythmic *per*^{Out} fly and an arrhythmic *per*^{01} fly.

[p] Konopka and Benzer measured the locomotor activity under free-run conditions via infrared light to determine the rhythmicity, whereas Helfrich and Engelmann observed the behavior in LD and evaluated morning and evening anticipation. For details see the materials and methods part in the appropriate papers cited in the text.

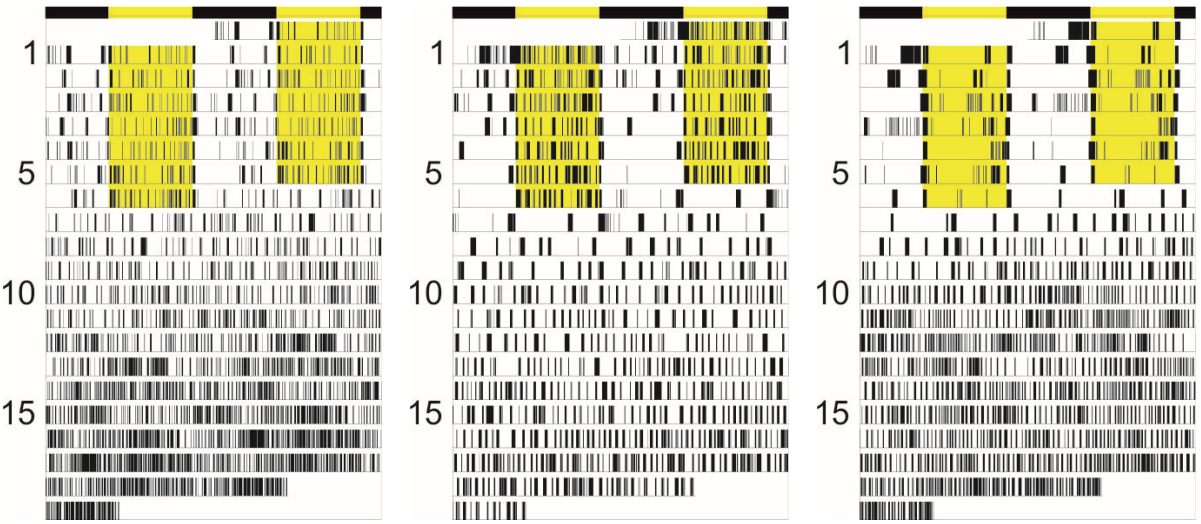

per^{Out} *red* (33.4 h) *per*^{Out} (arrhythmic) *per*^{01} (arrhythmic)

Figure 54: Actograms from a rhythmic and an arrhythmic *per*^{Out} fly with red eyes.

Black bars show crosses of the light beam inside the monitor by the fly. Numbers on the left side count the days of the experiment. The yellow/black bars on top show the existing light regime of the first 6 days. For a better view yellow background also shows timespans with lights-on. Left: The fly with the highest power value (18.22) and a calculated period of 33.4 h. Middle: A randomly picked *per*^{Out} arrhythmic fly. Right: Example for an arrhythmic *per*^{01} fly.

Judged by eye, it is hard to find a rhythm in the left as well as in the other actograms. Nevertheless, the program recognizes a weak 33.4 h rhythm on the left side, although one can observe an apparently consistent distribution of activity throughout the whole circadian cycle in free-run.

5.2.3.1 Potentially affected neighboring genes

The genomic region with the neighboring genes surrounding *per* is depicted in Figure 20.

In first studies, *HLH3B* was named *DroSCL*, because of its homology to the mammalian hematopoietic transcription factor *SCL* and a high conservation of putative secondary structures. As the name suggests it belongs to the gene group of *basic helix-loop-helix* (*bHLH*) genes in *Drosophila* (Varterasian et al. 1993) and '3B' implies its cytogenetic position on 3B1 on the X-chromosome. Due to this functional domain, one can propose that it is involved in protein dimerization activity and functions as a sequence-specific DNA binding transcription factor as it is known for other bHLH-proteins (Ledent and Vervoort 2001). For the latter case, they especially bind to variations of the E-box motif ('CANNTG'). Protein interaction groups are only described for *CG14894* (Rhee et al. 2014).

The only feature described for *CG2652* is attributed to its protein that belongs to the YEATS family (YNK7, ENL, AF-9, TFIIF small subunit). These proteins are thought to have a transcription stimulatory activity using DNA as template (http://flybase.org/). It is conspicuous that expression data shows that *CG2652* seems to be active nearly solely in the adult male testis.

CG2650 is notated as a gene encoding for a 0.9 kb RNA next to *per*, that is expressed - like his neighbor - under circadian control (Lorenz, Hall, and Rosbash 1989). A haemolymphe juvenile hormone binding site is predicted. This group of proteins is thought to carry the juvenile hormone from the place of its synthesis to its target position and thereby protecting this important protein from hydrolyses through unspecific esterases present in the insect haemolymph (Kolodziejczyk et al. 2003) (http://www.ebi.ac.uk/interpro/). Since *CG2650* is reported to be rhythmically expressed an influence on PER and/or circadian rhythmicity cannot be totally excluded. However, a connection to juvenile hormone is described and thus a role in development is more likely. There is a deficiency genotype (Df (l)TEM202/Df (l)64j4) containing a deletion of the *per* transcript, the 0.9 kb RNA of *CG2650* and at least two other transcripts (Bargiello and Young 1984, Reddy et al. 1984). Restoration of the adult circadian locomotor activity rhythm has been accomplished by P-element mediated transformation of arrhythmic *per* flies with *per* DNA alone (Bargiello and Young 1984, Hamblen et al. 1986), but rescue of the eclosion rhythm without the 0.9 kb transcript has yet to be demonstrated. A clear statement should be possible with a partial rescue including *CG2650* and leaving out *per* CDS or vice versa. This can be done quite easily, since we already divided the rescue construct in three functional parts (3.2.14).

ATPase and peptidase domains, zinc ion binding and involvement in proteolysis as an integral component of membranes is predicted for *CG2658* from online sources like InterPro or UniProtKB (http://www.ebi.ac.uk/interpro/, http://www.uniprot.org). But no research evidence is listed. Solely a non-rhythmic gene expression was shown (Huang et al. 2013).

The same tool from EMBL-EBI also predicts a zinc ion binding function and a sterile alpha motif (SAM) domain, for *CG2662*, the last involved neighbor gene. The SAM is a putative protein interaction domain that is present in various proteins and described to be involved in many biological processes (Schultz et al. 1997). Zink fingers are motifs containing finger-like protrusions, that make tandem contacts with target molecules like DNA, RNA, protein and/or lipid substrates (Klug 1999, Hall 2005, Brown 2005, Gamsjaeger et al. 2007, Matthews and Sunde 2002).

One possibility for answering the question of potential implications due to the accrued duplication or errors concerning the recombination would be to knock down these adjacent genes by RNAi. For all of them, RNAi-lines are listed on http://flybase.org. First, they have to be functionally tested, but this would be a possible way to go on after the observation of the *per* rescue flies.

5.3 Generating the knockout strain for *tim*

5.3.1 Why ends-out targeting of *tim*

The amorphic allele tim^{01} originates from a 64 bp deletion, causing a frame shift in the coding sequence. The residual peptide is predicted to consist of 714 AA, whereby additional 35 AA derive from a new reading frame after the mutation site (Myers et al. 1995). It was the first reported null mutant for *tim* discovered by Sehgal et al. in 1994 (Sehgal et al. 1994). Although, *tim* mRNA levels can be observed in this loss of function mutant at relatively high levels (Hardin 2011, Sehgal et al. 1995), *Clk* mRNA is reduced to constantly low levels. Nevertheless, these low levels indicate that residual TIM somehow activates *Clk* transcription (Bae et al. 1998) and a residual function of the truncated polypeptide cannot be ruled out. So, a well-defined null mutant without any remaining TIM protein could give new insights and studies with tim^{01} compared to tim^{Out} are one future aim, as well as observing the *Clk* mRNA levels in tim^{Out}. But as mentioned for per^{Out}, the initial idea was to design a rescue construct for *tim* coupled to a fluorescence tag, that can be activated and detected next to the marker connected to PER.

5.3.2 Genetic design of the *tim* knockout and rescue

The conditions for *tim* were a little easier concerning adjacent genes, since there is no overlap of the gene regions. On the 5' site (concerning *tim*) we included the whole intergenic region to the next adjacent gene into the knockout area and started the 5' homology arm in the 3' UTR of *CG31954* until the center of *CG33123* (Figure 26). The distance between *tim* and *CG15414* – the neighboring gene on the 3' site – was not included in total. Here we screened for not conserved regions inside the *Drosophila* genus with BLAST analyzes (http://flybase.org/blast/) and placed the beginning of the 3' homology arm inside one of that loci. The end was then located in the big intron region of *CG15414*. In this way, we tried to excise also regulatory sequences next to *tim*.

A complete restoration of the endogenous genomic region was not done so far, but is part of our future plans. Due to promising results in the epigenetic ADAR project, we decided to couple the ADAR- and tim^{Out} projects and started with a UAS-GAL4 based rescue system for *tim*. For that, the plan was to recombine a *tim*-GAL4 driver to the second chromosome next to our designed tim^{Out} allele. Additionally, we cloned four different UAS-*tim* constructs with different mutations on the editing sites that were integrated into the second chromosome via P-element insertion. If further results are still that striking, a complete rescue with or without mutations could also be an option.

5.3.3 The result - *tim^{Out}*

The integration frequency of the *tim* construct was reduced compared to *per*. The number of positive red-eyed flies collected from the screening cross was lower, although much more screening crosses were assessed (compare Table 27 and Table 29). We assume this was because of the larger size of the knockout region and maybe also based on the different genomic locus.

Due to the chromosomal constitution of *tim*, we had to start with the *reaper* attendance PCR for a first selection. In Figure 37, the positive control seems to be on a reduced height compared to the positively tested flies (#30 and #31). For space reasons, we left out the middle part of the gel picture that was not running evenly horizontal, thus the products on the right side seem to be of bigger size, although they are not. We tested both homology arms for the same reasons as for *per* and sequenced the products. In the end, after crossbreeding a homozygous strain, we verified the results by an additional *tim* attendance PCR (Figure 39).

Protein level analysis of fly heads on western blot verified the knockout of *tim*. There is no TIM detectable in homozygous *tim^{Out}* animals. Also the difference between the latter probe and the empty lane is plain – the smear on '*tim^{Out}* homozygous' proves that a head lysate was blotted. We did not blot a loading control, but nevertheless it can be seen that the TIM level in the heterozygous flies compared to the *tim^{Out}* controls is reduced to half (Figure 40). Albeit, comparing LD behavior of flies with different *tim* alleles (Figure 55) it can be seen that - despite of a reduced activity level - there is no striking difference between *tim^{Out} white* (two functional copies of *tim*) and *tim^{Out} red* (one functional copy of *tim*). The same is true for the period rhythms under DD, where both genotypes expressing *tim* in different dosages - *tim^{Out} white* and *tim^{Out} red* – display a similar period length of a little less than 24 h (Table 30). This verifies the postulation of Rothenfluh et al., that TIM is dosage insensitive (Rothenfluh et al. 2000), a feature that was only know from one other clock gene (*dbt*) so far (Price et al. 1998).

The Ends-out targeting of *tim* proceeded without complications or failures, that means the result was as predicted and no duplications occurred like it happened for *per*. The *tim^{Out}* animals look healthy and normal and also homozygous individuals are viable and can be sustained as a strain. We also floxed-out the marker gene *mini-white* without any change in viability. The result on the behavioral level is as suspected, a high level of arrhythmicity. Not all animals were arrhythmic, but corresponding power values are quite low and - judged by eye - no rhythms are discernible. Although it is prominent, that all detected rhythms were >29 h up to 34 h, this effect cannot be seen in the *tim^{01}* flies. Besides a higher amount of rhythmic animals, the periods of *tim^{01}* flies ranged from 21 to 34 h, but the wider range should result from quite low power values of the single behavioral data and the increased number of rhythmic individuals. An arrhythmicity rate of only 46%, like we measured (Table 30), is very low and

cannot be verified by results of former publications, in which 93% of arrhythmicity were observed (Sehgal et al. 1994). From this, it is possible that something went wrong in this experiment or that the *tim*^{01} strain we used got contaminated with a functional *tim* allele from outside. The fact that the *w*^{1118} and the white-eyed *tim*^{Out} seem to behave normal strengthens the theory of a contamination and weakens the possibility of an experimental failure. The white-eyed *tim*^{Out} flies were taken out of a heterozygous strain and chosen as controls, because they are genetically most closely related to their *tim*^{Out} red-eyed arrhythmic siblings. The LD daily averages in behavior additionally underline the assumption of a non-flawless *tim*^{01} negative control, because it also shows morning and evening anticipation and a prominent shift into the dark phase after lights-off. *tim*^{Out} in contrast shows neither morning nor evening anticipation or shifts activity towards day or night. The overall activity level is a little higher during the light phase and distinct reactions to lights-on/-off are observable, but besides these deviations the slope increases until lights-off, falls to nearly zero afterwards and rises again (Figure 41).

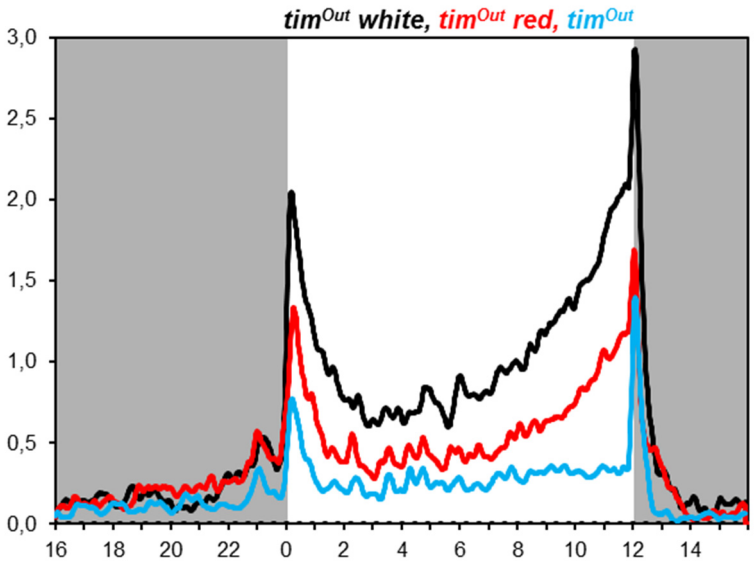

Figure 55: Comparison of flies with different amounts of TIM.

tim^{Out}: homozygous knockout flies. They do not show any anticipation, just a lights-on/-off reaction. *tim*^{Out} *red*: Contain one chromosome with an intact *tim* locus in trans with a knockout chromosome. These flies are less active than their wild type like siblings, but show an anticipation before lights-on and lights-off. *tim*^{Out} *white*: have a normal level of TIM due to two wild type alleles. The x-axis shows the ZT values, starting with ZT0 = lights-on. On the y-axis the activity is plotted in light beam disruptions per minute.

5.3.3.1 Genes adjacent to tim that could be affected by the knockout

The genomic region with the neighboring genes surrounding *tim* is depicted in Figure 26.

No molecular functions are described for *CG15414*, the adjacent gene upstream of *tim*. It consists of one very large intron region at its 5' end and one described exon that is predicted to result in a 320 AA long polypeptide (http://flybase.org/).

InterPro (http://www.ebi.ac.uk/interpro/) predicts a trypsin-like cysteine/serine peptidase domain for *CG31954*, or more specifically, belonging to the MEROPS (http://merops.sanger.ac.uk/) (Rawlings et

al. 2014) peptidase family S1 (chymotrypsin family, clan PA (S)) (Rawlings and Barrett 1994) involved in proteolytic processes. Chymotrypsins belong to serine proteases, a subfamily of peptidases with a serine residue in its catalytic center.

CG33123 shows a tRNA synthetase site putatively involved in aminoacetyl-tRNA editing activity, ATP binding (http://www.ebi.ac.uk/interpro/) and leucine-tRNA ligase activity (http://www.ncbi.nlm.nih.gov). A function in wound healing (Campos et al. 2010) and neurogenesis (Neumuller et al. 2011) is also proposed by experimental evidence.

5.4 TIM editing by ADAR - Important or just by chance?

5.4.1 Time specificity

The discovery of the editing sites, that are described in the prologue part of the *tim* rescue cloning result (4.3.1) were discovered by sequencing the whole *tim* transcript and searching for ADAR exchanges. A very interesting feature is the time point specific execution of the modification, which occurs mainly between ZT9 and ZT15 at both loci (Figure 44). So far it is known that *adar* gets highly transcribed in the embryonic nervous system, stays detectable throughout the development and peaks in pupal and adult stages (Jepson and Reenan 2010) in a variety of primary tissues and cells. Thereby its expression is controlled by two promoters in temporally distinct patterns (Palladino et al. 2000). We checked the expression levels of *adar* throughout the day (Figure 46). Our expression analysis showed no cycling *adar* mRNA level, thus another regulation mechanism could control ADAR function besides an expression variation of the enzyme, at least considered on the level of total heads[q]. *In situ* stainings against *adar* mRNA for example could hypothetically reveal a very different result for certain clusters or single clock neurons[r]. However, control mechanisms for enzymes are not unusual and are also described for ADAR. Examples for *Drosophila* are the *adar* gene itself, which controls its own transcript by editing, leading to an enzyme without catalytic region (Palladino et al. 2000) or the *para* Na^+ channel, that is developmentally regulated (Hanrahan et al. 2000). The exclusive and time point specific exchange of adenosine to inosine and the fact that we were not able to find the polymorphism in $adar^{hyp}$ flies made us assume that an editing process is responsible for the base pair exchange. $adar^{hyp}$ represents a hypomorphic allele with over 80% reduced enzymatic activity and decreased modification spectrum ranging from 70-100% depending on the editing site (Jepson et al. 2011). By sequencing, we were not able to detect any editing in these flies, at least for the investigated *tim* RNA,

[q] We used fly heads for RNA extraction and subsequent cDNA synthesis (3.2.5).
[r] This experiment was not done so far by us, but maybe in other labs.

thus we assume that the sites we observed do not belong to the 'high efficiency' group of ADAR-substrates, as they are proposed by Jepson et al. (Jepson et al. 2011).

5.4.2 Location - A serine-rich domain (SRD) that was part of other studies before

Another hint for the importance or expediency of the posttranscriptional modification is the location of the editing sites. Concerning the *tim* gene region, they can be found in exon two of the major transcript isoform *tim-RB*. It is almost astonishing, that exactly this region (altogether 96 bp in size) is spliced out as intron in two of the eight yet described transcript isoforms (Figure 6, http://flybase.org/reports/FBgn0014396). Interestingly, this region came into the focus of some scientists before. Myers et al. characterized the original *tim* cDNA lacking the 32 AA encoded by that sequence (Myers et al. 1995). Two years later, Ousley et al. performed phylogenetic and functional studies by searching for conserved regions within the *tim* locus through sequence alignments of *Drosophila melanogaster*, *Drosophila virilis* and *Drosophila hydei* (Ousley et al. 1998). Because they found exactly this region – later referred to as TIM SRD (serine-rich domain) by Meissner et al. (Meissner et al. 2008) – to be highly conserved and expressed in the other species, they performed RT-PCR experiments and were able to describe another transcript isoform including this domain. They went on with rescue studies by crossing transgenes with and without SRD in trans position to a tim^{01} allele and showed that the SRD is necessary to completely restore normal behavior. The tim^{UL} mutation (E260K) can also be found in this region, a mutation leading to a prolonged period of 33 h in homozygous constellation (Rothenfluh, Young, and Saez 2000). In close spatial proximity, only six AA C-terminal of this striking mutation (E^{260}), the first editing site is located (E^{266}) (Figure 43), making a mutual interference possible.

BLAST analyzes of the editing locus within the *Drosophila* genus revealed further evidence for a functional or structural important element. This is underlined by the high conservation of the locus throughout almost all species of the *Drosophila* and *Sophophora* subgenus. The comparison is shown in Figure 47 and coincides with the studies from Ousley et al. (Ousley et al. 1998). The first edited adenosine creates a new potential splicing site, but does not lead to an AA exchange. We did not observe, if there are alterations between different time points or $adar^{hyp}$ versus wild type flies concerning the relation of expression of the single transcripts, yet. It is already exchanged for a guanine in the genome of approximately half of the investigated *Drosophila* species. A possible effect on protein evolution, as it is postulated by Zinshteyn et al., could be assessed here. In contrast to a mutation, editing usually changes only a portion of the original transcript and thereby allows creation of new functions without destroying the old one in total (Zinshteyn and Nishikura 2009). The second edited adenosine is highly conserved in all species, which is also true for the next three or four adjacent

nucleotides on both sides. So the editing modifies a well conserved AA sequence and exchanges a glutamic acid with a glycine (acidic + negatively charged side chain is exchanged with a polar + neutral residue). But again, the potential role of this exchange has to be determined. An altered protein folding or a changed binding affinity towards its partner PER or modifying enzymes are only two conceivable possibilities.

5.4.3 Possible consequences of the editing process

Usually eukaryotic transcripts build stem-loop structures between intronic and exonic regions before splicing occurs. Hence, ADAR is able to catalyze the editing (ADAR needs double strands) resulting in an inosine in exchange for an adenosine, which is furthermore interpreted as a guanosine (Zinshteyn and Nishikura 2009). At the first editing site inside *tim*, there is an AA exchange from serine to glycine, whereas the second editing on E^{249} does not lead to substitution in the polypeptide sequence. But other effects besides changes in the coding capacity of the polypeptide sequence are also conceivable. Additionally, also intronic regions can be affected (Zinshteyn and Nishikura 2009). Further consequences could be altered miRNA or siRNA target populations, the formation of new secondary structures inside the ribonucleic acid strand, nuclear sequestration or altered splicing.

5.4.3.1 Splicing

Splicing can be influenced by modification of 3' and 5' splice sites or by elimination as a whole through modification of splice site donor or acceptor sequences (Zinshteyn and Nishikura 2009). Furthermore, subtle effects can result from changes in the secondary structure and with that the accessibility for the splicing machinery to the RNA. One example is the ADAR2 enzyme in mammals, which acts on his own pre-mRNA to create a new splice site (Rueter, Dawson, and Emeson 1999). In this case, an 'AA' is edited to an 'AI', acting like an 'AG'. Following the terms of canonical splicing, which makes up 99% of all splicing events, according to which introns contain an 'UG' at the 5' and an 'AG' at the 3' splice site (Black 2003), a new splice site is formed and the alternative splicing produces a new peptide lacking the catalytic domain amongst others (Bass 2002). For *Drosophila melanogaster*, the same self-targeting mechanism for ADAR could be shown (Palladino et al. 2000). In case of *tim*, this was also true for the second editing site, where ADAR creates an 'AI' out of an 'AA' (Figure 43). Studies using the qPCR technique should give indications about alterations in the ratio of different *tim* transcripts, depending on whether there is editing or not. But so far we could not find strong hints for such an alternative splicing at this site in our available *in silico* data.

5.4.3.2 Secondary structure

We tried distinct predictions for secondary structures of the *tim* pre-mRNA molecule in total, exon 2 alone or just the 96 bp SRD. The predicted structures mainly varied in the length and size of a stem-loop structure. As an example, one result is shown in Figure 45. However, compared to the total molecule, this structure is very small. Thus, overall considered our opinion is, the changes were not as tremendous, so an 'inaccessibility' of an important structure could be suspected. But here the state of evidence is totally missing yet.

5.4.3.3 Protein modification

Another aspect that was not discussed so far is the presence of multiple serine residues inside the 32 AA domain (SRD) regarding possible further modification. The tim^{UL} mutation changes a single guanosine into an adenosine. The result is an AA exchange from glutamic acid to lysine and with that a switch from a negative side chain to a positive one. The TIM SRD contains four predicted CK2 phosphorylation sites, one located on S^{256}, four residues upstream of tim^{UL}. It is known, that CK2 prefers serine or threonine residues 2-5 AA N-terminal to acidic AA (Meggio and Pinna 2003) and that the placement of basic residues near CK2 sites inhibits its phosphorylation of the target site (Marin et al. 1986). Meissner et al. claimed that the tim^{UL} mutation leads to a missing CK2 phosphorylation site on S^{256}, due to the acid-basic AA exchange. The theory is proven by the lack of significant mobility shifts in western blot experiments for a TIM polypeptide without SRD, what otherwise can be expected. They also expressed a dominant negative form of the *CK2α* allele, which shows typical behavioral effects on the period length of the circadian clock, which got reduced in tim^{UL} mutants - a further evidence for a disrupted phosphorylation by CK2 (Meissner et al. 2008).

The proximity (two AA N-terminal to S^{256} – the phosphorylation site affected by tim^{UL}) and the fact that the editing also leads to an exchange of a positive charged to a neutral AA let us assume a potential connection between the tim^{UL} mutation and the E254G exchange through editing. So we started behavioral studies as they were done by Meissner et al. (Meissner et al. 2008). Normally, after entrainment in a 12/12 LD cycle followed by free-run in DD, the majority of the $adar^{hyp}$ flies were arrhythmic (81.25%, Table 31). The portion of rhythmic flies showed a period of 26.6 h in DD. The averaged day activity showed no morning and a strongly decreased evening anticipation (Figure 48). A heterozygous tim^{UL} mutation leads to a postponed evening peak into the dark phase in LD average day graphs and a free-run period of 26 h in DD with a rhythmicity of 75% (Table 31). Since $adar^{hyp}$ and tim^{UL} are located on different chromosomes, both mutations can be combined in $adar^{hyp}; tim^{UL}/+$. These flies display a weak evening anticipation and were 100% rhythmic in DD with a period length of 26 h (Table 31, Figure 49). Actually, that allows only one assumption: the tim^{UL} mutation somehow mimics an

editing event. If both mutations were influencing two distinct pathways or processes, one would expect that the prolonged periods resulting from both single mutations would be more or less additive. The result would then be an even more prolonged period, for example of around 28 h. Likewise, this is indirect evidence, that the editing becomes manifested at the same site as tim^{UL}, because the result – a period length of around 26 h – is nearly similar. The work of Meissner et al. (Meissner et al. 2008) predicted a reduction in phosphorylation due to the tim^{UL} mutation at S^{256}, so maybe both modifications act on the same AA position!? To follow this question we also made *in silico* predictions for a phosphorylation probability by CK2 and other kinases on S^{256} with and without editing and/or tim^{UL} mutation (Figure 50). It turned out, that CK2 is most likely the catalyzing kinase and that in both cases - editing or tim^{UL} mutation - the score for a phosphorylation event and with that the probability was increased. Finally, it can be concluded, that the editing at E^{254} influences or regulates the phosphorylation by CK2 on S^{256}. A suppressed editing at this position keeps the glutamic acid at its position and with that prevents phosphorylation through CK2. One consequence of this is a strong arrhythmicity, that can be rescued in $adar^{hyp}; tim^{UL}/+$ animals. Here tim^{UL} blocks the otherwise overall phosphorylation through the prevented editing by $adar^{hyp}$ (Figure 56). A first western blot experiment verified this theory. Wild type animals are compared with male and female $adar^{hyp}$ flies at four different time points (Figure 51). Slight size shifts are discernible between the wild type and the $adar^{hyp}$ flies, implying a potential additional phosphor residue in the $adar^{hyp}$ animals due to phosphorylation.

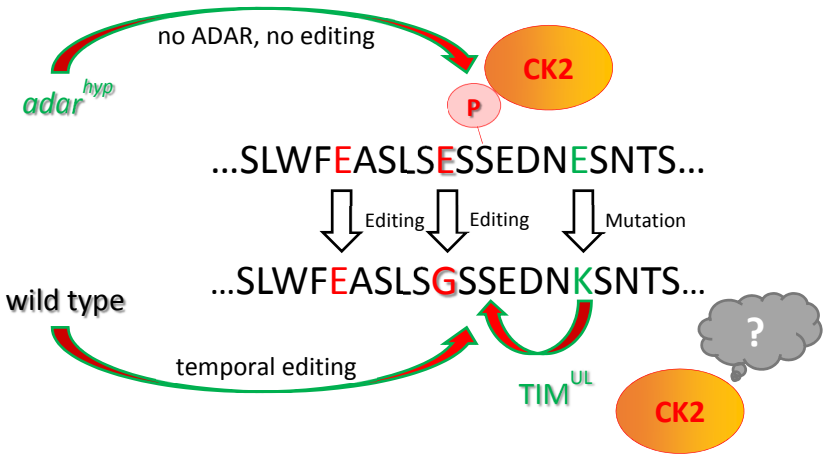

Figure 56: Current ADAR-CK2-phosphorylation-dependency model.

In wild type animals ADAR editing occurs in a time point specific manner. In case of the first editing site, this leads to an AA exchange. The corresponding loss of charge decreases CK2 dependent phosphorylation on the next but one serine. The same influence is given by the TIM^{UL} mutation. In $adar^{hyp}$ animals there is no ADAR and thus no editing. Phosphorylation can occur throughout the whole day, maybe resulting in arrhythmicity.

5.4.4 Outlook

For sure a lot of work has to be done to unravel the open questions concerning the editing process in this interesting region of the TIM protein. Size shifts on western blots should be verified. In a first try, we cloned truncated versions of TIM and transfected them into S2-cells with additional CK2 overexpression. Thereby we exchanged either one, both or no adenosine of the editing sites to a guanosine. This should mimic an editing event and theoretically prevent phosphorylation trough CK2 on E^{256}. A more distinct difference in size shifts should be observable due to the decreased size of the constructs. Immunoprecipitation assays could reveal a direct interaction of CK2 and TIM and first tests were already done, but did not succeed sufficiently (data not shown). For a phenotypical study we combined the *tim* knockout and ADAR project and designed rescue constructs for *tim* based on the GAL4-UAS system. The reintegration into the genome will be done through P-element insertion and selection/balancing to the second chromosome. The activation of the *tim* constructs thus should be enabled with an artificial *tim*-GAL4 driver. Therefore we cloned four different TIM CDS constructs under UAS control also containing adenosine to guanosine mutations at either one, both or at no editing site, respectively. Additionally, we try to recombine a *tim*-GAL4 driver on the *tim* knockout chromosome to get a most probable natural expression pattern. Since we can only speculate about possible effects of the editing so far, the hope is to get a useful tool for many further experiments answering questions about the connection between editing and changes in behavior as altered rhythms or even arrhythmicity. To look at the behavior is most probably the first test, due to the linkage to tim^{UL} and its prominent phenotype. Furthermore, it would be interesting to see if there are effects on RNA or protein level or if the affinity to other proteins of the circadian system is influenced. Surely, the next experiments will show the direction, where to go.

6 Appendix

6.1 SGG and its role in the circadian clock – Fischer et al., 2015 (submitted)

At the beginning of our work were two contradictory publications. The first was published in 2001 by Martinek et al. (Martinek et al. 2001). They already showed the period lengthening effect of a reduced SGG level and vice versa the shortened free-running period due to SGG overexpression under DD, a fact already mentioned in the introduction paragraph. The theory behind this is as follows: SGG phosphorylates TIM and thus causes a premature entrance of TIM into the nucleus resulting in a faster ticking clock. It was surprising when Stoleru et al. claimed that SGG overexpression results in a dramatic CRY stabilization even under LL conditions. Normally, constantly active CRY leads to a longer free-running period (Dissel et al. 2004). Arrhythmicity can be observed in wild type flies under LL conditions (Dubruille et al. 2009, Konopka, Pittendrigh, and Orr 1989), when CRY gets activated and degraded (Koh, Zheng, and Sehgal 2006). It was even more astonishing, when Stoleru et al. additionally described that the SGG induced CRY stabilization in LL leads to rhythmic flies (Stoleru et al. 2007) – until this date this was only known from *cry*-lacking flies (Dubruille et al. 2009, Patrick Emery 2000).

We were wondering about these results and tried to reproduce the experiments – and failed. Instead, we obtained opposite results in a yet unpublished western blot experiment (Figure 57). The fact, that we were not able to show a stabilizing effect for SGG on CRY levels were puzzling and made us trying to unravel the role of SGG in the circadian clock.

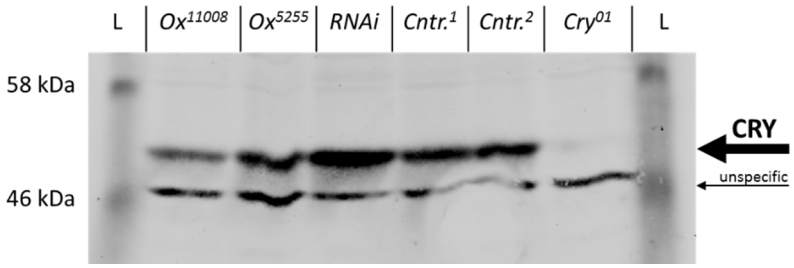

Figure 57: Anti-CRY western blot of flies with de- and increased levels of SGG.

Ox^{11008}: *UAS-SGG^{11008}* x *tim-GAL4*, overexpression of SGG as it was used from Stoleru et al., 2007 (Stoleru et al. 2007). Ox^{5255}: *UAS-SGG^{5255}* x *tim-GAL4*, described as constitutively active isoform of SGG on a P-element insertion. RNAi: *RNAi^{35364}* x *tim-GAL4*, RNAi against SGG. Cntr.^{1}: Just *RNAi^{35364}*. Cntr.^{2}: Just *tim-GAL4*. *cry^{01}*: Flies expressing no CRY. The western blot shows a yet unpublished result of a former work of us. It is obvious that there is no stabilization of CRY if SGG is overexpressed, rather it seems to be the other way around.

Title

GSK-3 beta interacts with Period and Timeless but not with Cryptochrome in the circadian clock of *Drosophila*

Short title

GSK-3 beta and *Drosophila's* circadian clock

Author list

Robin Fischer[1], Charlotte Helfrich-Förster[1] and Nicolai Peschel[1*]

[1] Neurobiology and Genetics, Biocenter, University of Würzburg, Würzburg, Germany

* Corresponding Author

Email: nicolaipeschel@biozentrum.uni-wuerzburg.de (NP)

Abstract

The molecular functioning of the circadian clock is one of the best-investigated biological mechanism. This outstanding knowledge makes it more difficult for the present generation of scientists to investigate the circadian clock. Consequently, current studies are going more and more into detail facing the problem, whether small behavioural changes are due to manipulation of a certain gene – or derive from a different genetic background. In this study we wanted to resolve the conundrum, why GSK-3 beta expression apparently stabilizes Cryptochrome (CRY) on the one hand, while this condition leads at the same time to rhythmic behaviour of the fly under constant light conditions, a situation that normally renders wild type animals arrhythmic, while animals lacking CRY stay rhythmic under those conditions.

Unexpectedly we could clarify the dissent by showing, that GSK-3 beta is not stabilizing CRY at all. We present evidence that the previously observed results were only due to a non-CRY-specific antibody. Our results suggest that GSK-3 beta and CRY do not interact and that genetic background effects caused the previously observed rhythmicity in constant light. Furthermore we could demonstrate, that GSK-3 beta mainly influences the circadian clock in the PDF expressing lateral neurons and thus the endogenous period in darkness, but not in the dorsal neurons, which are important to control activity rhythms under light.

Authors Summary

Every clock should have a reset button and a wheel to set a new time. The same is true for *Drosophila's* circadian clock. Light can push the flies reset button by activating the photoreceptor CRY and degrading the clock protein Timeless. So we were astonished to learn, that a stabilization of CRY leads to animals with a non-functioning reset button. Our hypothesis to the mechanism behind this irritating result was, that overexpression of GSK-3 beta not only makes CRY more stable, but at the same time inhibits CRYs ability to bind to Timeless and adjacently to reset the clock. In the end we were able to give an answer to this riddle – CRY is not stabilized by GSK-3 beta at all. This finding should thus adjust the model of the role of GSK3-beta plays in *Drosophila's* circadian clock.

Introduction

The circadian clock is an ancient mechanism in almost every living being on this planet, including bacteria, plants and animals (Schibler 2006). This truly sophisticated and magnificent evolved machinery allows us, to adapt to the daily 24 hours environmental changes on this planet – caused by

the earth's rotation round its own axis (Reppert and Weaver 2001). At different times of the day, the transcriptome and proteome of an animal might look very different. For instance, in diurnal animals the activity promoting hormone cortisol is maximally expressed at the beginning of the day – while the sleep hormone melatonin reaches its peak levels in the middle of the night (Masri and Sassone-Corsi 2013). In *Drosophila,* a transcriptionally regulated negative feedback loop controls the circadian clock. The two clock proteins Period (PER) and Timeless (TIM) inhibit the transcription factors Clock (CLK) and Cycle (CYC). CYC and CLK act as transcriptional activators of *per* and *tim*. The negative feedback loop and the resulting rhythmic expression of genes and proteins occur in about 150 neurons inside *Drosophila's* brain (Peschel and Helfrich-Förster 2011). The circadian clock is not only functional in the presence of the daily change of day and night, but it persists even under constant darkness conditions (DD). On the other hand the clock is plastic and can adapt to changing environmental conditions – migrating birds must adjust their behaviour according to the new environment, animals must adapt to the annual changes in day length, to sunsets and sunrises and the traveling *homo oeconomicus* has to battle jetlag and nightshifts by phase-shifting its circadian clock (Foster and Roenneberg 2008, Roenneberg, Kumar, and Merrow 2007). This adaptation is mainly caused by circadian photoreceptors (Foster, Hankins, and Peirson 2007). In *Drosophila* one of the most important photoreceptors is the blue light sensitive protein Cryptochrome (CRY) (Stanewsky et al. 1998, Emery et al. 1998). This photopigment changes its conformation upon light reception, allowing CRY to bind to TIM and subsequently leading to phosphorylation and ubiquitination of this important clock protein. Afterwards the proteasomal degradation of TIM is triggered (Yang et al. 1998, Suri et al. 1998). Consequently, the light induced degradation of the core clock protein TIM leads to a non-functional circadian clock under constant light exposure (LL) and the fruit fly forfeits its rhythmic behaviour. The loss of CRY on the other hand results in severe problems for *Drosophila* to adapt to a new light regime (Stanewsky et al. 1998). Furthermore *cry* mutants still display circadian rhythm under LL conditions (Emery, Stanewsky, Hall, et al. 2000). The light sensibility of *Drosophila's* clock and the degradation of TIM are dependent on several other factors. It was for example shown, that distinct TIM isoforms perform differently in the light – the longer TIM isoform has a reduced affinity towards CRY, leading to a more stable TIM protein in light conditions (Sandrelli et al. 2007). The E3 ubiquitin ligase Jetlag (JET) is another important factor, because JET induced ubiquitination of the phosphorylated TIM protein leads to TIM's degradation in light (Koh, Zheng, and Sehgal 2006, Peschel, Veleri, and Stanewsky 2006). A current model predicts that the light activated CRY binds to JET, TIM and to another F-Box protein called Ramshackle (BRWD3) (Ozturk et al. 2013). The preferred CRY target is the highly phosphorylated form of TIM. This conformation of the protein is mostly found in the cell's nucleus. Ubiquitination and degradation in the proteasome follows the binding of CRY and TIM. CRY itself is phosphorylated and ubiquitinated in light as well, to a larger extend by BRWD3 and to a smaller by JET (Ozturk et al. 2013,

Peschel et al. 2009, Lamba et al. 2014). The following degradation of CRY thus allows an adaptation and a reset of the circadian clock. Other proteins might be involved in this process of phosphorylation and/or degradation as well. To name a few: Kismet, Quasimodo or the Cop9 Signalosome (Dubruille et al. 2009, Chen et al. 2011, Knowles et al. 2009). The phosphorylation of CRY and TIM argues for participation of kinases and phosphatases. It was shown, that several proteins phosphorylate TIM, i.a. Casein Kinase 2 (CK2) and GSK-3 beta (Martinek et al. 2001, Meissner et al. 2008, Akten et al. 2003).

The aim of the present study was to investigate the phosphorylation and degradation of TIM and CRY under light conditions. We were especially interested in solving the conundrum, why a stabilization of the photoreceptor CRY leads to less light-sensitive animals, particularly in LL. It was already shown, that GSK-3 beta – in *Drosophila* called Shaggy (SGG) - is involved in this process (Martinek et al. 2001, Stoleru et al. 2007). Overexpression of SGG in clock neurons leads to a dramatic change in the behaviour of a fly under constant darkness conditions (DD). SGG phosphorylates TIM protein, leading to an earlier entry of TIM into the nucleus and subsequently to a shortened period of about 20 hrs (Martinek et al. 2001). Interestingly another publication demonstrated that SGG could stabilize CRY dramatically – even under constant illumination - leading to a behavioural phenotype under LL as well (Stoleru et al. 2007). When SGG is overexpressed in the clock neurons, especially in the Dorsal ones, the fly keeps its rhythmicity in light (Stoleru et al. 2007). In the following study we wanted to closer investigate this stabilization of CRY by SGG and examine why in animals with stabilized CRY, TIM protein is somehow protected from light induced degradation, thus leading to rhythmic animals under LL. Furthermore, we want to investigate the role of the F-Box proteins BRWD3 and JET in this process. The latter is of particular interest, because we found earlier that JET weakens CRY stability in LL (Peschel et al. 2009). Thus, JET and SGG may work antagonistically on CRY. To our great surprise, we could not repeat the stabilizing effect of SGG on CRY.

Results

CRY stabilization *in vitro*

Co-expression of SGG in S2 cells was reported to lead to a strong stabilization of CRY – even under constant light (LL) conditions (Stoleru et al. 2007), whereas JET makes CRY less stable, when the two proteins are co-expressed under the same conditions in LL (Peschel et al. 2009). Thus, we wanted to know whether co-expression of JET in the presence of SGG would diminish the stabilizing effect of SGG on CRY.

Remarkably we were not able to see the stabilization effect of SGG on CRY (Fig. 1 A). We transfected *Drosophila* S2 cells with cDNA of several genes under the control of a strong actin promoter. The cells were kept in darkness and were only exposed to light for a very short time, while we harvested the cells and extracted the protein. When *jet* or an only partly functional form of this gene, jet^{c}, was expressed in S2 cells, we could see a small reduction in CRY level. On the other hand, we could determine a small stabilization effect, when *tim* was co-expressed (as previously reported by us and others) (Peschel et al. 2009, Zoltowski et al. 2011). Because our positive and negative control worked well, we wondered why SGG expression does not influence CRY stability in our hands. To verify that the *pAc-sgg* plasmid (a generous gift from Pipat Nawathean) (Stoleru et al. 2007) was the correct one, we partially sequenced the plasmid and affirmed thereby that it was the proper plasmid (data not shown). Several repetitions of similar experiments yielded comparable results (data not shown); i.e., co-transfection and expression of *sgg* did not result in increased CRY levels. To confirm SGG expression in our S2 cell culture system we performed western blots using antibodies against the HIS-tag (Materials and Methods, Fig. 1B). In the *pAc-sgg* plasmid, *sgg* is directly fused to a V5 and HIS-tag.

CRY is expressed endogenously in S2 cells in a very low level (Lin et al. 2001). It was previously reported that this very low level of CRY protein in S2 cells can be stabilized dramatically (even under illumination) by co-expressing SGG (Stoleru et al. 2007). In our hands, co-expression of SGG did not stabilize the endogenous CRY protein neither in dark nor in light (Fig. 1C). Since SGG is a serine/threonine kinase, we were wondering if CRY's phosphorylation status is changed by the co-expression of *sgg*. If our CRY antibody is not able to detect the postulated highly phosphorylated, slow migrating, form of CRY, we would not be able to see this protein on western blots. Therefore, we dephosphorylated CRY. After phosphatase treatment, we were not able to see a difference on western blots (Fig. 1C). We concluded that endogenous CRY is not stabilized in darkness or illumination and that CRY phosphorylation is not dramatically changed in the presence of SGG kinase.

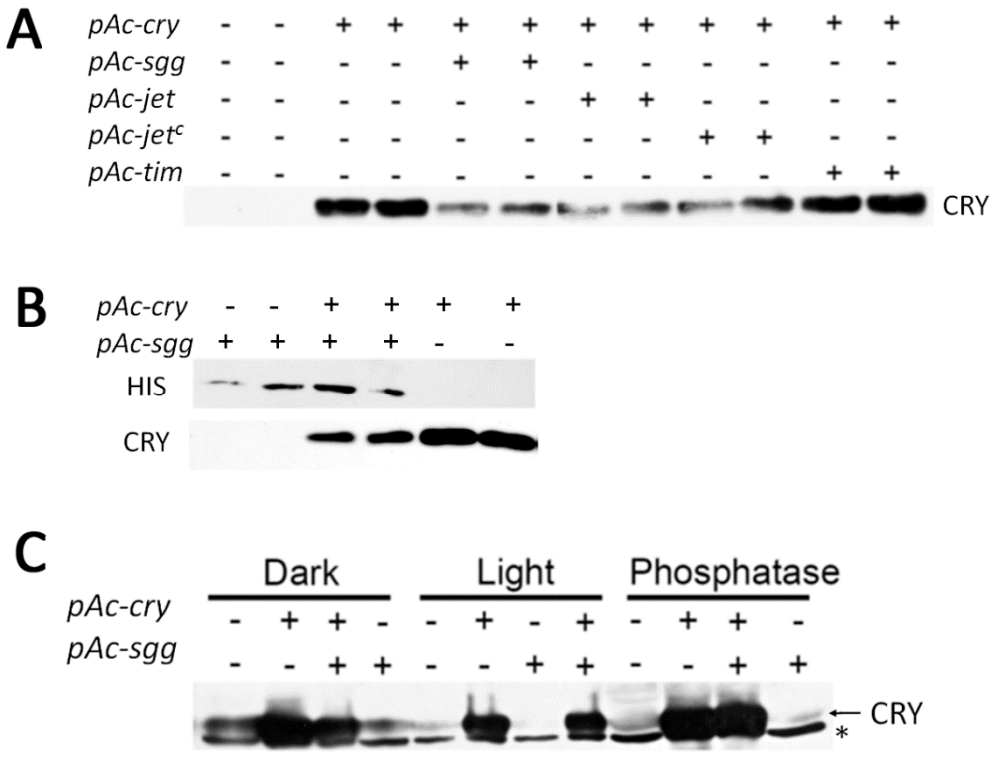

Figure 1.

Stability of CRY in *Drosophila* S2 cells

Drosophila Schneider S2 cells were used to overexpress different genes under the control of a strong actin promoter. The transfected plasmids are indicated at the top and left, while (+) is transfected, (-) indicates no transfection. If not indicated otherwise the cells were kept in darkness. The antibody used to detect CRY Protein is described in Yoshii et al. 2008 (Yoshii et al. 2008). (A) Representative blot of CRY stability in the presence of SGG, JET or TIM. (B) Representative blot of SGG-HIS expression in S2 cells. The antibody used to detect the SGG-HIS protein was anti-HIS (Invitrogen). (C) This western blot was strongly overexposed to visualize the only weakly expressed endogenous CRY. Cells were either sacrificed in darkness, in light or the protein was treated with a λ-phosphatase for 1 hour (after being in dark). The asterisk marks a non-specific band.

CRY stabilization *in vivo*

Next, we investigated the potential stabilization effect of SGG on CRY in adult *Drosophila* animals. Here we used a realtime luciferase assay to display the degradation of CRY under light/dark (LD) conditions (Peschel et al. 2009, Brandes et al. 1996). Therefore, we investigated flies carrying an *UAS-Luc-dCry* construct and a *timeless* driver (*tim*-Gal4) line to express the luciferase fusion protein in all clock cells. Because we (and others) could already show that CRY is stabilized, when TIM is co-expressed (Peschel et al. 2009, Zoltowski et al. 2011), we used two different *UAS-tim* lines as positive controls. To see whether SGG influences CRY stability we overexpressed or down-regulated *sgg* expression using *UAS-sgg* or *UAS-sgg*^{RNAi}, respectively. The flies were kept in a luciferase plate reader for 7 days under L/D 25°C conditions. Consistent with our current and previous (Peschel et al. 2009) S2 cell culture results, we found that only TIM overexpression stabilized CRY. Flies with SGG manipulation did not differ from the control. (Fig. 2)

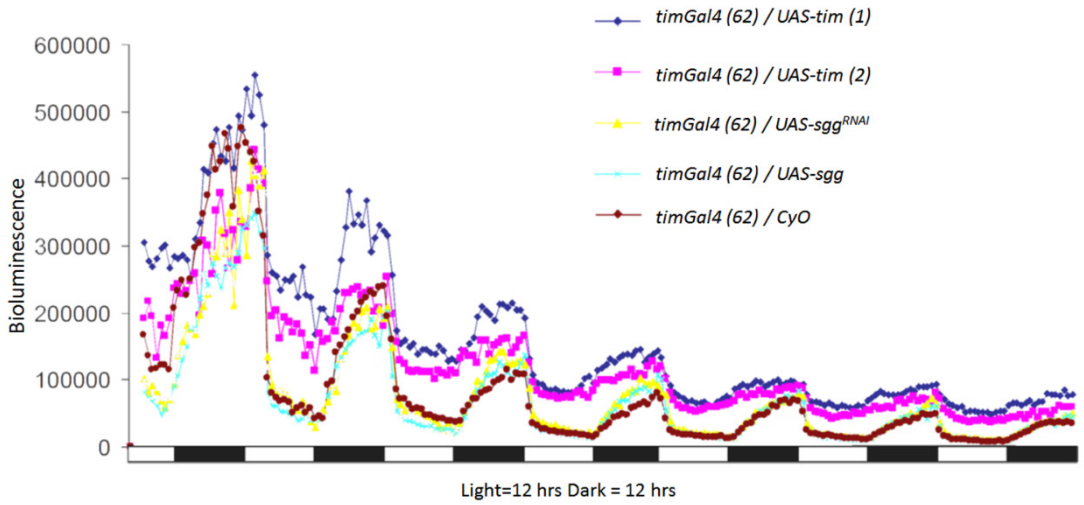

Figure 2.

Stability of CRY in living *Drosophila* animals

Bioluminescence of adult *Drosophila* animals carrying a *Luc-dCry* reporter. Adult *Drosophila* transgenic male flies were measured in a Packard Topcount machine. The genotype of the flies is displayed on the right. Furthermore all animals carried one chromosomal copy of an *UAS-Luc-dCry* insertion. The x-axis indicates the time, the black and white bars at the bottom indicate the daily change of light and

darkness (Light/Dark ratio 12:12 hrs). The y-axis indicates the bioluminescence level (in Counts per second CPS) and thus the luciferase amount. Per genotype 8 animals were investigated.

Behaviour of SGG manipulated animals

Animals overexpressing SGG in clock neurons display a shortened period under DD conditions. Additionally they show morning and evening peaks under LD, which are dramatically shifted towards the midday/midnight (Martinek et al. 2001). It has also been reported that *sgg* over-expression in all or dorsal subsets of the clock neurons leads to rhythmic behaviour in LL, with ~50% (all neurons) or >90% (dorsal neurons) of the flies exhibiting robust rhythmicity (Stoleru et al. 2007). Why a stabilization of CRY should make animals less sensitive towards light is not explained in detail. To unravel this paradox and to confirm these results we used two different fly strains for our overexpressing assay. One strain was carrying an *UAS-sgg* construct on the second chromosome, i.e. *P{UAS-sgg.B} MB5*, and another one that was previously used to demonstrate the behavioural effects of *sgg* expression in LL (*P{EP}sggEP1576*). This strain contained an UAS insertion in the *sgg* region that could be addressed by the GAL4 protein to overexpress SGG. We included *P{UAS-sgg.B} MB5,* because we and others (Martinek et al. 2001, Beckwith and Ceriani 2014) realized that this overexpression construct is much stronger than the original (*P{EP}sggEP1576*). Consistently we expected to see an even stronger phenotype with those animals. We used different driver lines to express *sgg* in several subsets of clock neurons in the *Drosophila* brain. While *tim*-Gal4 should address all clock neurons, *cry*-Gal4 is expressed mainly in the *cry* expressing cells (Yoshii et al. 2008). If the influence of SGG on CRY is the reason for the changed behaviour of those animals, we would expect so see the biggest effect here. *cry*-Gal4/*pdf*-Gal80 and *tim*-Gal4,*pdf*-Gal80 animals only overexpress SGG in the dorsally located cell groups, while the *Clk 4-1M* Gal4 only expresses in a subgroup of the dorsal neurons (Zhang et al. 2010) (further explanation in S1 Fig.). Moreover, we included animals, where the *sgg* mRNA was knocked down by RNAi, to see if those animals behave very sensitive towards light. Furthermore flies overexpressing the clock gene *per* are also behaviourally more rhythmic under constant light (Murad, Emery-Le, and Emery 2007). So we included *UAS-per* animals as well, as another control.

As expected, in DD overexpression of SGG in the ventral neurons shortened the period dramatically, especially when we used the *tim* driver line (Table 1) (Martinek et al. 2001). The only exception was the *P{EP}sggEP1576 w^{1118}; cry-Gal4/+* line. A reason for the lack of phenotype might be, that the *cry*-Gal4 driver is not expressed as strong as the *tim*-Gal4 driver in the s-LNvs – the neurons that are most important for driving rhythmic behaviour in DD (an effect seen by others as well (Stoleru et al. 2005)). On the other hand, the stronger effector line, *P{UAS-sgg.B} MB5*, led to a short period of about 21 hrs in combination with the *cry*-Gal4 driver line, demonstrating, that the driver line is functional. The

crossing of the combination of *P{UAS-sgg.B} MB5* and the strong *tim*-Gal4,*pdf*-Gal80 line did not yield in living offspring. In addition to the shortening or lengthening of the period in *sgg* manipulated animals a reduction in overall rhythmicity and in live span was observable. When we addressed different subsets of the dorsal neurons (*cry*-Gal4/*pdf*-Gal80 or *clk 4-1M* Gal4) we could not see an effect. While *cry*-Gal4/*pdf*-Gal80 addressed the *cry* expressing LNds and DN1s (Stoleru et al. 2004), *clk 4-1M* Gal4 is expressed in the DN1p only (Zhang et al. 2010) (S1 Fig.). Down-regulation of SGG resulted in long periods under DD conditions – again we could not see an effect, when we only down regulated SGG in the dorsal neurons (Table 1). We could detect a similar difference, when we investigated the LD behaviour of the animals (S2 Fig.). Our conclusion of those behaviour experiments is that *sgg* is only important in the lateral Neurons, especially in the *pdf* expressing small and large LNvs, but not in the dorsal Neurons – at least for LD and DD behaviour. Strikingly, in our hands over-expression of *sgg* in the entire or parts of clock network did not elicit strong behavioural rhythmicity in LL. We investigated the behaviour in constant light with the same animals as in DD. Because the intensity of the light plays a very important role for the behaviour, we performed the LL experiments under three different light intensities, i.e. 50 lux, 300 lux and 1500 lux. The high light intensity conditions was used in Stoleru et al. (2007) (Stoleru et al. 2007) so we expected to see a high number of rhythmic animals under LL conditions. While *cry* mutants showed the expected robustly rhythmic behaviour in LL, both *UAS-sgg* failed to produce significant LL rhythmicity when driven by the various clock-neuronal Gal4 lines (Table 2 and Table S1). We did not observe a dramatic difference between the three light conditions, therefore we merged the data. In low light conditions was a general trend, that the animals are more rhythmic in LL (Sup Table S1). This effect was especially pronounced in the two *pdf*-Gal80 driver lines, *cry*-Gal4/*pdf*-Gal80 and *tim*-Gal4,*pdf*-Gal80. But this higher number of rhythmic animals was mainly due to the driver line – the driver controls are almost as rhythmic as the *sgg* manipulated animals – and therefore the rhythm originates more likely from genetic background or darker eye colour, than from real *sgg* manipulation. The detected rhythms in all animals, except cry^{01}, was very weak and faint. In Fig. 3 we compiled examples showing the rhythms observed after SGG overexpression in comparison to cry^{01}. In contrast to cry^{01} mutants, almost none of the animals showed an obvious rhythm, which fits to the results of the periodogram analysis. Here one can see, that the LL rhythm in those animals is not very obvious. We performed a chi-square test to clarify if *sgg* manipulated animals differ from the control and could not find a significant difference (Chi^2 from 0,15 to 3,76 and p ranging from 0,07 to 0,93) In total, we were never able to see such a dramatic LL effect, as did Stoleru et al. (Stoleru et al. 2007) The animals where we overexpressed the *period* gene displayed a significantly stronger rhythm than the *sgg* manipulated animals (Chi^2 from 11,4 to 14,9 and p ranging from 0,003 to 0,0006) – though the number and power of the rhythm was never as high as in cry^{01} (Chi^2 124,06 and p=8,2 E-29) and as reported in the original publication. An explanation for the difference in rhythmic of *period*

overexpressing animals compared to the original publication can be, that we used a different UAS-*per* construct than Murad et al. (Murad, Emery-Le, and Emery 2007). When *per* was expressed in the Dorsal neurons only, we could not find a rhythm in those animals.

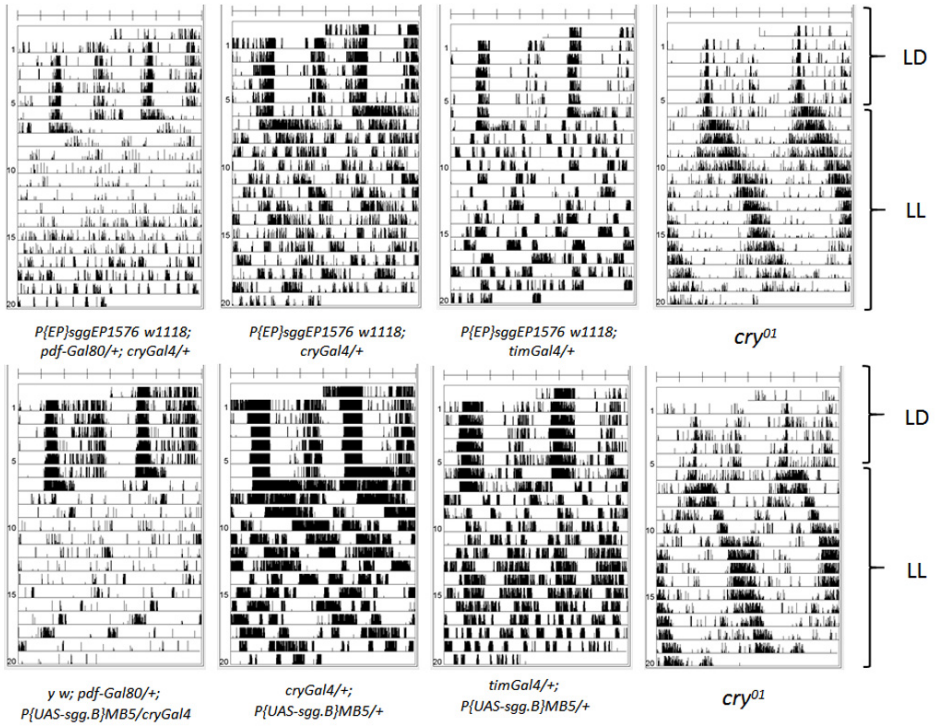

Figure 3.

Rhythmic behaviour of male *Drosophila* flies in LL after SGG overexpression

Double-plotted actograms of representative single males of the rhythmic genotypes are shown. On the y-axis the LD or LL setting is marked. While the SGG overexpressing animals only show a very weak rhythm in LL, *cry*^{01} animals still behave strongly rhythmic under these conditions.

Group	Genotype	n	period	sem	Rhythmic %
Over expression of *sgg*	*P{EP}sggEP1576 w^{1118}; Pdf*-Gal80*/+; cry*-Gal4*/+*	32	23,70	0,08	97
	P{EP}sggEP1576 w^{1118}; cry-Gal4*/+*	27	24,91	0,18	91
	P{EP}sggEP1576 w^{1118}; tim-Gal4*/+*	29	21,37	0,36	76
	P{EP}sggEP1576 w^{1118}; ; Clk 4-1M Gal4*/+*	16	24,38	0,06	100
	P{EP}sggEP1576 w^{1118};tim-Gal4,*pdf*-Gal80*/+*	14	24,83	0,13	89
Over expression of *sgg* (Uas)	*y w; Pdf-* Gal80*/+; P{*UAS-*sgg.B}MB5/cry*-Gal*4*	22	23,72	0,14	83
	cry-Gal4*/+;P{*UAS-*sgg.B}MB5/+*	29	20,94	0,14	77
	tim-Gal4*/+; P{*UAS-*sgg.B}MB5/+*	21	18,55	0,62	61
	*P{*UAS-*sgg.B}MB5/ Clk 4-1M* Gal4	16	24,16	0,07	100
Down regulation of *sgg* (RNAi)	*Pdf*-Gal80*/+; P{TRiP.GL00277 sgg RNAi}attP2/cry*-Gal4	29	24,20	0,14	93
	cry-Gal4*/+;P{TRiP.GL00277 sgg RNAi}attP2/+*	28	26,21	0,15	92
	tim-Gal4*/+; P{TRiP.GL00277 sgg RNAi}attP2/+*	31	27,03	0,14	100
	P{TRiP.GL00277 sgg RNAi}attP2/Clk 4-1M Gal4	16	24,36	0,23	100
	P{TRiP.GL00277 sgg RNAi}attP2;35364xtim-Gal4,*pdf-* Gal80*/+*	16	25,29	0,13	56
Over expression of *per*	*w*;*pdf*Gal80; UAS-*per16/*cry-Gal4	13	24,18	0,04	77
	w;cry-Gal4/+;UAS-*per16*/+	14	23,90	0,07	57
	w;tim-Gal4/+; UAS-*per16*/+	13	26,07	0,10	100
	*w;;*UAS-*per16/ Clk 4-1M* Gal4	13	24,64	0,10	92
	w;*tim*-Gal4,*pdf*-Gal80/+;UAS-*per16/+*	14	24,76	0,10	57
Control animals	*w^{1118}; pdf-* Gal80*/+;cry*-Gal4*/+*	29	23,66	0,12	97
	w^{1118}; cry-Gal4*/+*	28	24,69	0,17	92
	w^{1118}; tim-Gal4*/+*	29	23,84	0,11	97
	w^{1118}; ; Clk 4-1M Gal4*/+*	32	23,90	0,11	97
	w^{1118} ;tim-Gal4,*pdf-* Gal80*/+*	14	23,61	0,17	71
	P{EP}sggEP1576, w^{1118}	27	24,09	0,11	87
	w^{1118};;UAS-per16/+	13	23,63	0,08	92
	w^{1118};;P{UAS-sgg.B}MB5/+	30	23,47	0,13	93
	w^{1118};; P{TRiP.GL00277 sgg RNAi}attP2/+	31	23,52	0,15	90
Positiv Control	*cry^{01}*	29	23,07	0,08	97
	w^{1118}	31	23,78	0,09	93

Table 1.

Flies (only males) were recorded in LD 12:12 for 7 days and subsequently in DD for at least 14 days. The table displays the percentage of rhythmic flies, the period length and the rhythm of all investigated

genotypes in DD according to χ2-periodogram analysis. Furthermore, the number of investigated animals is indicated. Animals that died before the end of the experiment were excluded.

Group	Genotype	n	period	sem	Percent %
Over expression of *sgg*	*P{EP}sggEP1576 w^{1118}; Pdf*-Gal80*/+; cry*-Gal4*/+*	120	27,30	1,06	15,21
	P{EP}sggEP1576 w^{1118}; cry-Gal4*/+*	124	25,97	2,19	15,66
	P{EP}sggEP1576 w^{1118}; tim-Gal4*/+*	116	26,14	1,19	22,39
	P{EP}sggEP1576 w^{1118}; ; Clk 4-1M Gal4*/+*	48	25,80	0,91	10,69
	P{EP}sggEP1576 w^{1118};tim-Gal4,*pdf*-Gal80*/+*	123	23,30	1,04	26,71
Over expression of *sgg* (Uas)	*y w; Pdf-* Gal80*/+; P{*UAS-*sgg.B}MB5/cry*-Gal4	98	24,47	2,48	30,01
	cry-Gal4*/+;P{*UAS-*sgg.B}MB5/+*	115	25,37	1,63	30,52
	tim-Gal4*/+; P{*UAS-*sgg.B}MB5/+*	104	26,96	1,65	6,51
	*P{*UAS-*sgg.B}MB5/ Clk 4-1M* Gal4	48	7,77	0	2,22
Down regulation of *sgg* (RNAi)	*Pdf*-Gal80*/+; P{TRiP.GL00277 sgg RNAi}attP2/cry*-Gal4	112	25,67	1,22	15,94
	cry-Gal4*/+;P{TRiP.GL00277 sgg RNAi}attP2/+*	125	25,31	1,47	16,30
	tim-Gal4*/+; P{TRiP.GL00277 sgg RNAi}attP2/+*	118	24,67	2,14	13,68
	P{TRiP.GL00277 sgg RNAi}attP2/Clk 4-1M Gal4	48	15,83	0	4,46
	P{TRiP.GL00277 sgg RNAi}attP2;35364xtim-Gal4,*pdf-* Gal80*/+*	113	17,98	0,32	8,99
Over expression of *per*	*w*;*pdf*Gal80; UAS-*per16/*cry-Gal4	61	25,70	1,27	45,28
	w;cry-Gal4/+;UAS-*per16*/+	75	25,19	1,49	33,82
	w;tim-Gal4/+; UAS-*per16*/+	71	24,98	1,05	35,12
	*w;;*UAS-*per16/ Clk 4-1M* Gal4	74	27,1	0,53	7,68
	w;*tim*-Gal4,*pdf*-Gal80/+;UAS-*per16/+*	72	25,33	1,14	44,86
Control animals	*w^{1118}; pdf-* Gal80*/+;cry*-Gal4*/+*	121	25,73	1,09	27,29
	w^{1118}; cry-Gal4*/+*	122	25,84	1,01	14,27
	w^{1118}; tim-Gal4*/+*	115	26,47	1,17	13,63
	w^{1118}; ; Clk 4-1M Gal4*/+*	122	25,24	2,02	10,11
	w^{1118} ;tim-Gal4,*pdf-* Gal80*/+*	118	27,03	0,79	24,09
	P{EP}sggEP1576, w^{1118}	125	25,18	0,80	8,97
	w^{1118};;UAS-per16/+	70	23,36	1,52	17,41
	w^{1118};;P{UAS-sgg.B}MB5/+	122	24,91	0,43	9,18
	w^{1118};; P{TRiP.GL00277 sgg RNAi}attP2/+	114	26,54	0,35	7,94
Positiv Control	*cry^{01}*	109	24,74	0,28	81,96
	w^{1118}	123	26,26	2,39	9,33

Table 2.

Flies (only males) were recorded in LD 12:12 for 7 days and subsequently in LL for at least 14 days. The table displays the percentage of rhythmic flies, the period length and the rhythm of all investigated genotypes in LL according to χ2-periodogram analysis. Furthermore the number of investigated animals is indicated. Animals that died before the end of the experiment were excluded. The table displays a merge of all investigated LL settings, i.e. from LL50 – LL1500. The separate data can be seen in Supplementary Table S1.

Clock Neurons under SGG overexpression

Because western blots with whole heads or our luciferase assays with living animals showed us only the signal from the entirety of all clock neurons, we wanted to take a closer look at the single clock neurons. Overexpression of SGG under constant light could lead to a stabilization of CRY in only a small subset of clock neurons. Therefore, we used an immunohistochemical approach. We performed stainings of whole *Drosophila* brains.

The animals were first entrained in LD for three days and then released into LL conditions for 24 hrs. In this experiment, we overexpressed SGG or knocked SGG down by RNAi in all clock neurons. We performed triple stainings with antibodies against CRY, TIM and the Pigment-dispersing factor (PDF). The latter one helps identifying the ventral clock neurons. The staining of the SGG overexpressing animals and the controls did not reveal any clock neuron group in which CRY was stabilized. Quantification of staining intensity did not reveal any significant stabilization effect of SGG overexpression. Our statistical tests revealed a p value of $p>0.05$. CRY was similar low in all clock cells (Fig. 4). Furthermore, TIM and CRY expressions were restricted to the cytoplasm, never visible in the cell's nucleus (Fig. 4 A-C). The rhythmically migration of TIM from cytoplasm to the nucleus is important for proper clock function. Because we only investigated a single timepoint in LL conditions, we cannot rule out, that a whole series of different timepoints might reveal CRY in the nucleus as well. However, this seems unlikely because Stoleru et al. (Stoleru et al. 2007) showed that TIM protein is restricted to the cytoplasm, independent of the investigated timepoint in LL. On the other hand, CRY lacking animals - like cry^b – clearly showed nuclear TIM, leaving the question unanswered, what then could drive the LL rhythm in SGG overexpressing animals. We conclude that SGG manipulation does not neither significantly influence the light mediated degradation of TIM and CRY nor promote nuclear entry of CRY (Fig. 4 D and E).

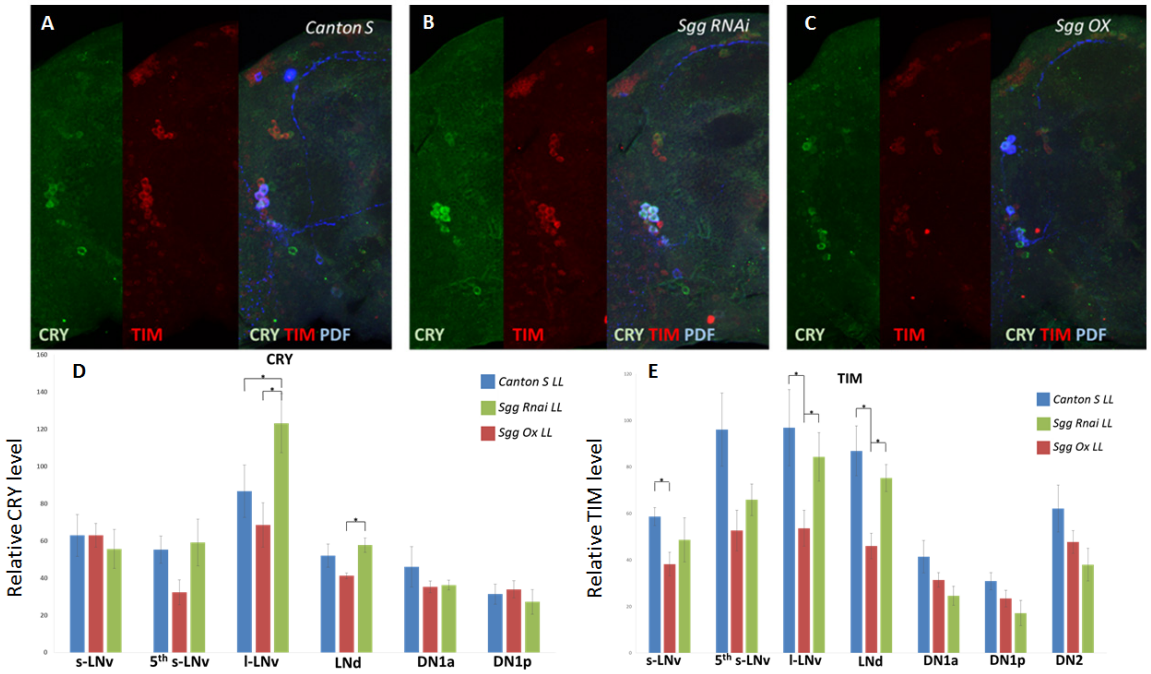

Figure 4.

Whole brains of the indicated genotypes were immunohistochemically investigated with anti-CRY (Yoshii et al. 2008), anti-TIM and anti-PDF antibodies. Animals were investigated on the first day in LL (300 Lux) at timepoint CT 21. (A-C) Representative pictures of the indicated genotypes are shown. (D) and (E) Staining intensity of the clock neurons was measured as described in Material and Methods and quantified. The x-axis displays the different subsets of clock neurons. Brains of at least five animals were averaged. No significant differences in staining intensity were found between *sgg* overexpressing flies and control flies. The only difference was a reduction of TIM in *sgg* overexpressing animals. Data were considered as significantly different at *p<0.05. Significances are indicated by asterisks in the graphs.

Detecting CRY with different antibodies

Because so far there was no evidence that SGG is stabilizing CRY, we wondered if there is a possibility, that we just missed a hint or fact from the original Cell publication from 2007. Finally, we found out, that we used a different antibody in our assay compared to Stoleru et al. (2007) (Stoleru et al. 2007). Our polyclonal antibody was raised against full-length dCRY protein (Yoshii et al.) (Yoshii et al. 2008), whereas the antibody used in the original publication (Stoleru et al.) (Stoleru et al. 2007) was raised against the N-terminal part of dCRY (AA 1-183) fused to a 6-HIS-tag (Rush et al.) (Rush et al. 2006), raising the possibility that the different antibodies may explain the conflicting results.

To compare the two antibodies we overexpressed *sgg* and *cry* in S2 cells, performed Western Blots and immunostained these in parallel with the two CRY-antibodies. Strikingly, we detected a strong signal in *sgg*-overexpressing flies with the CRY-antibody from Rush et al. (Rush et al. 2006) but not with the one of Yoshii et al. (Yoshii et al. 2008) (Fig. 5A). The newly appearing band was running slightly slower, compared to the one detected with our CRY serum (Fig. 5 A).

How can we explain the presence of the protein band and the different size of the protein detected by the Rush et al. antibody? There are two possible reasons. One possibility is that this antibody recognizes a different form of CRY, e.g. a phosphorylated form of this protein, though this does not explain why the faster migrating, presumably unphosphorylated CRY protein is not also visible. If the antibody by Yoshii et al. is not recognizing phosphorylated CRY protein, we would expect to see a strong band in SGG overexpression cells after phosphatase treatment. However, this was not the case (Fig. 1C) indicating that the Yoshii et al. antibody recognizes phosphorylated and unphosphorylated CRY. Another possibility to explain the results is that the Rush et al. antibody recognizes the overexpressed SGG protein itself. It is possible that the antibody not only recognizes CRY, but the HIS-tag epitope as well (a HIS-tagged CRY was used for the antibody production – and perhaps the tag was still part of the antigen). Because the overexpressed SGG (the same one as used in Stoleru et al. 2007) (Stoleru et al. 2007) was coupled to a HIS-tag, we decided to clone a new *pAc-sgg* vector, where we introduced a stop codon before the following V5 and HIS-tag sequence. Our prediction was, that the anti-CRY antibody (Rush et al.) (Rush et al. 2006) should not recognize this protein anymore. A western blot, where we expressed the SGG protein and the SGG-HIS protein in the presence and absence of CRY confirmed our hypothesis (Fig. 5 B). While the anti-CRY antibody from Yoshii et al. is recognizing only the overexpressed CRY protein, the antibody from Rush et al. recognizes the SGG-HIS protein too, but not the SGG protein without a tag.

To determine if the slower migrating band indeed corresponds to SGG, we incubated the western blot with an anti-GSK-3 antibody, which is directed against a region of the catalytic domain of the *Drosophila* GSK-3 enzyme. An overlay of the results, i.e. anti-GSK-3 in green, anti-CRY (Left side Rush et al., right side Yoshii et al.) in red, clearly shows that the anti-CRY (Rush et al.) antibody recognizes SGG-HIS protein in addition to CRY. The discrepancy between the previous study and our own results can therefore be explained by the different specificities of the CRY antibodies applied.

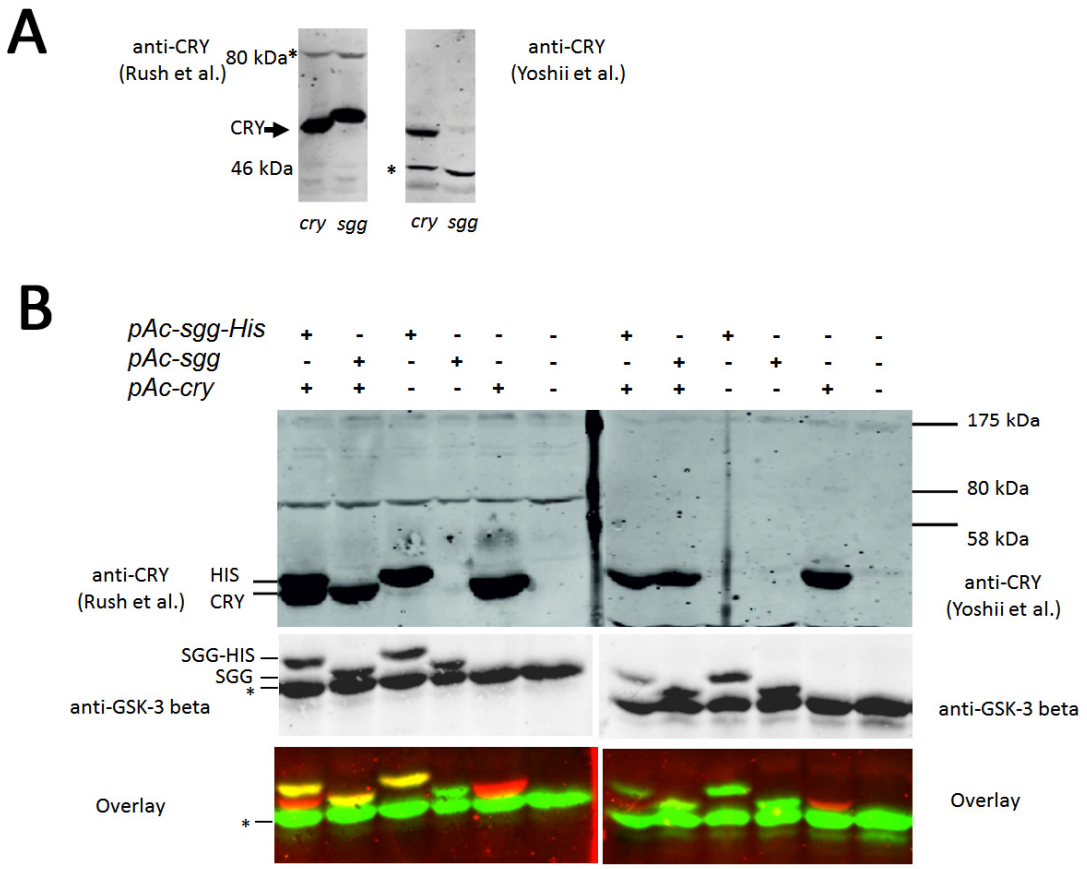

Figure 5.

CRY stability in S2 cells – with different antibodies.

(A) On the x-axis it is indicated if *pAc-sgg* or *pAc-cry* is expressed. The right western blot was treated with anti-CRY (Yoshii et al.) while for the left western blot another anti-CRY antibody was used (Rush et al.), but apart from the antibodies they were treated the same. The asterisk marks a non-specific band. The cells were kept in darkness. (B) The transfected plasmids are indicated at the top and left, while (+) is transfected, (-) indicates no transfection. Cells were kept in darkness and were released to light before harvesting. The right western blot was treated with anti-CRY (Yoshii et al.) while the left western blot was treated exactly the same, except of another anti-CRY antibody (Rush et al.). In the lower part, the western blot was incubated with anti-GSK-3 antibody. The asterisk marks a non-specific band. In the overlay anti-CRY antibody is coloured red, anti-GSK-3 is green and the overlay of both proteins results in a yellow colour.

Discussion

The Glycogen Synthase-kinase 3 beta plays an important role in regulating the circadian clock of different animals, like mice, humans or *Drosophila.* In the latter GSK-3 beta (in *Drosophila* called Shaggy) is directly interacting and phosphorylating master clock proteins like Period (Ko et al. 2010) or Timeless (Martinek et al. 2001) (and unpublished data). Recently it was reported, that another protein, the blue light photoreceptor Cryptochrome, is strongly stabilized by SGG. This stabilization is protecting the animals from constant light arrhythmicity. In our ongoing examination of how exactly this mechanism is working and to solve the conundrum how CRY stabilization leads to LL rhythmicity (Stoleru et al. 2007), we encountered the problem, that we were not able to reproduce the observed phenotype. When we overexpressed SGG in clock cells we could see, that the animals display a period of about 20 hrs in DD conditions (Martinek et al. 2001). The reason for this faster rhythm is that SGG is phosphorylating PER and TIM enabling the phosphorylated proteins to enter the cell's nucleus earlier. The observed changes in behaviour after overexpressing a protein does not necessarily mean that this protein really plays a role under normal, natural conditions. For example, it could be that endogenous SGG is not present in clock cells. However, RNAi down-regulation of SGG in the clock cells clearly demonstrated the importance of *sgg* for the clock. When we knocked down *sgg* in the ventrally located clock neurons, animals displayed a long period of more than 26 hrs in DD. This new result clearly demonstrates, that *sgg* plays an important role in the circadian clock, but that its influence is mainly restricted to the PDF expressing cells and that *sgg's* role in the Dorsal Neurons is of minor importance – at least in LD and DD conditions.

The highly phosphorylated form of TIM is more prone to the light induced degradation. Because of this effect, we expected that animals overexpressing SGG might be more sensitive towards light. Consistent with this idea, reducing the activity of SGG leads to a slightly more stable TIM protein and subsequently to animals, which are less sensitive to light (Yuan et al. 2005). For this reason we were intrigued by apparent opposite effect of SGG (Stoleru et al. 2007). Because we are not able to reproduce the data we started to doubt, that SGG is really directly influencing CRY. We could show that the previously reported stabilization effect of SGG on CRY was due to a misinterpretation of data obtained with a CRY antibody that recognizes CRY, but HIS-tagged proteins as well. We believe that the reason for this is found in the production of this antibody - a HIS-tagged CRY was used for the generation. Another awkward coincidence was that CRY and SGG are migrating at a similar size on western blots – explaining why the HIS-tagged SGG was mistakenly recognized as CRY.

In contrast to previous observations (Stoleru et al. 2007), we were not able to elicit rhythmic LL behaviour after overexpression of SGG nor were we able to see more light sensitive animals after down

regulating *sgg* via RNAi. We speculate that genetic background effects are responsible for this discrepancy (Stoleru et al. 2007). The beauty of the hundred-year-old model organism *Drosophila* in the genetic field has a big culprit. Because the animals are kept for a long time under unnatural laboratory conditions, they are accumulating more and more mutations, because they are living in a sort of land of milk and honey, without the pressure of natural selection and evolution. Unpublished experiments from our lab show, that for example "wild type" *CantonS* animals are so degenerated, that they are not able to survive in nature for a long time. Genetic tools, like the utilization of *P*-element insertions are another factor that introduces many problems/mutations for the investigator.

In a publication from 2006 we were able to show, that a certain spontaneous mutation in the *jetlag* gene is only phenotypical visible, when it is combined with a particular *tim* allele (Peschel, Veleri, and Stanewsky 2006), clearly demonstrating, that the genetic background of the animals is very important. Even more, because the mutation in the *jetlag* gene is lurking in a lot of common laboratory strains. Maybe a similar situation existed in the LL-rhythmic SGG-overexpressing flies (Stoleru et al. 2007). When we took a closer look at the *tim* allele polymorphism and *jetlag* mutation in our investigated experimental strains, we were not able to see a LL rhythm inducing combination of alleles (S3 Fig.). But most of the flies analysed in the current study carry the more light-sensitive s-TIM form and we were able to find further polymorphisms in the *jetlag* gene. It is possible, that the animals in Stoleru et al. carried the more stable ls-TIM version or the *jetlag* mutation, resulting in more LL rhythmic animals, or other genetic background defects, influencing the circadian clock. Reductions in DNA sequencing costs could create a new aid to solve problems with genetic background effects and thus improve future *Drosphila* genetic work.

Materials and Methods

Fly Strains

Flies were raised on a standard cornmeal/agar medium at 25°C in LD 12:12. For overexpression of *sgg* we used Bloomington strain #11008 *P{EP}sggEP1576* w^{1118} and #5361 w^{1118}*; P{UAS-sgg.B}MB5*. For RNAi knockdown we used #35364 *P{TRiP.GL00277}attP2*. The driver lines *cry*-Gal4#39 and *tim*-Gal4 are described in (Emery, Stanewsky, Helfrich-Förster, et al. 2000) and (Blau and Young 1999).Clk 4-1M Gal4/TM6B is described in (Zhang et al. 2010). y w; Pdf-Gal80/CyO; cry-Gal4/MKRS was a gift from C. Hermann-Luibl. w1118 is described in (Kurkulos et al. 1991). y w Pdf- Gal80,tim-Gal4/CyO was a gift from R. Stanewsky. Cry01 is described in (Dolezelova, Dolezel, and Hall 2007). w;;UAS-per16/+ is described in (Grima et al. 2004). For the luciferase assay we used in addition tim-Gal4 (62) as in (Kaneko and Hall 2000), the UAS-timeless lines are described in (Yang and Sehgal 2001) and UAS-Luc-dCry is

described in (Peschel et al. 2009) . For the wholemount stainings we used tim (UAS)-Gal4 (Blau and Young 1999) and Canton S (Konopka, Pittendrigh, and Orr 1989).

Behavioural analysis

Locomotor activity of individual flies was recorded using the *Drosophila* Activity Monitoring (DAM) System (Trikinetics) as previously described (Hermann et al. 2012). We investigated behaviour of 3–7 day old male flies in LD 12:12 for 7 days (with a light intensity of 50, 300 or 1500 lux in the light phase) followed by additional 14 days in constant darkness (DD) or constant light (LL). All recordings took place under constant 25°C in a climate–controlled chamber. Raw data of individual light beam crosses were collected in 1-minute bins and displayed as double-plotted actograms using ActogramJ. This program is a Java plug-in (Schmid, Helfrich-Förster, and Yoshii 2011) of ImageJ (that can be downloaded at http://rsb.info.nih.gov/ij/). For determining the individual free-running period (τ) of rhythmic flies, DD data from day 2–12 were analysed using χ^2-periodogram analysis and average period length of each genotype was calculated. Finally, data were averaged across the genotype. For determining the free-running period and rhythmicity, we analysed LL data from day 2-12 in the same way. Only cry^{01} showed a stable rhythm.

Cell Culture

The S2 cell line was derived from a primary culture of late stage (20-24 hours old) *Drosophila melanogaster* embryos (Schneider, 1972). The cells were grown in Insect Xpress medium (Cambrex) with 10% fetal bovine serum (Sigma-Aldrich) and 1% Penicillin-Streptomycin (PAA) at 25°C. Cells were transfected using FectoFly (polyPlus).

pAc-cry, pAc-jet, pAc-jet^c, pAc-tim are described in (Peschel et al. 2009). *pAc-sgg* (HIS) is a gift from P. Nawathean (Stoleru et al. 2007). We used a site-directed Mutagenesis kit (Agilent) to introduce a Stop-Codon for the generation of *pAc-sgg (noHIS)*.

Western Blots

Cells were harvested 72 hrs after transfection. They were homogenized in protein extraction buffer (20 mM HEPES pH 7.5; 100 mM KCl; 5% glycerol; 10 mM EDTA; 0.1% Triton X-100; 20 mM β-glycerophosphate; 0.1 mM Na3VO4 pH 11) containing a protease inhibitor cocktail (c0mplete Mini EDTA-free; Roche) and loaded onto a 10% gel. For dephosphorylation we treated the protein extract with λ-Phosphatase (Thermo Scientific) for 1 hour. For visualizing the different proteins, we incubated the western blots in primary and secondary fluorescent antibodies with following dilutions: rabbit anti-CRY 1:10000 (kindly provided by T. Yoshii), Alexa Fluor goat-anti-rabbit 680 1:5000 (Invitrogen), rabbit

anti-CRY 1:1000 (kindly provided by P. Emery), Mouse Anti-HIS 1:5000 (Invitrogen) Alexa Fluor goat-anti-mouse 1:5000 (Invitrogen), mouse anti-GSK-3 1:5000 (4G-1E; Millipore).

Fluorescent signals were detected using the Odyssey Imaging System (Licor Bioscience).

Luciferase Assay

Adult flies carrying the luciferase gene fused to dCryptochrome under the control of UAS were fed with luciferin containing food, the resulting bioluminescence measured with a Perkin Elmer TopCount NXT. This assay was performed as in (Stanewsky, Jamison, et al. 1997) and (Peschel et al. 2009). For the analysis we averaged the data from 8 different animals.

Immunohistochemistry

To investigate CRY and TIM stability in adult *Drosophila* brains, 3-7 days old male flies were entrained to LD 12:12 for at least 4 days and then released to constant light conditions. They were sacrificed after 24 hours in light. Flies were fixed in 4% paraformaldehyde (PFA) in 0.1M phosphate buffer (PB; pH 7.4) with 0.1% Triton X-100 for 2.5 hours. The fixation step was carried out on a shaker at room temperature. After dissection 5% normal goat serum (NGS) in PB with 0.5% Triton X-100 was used for blocking samples overnight at 4°C. The brains were incubated with primary antibodies that were diluted in PB with 0.5% Triton X-100, 5% NGS and 0.02% NaN_3 as follows: rat anti-TIM 1:1000 (kindly provided by I. Edery), mouse anti-PDF 1:1000 (Developmental Studies Hybridoma Bank; DSHB), rabbit anti-CRY 1:1000 (kindly provided by T. Yoshii). After 24–48 hours primary antibody incubation secondary antibodies were applied. Immunolabelings Alexa Fluor 488, Alexa Fluor 555 and Alexa Fluor 647 (all from Molecular Probes) were used as secondary antibodies in a dilution of 1:200 in PB with 5% NGS and 0.5% Triton X-100. After 2 hrs at room temperature secondary antibody solution was removed. Finally, brains were embedded in Vectashield mounting medium (Vector Laboratories). Confocal images were obtained using a Leica TCS SPE confocal microscope. Z-stack images were visualized and edited with the ImageJ distribution Fiji (http://fiji.sc/wiki/index.php/Fiji or http://rsb.info.nih.gov/ij/). Stacks were cropped and compiled as maximum projections. Brightness and contrast were adjusted. For intensity quantification, samples were processed in exactly the same way during the staining protocol and were scanned with identical laser settings. The quantifications were conducted in ImageJ (Fiji). For quantification a square-shaped area of 9 pixels (3 × 3 pixels) was placed on each cell of interest and the average pixel intensity was measured in the brightest focal plane. Cells of at least five different animals were analysed and the intensity values were first background corrected and then averaged for each neuronal group and genotype.

Statistics

Data were tested for normal distribution applying a onesample Kolmogorov–Smirnov test. To test for significant differences in normally distributed datasets, we then applied a one-way ANOVA followed by a post hoc pairwise comparison with Bonferroni's correction. Data that were not distributed normally were tested for significant differences with a Kruskal–Wallis test followed by pairwise comparison with Wilcoxon analysis. Data were considered as significantly different at *p<0.05. Significances are indicated by asterisks in the graphs.

PCR

For genotyping and identifying the timeless *s-tim* and *ls-tim* animals, we used the following oligonucleotide primers to amplify (and later to sequence) the genomic DNA: sense: 5'-TAGGTATCGCCCTCCAAG-3' and antisense: 5'-TAGGCAGCTCCACAATCA-3'. Sequencing of *jet* gDNA was performed by using oligonucleotides 5`-TGGGATAGAAGTCGTTCAAGT-3` (sense) and 5`-TGCCGATGGCTAACAGAT-3` (antisense) to determine the variants at the common ,rare and jetset (Lamba et al. 2014) sites within two LRR-encoding domains.

Acknowledgments

We would like to thank the members of the Förster and Stanewsky lab for fruitful discussions, B. Mühlbauer, G. Szabo for practical support and I. Wenzel for administrative help. We want to thank especially M. Schlichting and C. Hermann-Luibl for help with the statistics and data analysis. We are grateful for antibodies or fly strains from P. Emery, I. Edery, M. Rosbash and the Bloomington Drosophila Stock Center. Furthermore we would like to thank D. Stoleru for help and discussions and P. Nawathean for vectors. We would like to thank R. Stanewsky and A. Huber for critical comments on the manuscript. Finally, we would like to thank the Deutsche Forschungsgemeinschaft for funding and grants FKZ: Pe1798/2-1

References

1. Schibler U. Circadian time keeping: the daily ups and downs of genes, cells, and organisms. Progress in brain research. 2006;153:271-82. doi: 10.1016/S0079-6123 (06)53016-X. PubMed PMID: 16876581.

2. Reppert SM, Weaver DR. Molecular analysis of mammalian circadian rhythms. Annual review of physiology. 2001;63:647-76. doi: 10.1146/annurev.physiol.63.1.647. PubMed PMID: 11181971.

3. Masri S, Sassone-Corsi P. The circadian clock: a framework linking metabolism, epigenetics and neuronal function. Nature reviews Neuroscience. 2013;14 (1):69-75. doi: 10.1038/nrn3393. PubMed PMID: 23187814.

4. Peschel N, Helfrich-Förster C. Setting the clock--by nature: circadian rhythm in the fruitfly Drosophila melanogaster. FEBS Lett. 2011;585 (10):1435-42. doi: 10.1016/j.febslet.2011.02.028. PubMed PMID: 21354415.

5. Foster RG, Roenneberg T. Human responses to the geophysical daily, annual and lunar cycles. Current biology : CB. 2008;18 (17):R784-R94. doi: 10.1016/j.cub.2008.07.003. PubMed PMID: 18786384.

6. Roenneberg T, Kumar CJ, Merrow M. The human circadian clock entrains to sun time. Current biology : CB. 2007;17 (2):R44-5. doi: 10.1016/j.cub.2006.12.011. PubMed PMID: 17240323.

7. Foster RG, Hankins MW, Peirson SN. Light, photoreceptors, and circadian clocks. Methods in molecular biology. 2007;362:3-28. doi: 10.1007/978-1-59745-257-1_1. PubMed PMID: 17416998.

8. Stanewsky R, Kaneko M, Emery P, Beretta B, Wager-Smith K, Kay SA, et al. The cryb mutation identifies cryptochrome as a circadian photoreceptor in Drosophila. Cell. 1998;95 (5):681-92. PubMed PMID: 9845370.

9. Emery P, So WV, Kaneko M, Hall JC, Rosbash M. CRY, a Drosophila clock and light-regulated cryptochrome, is a major contributor to circadian rhythm resetting and photosensitivity. Cell. 1998;95 (5):669-79. PubMed PMID: 9845369.

10. Yang Z, Emerson M, Su HS, Sehgal A. Response of the timeless protein to light correlates with behavioral entrainment and suggests a nonvisual pathway for circadian photoreception. Neuron. 1998;21 (1):215-23. PubMed PMID: 9697865.

11. Suri V, Qian Z, Hall JC, Rosbash M. Evidence that the TIM light response is relevant to light-induced phase shifts in Drosophila melanogaster. Neuron. 1998;21 (1):225-34. PubMed PMID: 9697866.

12. Emery P, Stanewsky R, Hall JC, Rosbash M. A unique circadian-rhythm photoreceptor. Nature. 2000;404 (6777):456-7. doi: 10.1038/35006558. PubMed PMID: 10761904.

13. Sandrelli F, Tauber E, Pegoraro M, Mazzotta G, Cisotto P, Landskron J, et al. A molecular basis for natural selection at the timeless locus in Drosophila melanogaster. Science. 2007;316 (5833):1898-900. doi: 10.1126/science.1138426. PubMed PMID: 17600216.

14. Koh K, Zheng X, Sehgal A. JETLAG resets the Drosophila circadian clock by promoting light-induced degradation of TIMELESS. Science. 2006;312 (5781):1809-12. doi: 10.1126/science.1124951. PubMed PMID: 16794082; PubMed Central PMCID: PMC2767177.

15. Peschel N, Veleri S, Stanewsky R. Veela defines a molecular link between Cryptochrome and Timeless in the light-input pathway to Drosophila's circadian clock. Proceedings of the National Academy of Sciences of the United States of America. 2006;103 (46):17313-8. doi: 10.1073/pnas.0606675103. PubMed PMID: 17068124; PubMed Central PMCID: PMC1859927.

16. Ozturk N, VanVickle-Chavez SJ, Akileswaran L, Van Gelder RN, Sancar A. Ramshackle (Brwd3) promotes light-induced ubiquitylation of Drosophila Cryptochrome by DDB1-CUL4-ROC1 E3 ligase complex. Proceedings of the National Academy of Sciences of the United States of America. 2013;110 (13):4980-5. doi: 10.1073/pnas.1303234110. PubMed PMID: 23479607; PubMed Central PMCID: PMC3612607.

17. Peschel N, Chen KF, Szabo G, Stanewsky R. Light-dependent interactions between the Drosophila circadian clock factors cryptochrome, jetlag, and timeless. Current biology : CB. 2009;19 (3):241-7. doi: 10.1016/j.cub.2008.12.042. PubMed PMID: 19185492.

18. Lamba P, Bilodeau-Wentworth D, Emery P, Zhang Y. Morning and evening oscillators cooperate to reset circadian behavior in response to light input. Cell reports. 2014;7 (3):601-8. doi: 10.1016/j.celrep.2014.03.044. PubMed PMID: 24746814.

19. Dubruille R, Murad A, Rosbash M, Emery P. A constant light-genetic screen identifies KISMET as a regulator of circadian photoresponses. PLoS genetics. 2009;5 (12):e1000787. doi: 10.1371/journal.pgen.1000787. PubMed PMID: 20041201; PubMed Central PMCID: PMC2789323.

20. Chen KF, Peschel N, Zavodska R, Sehadova H, Stanewsky R. QUASIMODO, a Novel GPI-anchored zona pellucida protein involved in light input to the Drosophila circadian clock. Current biology : CB. 2011;21 (9):719-29. doi: 10.1016/j.cub.2011.03.049. PubMed PMID: 21530261.

21. Knowles A, Koh K, Wu JT, Chien CT, Chamovitz DA, Blau J. The COP9 signalosome is required for light-dependent timeless degradation and Drosophila clock resetting. The Journal of neuroscience : the official journal of the Society for Neuroscience. 2009;29 (4):1152-62. doi: 10.1523/JNEUROSCI.0429-08.2009. PubMed PMID: 19176824; PubMed Central PMCID: PMC2648809.

22. Martinek S, Inonog S, Manoukian AS, Young MW. A role for the segment polarity gene shaggy/GSK-3 in the Drosophila circadian clock. Cell. 2001;105 (6):769-79. PubMed PMID: 11440719.

23. Meissner RA, Kilman VL, Lin JM, Allada R. TIMELESS is an important mediator of CK2 effects on circadian clock function in vivo. The Journal of neuroscience : the official journal of the Society for Neuroscience. 2008;28 (39):9732-40. doi: 10.1523/JNEUROSCI.0840-08.2008. PubMed PMID: 18815259; PubMed Central PMCID: PMC3032400.

24. Akten B, Jauch E, Genova GK, Kim EY, Edery I, Raabe T, et al. A role for CK2 in the Drosophila circadian oscillator. Nature neuroscience. 2003;6 (3):251-7. doi: 10.1038/nn1007. PubMed PMID: 12563262.

25. Stoleru D, Nawathean P, Fernandez MP, Menet JS, Ceriani MF, Rosbash M. The Drosophila circadian network is a seasonal timer. Cell. 2007;129 (1):207-19. doi: 10.1016/j.cell.2007.02.038. PubMed PMID: 17418796.

26. Zoltowski BD, Vaidya AT, Top D, Widom J, Young MW, Crane BR. Structure of full-length Drosophila cryptochrome. Nature. 2011;480 (7377):396-U156. doi: Doi 10.1038/Nature10618. PubMed PMID: WOS:000298033000058.

27. Lin FJ, Song W, Meyer-Bernstein E, Naidoo N, Sehgal A. Photic signaling by cryptochrome in the Drosophila circadian system. Molecular and cellular biology. 2001;21 (21):7287-94. doi: Doi 10.1128/Mcb.21.21.7287-7294.2001. PubMed PMID: WOS:000171486900016.

28. Yoshii T, Todo T, Wulbeck C, Stanewsky R, Helfrich-Förster C. Cryptochrome is present in the compound eyes and a subset of Drosophila's clock neurons. The Journal of comparative neurology. 2008;508 (6):952-66. doi: 10.1002/cne.21702. PubMed PMID: 18399544.

29. Brandes C, Plautz JD, Stanewsky R, Jamison CF, Straume M, Wood KV, et al. Novel features of drosophila period Transcription revealed by real-time luciferase reporting. Neuron. 1996;16 (4):687-92. PubMed PMID: 8607986.

30. Beckwith EJ, Ceriani MF. Experimental assessment of the network properties of the Drosophila circadian clock. The Journal of comparative neurology. 2014. doi: 10.1002/cne.23728. PubMed PMID: 25504089.

31. Zhang L, Chung BY, Lear BC, Kilman VL, Liu Y, Mahesh G, et al. DN1 (p) circadian neurons coordinate acute light and PDF inputs to produce robust daily behavior in Drosophila. Current biology : CB. 2010;20 (7):591-9. doi: 10.1016/j.cub.2010.02.056. PubMed PMID: 20362452; PubMed Central PMCID: PMC2864127.

32. Murad A, Emery-Le M, Emery P. A subset of dorsal neurons modulates circadian behavior and light responses in Drosophila. Neuron. 2007;53 (5):689-701. doi: 10.1016/j.neuron.2007.01.034. PubMed PMID: 17329209; PubMed Central PMCID: PMC1852515.

33. Stoleru D, Peng Y, Nawathean P, Rosbash M. A resetting signal between Drosophila pacemakers synchronizes morning and evening activity. Nature. 2005;438 (7065):238-42. doi: 10.1038/nature04192. PubMed PMID: 16281038.

34. Stoleru D, Peng Y, Agosto J, Rosbash M. Coupled oscillators control morning and evening locomotor behaviour of Drosophila. Nature. 2004;431 (7010):862-8. doi: 10.1038/nature02926. PubMed PMID: 15483615.

35. Rush BL, Murad A, Emery P, Giebultowicz JM. Ectopic CRYPTOCHROME renders TIM light sensitive in the Drosophila ovary. Journal of biological rhythms. 2006;21 (4):272-8. doi: 10.1177/0748730406290416. PubMed PMID: 16864647.

36. Ko HW, Kim EY, Chiu J, Vanselow JT, Kramer A, Edery I. A hierarchical phosphorylation cascade that regulates the timing of PERIOD nuclear entry reveals novel roles for proline-directed kinases and GSK-3beta/SGG in circadian clocks. The Journal of neuroscience : the official journal of the Society for Neuroscience. 2010;30 (38):12664-75. doi: 10.1523/JNEUROSCI.1586-10.2010. PubMed PMID: 20861372; PubMed Central PMCID: PMC2957474.

37. Yuan Q, Lin F, Zheng X, Sehgal A. Serotonin modulates circadian entrainment in Drosophila. Neuron. 2005;47 (1):115-27. doi: 10.1016/j.neuron.2005.05.027. PubMed PMID: 15996552.

38. Emery P, Stanewsky R, Helfrich-Förster C, Emery-Le M, Hall JC, Rosbash M. Drosophila CRY is a deep brain circadian photoreceptor. Neuron. 2000;26 (2):493-504. PubMed PMID: 10839367.

39. Blau J, Young MW. Cycling vrille expression is required for a functional Drosophila clock. Cell. 1999;99 (6):661-71. PubMed PMID: 10612401.

40. Kurkulos M, Weinberg JM, Pepling ME, Mount SM. Polyadenylylation in copia requires unusually distant upstream sequences. Proceedings of the National Academy of Sciences of the United States of America. 1991;88 (8):3038-42. PubMed PMID: 1849643; PubMed Central PMCID: PMC51379.

41. Dolezelova E, Dolezel D, Hall JC. Rhythm defects caused by newly engineered null mutations in Drosophila's cryptochrome gene. Genetics. 2007;177 (1):329-45. doi: 10.1534/genetics.107.076513. PubMed PMID: 17720919; PubMed Central PMCID: PMC2013679.

42. Grima B, Chelot E, Xia R, Rouyer F. Morning and evening peaks of activity rely on different clock neurons of the Drosophila brain. Nature. 2004;431 (7010):869-73. doi: 10.1038/nature02935. PubMed PMID: 15483616.

43. Kaneko M, Hall JC. Neuroanatomy of cells expressing clock genes in Drosophila: transgenic manipulation of the period and timeless genes to mark the perikarya of circadian pacemaker neurons

and their projections. The Journal of comparative neurology. 2000;422 (1):66-94. PubMed PMID: 10842219.

44. Yang Z, Sehgal A. Role of molecular oscillations in generating behavioral rhythms in Drosophila. Neuron. 2001;29 (2):453-67. PubMed PMID: 11239435.

45. Konopka RJ, Pittendrigh C, Orr D. Reciprocal behaviour associated with altered homeostasis and photosensitivity of Drosophila clock mutants. J Neurogenet. 1989;6 (1):1-10. PubMed PMID: 2506319.

46. Hermann C, Yoshii T, Dusik V, Helfrich-Förster C. Neuropeptide F immunoreactive clock neurons modify evening locomotor activity and free-running period in Drosophila melanogaster. The Journal of comparative neurology. 2012;520 (5):970-87. doi: 10.1002/cne.22742. PubMed PMID: 21826659.

47. Schmid B, Helfrich-Förster C, Yoshii T. A new ImageJ plug-in "ActogramJ" for chronobiological analyses. Journal of biological rhythms. 2011;26 (5):464-7. doi: 10.1177/0748730411414264. PubMed PMID: 21921300.

48. Schneider I. Cell lines derived from late embryonic stages of Drosophila melanogaster. Journal of embryology and experimental morphology. 1972;27 (2):353-65. PubMed PMID: 4625067.

49. Stanewsky R, Jamison CF, Plautz JD, Kay SA, Hall JC. Multiple circadian-regulated elements contribute to cycling period gene expression in Drosophila. The EMBO journal. 1997;16 (16):5006-18. doi: 10.1093/emboj/16.16.5006. PubMed PMID: 9305642; PubMed Central PMCID: PMC1170135.

Supplementary Information

Genotype	n LL50	period LL50	sem LL50	rhythmic LL50
P{EP}sggEP1576 w^{1118}; Pdf-Gal80*/+; cry*-Gal4*/+*	46	28,33	0,81	13,04
P{EP}sggEP1576 w^{1118}; cry-Gal4*/+*	48	26	1,58	20,83
P{EP}sggEP1576 w^{1118}; tim-Gal4*/+*	44	26,36	1,87	24,15
P{EP}sggEP1576 w^{1118}; ; Clk 4-1M Gal4*/+*	16	27,75	1,34	12,50
P{EP}sggEP1576 w^{1118};tim-Gal4*,pdf*-Gal80*/+*	45	23,19	1,19	49
y w; Pdf- Gal80*/+; P{*UAS-*sgg.B}MB5/cry*-Gal*4*	39	23,83	1,33	26
cry-Gal4*/+;P{*UAS-*sgg.B}MB5/+*	41	24,44	1,89	26,83
tim-Gal4*/+; P{*UAS-*sgg.B}MB5/+*	36	27,30	3,32	2,78
*P{*UAS-*sgg.B}MB5/ Clk 4-1M* Gal4	16	0	0	0
Pdf-Gal80*/+; P{TRiP.GL00277 sgg RNAi}attP2/cry*-Gal4	42	25,57	2,25	11,90
cry-Gal4*/+;P{TRiP.GL00277 sgg RNAi}attP2/+*	46	25,02	0,91	21,89
tim-Gal4*/+; P{TRiP.GL00277 sgg RNAi}attP2/+*	43	26,07	2,08	21,55
P{TRiP.GL00277 sgg RNAi}attP2/Clk 4-1M Gal4	16	24,10	0	7,14
P{TRiP.GL00277 sgg RNAi}attP2;35364xtim-Gal4*,pdf-* Gal80*/+*	41	26,35	0,82	17,88
*w;pdf*Gal80; UAS-*per16/*cry-Gal4	22	26,56	2,01	50
*w;*cry-Gal4/+;UAS-*per16/+*	31	24,37	1,79	41,94
w;tim-Gal4/+; UAS-*per16/+*	27	24,11	1,14	44,44
*w;;*UAS-*per16/ Clk 4-1M* Gal4	27	0	0	7,41
w;*tim*-Gal4,*pdf*-Gal80/+;UAS-*per16/+*	30	24,91	1,29	63,33
w^{1118}; pdf- Gal80*/+;cry*-Gal4*/+*	46	26,47	0,62	38,55
w^{1118}; cry-Gal4*/+*	46	26,49	1,40	20,50
w^{1118}; tim-Gal4*/+*	43	27,08	1,35	13,95
w^{1118}; ; Clk 4-1M Gal4*/+*	45	28,06	2,53	16,15
w^{1118};tim-Gal4*,pdf-* Gal80*/+*	44	26,74	0,74	38,64
P{EP}sggEP1576, w^{1118}	46	25,72	0,48	11,16
w^{1118};;UAS-per16/+	29	16,04	1,86	20,69
w^{1118};;P{UAS-sgg.B}MB5/+	46	25,75	0,65	8,70
w^{1118};; P{TRiP.GL00277 sgg RNAi}attP2/+	40	30	0	2,50
cry^{01}	42	24,21	0,46	78,21
w^{1118}	45	24,43	1,33	11,11

Table S1 A

LL rhythmicity of animals investigated under 50 Lux illumination.

Genotype	n LL300	period LL300	sem LL300	rhythmic LL300
P{EP}sggEP1576 w^{1118}; Pdf-Gal80*/+; cry*-Gal4*/+*	30	27,01	1,51	16,67
P{EP}sggEP1576 w^{1118}; cry-Gal4*/+*	32	25,95	2,02	12,50
P{EP}sggEP1576 w^{1118}; tim-Gal4*/+*	28	27,13	0,68	25
P{EP}sggEP1576 w^{1118}; ; Clk 4-1M Gal4*/+*	16	22,35	1,40	13,33
P{EP}sggEP1576 w^{1118};tim-Gal4,*pdf*-Gal80*/+*	32	23,48	0,86	15,63
y w; Pdf- Gal80*/+; P{*UAS-*sgg.B}MB5/cry*-Gal*4*	22	24,54	3,91	27,27
cry-Gal4*/+;P{*UAS-*sgg.B}MB5/+*	30	26,25	0,79	37,92
tim-Gal4*/+; P{*UAS-*sgg.B}MB5/+*	27	26,80	0	7,16
*P{*UAS-*sgg.B}MB5/ Clk 4-1M* Gal4	16	23,30	0	6,67
Pdf-Gal80*/+; P{TRiP.GL00277 sgg RNAi}attP2/cry*-Gal4	27	26,72	0,70	14,81
cry-Gal4*/+;P{TRiP.GL00277 sgg RNAi}attP2/+*	32	26,23	2,05	9,38
tim-Gal4*/+; P{TRiP.GL00277 sgg RNAi}attP2/+*	32	23,03	2,05	12,50
P{TRiP.GL00277 sgg RNAi}attP2/Clk 4-1M Gal4	16	23,39	0	6,25
P{TRiP.GL00277 sgg RNAi}attP2;35364xtim-Gal4,*pdf*- Gal80*/+*	28	0	0	0
*w;pdf*Gal80; UAS-*per16/*cry-Gal4	15	24,87	1,07	40
*w;*cry-Gal4/+;UAS-*per16/+*	14	27,43	1,42	42,86
w;tim-Gal4/+; UAS-*per16/+*	15	26,30	0,99	33,33
*w;;*UAS-*per16/ Clk 4-1M* Gal4	15	0	0	0
w;*tim*-Gal4,*pdf*-Gal80/+;UAS-*per16/+*	11	25,36	1,01	45,45
w^{1118}; pdf- Gal80*/+;cry*-Gal4*/+*	30	26,37	0,77	30
w^{1118}; cry-Gal4*/+*	29	23,75	0,71	13,79
w^{1118}; tim-Gal4*/+*	28	25,14	1,06	17,86
w^{1118}; ; Clk 4-1M Gal4*/+*	31	23,47	1,56	9,68
w^{1118};tim-Gal4,*pdf*- Gal80*/+*	30	26,25	0,61	20
P{EP}sggEP1576, w^{1118}	32	25,93	1,92	9,38
w^{1118};;UAS-per16/+	15	27,10	1,89	20
w^{1118};;P{UAS-sgg.B}MB5/+	30	26,33	0	16,67
w^{1118};; P{TRiP.GL00277 sgg RNAi}attP2/+	31	23,57	0,74	9,68
cry^{01}	29	25,09	0,04	93,33
w^{1118}	32	29,90	4,53	3,13

Table S1 B

LL rhythmicity of animals investigated under 300 Lux illumination

Genotype	n LL1500	period LL1500	sem LL1500	rhythmic LL1500
P{EP}sggEP1576 w^{1118}; Pdf-Gal80*/+; cry*-Gal4*/+*	44	26,55	0,88	15,91
P{EP}sggEP1576 w^{1118}; cry-Gal4*/+*	44	25,96	2,96	13,64
P{EP}sggEP1576 w^{1118}; tim-Gal4*/+*	44	24,92	1,03	18,03
P{EP}sggEP1576 w^{1118}; ; Clk 4-1M Gal4*/+*	16	27,29	0	6,25
P{EP}sggEP1576 w^{1118};tim-Gal4,*pdf*-Gal80*/+*	46	23,24	1,08	15,51
y w; Pdf- Gal80*/+; P{*UAS-*sgg.B}MB5/cry*-Gal*4*	37	25,04	2,22	36,76
cry-Gal4*/+;P{*UAS-*sgg.B}MB5/+*	44	25,41	2,19	26,82
tim-Gal4*/+; P{*UAS-*sgg.B}MB5/+*	41	26,77	1,62	9,59
*P{*UAS-*sgg.B}MB5/ Clk 4-1M* Gal4	16	0	0	0
Pdf-Gal80*/+; P{TRiP.GL00277 sgg RNAi}attP2/cry*-Gal4	43	24,70	0,71	21,10
cry-Gal4*/+;P{TRiP.GL00277 sgg RNAi}attP2/+*	47	24,69	1,45	17,63
tim-Gal4*/+; P{TRiP.GL00277 sgg RNAi}attP2/+*	43	24,90	2,30	6,98
P{TRiP.GL00277 sgg RNAi}attP2/Clk 4-1M Gal4	16	0	0	0
P{TRiP.GL00277 sgg RNAi}attP2;35364xtim-Gal4,*pdf*- Gal80*/+*	44	27,60	0,13	9,09
*w;pdf*Gal80; UAS-*per16/*cry-Gal4	24	25,67	0,72	45,83
w;cry-Gal4/+;UAS-*per16/+*	30	23,76	1,26	16,67
w;tim-Gal4/+; UAS-*per16/+*	29	24,52	1,02	27,59
*w;;*UAS-*per16/ Clk 4-1M* Gal4	32	27,10	1,58	15,63
w;*tim*-Gal4,*pdf*-Gal80/+;UAS-*per16/+*	31	25,71	1,12	25,81
w^{1118}; pdf- Gal80*/+;cry*-Gal4*/+*	45	24,36	1,88	13,33
w^{1118}; cry-Gal4*/+*	47	27,30	0,92	8,51
w^{1118}; tim-Gal4*/+*	44	27,18	1,11	9,09
w^{1118}; ; Clk 4-1M Gal4*/+*	46	24,20	1,98	4,49
w^{1118} ;tim-Gal4,*pdf*- Gal80*/+*	44	28,11	1,03	13,64
P{EP}sggEP1576, w^{1118}	47	23,90	0	6,38
w^{1118};;UAS-per16/+	26	26,94	0,80	11,54
w^{1118};;P{UAS-sgg.B}MB5/+	46	22,65	0,65	2,17
w^{1118};; P{TRiP.GL00277 sgg RNAi}attP2/+	43	26,04	0,31	11,63
cry^{01}	38	24,93	0,33	74,34
w^{1118}	46	24,46	1,31	13,76

Table S1 C

LL rhythmicity of animals investigated under 1500 Lux illumination

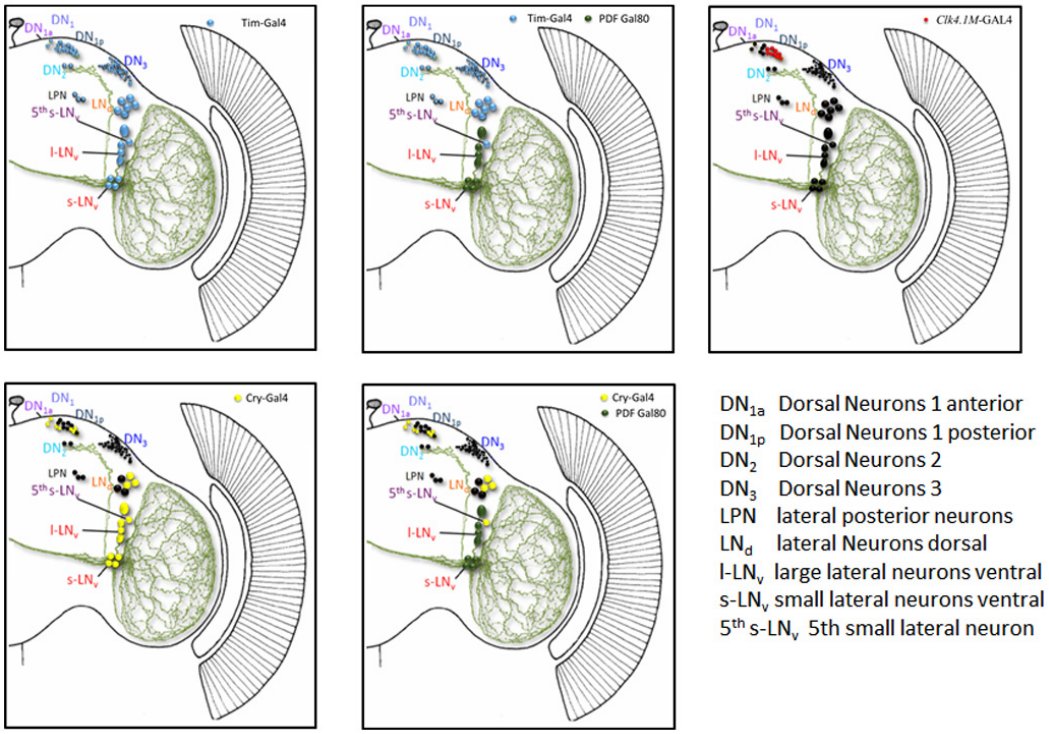

Figure S1

Overview of the *Drosophila melanogaster* brain, the clock neurons and their arborization.

The pictures illustrate the expression patterns of the driver lines that were used in the behavioural experiments. While the GAL4 protein is activating the UAS sequence and thus the following transcript, the GAL80 Protein is inhibiting the transcription of a gene following a UAS sequence.

The sophisticated system of activation and repression is working only to a certain extent, so that even in some cells, where GAL80 protein is produced, the inhibition of the UAS transcription might be not 100 %.

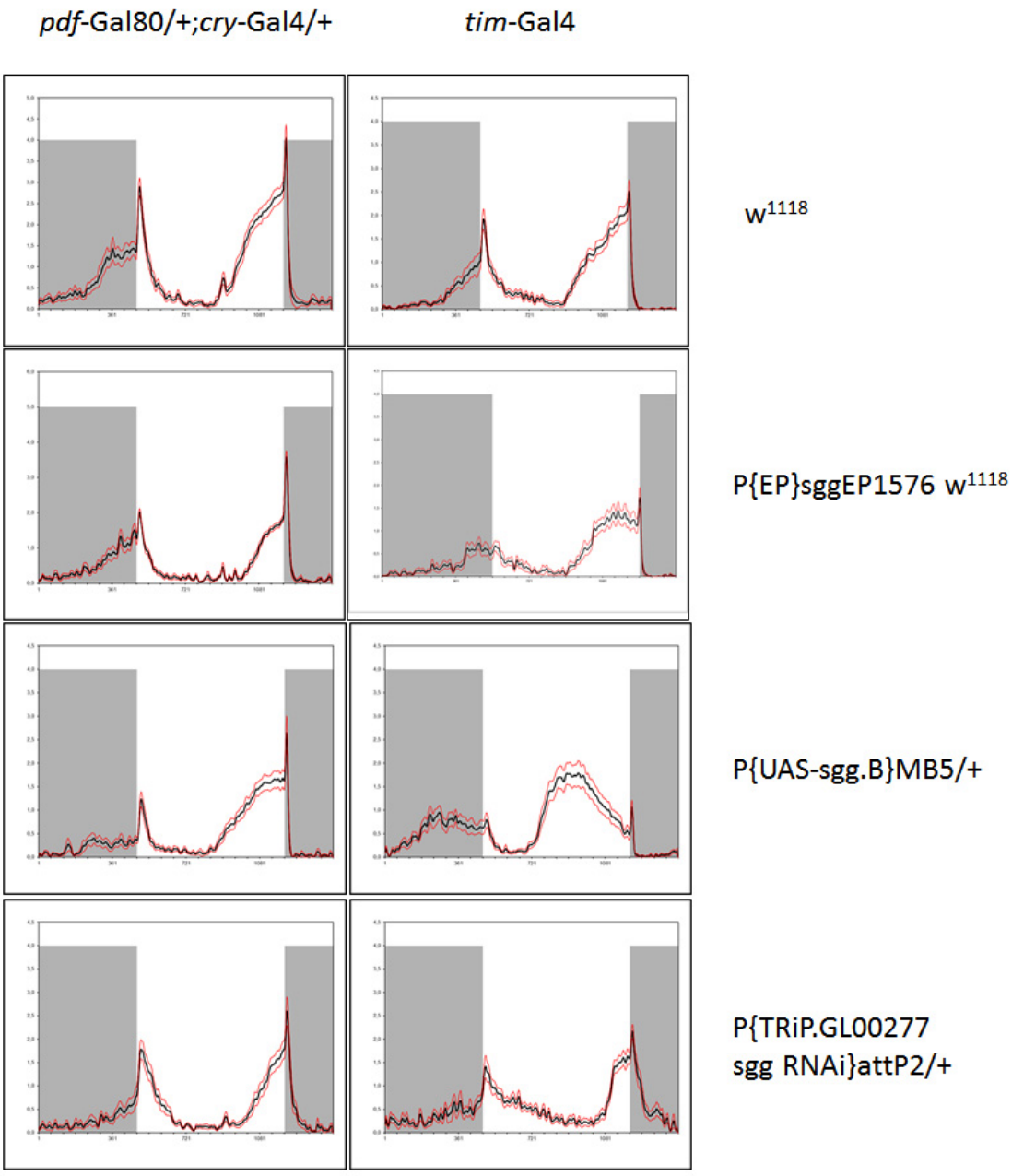

Figure S2

Behavior of *sgg* manipulated animals in LD conditions.

We investigated animals in L (50Lux) D, 25°C, for 7 consecutive days. The graph shows an average of 7 days and at least of 12 animals. The two driver lines *pdf*-Gal80/+;*cry*-Gal4/+ and *tim*-Gal4 were crossed versus wildtype or *sgg* manipulated animals. While an overexpression or knockdown of *sgg* in the TIM expressing cells leads to a shift of the evening/morning activity peak, the activity after a knockdown of

sgg is slightly shifted into the night. Expression in the Dorsal neurons or the white control did not yield in a change of the activity.

Genotype	*tim* allele
P{EP}sggEP1576	*s-tim*
P{TRiP.GL00277 sgg RNAi}attP2	*s-tim/ls-tim*
P{UAS-sgg.B}MB5	*s-tim*
clk4-1M Gal4	*s-tim/ls-tim*
cry-Gal4	*s-tim*
pdf-Gal80; cry-Gal4	*s-tim/ls-tim*
tim-Gal4	*s-tim*
CantonS	*ls-tim*
w^{1118}	*s-tim/ls-tim*

Figure S3

Jetlag and timeless changes in *Drosophila*

When we sequenced our *Drosophila* strains, that where investigated in locomotor behaviour, we were able to show, that different TIM isoforms were present in the strains. Furthermore we could show, that no jet^c, jet^r or jet^{set} mutation is in their *jetlag* gene. But we could see, that a lot more polymorphisms are present in *jetlag*, like L167I or L247V, demonstrating that a test of the proper genetic background is important.

Author contributions

Designed the experiments: RF, NP. Performed the experiments: RF, NP. Analysis and interpretation of data, technical support: RF, CHF, NP. Drafted the paper: NP, RF.

Competing interests

The authors declare that no competing interests exist.

Funding

Deutsche Forschungsgemeinschaft **FKZ: Pe1798/2-1**

The funders had no role in study design, data collection and interpretation, or the decision to submit the work for publication.

6.2 Amino acids

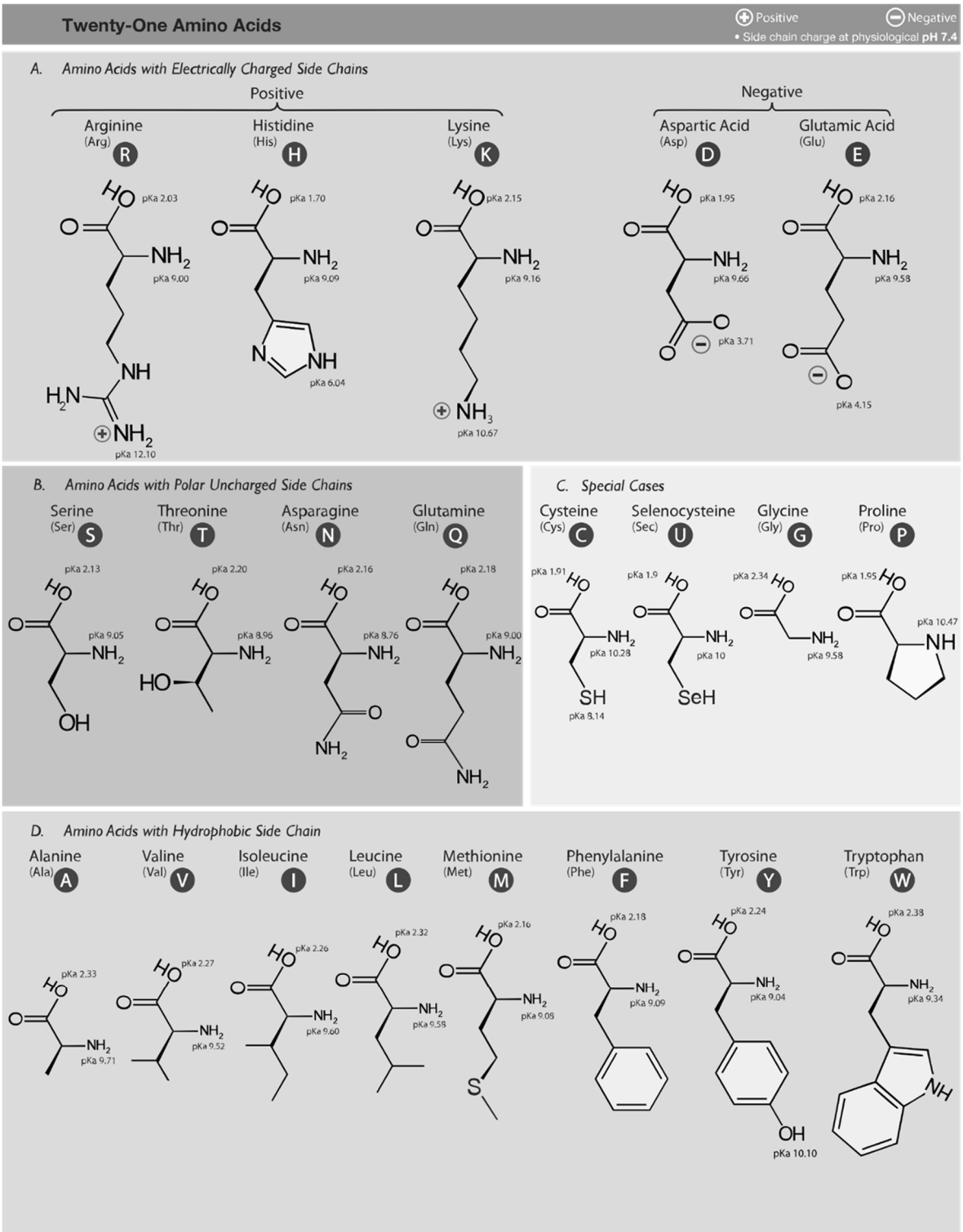

Figure 58: The 21 amino acids found in eukaryotes.

The AA are grouped according their side chains, acid dissociation constant and charges carried at pH 7.4. Single (used in the main text) and three letter abbreviations are noted above the structural formulas (http://wikipedia.org).

6.3 Literature

Akten, B., E. Jauch, G. K. Genova, E. Y. Kim, I. Edery, T. Raabe, and F. R. Jackson. 2003. "A role for CK2 in the Drosophila circadian oscillator." *Nature neuroscience* 6 (3):251-7. doi: 10.1038/nn1007.

Bae, K., C. Lee, D. Sidote, K. Y. Chuang, and I. Edery. 1998. "Circadian regulation of a Drosophila homolog of the mammalian Clock gene: PER and TIM function as positive regulators." *Mol Cell Biol* 18 (10):6142-51.

Bargiello, T. A., and M. W. Young. 1984. "Molecular genetics of a biological clock in Drosophila." *Proc Natl Acad Sci U S A* 81 (7):2142-6.

Bassett, A. R., and J. L. Liu. 2014. "CRISPR/Cas9 and genome editing in Drosophila." *J Genet Genomics* 41 (1):7-19. doi: 10.1016/j.jgg.2013.12.004.

Baylies, M. K., L. B. Vosshall, A. Sehgal, and M. W. Young. 1992. "New short period mutations of the Drosophila clock gene per." *Neuron* 9 (3):575-81.

Beckwith, E. J., and M. F. Ceriani. 2014. "Experimental assessment of the network properties of the Drosophila circadian clock." *J Comp Neurol*. doi: 10.1002/cne.23728.

Black, D. L. 2003. "Mechanisms of alternative pre-messenger RNA splicing." *Annu Rev Biochem* 72:291-336. doi: 10.1146/annurev.biochem.72.121801.161720.

Blau, J., and M. W. Young. 1999. "Cycling vrille expression is required for a functional Drosophila clock." *Cell* 99 (6):661-71.

Blom, N., T. Sicheritz-Ponten, R. Gupta, S. Gammeltoft, and S. Brunak. 2004. "Prediction of post-translational glycosylation and phosphorylation of proteins from the amino acid sequence." *Proteomics* 4 (6):1633-49. doi: 10.1002/pmic.200300771.

Brand, A. H., and N. Perrimon. 1993. "Targeted gene expression as a means of altering cell fates and generating dominant phenotypes." *Development* 118 (2):401-15.

Brandes, C., J. D. Plautz, R. Stanewsky, C. F. Jamison, M. Straume, K. V. Wood, S. A. Kay, and J. C. Hall. 1996. "Novel features of drosophila period Transcription revealed by real-time luciferase reporting." *Neuron* 16 (4):687-92.

Brown, R. S. 2005. "Zinc finger proteins: getting a grip on RNA." *Curr Opin Struct Biol* 15 (1):94-8. doi: 10.1016/j.sbi.2005.01.006.

Busza, A., M. Emery-Le, M. Rosbash, and P. Emery. 2004. "Roles of the two Drosophila CRYPTOCHROME structural domains in circadian photoreception." *Science* 304 (5676):1503-6. doi: 10.1126/science.1096973.

Bywalez, W., P. Menegazzi, D. Rieger, B. Schmid, C. Helfrich-Förster, and T. Yoshii. 2012. "The dual-oscillator system of Drosophila melanogaster under natural-like temperature cycles." *Chronobiol Int* 29 (4):395-407. doi: 10.3109/07420528.2012.668505.

Campos, I., J. A. Geiger, A. C. Santos, V. Carlos, and A. Jacinto. 2010. "Genetic screen in Drosophila melanogaster uncovers a novel set of genes required for embryonic epithelial repair." *Genetics* 184 (1):129-40. doi: 10.1534/genetics.109.110288.

Cashmore, A. R. 2003. "Cryptochromes: enabling plants and animals to determine circadian time." *Cell* 114 (5):537-43.

Ceriani, M. F., T. K. Darlington, D. Staknis, P. Mas, A. A. Petti, C. J. Weitz, and S. A. Kay. 1999. "Light-dependent sequestration of TIMELESS by CRYPTOCHROME." *Science* 285 (5427):553-6.

Chen, K. F., N. Peschel, R. Zavodska, H. Sehadova, and R. Stanewsky. 2011. "QUASIMODO, a Novel GPI-anchored zona pellucida protein involved in light input to the Drosophila circadian clock." *Curr Biol* 21 (9):719-29. doi: 10.1016/j.cub.2011.03.049.

Collins, B. H., S. Dissel, E. Gaten, E. Rosato, and C. P. Kyriacou. 2005. "Disruption of Cryptochrome partially restores circadian rhythmicity to the arrhythmic period mutant of Drosophila." *Proc Natl Acad Sci U S A* 102 (52):19021-6. doi: 10.1073/pnas.0505392102.

Cooley, L., R. Kelley, and A. Spradling. 1988. "Insertional mutagenesis of the Drosophila genome with single P elements." *Science* 239 (4844):1121-8.

Daan, S., and C. S. Pittendrigh. 1976. "Functional-Analysis of Circadian Pacemakers in Nocturnal Rodents .2. Variability of Phase Response Curves." *Journal of Comparative Physiology* 106 (3):253-266.

Dissel, S., V. Codd, R. Fedic, K. J. Garner, R. Costa, C. P. Kyriacou, and E. Rosato. 2004. "A constitutively active cryptochrome in Drosophila melanogaster." *Nature neuroscience* 7 (8):834-40. doi: 10.1038/nn1285.

Dolezelova, E., D. Dolezel, and J. C. Hall. 2007. "Rhythm defects caused by newly engineered null mutations in Drosophila's cryptochrome gene." *Genetics* 177 (1):329-45. doi: 10.1534/genetics.107.076513.

Dowse, H. B., J. C. Hall, and J. M. Ringo. 1987. "Circadian and ultradian rhythms in period mutants of Drosophila melanogaster." *Behav Genet* 17 (1):19-35.

Dubruille, R., and P. Emery. 2008. "A plastic clock: how circadian rhythms respond to environmental cues in Drosophila." *Molecular neurobiology* 38 (2):129-45. doi: 10.1007/s12035-008-8035-y.

Dubruille, R., A. Murad, M. Rosbash, and P. Emery. 2009. "A constant light-genetic screen identifies KISMET as a regulator of circadian photoresponses." *PLoS genetics* 5 (12):e1000787. doi: 10.1371/journal.pgen.1000787.

Emery, P., W. V. So, M. Kaneko, J. C. Hall, and M. Rosbash. 1998. "CRY, a Drosophila clock and light-regulated cryptochrome, is a major contributor to circadian rhythm resetting and photosensitivity." *Cell* 95 (5):669-79.

Emery, P., R. Stanewsky, J. C. Hall, and M. Rosbash. 2000. "A unique circadian-rhythm photoreceptor." *Nature* 404 (6777):456-7. doi: 10.1038/35006558.

Emery, P., R. Stanewsky, C. Helfrich-Förster, M. Emery-Le, J. C. Hall, and M. Rosbash. 2000. "Drosophila CRY is a deep brain circadian photoreceptor." *Neuron* 26 (2):493-504.

Fang, Y., S. Sathyanarayanan, and A. Sehgal. 2007. "Post-translational regulation of the Drosophila circadian clock requires protein phosphatase 1 (PP1)." *Genes & development* 21 (12):1506-18. doi: 10.1101/gad.1541607.

Foster, R. G., M. W. Hankins, and S. N. Peirson. 2007. "Light, photoreceptors, and circadian clocks." *Methods Mol Biol* 362:3-28. doi: 10.1007/978-1-59745-257-1_1.

Foster, R. G., and T. Roenneberg. 2008. "Human responses to the geophysical daily, annual and lunar cycles." *Curr Biol* 18 (17):R784-R794. doi: 10.1016/j.cub.2008.07.003.

Frame, S., and P. Cohen. 2001. "GSK3 takes centre stage more than 20 years after its discovery." *Biochemical Journal* 359:1-16.

Gamsjaeger, R., C. K. Liew, F. E. Loughlin, M. Crossley, and J. P. Mackay. 2007. "Sticky fingers: zinc-fingers as protein-recognition motifs." *Trends Biochem Sci* 32 (2):63-70. doi: 10.1016/j.tibs.2006.12.007.

Garbe, D. S., Y. Fang, X. Zheng, M. Sowcik, R. Anjum, S. P. Gygi, and A. Sehgal. 2013. "Cooperative interaction between phosphorylation sites on PERIOD maintains circadian period in Drosophila." *PLoS Genet* 9 (9):e1003749. doi: 10.1371/journal.pgen.1003749.

Gekakis, N., L. Saez, A. M. Delahaye-Brown, M. P. Myers, A. Sehgal, M. W. Young, and C. J. Weitz. 1995. "Isolation of timeless by PER protein interaction: defective interaction between timeless protein and long-period mutant PERL." *Science* 270 (5237):811-5.

Golic, K. G., and S. Lindquist. 1989. "The FLP recombinase of yeast catalyzes site-specific recombination in the Drosophila genome." *Cell* 59 (3):499-509.

Gong, W. J., and K. G. Golic. 2003. "Ends-out, or replacement, gene targeting in Drosophila." *Proceedings of the National Academy of Sciences of the United States of America* 100 (5):2556-61. doi: 10.1073/pnas.0535280100.

Grether, M. E., J. M. Abrams, J. Agapite, K. White, and H. Steller. 1995. "The head involution defective gene of Drosophila melanogaster functions in programmed cell death." *Genes & development* 9 (14):1694-708.

Grima, B., E. Chelot, R. Xia, and F. Rouyer. 2004. "Morning and evening peaks of activity rely on different clock neurons of the Drosophila brain." *Nature* 431 (7010):869-73. doi: 10.1038/nature02935.

Hall, T. M. 2005. "Multiple modes of RNA recognition by zinc finger proteins." *Curr Opin Struct Biol* 15 (3):367-73. doi: 10.1016/j.sbi.2005.04.004.

Hamblen, M., W. A. Zehring, C. P. Kyriacou, P. Reddy, Q. Yu, D. A. Wheeler, L. J. Zwiebel, R. J. Konopka, M. Rosbash, and J. C. Hall. 1986. "Germ-line transformation involving DNA from the period locus in Drosophila melanogaster: overlapping genomic fragments that restore circadian and ultradian rhythmicity to per0 and per- mutants." *J Neurogenet* 3 (5):249-91.

Hanrahan, C. J., M. J. Palladino, B. Ganetzky, and R. A. Reenan. 2000. "RNA editing of the Drosophila para Na(+) channel transcript. Evolutionary conservation and developmental regulation." *Genetics* 155 (3):1149-60.

Hardin, P. E. 2005. "The circadian timekeeping system of Drosophila." *Current biology : CB* 15 (17):R714-22. doi: 10.1016/j.cub.2005.08.019.

Hardin, P. E. 2011. "Molecular genetic analysis of circadian timekeeping in Drosophila." *Adv Genet* 74:141-73. doi: 10.1016/B978-0-12-387690-4.00005-2.

Hardin, P. E., J. C. Hall, and M. Rosbash. 1990. "Feedback of the Drosophila period gene product on circadian cycling of its messenger RNA levels." *Nature* 343 (6258):536-40. doi: 10.1038/343536a0.

Hardin, P. E., J. C. Hall, and M. Rosbash. 1992. "Circadian oscillations in period gene mRNA levels are transcriptionally regulated." *Proc Natl Acad Sci U S A* 89 (24):11711-5.

Harwood, A. J. 2001. "Regulation of GSK-3: a cellular multiprocessor." *Cell* 105 (7):821-4.

Helfrich-Förster, C. 2001. "The locomotor activity rhythm of Drosophila melanogaster is controlled by a dual oscillator system." *Journal of Insect Physiology* 47 (8):877-887. doi: Doi 10.1016/S0022-1910(01)00060-9.

Helfrich-Förster, C. 2002. "The circadian system of Drosophila melanogaster and its light input pathways." *Zoology* 105 (4):297-312. doi: Doi 10.1078/0944-2006-00074.

Helfrich-Förster, C. 2004. "The circadian clock in the brain: a structural and functional comparison between mammals and insects." *Journal of Comparative Physiology a-Neuroethology Sensory Neural and Behavioral Physiology* 190 (8):601-613. doi: DOI 10.1007/s00359-004-0527-2.

Helfrich-Förster, C., C. Winter, A. Hofbauer, J. C. Hall, and R. Stanewsky. 2001. "The circadian clock of fruit flies is blind after elimination of all known photoreceptors." *Neuron* 30 (1):249-61.

Helfrich, C., and W. Engelmann. 1987. "Evidences for circadian rhythmicity in the per0 mutant of Drosophila melanogaster." *Z Naturforsch C* 42 (11-12):1335-8.

Hermann, C., T. Yoshii, V. Dusik, and C. Helfrich-Förster. 2012. "Neuropeptide F immunoreactive clock neurons modify evening locomotor activity and free-running period in Drosophila melanogaster." *J Comp Neurol* 520 (5):970-87. doi: 10.1002/cne.22742.

Huang, J., W. Zhou, W. Dong, and Y. Hong. 2009. "Targeted engineering of the Drosophila genome." *Fly* 3 (4):274-7.

Huang, J., W. Zhou, W. Dong, A. M. Watson, and Y. Hong. 2009. "From the Cover: Directed, efficient, and versatile modifications of the Drosophila genome by genomic engineering." *Proceedings of the National Academy of Sciences of the United States of America* 106 (20):8284-9. doi: 10.1073/pnas.0900641106.

Huang, J., W. Zhou, A. M. Watson, Y. N. Jan, and Y. Hong. 2008. "Efficient ends-out gene targeting in Drosophila." *Genetics* 180 (1):703-7. doi: 10.1534/genetics.108.090563.

Huang, Y., J. A. Ainsley, L. G. Reijmers, and F. R. Jackson. 2013. "Translational profiling of clock cells reveals circadianly synchronized protein synthesis." *PLoS Biol* 11 (11):e1001703. doi: 10.1371/journal.pbio.1001703.

Jepson, J. E., and R. A. Reenan. 2010. "Unraveling pleiotropic functions of A-to-I RNA editing in Drosophila." *Fly (Austin)* 4 (2):154-8.

Jepson, J. E., Y. A. Savva, C. Yokose, A. U. Sugden, A. Sahin, and R. A. Reenan. 2011. "Engineered alterations in RNA editing modulate complex behavior in Drosophila: regulatory diversity of adenosine deaminase acting on RNA (ADAR) targets." *The Journal of biological chemistry* 286 (10):8325-37. doi: 10.1074/jbc.M110.186817.

Kaneko, M., and J. C. Hall. 2000. "Neuroanatomy of cells expressing clock genes in Drosophila: transgenic manipulation of the period and timeless genes to mark the perikarya of circadian pacemaker neurons and their projections." *J Comp Neurol* 422 (1):66-94.

Kempinger, L., R. Dittmann, D. Rieger, and C. Helfrich-Förster. 2009. "The Nocturnal Activity of Fruit Flies Exposed to Artificial Moonlight Is Partly Caused by Direct Light Effects on the Activity Level That Bypass the Endogenous Clock." *Chronobiology International* 26 (2):151-166. doi: Pii 908654298 Doi 10.1080/07420520902747124.

Kim, E. Y., K. Bae, F. S. Ng, N. R. Glossop, P. E. Hardin, and I. Edery. 2002. "Drosophila CLOCK protein is under posttranscriptional control and influences light-induced activity." *Neuron* 34 (1):69-81.

Kim, E. Y., and I. Edery. 2006. "Balance between DBT/CKIepsilon kinase and protein phosphatase activities regulate phosphorylation and stability of Drosophila CLOCK protein." *Proc Natl Acad Sci U S A* 103 (16):6178-83. doi: 10.1073/pnas.0511215103.

Kloss, B., J. L. Price, L. Saez, J. Blau, A. Rothenfluh, C. S. Wesley, and M. W. Young. 1998. "The Drosophila clock gene double-time encodes a protein closely related to human casein kinase Iepsilon." *Cell* 94 (1):97-107.

Klug, A. 1999. "Zinc finger peptides for the regulation of gene expression." *J Mol Biol* 293 (2):215-8. doi: 10.1006/jmbi.1999.3007.

Knowles, A., K. Koh, J. T. Wu, C. T. Chien, D. A. Chamovitz, and J. Blau. 2009. "The COP9 signalosome is required for light-dependent timeless degradation and Drosophila clock resetting." *J Neurosci* 29 (4):1152-62. doi: 10.1523/JNEUROSCI.0429-08.2009.

Ko, H. W., S. DiMassa, E. Y. Kim, K. Bae, and I. Edery. 2007. "Cis-combination of the classic per(S) and per(L) mutations results in arrhythmic Drosophila with ectopic accumulation of hyperphosphorylated PERIOD protein." *J Biol Rhythms* 22 (6):488-501. doi: 10.1177/0748730407306929.

Ko, H. W., J. Jiang, and I. Edery. 2002. "Role for Slimb in the degradation of Drosophila Period protein phosphorylated by Doubletime." *Nature* 420 (6916):673-8. doi: 10.1038/nature01272.

Ko, H. W., E. Y. Kim, J. Chiu, J. T. Vanselow, A. Kramer, and I. Edery. 2010. "A hierarchical phosphorylation cascade that regulates the timing of PERIOD nuclear entry reveals novel roles for proline-directed kinases and GSK-3beta/SGG in circadian clocks." *The Journal of neuroscience : the official journal of the Society for Neuroscience* 30 (38):12664-75. doi: 10.1523/JNEUROSCI.1586-10.2010.

Koh, K., X. Zheng, and A. Sehgal. 2006. "JETLAG resets the Drosophila circadian clock by promoting light-induced degradation of TIMELESS." *Science* 312 (5781):1809-12. doi: 10.1126/science.1124951.

Kolodziejczyk, R., M. Kochman, G. Bujacz, P. Dobryszycki, A. Ozyhar, and M. Jaskolski. 2003. "Crystallization and preliminary crystallographic studies of juvenile hormone-binding protein from Galleria mellonella haemolymph." *Acta Crystallogr D Biol Crystallogr* 59 (Pt 3):519-21.

Konopka, R. J., and S. Benzer. 1971. "Clock mutants of Drosophila melanogaster." *Proc Natl Acad Sci U S A* 68 (9):2112-6.

Konopka, R. J., C. Pittendrigh, and D. Orr. 1989. "Reciprocal behaviour associated with altered homeostasis and photosensitivity of Drosophila clock mutants." *J Neurogenet* 6 (1):1-10.

Kowalczykowski, S. C., D. A. Dixon, A. K. Eggleston, S. D. Lauder, and W. M. Rehrauer. 1994. "Biochemistry of Homologous Recombination in Escherichia-Coli." *Microbiological Reviews* 58 (3):401-465.

Krishnan, B., S. E. Dryer, and P. E. Hardin. 1999. "Circadian rhythms in olfactory responses of Drosophila melanogaster." *Nature* 400 (6742):375-8. doi: 10.1038/22566.

Krishnan, B., J. D. Levine, M. K. Lynch, H. B. Dowse, P. Funes, J. C. Hall, P. E. Hardin, and S. E. Dryer. 2001. "A new role for cryptochrome in a Drosophila circadian oscillator." *Nature* 411 (6835):313-7. doi: 10.1038/35077094.

Kurkulos, M., J. M. Weinberg, M. E. Pepling, and S. M. Mount. 1991. "Polyadenylylation in copia requires unusually distant upstream sequences." *Proc Natl Acad Sci U S A* 88 (8):3038-42.

Kyriacou, C. P., and M. Hastings. 2001. "Keystone clocks." *Trends Neurosci* 24 (8):434-5.

Lamba, P., D. Bilodeau-Wentworth, P. Emery, and Y. Zhang. 2014. "Morning and evening oscillators cooperate to reset circadian behavior in response to light input." *Cell Rep* 7 (3):601-8. doi: 10.1016/j.celrep.2014.03.044.

Ledent, V., and M. Vervoort. 2001. "The basic helix-loop-helix protein family: comparative genomics and phylogenetic analysis." *Genome Res* 11 (5):754-70. doi: 10.1101/gr.177001.

Lin, F. J., W. Song, E. Meyer-Bernstein, N. Naidoo, and A. Sehgal. 2001. "Photic signaling by cryptochrome in the Drosophila circadian system." *Mol Cell Biol* 21 (21):7287-94. doi: 10.1128/MCB.21.21.7287-7294.2001.

Lin, J. M., V. L. Kilman, K. Keegan, B. Paddock, M. Emery-Le, M. Rosbash, and R. Allada. 2002. "A role for casein kinase 2alpha in the Drosophila circadian clock." *Nature* 420 (6917):816-20. doi: 10.1038/nature01235.

Lorenz, L. J., J. C. Hall, and M. Rosbash. 1989. "Expression of a Drosophila mRNA is under circadian clock control during pupation." *Development* 107 (4):869-80.

Maggert, K. A., W. J. Gong, and K. G. Golic. 2008. "Methods for homologous recombination in Drosophila." *Methods in molecular biology* 420:155-74. doi: 10.1007/978-1-59745-583-1_9.

Marin, O., F. Meggio, F. Marchiori, G. Borin, and L. A. Pinna. 1986. "Site specificity of casein kinase-2 (TS) from rat liver cytosol. A study with model peptide substrates." *Eur J Biochem* 160 (2):239-44.

Martinek, S., S. Inonog, A. S. Manoukian, and M. W. Young. 2001. "A role for the segment polarity gene shaggy/GSK-3 in the Drosophila circadian clock." *Cell* 105 (6):769-79.

Masri, S., and P. Sassone-Corsi. 2013. "The circadian clock: a framework linking metabolism, epigenetics and neuronal function." *Nat Rev Neurosci* 14 (1):69-75. doi: 10.1038/nrn3393.

Matthews, J. M., and M. Sunde. 2002. "Zinc fingers--folds for many occasions." *IUBMB Life* 54 (6):351-5. doi: 10.1080/15216540216035.

Meggio, F., and L. A. Pinna. 2003. "One-thousand-and-one substrates of protein kinase CK2?" *FASEB J* 17 (3):349-68. doi: 10.1096/fj.02-0473rev.

Meissner, R. A., V. L. Kilman, J. M. Lin, and R. Allada. 2008. "TIMELESS is an important mediator of CK2 effects on circadian clock function in vivo." *The Journal of neuroscience : the official journal of the Society for Neuroscience* 28 (39):9732-40. doi: 10.1523/JNEUROSCI.0840-08.2008.

Menegazzi, P., T. Yoshii, and C. Helfrich-Förster. 2012. "Laboratory versus nature: the two sides of the Drosophila circadian clock." *J Biol Rhythms* 27 (6):433-42. doi: 10.1177/0748730412463181.

Murad, A., M. Emery-Le, and P. Emery. 2007. "A subset of dorsal neurons modulates circadian behavior and light responses in Drosophila." *Neuron* 53 (5):689-701. doi: 10.1016/j.neuron.2007.01.034.

Myers, M. P., K. Wager-Smith, C. S. Wesley, M. W. Young, and A. Sehgal. 1995. "Positional cloning and sequence analysis of the Drosophila clock gene, timeless." *Science* 270 (5237):805-8.

Naidoo, N., W. Song, M. Hunter-Ensor, and A. Sehgal. 1999. "A role for the proteasome in the light response of the timeless clock protein." *Science* 285 (5434):1737-41.

Neumuller, R. A., C. Richter, A. Fischer, M. Novatchkova, K. G. Neumuller, and J. A. Knoblich. 2011. "Genome-wide analysis of self-renewal in Drosophila neural stem cells by transgenic RNAi." *Cell Stem Cell* 8 (5):580-93. doi: 10.1016/j.stem.2011.02.022.

Ni, J. Q., L. P. Liu, R. Binari, R. Hardy, H. S. Shim, A. Cavallaro, M. Booker, B. D. Pfeiffer, M. Markstein, H. Wang, C. Villalta, T. R. Laverty, L. A. Perkins, and N. Perrimon. 2009. "A Drosophila resource of transgenic RNAi lines for neurogenetics." *Genetics* 182 (4):1089-100. doi: 10.1534/genetics.109.103630.

Ousley, A., K. Zafarullah, Y. Chen, M. Emerson, L. Hickman, and A. Sehgal. 1998. "Conserved regions of the timeless (tim) clock gene in Drosophila analyzed through phylogenetic and functional studies." *Genetics* 148 (2):815-25.

Ozturk, N., S. J. VanVickle-Chavez, L. Akileswaran, R. N. Van Gelder, and A. Sancar. 2013. "Ramshackle (Brwd3) promotes light-induced ubiquitylation of Drosophila Cryptochrome by DDB1-CUL4-ROC1 E3 ligase complex." *Proc Natl Acad Sci U S A* 110 (13):4980-5. doi: 10.1073/pnas.1303234110.

Palladino, M. J., L. P. Keegan, M. A. O'Connell, and R. A. Reenan. 2000. "dADAR, a Drosophila double-stranded RNA-specific adenosine deaminase is highly developmentally regulated and is itself a target for RNA editing." *RNA* 6 (7):1004-18.

Patrick Emery, Ralf Stanewsky, Jeffrey C. Hall, Michael Rosbash. 2000. "A unique circardian rhythm photoreceptor." *Nature* 404.

Peschel, N., K. F. Chen, G. Szabo, and R. Stanewsky. 2009. "Light-dependent interactions between the Drosophila circadian clock factors cryptochrome, jetlag, and timeless." *Curr Biol* 19 (3):241-7. doi: 10.1016/j.cub.2008.12.042.

Peschel, N., and C. Helfrich-Förster. 2011. "Setting the clock - by nature: Circadian rhythm in the fruitfly Drosophila melanogaster." *FEBS letters* 585 (10):1435-42. doi: 10.1016/j.febslet.2011.02.028.

Peschel, N., S. Veleri, and R. Stanewsky. 2006. "Veela defines a molecular link between Cryptochrome and Timeless in the light-input pathway to Drosophila's circadian clock." *Proc Natl Acad Sci U S A* 103 (46):17313-8. doi: 10.1073/pnas.0606675103.

Price, J. L., J. Blau, A. Rothenfluh, M. Abodeely, B. Kloss, and M. W. Young. 1998. "double-time is a novel Drosophila clock gene that regulates PERIOD protein accumulation." *Cell* 94 (1):83-95.

Rawlings, N. D., and A. J. Barrett. 1994. "Families of serine peptidases." *Methods Enzymol* 244:19-61.

Rawlings, N. D., M. Waller, A. J. Barrett, and A. Bateman. 2014. "MEROPS: the database of proteolytic enzymes, their substrates and inhibitors." *Nucleic Acids Research* 42 (D1):D503-D509. doi: DOI 10.1093/nar/gkt953.

Reddy, P., W. A. Zehring, D. A. Wheeler, V. Pirrotta, C. Hadfield, J. C. Hall, and M. Rosbash. 1984. "Molecular analysis of the period locus in Drosophila melanogaster and identification of a transcript involved in biological rhythms." *Cell* 38 (3):701-10.

Renn, S. C., J. H. Park, M. Rosbash, J. C. Hall, and P. H. Taghert. 1999. "A pdf neuropeptide gene mutation and ablation of PDF neurons each cause severe abnormalities of behavioral circadian rhythms in Drosophila." *Cell* 99 (7):791-802.

Reppert, S. M., and D. R. Weaver. 2001. "Molecular analysis of mammalian circadian rhythms." *Annu Rev Physiol* 63:647-76. doi: 10.1146/annurev.physiol.63.1.647.

Rhee, D. Y., D. Y. Cho, B. Zhai, M. Slattery, L. Ma, J. Mintseris, C. Y. Wong, K. P. White, S. E. Celniker, T. M. Przytycka, S. P. Gygi, R. A. Obar, and S. Artavanis-Tsakonas. 2014. "Transcription factor networks in Drosophila melanogaster." *Cell Rep* 8 (6):2031-43. doi: 10.1016/j.celrep.2014.08.038.

Rieger, D., O. T. Shafer, K. Tomioka, and C. Helfrich-Förster. 2006. "Functional analysis of circadian pacemaker neurons in Drosophila melanogaster." *J Neurosci* 26 (9):2531-43. doi: 10.1523/JNEUROSCI.1234-05.2006.

Rieger, D., R. Stanewsky, and C. Helfrich-Förster. 2003. "Cryptochrome, compound eyes, Hofbauer-Buchner eyelets, and ocelli play different roles in the entrainment and masking pathway of the locomotor activity rhythm in the fruit fly Drosophila melanogaster." *J Biol Rhythms* 18 (5):377-91.

Roenneberg, T., C. J. Kumar, and M. Merrow. 2007. "The human circadian clock entrains to sun time." *Curr Biol* 17 (2):R44-5. doi: 10.1016/j.cub.2006.12.011.

Rong, Y. S., and K. G. Golic. 2000. "Gene targeting by homologous recombination in Drosophila." *Science* 288 (5473):2013-8.

Rothenfluh, A., M. Abodeely, J. L. Price, and M. W. Young. 2000. "Isolation and analysis of six timeless alleles that cause short- or long-period circadian rhythms in Drosophila." *Genetics* 156 (2):665-75.

Rothenfluh, A., M. W. Young, and L. Saez. 2000. "A TIMELESS-independent function for PERIOD proteins in the Drosophila clock." *Neuron* 26 (2):505-14.

Rueter, S. M., T. R. Dawson, and R. B. Emeson. 1999. "Regulation of alternative splicing by RNA editing." *Nature* 399 (6731):75-80. doi: 10.1038/19992.

Rush, B. L., A. Murad, P. Emery, and J. M. Giebultowicz. 2006. "Ectopic CRYPTOCHROME renders TIM light sensitive in the Drosophila ovary." *J Biol Rhythms* 21 (4):272-8. doi: 10.1177/0748730406290416.

Saez, L., and M. W. Young. 1996. "Regulation of nuclear entry of the Drosophila clock proteins period and timeless." *Neuron* 17 (5):911-920. doi: Doi 10.1016/S0896-6273(00)80222-6.

Sandrelli, F., E. Tauber, M. Pegoraro, G. Mazzotta, P. Cisotto, J. Landskron, R. Stanewsky, A. Piccin, E. Rosato, M. Zordan, R. Costa, and C. P. Kyriacou. 2007. "A molecular basis for natural selection at the timeless locus in Drosophila melanogaster." *Science* 316 (5833):1898-900. doi: 10.1126/science.1138426.

Sathyanarayanan, S., X. Zheng, S. Kumar, C. H. Chen, D. Chen, B. Hay, and A. Sehgal. 2008. "Identification of novel genes involved in light-dependent CRY degradation through a genome-wide RNAi screen." *Genes Dev* 22 (11):1522-33. doi: 10.1101/gad.1652308.

Schibler, U. 2006. "Circadian time keeping: the daily ups and downs of genes, cells, and organisms." *Prog Brain Res* 153:271-82. doi: 10.1016/S0079-6123(06)53016-X.

Schmid, B., C. Helfrich-Förster, and T. Yoshii. 2011. "A new ImageJ plug-in "ActogramJ" for chronobiological analyses." *J Biol Rhythms* 26 (5):464-7. doi: 10.1177/0748730411414264.

Scholz, N., J. Gehring, C. Guan, D. Ljaschenko, R. Fischer, V. Lakshmanan, R. J. Kittel, and T. Langenhan. 2015. "The Adhesion GPCR Latrophilin/CIRL Shapes Mechanosensation." *Cell Rep*. doi: 10.1016/j.celrep.2015.04.008.

Schultz, J., C. P. Ponting, K. Hofmann, and P. Bork. 1997. "SAM as a protein interaction domain involved in developmental regulation." *Protein Sci* 6 (1):249-53. doi: 10.1002/pro.5560060128.

Sehgal, A., J. L. Price, B. Man, and M. W. Young. 1994. "Loss of circadian behavioral rhythms and per RNA oscillations in the Drosophila mutant timeless." *Science* 263 (5153):1603-6.

Sehgal, A., A. Rothenfluh-Hilfiker, M. Hunter-Ensor, Y. Chen, M. P. Myers, and M. W. Young. 1995. "Rhythmic expression of timeless: a basis for promoting circadian cycles in period gene autoregulation." *Science* 270 (5237):808-10.

Shafer, O. T., M. Rosbash, and J. W. Truman. 2002. "Sequential nuclear accumulation of the clock proteins period and timeless in the pacemaker neurons of Drosophila melanogaster." *J Neurosci* 22 (14):5946-54. doi: 20026628.

Shafer, O. T., and Z. Yao. 2014. "Pigment-Dispersing Factor Signaling and Circadian Rhythms in Insect Locomotor Activity." *Curr Opin Insect Sci* 1:73-80. doi: 10.1016/j.cois.2014.05.002.

Sidote, D., J. Majercak, V. Parikh, and I. Edery. 1998. "Differential effects of light and heat on the Drosophila circadian clock proteins PER and TIM." *Mol Cell Biol* 18 (4):2004-13.

Siegal, M. L., and D. L. Hartl. 2000. "Application of Cre/loxP in Drosophila. Site-specific recombination and transgene coplacement." *Methods Mol Biol* 136:487-95. doi: 10.1385/1-59259-065-9:487.

Smith, E. M., J. M. Lin, R. A. Meissner, and R. Allada. 2008. "Dominant-negative CK2alpha induces potent effects on circadian rhythmicity." *PLoS genetics* 4 (1):e12. doi: 10.1371/journal.pgen.0040012.

Stanewsky, R. 2002. "Clock mechanisms in Drosophila." *Cell Tissue Res* 309 (1):11-26. doi: 10.1007/s00441-002-0569-0.

Stanewsky, R., B. Frisch, C. Brandes, M. J. Hamblen-Coyle, M. Rosbash, and J. C. Hall. 1997. "Temporal and spatial expression patterns of transgenes containing increasing amounts of the Drosophila

clock gene period and a lacZ reporter: mapping elements of the PER protein involved in circadian cycling." *J Neurosci* 17 (2):676-96.

Stanewsky, R., C. F. Jamison, J. D. Plautz, S. A. Kay, and J. C. Hall. 1997. "Multiple circadian-regulated elements contribute to cycling period gene expression in Drosophila." *EMBO J* 16 (16):5006-18. doi: 10.1093/emboj/16.16.5006.

Stanewsky, R., M. Kaneko, P. Emery, B. Beretta, K. Wager-Smith, S. A. Kay, M. Rosbash, and J. C. Hall. 1998. "The cryb mutation identifies cryptochrome as a circadian photoreceptor in Drosophila." *Cell* 95 (5):681-92.

Stoleru, D., P. Nawathean, M. P. Fernandez, J. S. Menet, M. F. Ceriani, and M. Rosbash. 2007. "The Drosophila circadian network is a seasonal timer." *Cell* 129 (1):207-19. doi: 10.1016/j.cell.2007.02.038.

Stoleru, D., Y. Peng, J. Agosto, and M. Rosbash. 2004. "Coupled oscillators control morning and evening locomotor behaviour of Drosophila." *Nature* 431 (7010):862-8. doi: 10.1038/nature02926.

Stoleru, D., Y. Peng, P. Nawathean, and M. Rosbash. 2005. "A resetting signal between Drosophila pacemakers synchronizes morning and evening activity." *Nature* 438 (7065):238-42. doi: 10.1038/nature04192.

Suri, V., Z. Qian, J. C. Hall, and M. Rosbash. 1998. "Evidence that the TIM light response is relevant to light-induced phase shifts in Drosophila melanogaster." *Neuron* 21 (1):225-34.

Tauber, E., M. Zordan, F. Sandrelli, M. Pegoraro, N. Osterwalder, C. Breda, A. Daga, A. Selmin, K. Monger, C. Benna, E. Rosato, C. P. Kyriacou, and R. Costa. 2007. "Natural selection favors a newly derived timeless allele in Drosophila melanogaster." *Science* 316 (5833):1895-8. doi: 10.1126/science.1138412.

Vanin, S., S. Bhutani, S. Montelli, P. Menegazzi, E. W. Green, M. Pegoraro, F. Sandrelli, R. Costa, and C. P. Kyriacou. 2012. "Unexpected features of Drosophila circadian behavioural rhythms under natural conditions." *Nature* 484 (7394):371-5. doi: 10.1038/nature10991.

Varterasian, M., S. Lipkowitz, I. Karsch-Mizrachi, B. Paterson, and I. Kirsch. 1993. "Two new Drosophila genes related to human hematopoietic and neurogenic transcription factors." *Cell Growth Differ* 4 (11):885-9.

Veleri, S., D. Rieger, C. Helfrich-Förster, and R. Stanewsky. 2007. "Hofbauer-Buchner eyelet affects circadian photosensitivity and coordinates TIM and PER expression in Drosophila clock neurons." *J Biol Rhythms* 22 (1):29-42. doi: 10.1177/0748730406295754.

White, K., E. Tahaoglu, and H. Steller. 1996. "Cell killing by the Drosophila gene reaper." *Science* 271 (5250):805-7.

Yang, Z., M. Emerson, H. S. Su, and A. Sehgal. 1998. "Response of the timeless protein to light correlates with behavioral entrainment and suggests a nonvisual pathway for circadian photoreception." *Neuron* 21 (1):215-23.

Yang, Z., and A. Sehgal. 2001. "Role of molecular oscillations in generating behavioral rhythms in Drosophila." *Neuron* 29 (2):453-67.

Yoshii, T., Y. Funada, T. Ibuki-Ishibashi, A. Matsumoto, T. Tanimura, and K. Tomioka. 2004. "Drosophila cryb mutation reveals two circadian clocks that drive locomotor rhythm and have different responsiveness to light." *J Insect Physiol* 50 (6):479-88. doi: 10.1016/j.jinsphys.2004.02.011.

Yoshii, T., D. Rieger, and C. Helfrich-Förster. 2012. "Two clocks in the brain: an update of the morning and evening oscillator model in Drosophila." *Prog Brain Res* 199:59-82. doi: 10.1016/B978-0-444-59427-3.00027-7.

Yoshii, T., T. Todo, C. Wulbeck, R. Stanewsky, and C. Helfrich-Förster. 2008. "Cryptochrome is present in the compound eyes and a subset of Drosophila's clock neurons." *J Comp Neurol* 508 (6):952-66. doi: 10.1002/cne.21702.

Yu, Q., A. C. Jacquier, Y. Citri, M. Hamblen, J. C. Hall, and M. Rosbash. 1987. "Molecular mapping of point mutations in the period gene that stop or speed up biological clocks in Drosophila melanogaster." *Proc Natl Acad Sci U S A* 84 (3):784-8.

Yuan, Q., F. Lin, X. Zheng, and A. Sehgal. 2005. "Serotonin modulates circadian entrainment in Drosophila." *Neuron* 47 (1):115-27. doi: 10.1016/j.neuron.2005.05.027.

Zhang, L., B. Y. Chung, B. C. Lear, V. L. Kilman, Y. Liu, G. Mahesh, R. A. Meissner, P. E. Hardin, and R. Allada. 2010. "DN1(p) circadian neurons coordinate acute light and PDF inputs to produce robust daily behavior in Drosophila." *Curr Biol* 20 (7):591-9. doi: 10.1016/j.cub.2010.02.056.

Zinshteyn, B., and K. Nishikura. 2009. "Adenosine-to-inosine RNA editing." *Wiley Interdiscip Rev Syst Biol Med* 1 (2):202-9. doi: 10.1002/wsbm.10.

Zoltowski, B. D., A. T. Vaidya, D. Top, J. Widom, M. W. Young, and B. R. Crane. 2011. "Structure of full-length Drosophila cryptochrome." *Nature* 480 (7377):396-9. doi: 10.1038/nature10618.

6.4 Figures

6.5 Tables

6.6 Abbreviations

Adar	Adenosine deaminase acting on RNA	HLH3B	Helix loop helix protein 3B
AA	Amino acid	Jet	Jetlag
attP/B	Attachment site on the phage/bacterial part	LD	Light-dark
BDSC or Bl	Bloomington *Drosophila* Stock Center (IN, USA)	LL	Light-light
gDNA	Genomic DNA	loxP	Locus over X-over P1
BLAST	Basic Local Alignment Search Tool	PCR	Polymerase chain reaction
Bp	Base pairs	Pdf	Pigment dispersing factor
cDNA	Complementary DNA	Pdp1	Pyruvate dehydrogenase phosphatase catalytic subunit 1
CK	Casein kinase	Per	Period
Fw	forward	qPCR	Quantitative PCR
FRT	Flippase recognition site	rtPCR	Reverse transcriptase PCR
Clk	Clock	Rv	reverse
Cry	Cryptochrome	SGG	Shaggy
Cyc	Cycle	Tim	Timeless
DBT	Double-time	UAS	Upstream activating sequence
DNA	Deoxyribonucleic acid	Vri	Vrille
Flp	Flippase	ZT	Zeitgeber time

6.7 Publications and presentations

Publications

Fischer R., Helfrich-Förster C. and Peschel N. 2015. “GSK-3 beta interacts with Period and Timeless but not with Cryptochrome in the circadian clock of Drosophila”. (under revision)

Poster

Fischer R., Helfrich-Förster C. and Peschel N., Neurofly 2012, Padua, Italy. „Frizzled2 and Shaggy: Two members of the Wnt pathway with influence on the circadian clock.”

Fischer R., Helfrich-Förster C. and Peschel N., *Drosophila* research conference 2013, Washington, USA. “New insights into the influences of SHAGGY (SGG) on the circadian clock.”

Fischer R., Cao F., Helfrich-Förster C. and Peschel N., Neurofly 2014, Hersonissos, Greece. „A new way of setting the clock – Adenine to Inosine editing of timeless RNA depending on circadian rhythm.”

6.8 Acknowledgements

Zunächst möchte ich mich bei Prof. Dr. Charlotte Förster bedanken, dass ich an ihrem Lehrstuhl die Räumlichkeiten und Materialien nutzen durfte um meine Dissertation anzufertigen. Ebenfalls gilt mein Dank für die wertvolle Zeit mit vielen hilfreichen Diskussionen die zur Verbesserung meiner Arbeit maßgeblich beigetragen haben.

Mein größter Dank gilt Dr. Nicolai Peschel, meinem Erstgutachter, Betreuer und Arbeitgeber, der mir die Möglichkeit gegeben hat meine Arbeit in seiner Arbeitsgruppe am Lehrstuhl für Neurobiologie und Genetik durchzuführen. Im Besonderen möchte ich mich für viele hilfreiche Diskussionen, Geduld, Motivation und Vertrauen, sowie dauerhafter, bedingungsloser Unterstützung während meiner Zeit im Labor, als auch in der Schreibphase bedanken. Ich habe mich zu jeder Zeit sehr wohl gefühlt, es hat mir nie an etwas gefehlt und ich bekam zu jeder Zeit ein offenes Ohr für Hilfe und Rat!

Natürlich möchte ich mich auch bei allen meinen Kollegen für ein wirklich harmonisches Arbeitsklima, erholsame Kaffeepausen und eine schöne, entspannte Zeit im Labor und auch nach Feierabend bedanken. Dies gilt besonders auch meiner ehemaligen Mitstreiterin Fang Cao und unserer technischen Assistentin Barbara Mühlbauer, die mir bei zahlreichen Experimenten hilfreich unter die Arme gegriffen hat. Besonderer Dank geht auch an Dr. Christiane Luibl und Dr. Matthias Schlichting für die Hilfe bei statistischen Auswertungen, sowie an Dr. Pamela Menegazzi für viele gewinnbringende Diskussionen und Hilfe bei Fragen. Nicht vergessen möchte ich auch die Hilfe durch Studenten, speziell für die Verifizierung des Period Knock-out durch Stephanie Lichtblau und die Klonierung des Period Rescue Konstrukts durch Peter Deppisch. Die Zusammenarbeit mit euch allen hat zu jeder Zeit sehr viel Freude bereitet!

Allen meinen Freunden inner- und außerhalb Würzburgs für Motivation, Unterstützung und ein tolles Leben außerhalb der Arbeit. Ganz besonders meinen Eltern, die mich stets unterstützt, mein Studium mitfinanziert und nie an mir gezweifelt haben.

Zum Schluss gilt mein Dank in ganz besonderer Weise meiner Frau Annette. Ohne deine Unterstützung und Liebe im Privaten, aber auch Diskussionen und Ratschläge im Fachlichen, wäre ich bestimmt nicht hier wo ich jetzt bin! Danke für Alles!

6.10 Declarations

Affidavit

I hereby confirm that my thesis “Generating useful tools for future studies in the center of the circadian clock – defined knockout mutants for PERIOD and TIMELESS” is the result of my own work. I did not receive any help or support from commercial consultants. All sources and/or materials applied are listed and specified in the thesis.

Furthermore, I confirm that this thesis has not yet been submitted as part of another examination process neither in identical nor in similar form.

Würzburg, 19.06.2015

Place, Date Signature

Eidesstattliche Erklärung

Hiermit erkläre ich an Eides statt, die Dissertation „Entwicklung nützlicher Hilfsmittel für zukünftige Studien im Zentrum der inneren Uhr – definierte knockout Mutanten für PERIOD und TIMELESS“ eigenhändig, d.h. insbesondere selbständig und ohne Hilfe eines kommerziellen Promotionsberaters, angefertigt und keine anderen als die von mir angegebenen Quellen und Hilfsmittel verwendet zu haben.

Ich erkläre außerdem, dass die Dissertation weder in gleicher noch in ähnlicher Form bereits in einem anderen Prüfungsverfahren vorgelegen hat.

Ich habe früher, außer den mit dem Zulassungsgesuch urkundlich vorgelegten Graden, keine weiteren akademischen Grade erworben oder zu erwerben versucht.

Würzburg, 19.06.2015

Ort, Datum Unterschrift